ISTANBUL TECHNICAL UNIVERSITY ★ GRADUATE SCHOOL OF SCIENCE ENGINEERING AND TECHNOLOGY

PEPTITE–BASED DESIGNED BIOMATERIALS FOR MEDICAL APPLICATIONS THROUGH BIOMIMETIC APPROACH

Ph.D. THESIS

Hilal YAZICI

Department of Molecular Biology and Genetics

Molecular Biology-Genetics and Biotechnology Programme

DECEMBER 2011

ISTANBUL TECHNICAL UNIVERSITY ★ GRADUATE SCHOOL OF SCIENCE ENGINEERING AND TECHNOLOGY

PEPTITE–BASED DESIGNED BIOMATERIALS FOR MEDICAL APPLICATIONS THROUGH BIOMIMETIC APPROACH

Ph.D. THESIS

Hilal YAZICI
(521042216)

Department of Molecular Biology and Genetics

Molecular Biology-Genetics and Biotechnology Programme

Thesis Advisor: Prof. Dr. Candan TAMERLER
Co-Advisor: Prof. Dr. Mehmet SARIKAYA

DECEMBER 2011

İSTANBUL TEKNİK ÜNİVERSİTESİ ★ FEN BİLİMLERİ ENSTİTÜSÜ

BİOMİMETİK YAKLAŞIMI İLE PEPTİD BAZLI BİYOMALZEMELERİN MEDİKAL UYGULAMALAR İÇİN GELİŞTİRİLMESİ

DOKTORA TEZİ

Hilal YAZICI
(521042216)

Mühendislikte İleri Teknolojiler Anabilim Dalı

Mokelüler Biyoloji-Genetik Biyoteknoloji Programı

Tez Danışmanı: Prof. Dr. Candan TAMERLER
Eş Danışman: Prof. Dr. Mehmet SARIKAYA

ARALIK 2011

Hilal YAZICI, **a Ph.D.** student of ITU **Graduate School of Science Engineering and Technology** student ID 521042216, successfully defended the **dissertation** entitled "**PEPTITE–BASED DESIGNED BIOMATERIALS FOR MEDICAL APPLICATIONS THROUGH BIOMIMETIC APPROACH**", which she prepared after fulfilling the requirements specified in the associated legislations, before the jury whose signatures are below.

Thesis Advisor :	**Prof. Dr. Candan TAMERLER** İstanbul Technical University University of Washington	.....
Co-advisor :	**Prof. Dr. Mehmet SARIKAYA** University of Washington	.....
Jury Members :	**Prof. Dr. Mustafa ÜRGEN** İstanbul Technical University	.....
	Assoc. Prof. Dr. Ayten Yazgan KARATAŞ İstanbul Technical University	.....
	Assoc. Prof. Dr. Nevin Gül KARAGÜLER İstanbul Technical University	.....
	Assoc. Prof. Dr. Levent TRABZON İstanbul Technical University	.....
	Prof. Dr. Gamze Torun KÖSE Yeditepe University	.....

Date of Submission : 10 February 2011
Date of Defense : 28 December 2011

To my mon (Saadet YAZICI) and my dad (Ali Kemal YAZICI),

FOREWORD

Looking back, it was a long journey. While very close to end after all fails and stumbling, I am surprised, at the same time very greatful for all I have received throughout these years. It has certainly shaped me as a person and has led me where I am now. All these years of PhD studies are full of such gifts.

To acknowledge the many people who have involved, contributed to reveal this work in full is the last and difficult task. This assiduous hike wouldn't have accomplished without tremendous help and support I gratefully received from many individuals as highlighted below.

First and foremost, I wish express my gratitude to my supervisors Prof. Candan Tamerler and Prof. Mehmet Sarikaya for their continuous encouragements, invaluable suggestions and guidance to make my PhD experience more productive, stimulating and challenging. Especially, Prof Sarikaya has provided me with his excellent vision to conduct investigations and concentrate on the important matters. Prof Tamerler` s infinite enthusiasm, energy, initiative and positive thinking made this work more dynamic.

I would like to especially thank to Prof Martha Sommermon, Assoc Prof. Hai Zang, Assist Prof Sami Dogan and Prof John S. Evans and their research group supported us with their knowledge, experience on various areas that gave us perspective for utilization of GEPIs on new application areas. I am thankful to them.

This study could not have been accomplished without the financial support of Turkish State Planing Organization via Advanced Technologies in Engineering Program and Institute of Science and Technology via Graduate Thesis Supporting Fund at Istanbul Technical University (Project number: 34009). It was also provided by TUBITAK/NSF-IRES project (Contract grant number: 107T250) and by Genetically Engineered Materials Science and Engineering Center through NSF-MRSEC Program at University of Washington.

The research presented in this dissertation was largely an outcome of a collaborative work involving essential contributions from institutions and it was performed in the facilities of Molecular Biology-Biotechnology & Genetics Research Center (MOBGAM) at Istanbul Technical University and Material Science and Engineering Department and GEMSEC (Genetically Engineered Materials Science and Engineering Center) at University of Washington, Seattle, USA. I want to express my gratitude to the staff in these institutions.

I would like thank to my colleges and my research partners. Dr. Brandon Wilson, Dr. Marketa Hnilova, Dr. Turgay Kacar, Dr. Mustafa Gungormus, Dr.Yuhei Hayamizu, Dr. Christopher So for their extremely valuable experience, supports and insights and being such a good friend in all the times. I want to thank to Dr. Hanson Fong for his willingness to help especially while performing AFM and SEM and writing my papers. Dr. E. Emre Oren is another person who gave insights to this work with his data support.

I would like to thank to Mary Rood. It was a pleasure and great experience to work with her as a junior mentor. I would like to send special thanks to Carolyn Gresswell who is the nice person with her willingness help, research partnership and being so supportive, positive during my studies at University of Washington. Many thanks go to all the members of the Biomimetics Research group at UW, for their moral and technical support.

The years spent in Seattle would not have been wonderful without lots of friends. There were some moments that shaped with lots of people and I never ever forget through my life. One of the people among them is Athena Foundulis. I would like to send my special thanks to her who support me sometimes as a big sister, sometimes as a mom or as a good friend whenever I felt exhausted and couldn`t continue on my way and while I was miles and miles far away from my country, she made my home (Eta Beta) in Seattle warmer.

It is really difficult finding the right words to express my depth gratitude to Christine Tasai for her infinite help, sweat heart, positive energy which makes me every time powerful.

I would like to thank to Holly Shelton and Derya Kaltakci who can understand my tiredness the best after long hours working and try to put a smile on my face enjoying with their Halloween, tea and dinner parties, dancing classes, Easter sports, trekking. In crazy journey between Seattle and Istanbul, Sibel Cetinel, Banu Taktak and Esra Yuca are accompanied to me sometimes as a lab partner, as a roommate, as a good friend. I would like to thank all of them for lots of shared unforgettable and enjoyable moments.

After long time in Seattle, I would like to thank to Senem Donatan and Derya Canbaz to make my adaptation for everything faster with their moral support.

I owe a special distinction to Volkan Demir who every time staying by my side, taking care and thinking of me. I am infinitively thankful to him.

At last, but not least, I would like to thank my family, especially to my mom how to teach me to be strong, resistant and persist against the every challenge in my life and to my dad, showing me how to be patient while running though the life. Finally, I would like thank to one of the most important people in my life, my older sister Prof Hulya Yazici. It is really difficult to find proper words for her who loves me a lot, believed in me, motivated and encourage me though all of my life.

December 2011

Hilal YAZICI
(Molecular Biologist)

TABLE OF CONTENTS

Page

FOREWORD ..... **xix**
TABLE OF CONTENTS ..... **xi**
ABBREVIATIONS ..... **xv**
LIST OF TABLES ..... **xvii**
LIST OF FIGURES ..... **xix**
SUMMARY ..... **xxv**
ÖZET ..... **xxix**
1. INTRODUCTION **1**
1.1 Bionanotechnology and Biomaterials 1
1.2 Implant Materials for Tissue Restoration 4
1.2.1 Metallic materials 5
1.2.1.1 Titanium and its alloys 6
1.2.1.2 Stinless steel 7
1.2.1.3 Cobalt chromium alloys 8
1.2.1.4 Ceramics 8
1.2.2 Polymers 8
1.2.3 Composites 9
1.2.4 Natural Materials 11
1.3 Performance Factors for Implant Materials 11
1.3.1 Chemical composition 12
1.3.2 Mechanical behavior 13
1.3.3 Corrosion 13
1.3.4 Surface characteristics 14
1.3.4.1 Surface chemistry 15
1.3.4.2 Surface hydrophobicity (wettability) 16
1.3.4.3 Surface topographyand roughness 17
1.3.4.4 Surface porosity 18
1.3.5 Biocompatibility 19
1.4 Biomaterials Induced Biological Response at Implant-Tissue Interface 21
1.4.1 Material-host interactions 21
1.4.2 Cell-surface interactions 23
1.4.2.1 Protein adsorption 23
1.4.2.2 Cell adhesion 26
1.4.2.3 Cell morphology and motility 28
1.4.2.4 Cell proliferation and differentiation 29
1.5 Challenges at Implant-Tissue Interface 30
1.5.1 Osseointegration 30
1.5.1.1 Prerequisites for osseointegration 31
1.5.2 Bacterial infection 32
1.5.2.1 Main pathogen bacteria involved in implant infections osseointegration 36

1.6 Approaches for Implant-Tissue integration 39
1.6.1 Implant surface modifications for better osseointegration 39
1.6.1.1 Chemical surface modification 40
1.6.1.2 Physical surface modification 44
1.6.1.3 Biological surface modification 45
1.6.2 Strategies to prevent implant infections 50
1.6.2.1 Antibiotic treatment 50
1.6.2.2 Antimicrobial agents 54
1.6.2.3 Nonfouling surfaces 55
1.6.2.4 Antimicrobial peptides 56
1.7 Biomolecule Immobilization Approaches to Functionalize Implant Surfaces 61
1.7.1 Physical immobilization 61
1.7.2 Chemical immobilization 63
1.8 Genetically Engineered Peptides for Inorganics-GEPI in Bionanotechnology 65
1.8.1 Biocombinatorial Selection of GEPIs 66
1.8.2 Theoretical design and molecular binding characterization of GEPIs 69
1.8.3 Current and potential applications of GEPI`s in bionanotechnology 73
2. MATERIALS AND METHODS 79
2.1 Combinatorial Selection Methods 79
2.1.1 Cell surface display selection 79
2.1.1.1 Target material preparation 79
2.1.1.2 FliTRx random peptide display library 79
2.1.1.3 Cell surface display 80
2.1.1.4 Initial binding characterization of selected clones via fluorescence microscopy 82
2.2 Solid State Peptide Synthesis 83
2.3 Molecular Structure and Modeling Methods 87
2.3.1 Circular dichroism spectroscopy 87
2.3.2 Molecular modeling 87
2.4 Quantitative Peptide Binding Characterization Methods 88
2.4.1Quartz crystal microbalance 88
2.4.1.1 Quantification of peptide binding affinity via QCM 89
2.4.1.2 *In vitro* monitoring of peptide-mediated mineralization via QCM 90
2.5 Material Surface Characterization Methods 90
2.5.1 Scanning electron microscopy 90
2.5.2 Atomic force microscopy 91
2.5.3 Transmission electron microscopy 92
2.6 Preparation of PDMS Stamps for μCP 93
2.6.1 Master preparation 93
2.6.2 PDMS stamp preparation 94
2.7 Cytotoxicity Assays for Peptide Functionalized Titanium Surfaces 94
2.7.1 Cell culture maintenance 94
2.7.2 Cell viability (MTT assay) 94
2.7.3 Cell adhesion and spreading 95
2.8 Antimicrobial Assays for Peptide Functionalized Titanium Surfaces 96
2.8.1 Bacterial maintenance and culturing 96
2.8.2 In solution antimicrobial activity of TiBP-AMP conjugates 96
2.8.3 Titanium substrate preparation and peptide immobilization 97
2.8.4 Mid-log culture and preparation of 10^8 cells/mL cell suspension 97
2.8.5 Fixation of adhered bacteria to peptide-modified titanium surfaces 98

2.8.6 Micro-contact printing of TiBP1-AMP with *S.mutans*.....98
2.8.7 Visualization and quantification of bacterial adhesion on GEPI-modified titanium substrate 98
2.9 Statistical Analysis 99
3. RESULTS AND DISCUSSION 101
3.1 Selection and Characterization of Titanium Binding Peptides (TiBPs) as a Molecular Linker 101
3.1.1 Biocombinatorial selection and characterization of TiBPs.....101
3.1.2 Conformational properties of TiBPIs 105
3.1.3 Adsorption behavior of TiBPs on titanium and other implantable surface……...109
3.1.4 Surface topography of cp Grade 4 and cp Grade 1 titanium dental implant materials.....115
3.1.5 Cell viability (MTT assay).....118
3.2 TiBPs as a Molecular Linker for Bioactive Implant Surface Functionalization…..120
3.2.1 Biocompatibility of TiBPs functionalized titanium dental implant surface……...120
3.2.2 TiBP-RGDS mediated bioactive surface modifications 123
3.3 GEPI Mediated Antimicrobial Titanium Surface Modifications.....128
3.3.1 Designing of TiBP-AMP bi-fucntional conjugates 129
3.3.2 Adsorption behavior of TiBP-AMP bi-fucntional peptides on titanium..130
3.3.3 Conformational properties of TiBP-AMP bi-fucntional peptides.....131
3.3.4 In solution antimicrobial activity of TiBP-AMP bi-fucntional peptides……..133
3.3.5 On the surface antimicrobial activity of TiBP-AMP bi-fucntional peptides……..140
3.3.6 Micro-contact printing of TiBP-AMPon titanium surface.....143
3.4 In situ Mineralization of Hydroxapatite Films on Titanium Surface via Bi-functional Peptide 145
3.4.1 Bioinformatics design of peptides derived from natural proteins: Amelogenin case study..146
3.4.1.1 Binding characterization of ADPs 148
3.4.1.2 Biomineralization characteristics of ADPs 149
3.4.2 Designing of TiBP-ADP(s) bi-functional conjugates for hydroxyapatite mineralization on titanium..151
3.4.3 Adsorption behavior of TiBP-ADP(s) bi-functional peptides on titanium……..153
3.4.4 Kinetics of bi-functional peptides facilitated biomineralization.....154
3.4.5 Mineralization characteristics of bi-functional peptides on titanium 155
4. CONCLUSION 157
REFERENCES 161
APPENDICES 199
APPENDIX A.1.....**200**
CURRICULUM VITAE.....207

ABBREVIATION

aa : Amino acid
A (Ala) : Alanine
R (Arg) : Arginine
N (Asn) : Asparagine
D (Asp) : Aspartic acid
C (Cys) : Cysteine
E (Glu) : Glutamic acid
Q (Gln) : Glutamine
G (Gly) : Glycine
H (His) : Histidine
I (Ile) : Isoleucine
L (Leu) : Leucine
K (Lys) : Lysine
M (Met) : Methionine
F (Phe) : Phenylalanine
P (Pro) : Proline
S (Ser) : Serine
T (Thr) : Threonine
W (Trp) : Tryptophan
Y (Tyr) : Tyrosine
V (Val) : Valine
ALP : Alkaline Phosphatase
ADP : Amelogenin Derived Peptide
AMP : Antimicrobial Peptide
AFM : Atomic Force Microscopy
Bi-GEPI : Bifunctional GEPI
BMP : Bone Morphogenetic Protein
CaP : Calcium Phosphate
CD : Circular Dichroism
Cp : Commerrially pure
CVD : Chemical Vapor Deposition
DEAE : Diethylaminoethyl
DF : Darf-field
DCP : Dicumyl Peroxide
DMF : Dimethylformamide
DMSO : Dimethyl sulfoxide
DPN : Dip-pen nanolithographye
EBL : Electron Beam Lithography
EDX : Energy-Dispersive X-ray
ELISA : Enzyme-Linked Immunosorbent Assay
ECM : Extracellular Matrix
EVAc : Ethylene Vinyl Acetate

FGF : Fibroblast Growth Factor
FITC : Fluorescein isothiocyanate
FM : Fluorescence Microscopy
GEPI : Genetically Engineered Inorganic Binding Peptides
HA : Hydroxyapatite
HABP : Hydroxyapapite Binding Peptide
IPTG : Isopropyl β-D-1-thiogalactopyranoside
IGF : Insulin-like Growth Factor
NMR : Nuclear Magnetic Resonance
PBS : Phosphate Buffer Saline
PDGF : Platelet Derived Growth Factor
PDMS : Polydimethylsiloxane
PEEK : Polyetheretherketone
PEG : Polyethyleneglycol
PEO : Polyethyleneoxide
PGA : Polyglycolic acid
PHB : Polyhydroxybutyrate
Pi : Inorganic Phosphate
PLA : Poly(lactic acid)
PLGA : Polylactic-co-glycolic acid
PLL : Poly(L-lysine)
PMMA : Poly(methyl methacrylate)
PDLLA : Poly(D,L-lactide)
PPi : Extracellular Pyrophosphate
PVD : Physical Vapor Deposition
QAC : Quaternary ammonia compounds
RGD : Arginine-Glycine-Aspartic acid
SMH : Shai-Matsuzaki- Huang
SPR : Surface Plasmon Resonance
SS : Stainless Steel
QCM : Quartz Crystal Microbalance
SAM : Self Assembled Monolayers
SEM : Scanning Electron Microscopy
TCP : Tricalcium Phosphate
TGF-β : Transforming Growth Factor Beta
TiBP : Titanium Binding Peptide
TOF-SIMS : Time of Flight Secondary Ion Mass Spectroscopy
TEM : Transmission Electron Microscopy
UHMWPE : Ultra high Molecular weight polyethylene
XPS : X-ray photoelectron spectroscopy

LIST OF TABLES

Page

Table 1.1: Examples of polymers used as biomaterials. 9
Table 1.2: Classification of biomaterials based on its interaction with its surrounding.....20
Table 2.1: Sequence, MW, pI and Net Charge of Synthesized Peptides 86
Table 3.1: Amino acid sequence and physicochemical properties of TiBP1, TiBP2 105
Table 3.2: Secondary structure classifications of TiBP1, TiBP2 and TiBP60.....106
Table 3.3: Observed K_d and ΔG values of TiBP1, TiBP2 and TiBP60 111
Table 3.4: QCM analysis of TiBP1and TiBP2 on SiO_x and Hydroxapatite.....115
Table 3.5: Sequence, MW, pI and net charge of TiBP-AMP bi-functional peptides 130
Table 3.6: Binding Affinity Analysis of AMP and TiBP-AMP bi-functional peptides 131
Table 3.7: Secondary Structure Classifications of AMP, TiBP1-AMP, TiBP2-AMP. 132
Table 3.8: K_D (μM) values of TiBP2-ADP5 and TiBP2-ADP7 on titanium 153

LIST OF FIGURES

Page

Figure 1.1 : a) Mammalian tooth is a hierarchical multimaterial system composed of enamel (E), dentin (D), pulp (P), cementum (C) and periodontal ligaments (PDL). b) The nanostructured hierarchal self-assembly of bone. c) Plywood-like structure present in lamellar bone (left), Radial fibril arrays (right).....2
Figure 1.2 : Nanotechnology and implant applications.....3
Figure 1.3 : a) A dental implant b) A replacement heart valve.....6
Figure 1.4 : Orthopedic Implant devices used for load bearing applications: (a) hip implant (b) knee implant (c) shoulder implant and (d) elbow.....7
Figure 1.5 : Illustrating the use of UHMWPE as a bearing metal for (a) hip joint and (b) knee joint prosthesis.....10
Figure 1.6 : Surface composition, roughness, topography, and energy are interelated surface characteristics that dictate the biological response to an implanted device.....12
Figure 1.7 : Schematic illustration of (a) a hydrophobic or non wetting surface (b) a hydrophilic or wetting surface.....16
Figure 1.8 : An example of biomaterial- tissue interactions, e.g., Implant- bone interactions 23
Figure 1.9 : Schematic representation of events consecutively taking place at the titanium surface after implantation into living bone tissue. Water binds to the surface, followed by incorporation of hydrated ions, adsorption and desorption of proteins, eventually leading to cell attachment. After differentiation, mature osteoblasts produce the extracellular matrix (ECM).....25
Figure 1.10 : Schematic drawing to depict the protein: biomaterial interactions which often lead to conformational changes of adsorbed proteins and the subsequent exposure of hidden proinflammatory epitopes.....26
Figure 1.11 : Initial protein interactions leading to cell recognition of implants.....28
Figure1.12 : a) Biofilm formation, b) Representation of bacterial adhesion to a biomaterial substrate. Phase I adhesion involves reversible cellular association with the surface. During Phase II, bacteria undergo irreversible molecular bridging with the substrate through cell surface adhesin compounds. After approximately 1d, certain bacterial species are capable of secreting a protective exopolysaccharide matrix (biofilm) that protects the adhered bacteria from host defences and systemically-administered antibiotics 35
Figure 1.13 : Frequency of main pathogenic species among orthopedic clinical isolates of implant-associated infections.....37

Figure 1.14 : Diagram of the association among subgingival species 38
Figure 1.15 : SEM micrographs of the dental implants surfaces. (A) machined, (B) acid etched, (C) sandblasted and (D) anodized 40
Figure 1.16 : Scanning electron microscopy (SEM) images illustrating various microtextures achieved on Ti after etching in 48% H_2SO_4 at 60 ^{0}C for 0.25, 0.5, 1, 3, and 8 h. The upper row displays micrographs with higher magnification 41
Figure 1.17 : SEM image of nanotubular structures created by anodization of Ti. 42
Figure 1.18 : SEM image of the characteristic nanometric sponge-like strudture that is achieved by treatment of Ti with H_2SO_4/H_2O_2 43
Figure 1.19 : SEM images of rod-like structures resulting from the treatment of Nb with NaOH at a) 60^{0}C (diameter of the rods in the 100–300-nm range) and b) 80^{0}C (diameter of the rods in the 50–100-nm range) 43
Figure 1.20 : SEM images of an electrochemically deposited coating of calcium phosphate on smooth Ti. a) Microporous structure. b) Crystal grains on the nanometer scale. 44
Figure 1.21 : Three hypotheses for mechanisms of antibiotic resistance in biofilms. 53
Figure 1.22 : Clustering of cationic and hydrophobic amino acids into distinct domains in several antimicrobial peptides of different structural classes. This `amphipathic' design is evident in many, but not all, antimicrobial peptides. Red, basic (positively charged) amino acids; green, hydrophobic (`oily') amino acids. Other amino acids are not shown. Magainin is depicted in its a-helical configuration. 57
Figure 1.23 : The membrane target of antimicrobial peptides of multicellular organisms and the basis of specificity. 58
Figure 1.24 : The Shai-Matsuzaki-Huang model of the mechanism of action of an antimicrobial peptide. An alpha-helical peptide is depicted. a, Carpeting of the outer leaflet with peptides. b, Integration of the peptide into the membrane and thinning of the outer leaflet. The surface area of the outer leaflet expands relative to the inner leaflet, resulting in strain within the bilayer (jagged arrows). c, Phase transition and `wormhole' formation. Transient pores form at this stage. d, Transport of lipids and peptides into the inner leaflet. e, Diffusion of peptides onto intracellular targets (in some cases). f, Collapse of the membrane into fragments and physical disruption of the target cell's membrane. Lipids with yellow headgroups are acidic, or negatively charged. Lipids with black headgroups have no net charge 59
Figure 1.25 : Standard approaches for creating SAMs on noble metal and oxide surfaces using alkanethiol and silane chemistry..... 65
Figure 1.26 : Schematic diagram for phage and cell-surface display technique 68
Figure 1.27 : Design of second generation GEPI using bioinformatic approach. Experimentally selected and categorized peptide sequences (upper) are used to calculate similarity scoring matrices (lower) 72
Figure 1.28 : (A) Rate of Ca^{2+} consumption in the presence of peptides; inset: the consumption rate during the first 6 h. (B) Ca/P ratio of the mineral phase at different time points. The final morphology of the minerals after 96 hours of mineralization in the presence of (C) no

peptide, (D) weak binding control peptide and (e) strong binding peptide, HABP1 75
Figure 1.29 **:** (A) Directed assembly—GEPI is conjugated with the active molecule before immobilization on the substrate. (B) Targeted assembly—GEPI is immobilized on the substrate alone, then conjugated with the active molecule by secondary means, such as Schiff base chemistry. 76
Figure 1.30 **:** (A) Light optical microscopy images of NIH3T3 fibroblast cells ($3x10^5$ cells, 1.5 hrs, 200X) on gold substrate modified with GEPI-PEG conjugate; (B) Scanning electron microscopy (SEM) images of NIH3T3 (5 3 103 cells, 24 hrs) on glass substrate modified with GEPI-RGD conjugate; (C) SEM images of NIH3T3 ($8x10^4$ cells, 24 hrs) on titanium surface modified with GEPI-RGD conjugate 77
Figure 1.31 **:** ALP activity was assessed by staining with BCIP/NBT. 77
Figure 2.1 **:**Schematic of library construction and displayed peptide on the surface of E. *coli*. 80
Figure 2.2 **:** Schematic representation of selection of titanium binding peptides by cell surface display 81
Figure 2.3 **:**The optical microscope dedicated for fliorescence and dark field imaging. 82
Figure 2.4 **:** Initial binding characterization of titanium binding peptides via fluorescence microscopy 83
Figure 2.5 **:** Image of CS-Bio peptide synthesizer 85
Figure 2.6 **:** Image of Waters HPLC 85
Figure 2.7 **:** (A) The quartz crystal used in the QCM-D. (B) Applying of the direct current to the crystal (C) Applying alternative current to the quartz crystal (D) The change in the frequency upon adsorption of a layer onto the quartz crystal. (E) The change in the dissipation upon adsorption of a viscoelastic layer on to the quartz crystal (reproduced form the user guide of QCM-D apparatus, Q-Sense AB, Sweden) 88
Figure 2.8 **:** The picture of the Quartz Crystal System. The temperature of the QCMD system is controlled with a Peltier embedded systems coupled with a temperature controller system. 89
Figure 2.9 **:** JEOL JSM-7000F Scanning Electron Microscope with EDX detector. 91
Figure 2.10 **:** The image of the Atomic Force Microscope in the chamber for acoustic and mechanical isolation 92
Figure 2.11 **:** Philips EM420 Transmission Electron Microscope 93
Figure 3.1 **:** Florescence microscopy images of titanium binding peptides with various binding affinities. 102
Figure 3.2 **:** Categorization of titanium binding clones via fluorescence microscopy. 102
Figure 3.3 **:** Relative abundance of amino acids in strong and weak binding groups of titanium binding peptides 103
Figure 3.4 **:** CD spectra of 30 μM TiBPs (TiBP1, TiBP2, TiBP60) in the presence of varying volume percentages of TFE in 100 μM Tris–HCl, pH 7.4. Arrow indicates increasing sample TFE concentration (0, 10, 20, 30, 40, 50, 75 %). 107

Figure 3.5 **:** a) Overlapped ribbon and CPK models of the predicted structures of the (a) TiBP1, (b) TiBP2 and (c) TiBP60. The residues are colored according to residue type (Basic: blue, Acidic: red, Polar: green, Nonpolar: gray). The backbone is colored according to secondary structure (Turn: cyan, Random Coil: Gray, Isolated Bridge: Tan). *Water is omitted for clarity.* 109
Figure 3.6 **:** Surface coverage of TiBP1, TiBP2 and TiBP60 on titanium via QCM. 111
Figure 3.7 **:** Surface Coverage and K_D (μM) of TiBPs on various implantable surfaces (SiO_x and Hydroxapatite). a) TiBP1 (b) TiBP2. 113
Figure 3.8 **:** AFM scans in 3D view with the 30 μm by 30 μm cut-out (a) cp Grade 4 (b) cp Grade 1 116
Figure 3.9 **:** SEM scans titanium implant surfaces (a) cp Grade 4 (b) cp Grade 1. The inset represents EDS spectra of each surfaces. 117
Figure 3.10 **:** Schematic representation of peptide functionalized dental implant surface 118
Figure 3.11 **:** TiBP1 and TiBP2 functionalized cp Grade 4 titanium implant surface 119
Figure 3.12 **:** TiBP1 and TiBP2 functionalized cp Grade 1 titanium implant surface 119
Figure 3.13 **:** FM micrographs of phalloidin stained MC3T3-E1 cells on cp Grade 4 and Grade 1 titanium implant surfaces. 121
Figure 3.14 **:** The number of adhered MC3T3-E1 cells per cm^2 in serum free conditions on two titanium implant surfaces 122
Figure 3.15 **:** Average cell spreading per μm^2 on TiBP1 and TiBP2 functionalized cp Grade1 and cp Grade4 titanium dental implant surfaces 123
Figure 3.16 **:** FM micrographs of phalloidin stained MC3T3-E1 cells on RGDS, TiBP1-RGDS and TiBP2-RGDS functionalized cp Grade 4 titanium dental implant surfaces 124
Figure 3.17 **:** The number of adhered MC3T3-E1 cells per mm^2 in serum free conditions on peptide functionalized cp Grade 4 titanium dental implant surfaces 125
Figure 3.18 **:** Average cell spreading per μm^2on peptide functionalized cp Grade 4 titanium dental implant surfaces 125
Figure 3.19 **:** FM micrographs of phalloidin stained NIH3T3 cells on titanium coated glass surfaces 126
Figure 3.20 **:** The number of adhered NIH3T3 cells per mm^2 in serum free conditions on peptide functionalized titanium coated glass surfaces . 127
Figure 3.21 **:** Average cell spreading per μm^2 on peptide functionalized titanium coated glass substrate. 127
Figure 3.22 **:** CD Spectra of 50 μM AMP, TiBP-AMP bi-functional peptides in the presence PBS. 132
Figure 3.23 **:** Models of the predicted structures of the a) AMP, b) TiBP1-GGG-AMP, c) TiBP2-GGG-AMP 133
Figure 3.24 **:** In solution antimicrobial activity of bi-functional peptides (TiBP1-AMP, TiBP2-AMP) in the presence of gradually increased peptide concentrations a)10 μM, b) 25 μM c) 50 μM, d) 100 μM including positive (only *S. mutans*), negative control (only AMP) ... 135

Figure 3.25 : In solution antimicrobial activity of bi-functional peptides (TiBP1-AMP, TiBP2-AMP) in the presence of gradually increased peptide concentrations a)10 μM, b) 25 μM including positive (only *S. epidermidis*), negative control (only AMP) 136
Figure 3.26 : In solution antimicrobial activity of bi-functional peptides (TiBP1-AMP, TiBP2-AMP) in the presence of gradually increased peptide concentrations a)10 μM, b) 25 μM including positive (only *E. coli*), negative control (only AMP) 137
Figure 3.27 : Minimum growth inhibition concentration of AMP, TiBP1-GGG-AMP, TiBP2-GGG-AMP in the presence of various bacteria type a) *Streptococcus mutans*, b) *Staphylococcus epidermidis*, c) *Escherichia coli*. 138
Figure 3.28 : In solution antimicrobial activity of TiBP1 and TiBP2 at minimum inhibitory concentration of their bi-functional conjugates against a) *Streptococcus mutans,* b) *Staphylococcus epidermidis,* c) *Escherichia coli*. 139
Figure 3.29 : Bacterial adhesion on AMP, TiBP1-GGG-AMP, TiBP2-GGG-AMP peptide modified titanium surfaces against *Streptococcus mutans* (left column), *Staphylococcus epidermidis* (middle column), *Escherichia coli* (right column) 141
Figure 3.30 : Surface coverage analysis on AMP, TiBP1-GGG-AMP, TiBP2-GGG-AMP peptide modified titanium surfaces against a) *Streptococcus mutans,* b) *Staphylococcus epidermidis,* c) *Escherichia coli* 142
Figure 3.31 : a) Schematic representation for PDMS patterning of TiBP1-GGG-AMP on titanium. b) Adhesion of *S.mutans* (10^8 cell/ml) from log-phase on peptide modified surfaces after 2 hours incubation. c) FM images of Syto9 labeled *S.mutans* on patterned peptide array. 143
Figure 3.32 : Mouse amelogenin sequence (P63277|AMELX_MOUSE) and predicted high (red) and low (teal) similarity sequence domains.....148
Figure 3.33 : SEM micrographs of the minerals formed by the ADPs. The morphologies ADP5 and ADP7 yielded (Oren & Gungormus et.al unpublished data).....150
Figure 3.34 : TEM micrographs of the minerals formed by ADP7 and the full length recombinant amelogenin, and a literature [448] comparison to a mineral formed by the same full length amelogenin. The control mineral was formed in the presence of no peptide 150
Figure 3.35 : Binding affinity of TiBP2, ADP5 and ADP7on titanium and HA respectively.....152
Figure 3.36 : Surface Coverage of TiBP2-ADP5 and TiBP2-ADP7 on Titanium Surface.....153
Figure 3.37 : In situ monitoring of bi-functional peptide mediated $Ca_5(PO_4)_3OH$ mineralization via QCM.....154
Figure 3.38 : SEM micrographs of minerals formed by bi-functional peptides (TiBP2-ADP5, TiBP2-ADP7) including positive and negative controls.....156
Figure 3.39 : TEM images of the minerals formed in the presence of TiBP2-ADP5. The inset is the corresponding selected area diffraction patterns of the minerals. 156

Figure A.1 : The MALDI/TOF spectrum of synthesized TiBP1 200
Figure A.2 : The MALDI/TOF spectrum of synthesized TiBP2 200
Figure A.3 : The MALDI/TOF spectrum of synthesized TiBP60 201
Figure A.4 : The MALDI/TOF spectrum of synthesized TiBP1-GGG-RGDS 202
Figure A.5 : The MALDI/TOF spectrum of synthesized TiBP2-GGG-RGDS 202
Figure A.6 : The MALDI/TOF spectrum of synthesized RGDS 202
Figure A.7 : The MALDI/TOF spectrum of synthesized TiBP1-GGG-AMP 203
Figure A.8 : The MALDI/TOF spectrum of synthesized TiBP2-GGG-AMP 203
Figure A.9 : The MALDI/TOF spectrum of synthesized AMP 204
Figure A.10: The MALDI/TOF spectrum of synthesized TiBP1-GGG-ADP5 204
Figure A.11: The MALDI/TOF spectrum of synthesized TiBP1-GGG-ADP7 205
Figure A.12: The MALDI/TOF spectrum of synthesized ADP5 205
Figure A.13: The MALDI/TOF spectrum of synthesized ADP7 206

PEPTIDE-BASED DESIGNED BIOMATERIALS FOR MEDICAL APPLICATIONS THROUGH BIOMIMETIC APPROACH

SUMMARY

Biomaterials used in implants have traditionally been selected based on their mechanical properties, chemical stability and biocompatibility. Titanium and titanium alloys are current widely used biomaterials for dental and orthopedic implants due to their superior properties. Although, they are the most preferential materials in implantation, improper implant–tissue integration into surrounding bone often occurs due to unwanted biological response includes bacterial colonization subsequently bacterial infection and fibrous capsule formation. Biological response at the implant-tissue interface is a surface phenomenon. Surface properties such as topography, morphology and chemistry play a major role in determining both the biological response to implants and the material response to the physiological condition. Hence, surface engineering focuses on modifying the surface properties of titanium to control the interaction between the implants and its biological surroundings by altering cell attachment, growth and tissue formation. Due to the ultimate role of surface properties on the rate and quality of implant–tissue integration or osseointegration, a variety of surface modification approaches including physical, chemical and biological ones have been utilized. Among them, to create biologically active surfaces that are mimicking natural environment and organization of bone tissues is emerged as a current approach to induce controlled, guided and rapid cellular response.

In course of implantation; a competition occurs between integration of the material into the surrounding tissue and adhesion of bacteria onto the implant surface. These two concurrent events followed by mineralization are critical steps for the successful osseointegration. Thus, biological surface modifications have a potential to bring solutions for better implant materials firstly in designing nonfouling and antimicrobial surfaces, secondly in creating bioactive surfaces that enhance short and long term cellular response subsequently mineralization at implant-tissue interface. To design surfaces with targeted goal, various biomolecules have been immobilized on to implant surfaces via different immobilization techniques. Depending on current design parameters under biological surface modifications for nonfouling and antimicrobial surfaces, PEO, PEG and antimicrobial peptides are the most favorable biomolecules to prevent bacterial adhesion that is primary cause of implant failures. In case of bioactive surfaces, engineered peptide motive arginine-glycine-aspartic acid (RGD) derived from cell adhesive proteins present in the extracellular matrix (ECM) of bone, (such as fibronectin, bone sialoprotein, and osteopontin), have been immobilized on implant materials. Besides, Ca-P coatings and its combination with organic molecules such as albumin, collagen, BMPs, biphosphate and amlogenins due to their similar composition with bone and its extracellular environment, are another type of biological surface modifications to trigger mineral formation for optimal osseointegration.

The success of biological surface modifications relies on the choice of immobilization methods (i.e. physical or chemical) which control functionality, stability of biomolecules. Physical immobilization with simple adsorption principle is lack of controlling amount and density of adsorbed molecules. Covalent attachment as a chemical immobilization method utilizing self assembled monolayers (SAMs) is often applicable only to a limited range of materials and requires the presence of specific functional groups which are themselves non-specific to surfaces and synthetic pathways which requires extensive chemistry. Both of the techniques are poor to control orientation, structural conformation that effect function of molecule to fully retain biological activity. Controlling the bio-material interfaces is the common major challenge in all of these surface treatments.

There is a need for a new generation of molecular linkers that can induce controlled and predictable interactions at bio-material interface with high material binding affinity, specificity. These properties can only be achieved with material recognition capability for desired surface that allow us precise control density, functionality, accessibility of biomolecules. Molecular recognition is the basis of biological interactions, therefore molecular biomimetics approch offers unique premises to generate biological molecules, which are truly self assembled, can be genetically programmable, and have molecular recognition properties. Genetically engineered peptides for inorganics (GEPI) can be designed as novel alternative biomolecular linkers to immobilize biological molecules onto implant surfaces. Their high binding affinity and specificity towards inorganic surface, high conjugation capability with biomolecules to produce mutlifunctional molecular probes, easy production are unique features to be implemented in restorative medicine.

In this dissertation, we first generated a set of sequence that have affinity to titanium dental implant surface (cp Grade 4) via cell surface display and then each of the selected titanium binding peptides (TiBPs) was characterized semi-quantitatively *via* fluorescence microscopy (FM) for binding to their respective titanium surface. Peptides with strong binding affinity (TiBP1 and TiBP2) and weak binding affinity (TiBP60) were further subjected to quantitative binding characterization *via* quartz crystal microbalance (QCM) as well as analysis of the molecular conformation properties by protein structure interrogation techniques. The high binding subset of TiBPs (TiBP1 and TiBP2) were then examined for their material selectivity and cytotoxicity properties. Next, their potential applicability for biological surface modifications as peptide based molecular linker was shown with three examples that are critical for osseointegration.

In the first approach, bi-functional peptides were designed in conjugation with two different titanium binding peptides (TiBP1 and TiBP2) and integrin binding domain Arg-Gly-Asp-Ser (RGDS) for bioactive surface modifications. Effects of two bi-funtional peptides on cell viability, adhesion and spreading were examined on different implant surfaces with distinct surface roughness and topography such as cp Grade 4, cp Grade 1 titanium dental implant and titanium coated glass surfaces in the presence of osteoblast and fibroblast. Cell adhesion and spreading assays demonstrated that bi-functional peptide within single peptide domain preserved its dual functionality effectively while peptide facilitating the titanium surface functionalization, also kept its functionality as a recognition site for cells. The increase in cell number and spreading on three different surfaces also supports us utilization of the TiBPs as a molecular linker for bioactive surface modfications.

In the second approach, to bring a new surface modification metdology in the area of implant infections, TiBP and antimicrobial peptide (AMP) were conjugated as a bi-functional peptide to impart the bacterial resitance or antimicrobial properties to titanium surface. Two bi-functional (TiBP1-AMP and TiBP2-AMP) peptides were designed based on their charge, binding affinity and structurual properties and then evaluated detail in terms of their binding and antimicrobial activity. To evaluate efficiency of the method as a biological surface modification, in solution and on the surface antimicrobial activity were examined against *Streptococcus mutans, Staphylococcus epidermidis,* and *Escherichia coli*. Modified surfaces with two different bi-functional peptides were found to significantly reduce bacterial adhesion on titanium against all three bacteria. The results indicate us surface modification with conjugated molecules consisting of antimicrobial and titanium binding peptides is a promising approach to prevent bacterial infection on implant surfaces.

In the third approach, utilization of GEPI`s for mineral deposition on the implant surface which is one of the major challenge in osteointegration were shown. To achive to induce and control mineral formation, molecular linker and material synthesizer capability of GEPIs` were combined in a bi-functional peptide. TiBP2 with two different *de novo* designed peptides (ADP5 and ADP7), which are very well characterized in terms of their binding affinity to hyrodxapatite (HA) with controllable mineralization capability, were conjugated to create a bi-functional peptide. After performing complete characterization of the bi-functional peptides for inorganic binding, real time monitoring of the $CaPO_4$ biomineralization were successfully achieved on the surface of titanium via QCM. The mineral morphology and crystal structure were examined with Transmission Electron Microscopy (TEM) and Scanning Electron Microscopy (SEM). This part of work indicates that GEPI may provide the ways for genetic control on biomineralization from tissue restoration to regeneration. *In vitro* studies reveal that the bi-functional peptides form hyrodxapatite (HA) on the implant surface while promoting the cell adhesion on titanium surface.

In scope of this thesis, the remarkable potential of GEPIs were shown in controlling not only cell-surface interactions through controlled immobilization of peptide based multifunctional molecular linkers on the implant surfaces but also controlled mineral formation was demonstrated addressably at implant-tissue interphase.

Titanium binding peptides can be a candidate to serve as biomolecular linker to functionalize implant surfaces by providing modular domains that ease their conjugation to biologically active signaling molecules while retaining their remarkable binding and selectivity to the solid substrate with the absence of cytotoxicity properties. Since material surface binding peptides can be conjugated with a variety of bioactive molecules that can enhance cell attachment, cell proliferation, cellular spreading and other fundamental properties of cell behavior, the TiBPs studied here offer a unique utility for tissue engineering studies. The proposed peptide based surface coating is universal and can be applied to induce various desired biological activity on any implant material from dental to orthopedic surgery using an easily adaptable single-step biologically relevant condition.

BİYOMİMETİK YAKLAŞIMI İLE PEPTİD BAZLI BİYOMALZEMELERİN MEDİKAL UYGULAMALAR İÇİN GELİŞTİRİLMESİ

ÖZET

İmplantlarda kullanılan biyomalzemeler geleneksel olarak mekanik özellikleri, kimyasal kararlılıkları ve biyouyumluluklarına göre seçilirler. Titanyum ve titanyum alaşımları ortopedik ve diş implantları için seçkin özellikleri dolayısıyla günümüzde oldukça kullanılmaktadır. Titanyum ve alaşımları, implantasyon da çok tercih edilen malzemeler olmalarına rağmen; bakteriyel kolonizasyon ve sonrasındaki bakteriyel enfeksiyonu, fibroz kapsül oluşumunu içeren, istenmeyen biyolojik cevap dolayısıyla implantın çevredeki kemik dokusuyla uyumsuzluğuna çok sık rastlanmaktadır. Implant-doku ara kesitindeki biyolojik cevap yüzey olgusudur. Yüzey topografisi, kimyası ve morfolojisi gibi özellikler, implanta karşı biyolojik cevabın ve fizyolojik ortama malzemenin cevabının belirlenmesinde önemli rol oynamaktadırlar. Yüzey mühendisliği; implant ve biyolojik çevresinin arasındaki etkileşimi, titanyumun yüzey özelliklerini değistirerek ve böylelikle hücre bağlanması, büyümesi ve doku oluşumunu etkileyerek kontrol etmeyi hedeflemektedir. Yüzey özelliklerinin; implat–doku uyumunun oranı ve hızına olan temel etkisi dolayısıyla; fiziksel, kimyasal ve biyolojik olan çok farklı yüzey modifikasyonları kullanılmaktadır. Bunlar arasında, kemik doğal ortamına benzeyen biyolojik aktif yüzeyler günümüzde kontrollü, yönlendirilmiş ve hızlı hücre cevabına neden olan yaklaşımlar olarak ortaya çıkmaktadır.

İmplantasyon sırasında, malzemelerin çevresindeki doku ile uyumu ve bakterilerin yüzeye tutunması arasında yarışmacı bir durum oluşur. Eş zamanlı ve akabinde mineralizasyonun gercekleştiği bu iki olay; etkin osseointegrasyon için kritik olan aşamalardır. Böylelikle, biyolojik yüzey modifikasyonları ilk olarak; antimikrobiyel yüzeylerin, ikici olarak; hücrelerin kısa ve uzun süreli cevabını ve sonrasında implant-doku ara kesitindeki mineralizasyonu arttıran biyoaktif yüzeylerin oluşturulmasına daha iyi implant mazlemeler için çözümler getirme potensiyeline sahiptir. Hedef odaklı malzeme tasarlamak için, çok çesitli biyomoleküller implant yüzeyler üzerine farklı immobilizasyon yöntemleri ile tutturulmuşlardır. Günümüzde antimikrobiyel ve kirlenmemiş yüzeyler için biyolojik yüzey modifikasyonlarının tasarım kriterlerine bağlı olarak; implant başarısızlıklarının temel sebebi olan bakteriyel yapışmayı engelemek amacıyla PEO, PEG ve antimiktobiyel peptitler en çok tercih edilen moleküller arasındadırlar. Biyoaktif yüzeyler için, kemik hücre dışı matriksinde bulunan hücre etkileştirici proteinlerden (fibronektin, kemik sialoprotein ve osteopontin) türetilerek tasarlanmış arjinin-glisin-aspartik asit (RGD) peptit motifi implant malzemeler üzerine immobilize edimişlerdir. Bunun dışında, Ca-P kaplamaları ve bunların albumin, kologen, kemik morfogenetik proteinleri, bifosfat ve amelojenin gibi kemik yapısına ve hücre dışı ortamına benzerlikleri olan organik moleküllerle bileşimi optimal osseointegrasyon için mineral oluşumunu tetikleyen diğer bir biyolojik yüzey modifikasyon çeşididir.

Biyolojik yüzey modifikasyonlarının başarısı, biyomoleküllerin kararlılığını, fonskiyonelliğini kontol eden immobilizasyon yöntemlerine (örneğin fiziksel ve kimyasal yöntemler) bağlıdır. Basit adsorpsiyon prensibine bağlı olan fiziksel immobilizasyon, adsorplanan biyomoleküllerin miktarını ve yoğunluğunu kontrol etmekten yoksundur. Kovalent bağlanma, kendiliğinden oluşan tek tabakaları kullanan kimyasal bir immobilizayon yöntemi olarak özgün foknsiyonel gruplar ve sentetik yollar gerektirir, çoğunlukla sınırlı sayıda malzemelerle uygulanır. Her iki teknik de biyomolekülün fonksiyonunu etkileyen yönelim ve yapısal konformasyonun kontrolü zayıftır. Fiziksel ve kimyasal immobilizasyonun eksiklerinin gösterilmesi, hedef yüzey için yüksek bağlanma, özgünlük ve tanıma kapasitesi olan ve biyomolekülün fonksiyonelliği erişilebilirliği, yoğunluğunu kontrol edilebilmesine izin veren yeni moleküler bağlayıcıların geliştirilmesine ihtiyaç vardı. Tüm yüzey modifikasyonlarında doku-malzeme ara kesitinin kontrol edilmesi başta gelen sorunlardan biridir.

Doku-malzeme ara kesitinde, kontrol edilebilir etkileşimini tetikleyecek malzemeye yüksek bağlanma ilgisi ve özgünlüğü olan yeni bağlayıcı moleküllere ihtiyaç vardır. Bu özellikler sadece biyomoleküllerin yoğunluğunu, fonksiyonelliğini ve ulaşılabilirliliğini kontrol edebilmeye izin veren ve istenilen yüzeye özgü moleküler tanıma kapatitesi sayesinde elde edilebilir. Moleküler tanıma biyolojik etkileşimlerin temelinidir ve böylelikle moleküler biyomimetik yaklaşımı da kendiliğinden oluşan, genetik olarak programalanabilen ve moleküler tanıma özelliklerine sahip olan biyolomoküllerin oluşturulmasında özgün bir yol oluşturmaktadır. Genetik olarak tasarlanmış peptitler (GEPI), biyolojik moleküllerin implant yüzeylerine immobilizasyonu için moleküler bağlayıcı olarak alternatif bir method olabilirler. GEPI`lerin inorganik yüzeylere yüksek bağlanma ilgisi, özgünlüğü, biyomoleküllerle yüksek konjugasyon kapasitesi, kimyasal yapısını kesin olarak kontrolüne izin veren kolay üretimi diğer immobilizasyon metodları üzerine dikkat çekici özellikleridir. Moleküllerin bu özellikleri implantasyon alanında uygulanmasına sebep olmaktadır.

Bu tez çalışmasında, ilk olarak titanyum diş implant yüzeyine (cp Grade4) ilgisi olan peptitleri hücre yüzey gösterim teknolojisi ile elde ettik ve sonrasında her bir seçilmiş titanyuma özgül olarak bağlanan peptitler yarı kantitatif olarak floresan mikroskopu (FM) methodu ile titanyum yüzeyine bağlanma ilgilerine göre karakterize edildiler. Yüksek bağlanma ilgisi olan (TiBP1 ve TiBP2) ve zayıf bağlanma (TiBP60) ilgilisi olan peptidlerin bağlanma ilgileri, kuvars kristal mikroterazi (QCM) methodu ile kantitatif olarak ve aynı zamanda moleküler konformasyonu da protein yapısı analiz methodlari ile karakterize edildi. Yüksek bağlanma ilgisi olan gruptaki TiBP1 ve TiBP2`nin malzemeye seçici bağlanma ilgileri ve sitotoksite özellikleri açısından incelendi. Sonrasında, peptidlerin biyolojik yüzey modifikasyonları için moleküler bağlayıcı olarak potensiyel uygulanabilirliği osseointegrasyon için kritik olan üç farklı örnekle gösterilmiştir.

İlk yaklaşımda, titanyum`a bağlanan iki farkli peptitle (TiBP1 ve TiBP2) ve integrin bağlanma bölgesi RGDS`nin birleştirilmesiyle biyoaktif yüzey modifikasyonları için çift fonkisyonlu peptit tasarlammıştır. İki çift fonskiyonlu peptidin hücre canlılığı, bağlanması ve yayılması üzerine etkisi yüzey pürüzlülüğü ve topografisi farklı olan iki cp Grade 1 ve cp Grade 4 diş implant yüzeyleriyle, titanyum kaplanmış cam yüzey üzerinde osteoblast ve fibroblast hücreleri ortamında incelendi. Hücre

bağlanma ve yayılma deneyleri çift fonsiyonlu peptidin tek bir parça içersinde titanyum yüzeyini fonksiyonelleştirme ve hücre tanıma özellikleri gibi iki farklı fonksiyonu barındırdığını göstermiştir. Üç farklı yüzey üzerinde hücre sayısında ve yayılmasındaki artış TiBP`lerin moleküler bağlayıcı olarak biyoaktif yüzey modifikasyonlarında kullanılabileceğini desteklemektedir.

İkinci yaklaşımda, implant enfeksiyoları alanına yeni yüzey modifikasyon methodları getirmek için TiBP ve antimikrobiyal peptidler (AMP) titanyum yüzeyine antimikrobiyal özellik kazandırmak ve bakteriye karşı dirençli hale getirmek amacıyla birleştirilip çift fonksiyonlu peptit oluşturuldu. Çift fonksiyonlu (TiBP1-AMP ve TiBP2-AMP) peptitler her bir peptidin yük, bağlanma ilgileri ve yapısal özelliklerine bağlı olarak tasarlandı ve sonrasında yüzeye bağlanma ilgileri ve antimikrobiyal özellikleri açısından değerlendirildi. Metodun biyolojik yüzey modifikasyonu olarak etkinliğini değerlendirmek için peptidin hem solusyon içindeki hem de yüzeydeki aktivitesi *Streptococcus mutans, Staphylococcus epidermidis,* and *Escherichia coli*`e karşı incelendi. İki farklı çift fonksiyonlu peptitle modifiye olmuş yüzeylerde üç bakteriye karsı, hücre tutunmasında önemli bir azalma görülmüştür. Sonuçlar antimikrobiyal ve titanyuma bağlanma özelliği olan birleşmiş peptitlerin implant yüzeylerde bakteriyel enfeksiyonu önlemek için yüzey modifikasyonlarında kullanılabileceğini gösterir.

Üçüncü yaklaşımda, osseointegrasyonda önemli bir sorun olan implant yüzeylerinde mineral depolanmasında GEPI`lerden nasıl yararlanılacağı gösterilmiştir. Mineral oluşumunu implant yüzeyinde tetiklemek için, GEPI`lerin moleküler bağlanma ve malzeme sentezleme kapasitesi tek bir çift fonksiyonlu peptidi tasarlanmıştır. TiBP2, *de novo* methodu ile tasarlanmış kontrol edilebilir mineralizasyon yapabilme kapasitesi ve hidroksiapatit yüzeyine yüksek bağlanma ilgisi açısından iyice karakterize edilmiş iki farklı peptit ile (ADP5 ve ADP7) ile birleştirilerek çift fonksiyonlu peptit oluşturulmuştur. Çift fonksiyonlu peptidin anorganiklere baglanma karakterizasyonunun tamamlanmasının ardından, gerçek zamanlı olarak $CaPO_4$ mineralizasyonu QCM kullanılarak gözlenmiştir. Mineral morfolojisi ve kristal yapısı TEM ve SEM kullanılarak incelenmiştir. Bu kısımdaki çalışmayla, GEPI`lerin doku onarımından ve yenilenmesine kadar olan alanlardaki mineral oluşum sürecinin genetik olarak kontrol edilebilir olduğu gösterilmektedir. *In vitro* çalışmalarda implant yüzeyinde çift fonksiyonlu peptidlerin hücre adhezyonu tetiklerken aynı zamnada HA mineralizasyonu da yapabileceğini göstermektedir.

Bu tezin kapsamında, GEPI`lerin moleküler bağlayıcı olarak dikkat çekici potensiyeli implant-doku ara kesitinde, hücre-yüzey arasındaki ilişkinin yanısıra mineralizasyonunu da fonkiyonel moleküllerin immobilzasyonuyla kontrol edebildiği gösterilmiştir.

Titanyuma bağlanan peptitler biyolojik olarak aktif sinyal molekülleri ile kolay birleşebilen ve birleşirken de hücre toksitesileri olmayan, katı yüzeylere olan belirgin bağlanma ve seçiciliklerini koruma özelliklerinden dolayı biyomoleküler bağlayıcı olarak implant yüzeylerin fonksiyonelleştirilmesinde kullanılmaya adaydırlar. Malzemeye bağlanan peptidler, hücre bağlanması, yayılması, proliferasyonunu ve hücre davranışının diğer temel özelliklerini arttıran çok çeşitli biyoaktif moleküllerle birleşebilirler. Burada çalısılan TiBP`lerin doku mühendisliği çalışmaları için özgün bir yararlılığı olacaktır. Önerilen peptid bazlı kaplamalar, diş implantlarından ortopedik implantlarin yüzeyine kazandırılması istenilen biyolojik aktivite için yaygın şekilde ve kolaylıkla tek basamakta biyolojik olarak uygun koşullarda uygulanabilecek bir tekniktir.

1 INTRODUCTION

1.1. Bionanotechnology and Biomaterials

Nanotechnology, a new focus in the area of biomedical research, involves visualization, manipulation, and fabrication of materials on the smallest scales, in dimensions of 1 μm down to 10°A [1-3]. The range below 100 nanometers is important because at this small size, the classic laws of physics change. The result is novel properties that enable researchers to produce new materials with the exact characteristics they desire: smaller, stronger, and tougher than current materials.

Nature enables to produce materials with unique features applying proper nanotechnology since at the beginning of the life. The biological systems in cells and in nature contain examples of many nanoscale systems. Firstly, proteins, nucleic acids, lipids and carbohydrates are the building block of life and they are the examples of materials that possess unique properties determined by size, folding and patterns at the nanoscale [4-6]. Specifically, bone and tooth are composed of numerous nanostructures, such as collagen and hydroxyapatite, which provide a unique nanostructure for protein and bone cell interactions in the body [7-12] (Figure1.1).

Most of the current macro- or micro fabrication techniques are unable to create these sophisticated structures. Recent paradigm shifts from these fabrication techniques to nano-enabled techniques have significantly enhanced our ability to design new materials for various fields [13]. However, this unique feature and ability of nanotechnology requires an integrated understanding of and collaboration between multiple scientific fields, including biology, physics, chemistry, materials science, computer science, mechanical engineering, and electrical engineering [14, 15].

Biomimetics can be considered as a promising way for realizing nano and bionanotechnology by taking inspiration from mother nature`s biological

structures to design practical materials and systems for engineering [16]. Traditionally, biomimetics have focused on imitating biosystems using mostly synthetic components and conventional approaches [17].With a growing understanding of the processes involved in biology, novel routes were created in material assembly and fabrication for technological applications [15]. Recent advances in molecular biology with merging engineering disciplines open a new route in biomimetics. The new emerging field as molecular biomimetics shifts biomimetic material science to the molecular level [9].

All accumulated knowledge in various fields as described above thorugh nanotechnology can lead fabrication of new nanomaterials from metals, ceramics, polymers to composite materials, which demonstrate novel properties compared to conventional materials due to their nanoscale features [18, 14, 19, 20, 8].

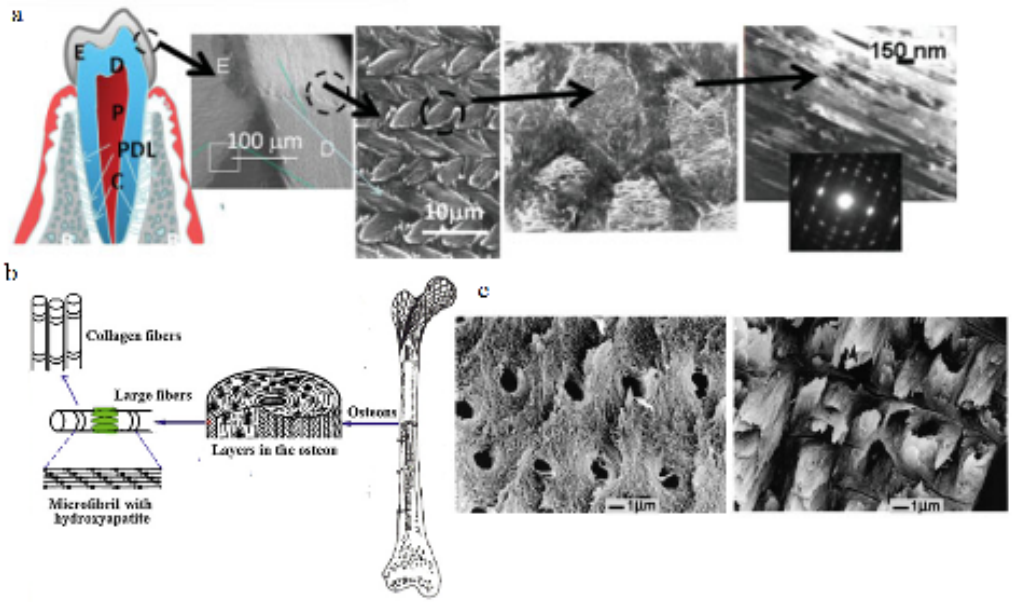

Figure 1.1: a) Mammalian tooth is a hierarchical multimaterial system composed of enamel (E), dentin (D), pulp (P), cementum (C) and periodontal ligaments (PDL) [9].b) The nanostructured hierarchal self-assembly of bone[8]. c) Plywood-like structure present in lamellar bone (left), Radial fibril arrays (right) [10].

At the nanoscale, materials possess several novel properties including extremely high surface area, tunable optical emission, enhanced mechanical properties, and super paramagnetic behavior, which contrast the properties that are important when working with the bulk parent materials [21, 8].

In recent years, bionanotechnology, as a branch of nanotechnology for application of biology, can be broadly defined an area, which utilize molecular tools and knowledge of the human body for diagnosis, treatment and prevention of diseases [22]. Applications of bionantechnology and/or nanomedicine can be roughly classified into diagnostics, imaging, nanobiomaterials, nanodevices/implants, novel drug delivery systems [22-24]. Several biomaterials in the form of self-assembled nanofibers/nanoparticles, electrospun nanofibers and nanocomposites and hydroxapaptite are also being used as a part of biomedical devices to enhance their performance (Figure 1.2) [23, 12].

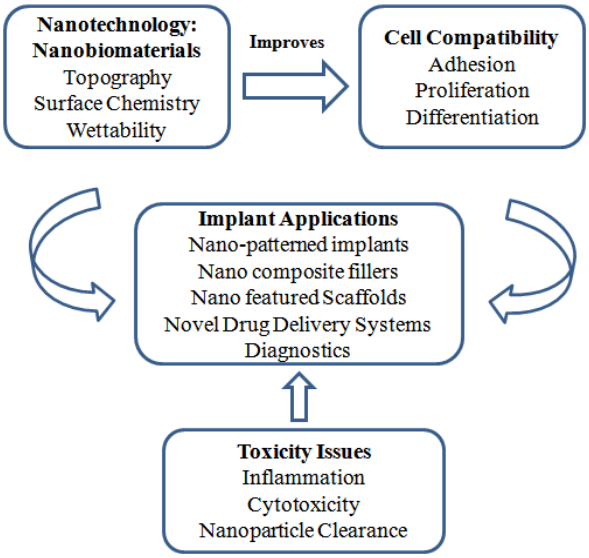

Figure 1.2: Nanotechnology and implant applications [12].

Nanobiomaterials have an increased number of atoms and crystal grains at their surfaces and possess a higher surface area to volume ratio than conventional microscale biomaterials. Novel physiochemical properties of nanobiomaterials dramatically change after decreasing material size into nanoscale by creating different surface topographies [13, 25]. They have been proposed as the next generation of improved implant materials, with the aim of improving surface properties to create an environment more conducive for osteoblast function and bone ingrowth [26]. Nanotubes, building blocks for macro nanostructures, are about one-sixth the weight and nearly 100 times stronger than steel. For example, nanostructured ceramics can reduce friction and wear problems associated with joint replacement components [27]. Biologically active molecules, added to the implant surface via nanotechnology for the guided interfacial osteogenesis. Nanostructured

titanium implant surfaces promote bone cell responses leading to accelerated calcium deposition improving integration with surrounding bone compared to conventional titanium surfaces [18, 28, 20, 29, 30]. But bone is not the only application of nanobimaterials in nanomedicine. For cartilage applications, nano-structured polylactic- co-glycolic acid (PLGA) surfaces have been shown to accelerate chondrocyte adhesion and proliferation, as well as extracellular matrix production [31-33]. Furthermore, vascular graft (PLGA) and stent (titanium) surfaces with nanometer surface roughness values improve endothelial (inner vessel cells) cell functions as compared to nanosmooth polymer and titanium surfaces [34-38]. In addition to the incorporation of nanometer surface features on conventional biomaterials, intrinsic nano-sized materials such as carbon nanotubes (hydrophobic) [39-42] and helical rosette nanotubes (hydrophilic) [43] are under intense investigation in regenerative medicine. Both types of these novel carbon based nanomaterials promote cellular interactions over currently implanted materials. Such data strongly supports the hypothesis that nano surface topography, in addition to surface chemistry, dictate initial protein adsorption and bioactivity (since initial protein interactions mediate cellular adhesion) as well as subsequent cellular adhesion [44].

1.2 Implant Materials for Tissue Restoration

Biomaterials are artificial or natural materials and they have role to restore the function of lost and diseased biological structures. Thus biomaterials help to enhance the quality of life and longevity of human beings. The field of biomaterials has shown rapid increase to keep with the demands of an aging population [45]. Many synthetic materials are used in the medicine for a variety of applications ranging from total replacement of hard or soft tissues (such as bone plates, pins, total joint replacement, dental implants, intra-ocular lenses, etc.), repair, diagnostic or corrective devices (such as pacemakers, catheters, heart valves, etc.) [46].

The material or system of materials were chosen for the appropriate mechanical properties such as elasticity, yield stress, ductility, toughness, wear resistance, etc. [47] depending on desired function. Further it should be amenable to being formed or machined into different shapes, at relatively low cost and be readily available. A proper design of an implant material is aimed to provide the requisite durability,

functionality and biological response. Durability and functionality are governed by the bulk properties of the material, whereas biological response depends on the surface chemistry, surface topography, surface roughness, wettability, surface charge, and surface energy [48-51]. Biocompatibility can be defined as the acceptance of the implant material by the surrounding tissues without any adverse response from the body and vice versa. Therefore, a biocompatible implant material should be nontoxic, noncarcinogenic, with little or no foreign body reaction and be chemically stable or corrosion resistant [51, 52, 47]. Depending on required parameters that listed above, various types of synthetic materials have been developed in order to fulfill with its function. They belong to the following main material classes [52]:

i. Metals- titanium, titanium alloys, stainless steel, cobalt–chromium alloys.
ii. Ceramics- aluminum oxide, carbon, calcium phosphates, glass–ceramics.
iii. Polymers- silicon, poly (methylmethacrylate), poly lactide, poly (urethane), ultra high molecular weight poly ethylene.
iv. Composites- ceramic coating on metal implants, or ceramic-reinforced polymers.
v. Natural materials

The choice of one material above another will depend on the application and the type of function that needs replacement. Unfortunately, none of the existing biomaterials can meet all of the requirements. The following section explains utilization of each material based on their required function.

1.2.1 Metallic materials

Metallic materials are most commonly used for load bearing implants and internal fixation devices. The properties of metals can be determined processing method and purity of the materials. Some featured properties of a metallic material are its high tensile strength, high yield strength, resistance to cyclic loading (fatigue), resistance to time dependent deformation (creep) and its corrosion resistance. They generally find applications in the fabrication of implant devices such as hip joint prosthesis, knee joint prosthesis, dental implants, cardiovascular devices, surgical instruments,

etc. The most commonly used metals and alloys for medical device applications include stainless steels, commercially pure titanium and its alloys, and cobalt-based alloys [52, 45-47].

1.2.1.1 Titanium and its alloys

Titanium as a pure metal is a well-tolerated material especially compared to stainless steel and Co–Cr based alloys under *in vivo* conditions. The two most commercially used specifications for implants are pure Ti (ASTM F67) and Ti–6Al–4V (ASTM F136). These alloys have driven a lot of interest for load bearing implants because of their superior mechanical properties (tensile strength and fatigue strength), chemical stability (corrosion resistance), and biocompatibility under *in vivo* conditions [53-57]. Commercially pure Ti is one of the preferable materials for applications where corrosion resistance is much important than its mechanical properties.

In the recent past, however there has been a great concern about the dissolution of aluminum and vanadium ions into the body fluid and the possibility of any toxic effect, as a result of the passivation layer break down during wear in Ti–6Al–4V. Figure 1.3 and Figure 1.4 shows the different types of Ti-based implants. Although titanium and its alloys are very promising in various fields, their bone-bonding activity is insufficient compared to other ceramic based materials. Thus a large amount or research in recent decades has been focued to surface modification of implant materials [47, 51].

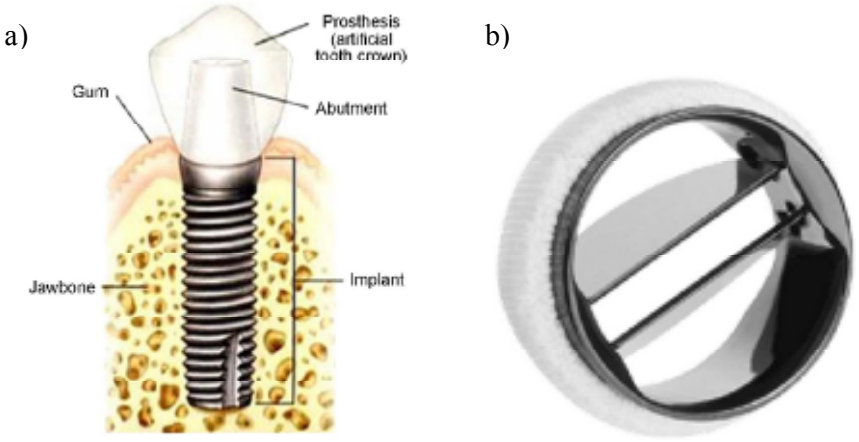

Figure 1.3: a) A dental implant b) A replacement heart valve [52].

1.2.1.2 Stainless steel

Despite having a high content of Ni – a metal that provokes a strong dermatological allergic reaction in many people – and Cr, which in one of its oxidation states is a human carcinogen, stainless steel is surprisingly biocompatible and has been used for many decades as a permanent surgical implant material [46]. The type of stainless steel that is normally used for implants is 316L. It achieves its biocompatibility by being highly corrosion-resistant due to the formation of a thin protective chromium oxide layer on its surface. The environment that stainless steel must deal with in the body is, however, rather complex and, if corrosion occurs, release of potentially harmful material could ensue [52]. Due to the fact that stronger and more corrosion-resistant materials are available and also that a growing number of people are displaying Ni sensitivity (apparently due to the increasing practice of body piercing), other alloys are now usually preferred for permanent prosthetic devices.

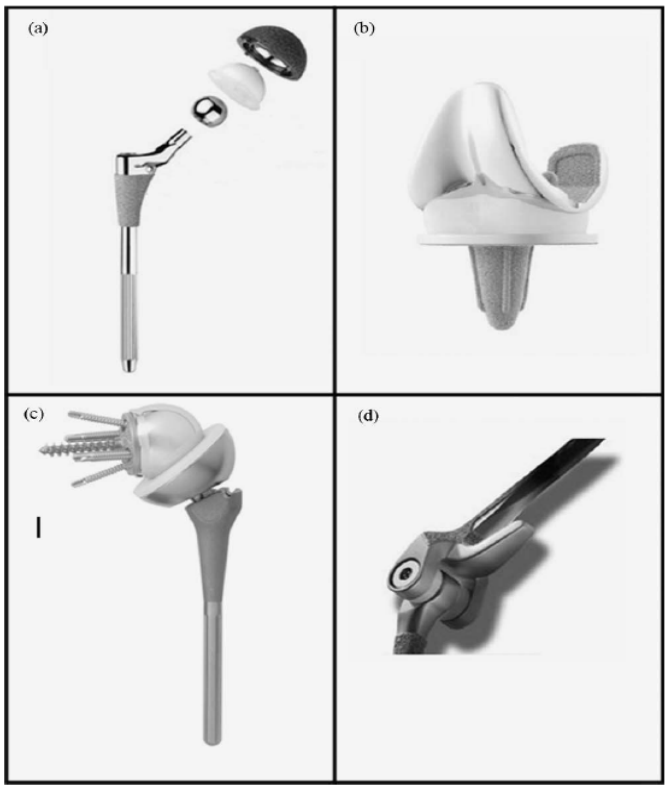

Figure 1.4: Orthopedic Implant devices used for load bearing applications: (a) hip implant (b) knee implant (c) shoulder implant and (d) elbow [52].

Stainless steels are more suitable for nonpermanent implants and are still employed for permanent implantation in certain circumstances [47, 58].

1.2.1.3 Cobalt chromium alloys

CoCr alloys have excellent mechanical properties and are widely used in orthopaedic implants. The alloys are generally CoCrMo or CoNiCrMo, and may also include other elements such as tungsten or iron (Fe).Bedises these elements, Ni can be avoided in the formulation, CoCr alloys have advantages over stainless steel in terms of better corrosion resistance and somewhat better mechanical properties for certain applications. Both wrought and cast CoCr alloys are used in prosthetic devices, each version having distinct properties. They are often used as components in modular prosthetic devices such as hip or knee joints, being the most suitable for bearing surfaces (often against ultra-high-molecular-weight polyethylene) [46, 52, 58].

1.2.1.4 Ceramics

Ceramics are inorganic compounds of metallic or nonmetallic materials, with interatomic bonding as ionic or covalent and which are generally formed at elevated temperatures. A class of such materials used for skeletal or hard tissue repair is commonly referred to bioceramics. These bioceramics may be bioinert (alumina, zirconia), bioresorbable (tricalcium phosphate), bioactive (hydroxyapatite, bioactive glasses, and glass ceramics), or porous for tissue in growth (hydroxyapatite coating, and bioglass coating on metallic materials) [59, 60]. Their success depends on their ability to induce bone regeneration and bone in growth at the tissue–implant interface without the intermediate fibrous tissue layer. The featured clinical applications include their use in orthopedics as (a) bone plates and screws, (b) total and partial hip components, (c) coatings on metal prosthesis for controlled implant or tissue interfacial response, (d) space fillings of diseased bone [61, 52].

1.2.2 Polymers

Polymers are long chain molecules consisting of large number of small repeating units known as monomers. They belong to the family of macromolecules and represent the largest class of biomaterials. Polymers can be derived either from natural sources or from synthetic organic sources. The different types of polymers and their corresponding medical applications are listed in Table 1.1

Table 1.1: Examples of polymers used as biomaterials [62, 52, 63].

Applications	Polymer
Knee, hip, shoulder joints	Ultrahigh-molecular-weight polyethylene
Finger joints	Silicone
Sutures	Polylactic and polyglycolic acid
Tracheal tubes	Silicone, acrylic,nylon
Heart Pacemaker	Acetal, polyethylene, polyurethane
Blood vessels	Polyester,polyetrafluroethylene,PVC
Gastrointestinal segments	Nylon, PVC, silicones
Facial Prostheses	Polydimethyl siloxane,polyurethane,PVC
Bone Cement	Polymethylmethacrylate

Figure 1.5 shows the use of UHMWPE as a bearing material for hip joint and knee joint prostheses. Some advantages associated with polymers, for use as biomaterials can be listed as follows:

- Polymers can be easily fabricated to various complex shapes and structures.
- Provide wide range of bulk compositions and physical properties.
- Surface properties can be easily tuned.

On the other hand their disadvantages include:

- Difficulty in sterilization.
- Easily absorb water and biomolecule from the surroundings and thereby alter the surface chemistry.
- Being soft materials may undergo mechanical wear and breakdown.
- May leach some harmful compounds to the body under in vivo conditions.

1.2.3 Composites

A composite defines as combination of two or more materials each with distinct physical or chemical properties. It is designed to have best characteristic of each component materials. Biomedical composites are often designed to provide superior mechanical and biological compatibility. They can be classified based on the matrix material or on the bioactivity of the composites. Considering matrix material as the basis for classification, there are three different types of biomedical composites [64]:

- Polymer matrix composites, e.g., carbon/PEEK (polyetheretherketone), HA/HDPE.
- Metal matrix composites, e.g., HA/Ti, HA/Ti–6Al–4V.
- Ceramic matrix composites, e.g., stainless steel/HA, glass/HA.

Considering bioactivity of the composite as the basis for classification, there are three different types of biomedical composites.

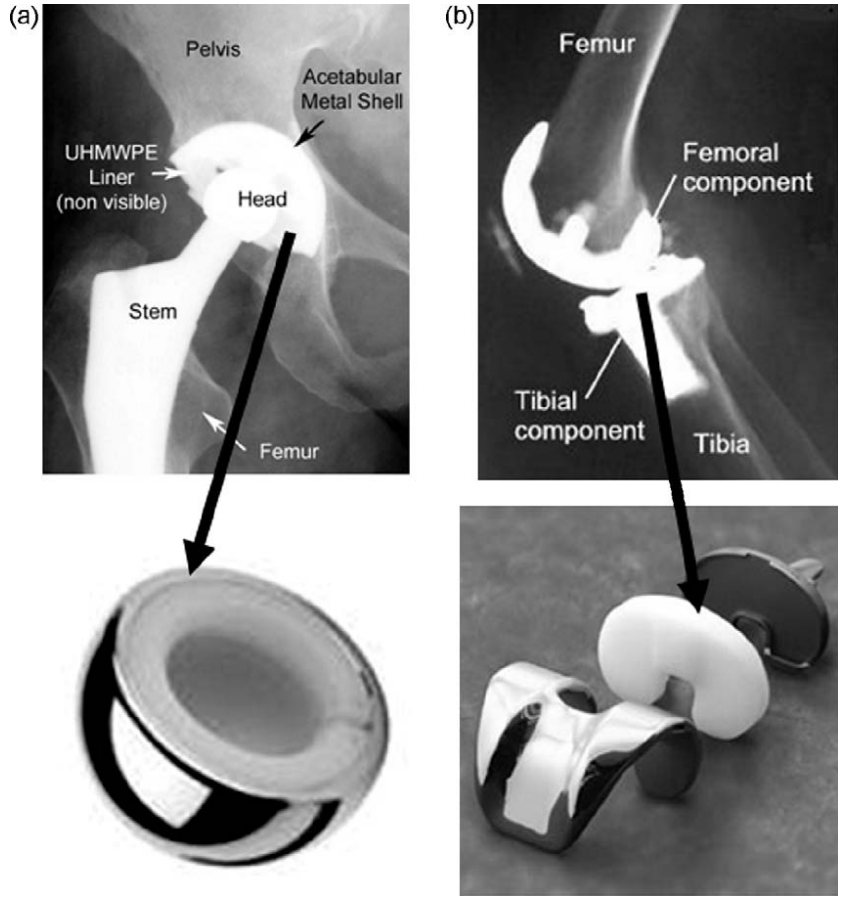

Figure 1.5: Illustrating the use of UHMWPE as a bearing metal for (a) hip joint and (b) knee joint prosthesis [52].

- Bioinert composites, e.g., carbon/carbon, carbon/PEEK.
- Bioactive composites, e.g., stainless steel/bioglass, HA/HDPE, HA/Ti–6Al–4V.
- Bioresorbable composites, e.g., tricalcium phosphate (TCP)/polylactic acid (PLA), TCP/polyhydroxybutyrate (PHB).

The various factors that affect the performance of a biomedical composite material can be listed as follows [64]:

- shape, size and distribution of reinforcement;
- reinforcement properties and volume percentage;
- bioactivity of the reinforcement;
- matrix properties such as molecular weight and grain size;
- reinforcement-matrix interfacial state.

1.2.4 Natural materials

Natural polymers such as collagen and glycosaminoglycans are the most commonly used natural materials for clinical applications [65, 63, 66, 67]. Collagen is a fibrous protein that connects and supports other bodily tissues such as skin, bone, tendons, muscles, and cartilage. It is the most plentiful available protein present in the bodies of mammals, including humans. Glycosaminoglycan is the most abundant heteropolysaccharide present in the body. Glycosaminoglycans occur primarily on the surface of the cells or in the extracellular matrix (ECM). The advantages associated with these natural biomaterials can be listed as follows:

- These materials being similar to the macromolecular substances get easily recognized by the biological environment and therefore deal metabolically.
- Problems of toxicity, chronic inflammation, and lack of recognition by cells which occurs mostly with synthetic materials can be avoided.
- These materials are biodegradable, and therefore it can be used for applications where it is desired to deliver a specific function for a temporary period of time [52].

1.3 Performance Factors for Implant Materials

The design and selection of biomaterials depend on the function of the implant which allows researchers to create new materials with desired pyhical, chemical and biological properties. Thus, development of new biomaterials often requires a collaborative work between diffent disciplines from material scientists, engineers to clinicians [45].

It is well established that the bulk and surface properties of synthetic biomaterials, determine their long-term performance and stability under in vivo conditions. The bulk properties of an implant material can be characterized by its mechanical behavior and chemical stability under *in vivo* conditions. Based on the intended application and normal activity of the patient, an implant material may fail due to yielding, plastic deformation, rupture, fatigue, creep, corrosion, wear, and impact fracture. Further, since the atoms at the surface are highly unstable and drive most of the biological reactions at the tissue–implant interface, characterization and evaluation of surface properties plays an important role in determining its

biocompatibility to the surrounding environment. The various surface parameters that dictate the biological response to surfaces include surface roughness, surface morphology, wettability, chemical composition, charge, crystallinity, and heterogeneity (Figure 1.6).

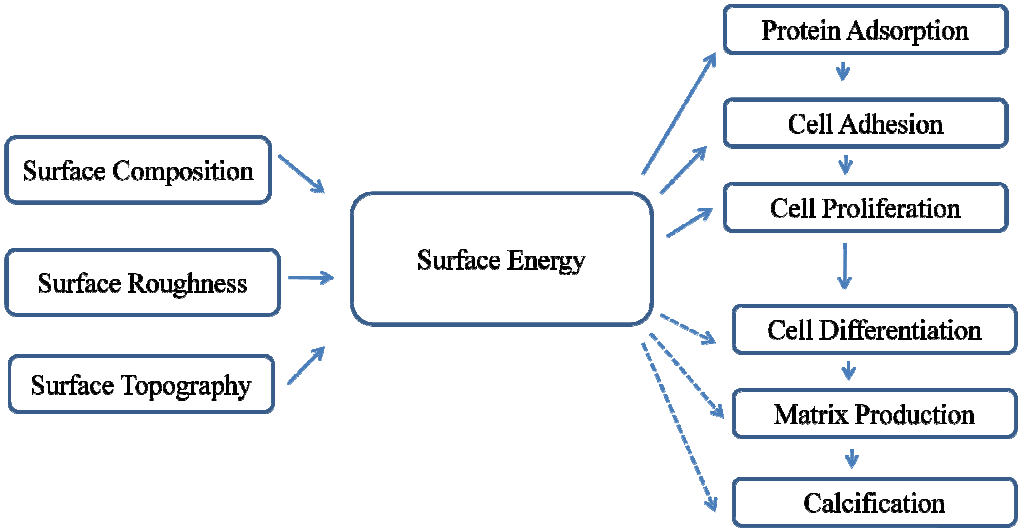

Figure 1.6: Surface composition, roughness, topography, and energy are interelated surface characteristics that dictate the biological response to an implanted device [45].

1.3.1 Chemical composition

The chemical composition and charges on implant surfaces can be different depending on their bulk composition as well as surface treatments. It is well known that the composition and charges are critical for protein adsorption and cell attachment. The surface chemical composition of implants affects the hydrophilicity of the implant surface [68].

Commercially pure titanium or titanium alloys are preferred materials for dental and orthopedic implants. Commercially pure titanium (cpTi) has various degrees of purity (graded from 1 to 4). This purity is characterized by oxygen, carbon and iron content. Most dental implants are made from grade 4 cpTi as it is stronger than other grades. Titanium alloys are mainly composed of Ti6Al4V (grade 5 titanium alloy) with greater yield strength and fatigue properties than pure titanium [69, 70]. Due to the effect of chemical composition and various surface treatments on surface hydrophobicity, contact angle measurements of titanium implant surface is ranging from 0° (hydrophilic) to 140° (hydrophobic). Highly hydrophilic surfaces seem to be

more desirable than hydrophobic ones because of their interactions with biological fluids, cells and tissues [71-73]. Recent studies was shown in an animal model that a hydrophilic sand-blasted, acid-etched (SLA) implant surface yielded higher bone-to implant contact than a regular SLA surface [71].

1.3.2 Mechanical behavior

The mechanical properties are one the major issue to decide the type of material for a specific application. There are various parameters need to be consired such as hardness, tensile strength, modulus and elongation to design implant for proper function. Among them, the fatigue strength of the material that is directly related the material response mostly determined by the repeated cyclic loads or strains. This feature determines the long-term success and usability of the implant that is subjected to cyclic loading. If an implant fractures due to poor strength or mismatch in mechanical property between the bone and implant, then this is referred to as biomechanical incompatibility. The implant material replaced for bone is expected to have a modulus equivalent to that bone. The bone modulus varies in the magnitude from 4 to 30 Gpa depending on the type of the bone and the direction of measurement [74, 45]. The current applicable implant materials shouldn`t have higher stiffness than bone. Higher stiffness prevents the needed stress being transferred to adjacent bone. The problem ended in bone resorption around the implant and consequently to implant loosening. This biomechanical incompatibility that cause to death of bone cells and this phenomena is called as ‘‘stress shielding effect” [75]. Thus a material with excellent combination of high strength and low modulus closer to bone has to be design for implantation due to the prevention loosening of implants and higher service period for revision of surgery [52].

1.3.3 Corrosion

Corrosion is the weaknees of a material as a result of chemical and electrochemical reactions with its surrounding environment. It is a fact that most pure metals and alloys are chemically unstable in many everyday environments due to their tendency to corrosion. Gold is the obvious exception to this rule in typical terrestrial environments. In the complex environment of the human body, alloys are subject to electrochemical corrosion mechanisms, with body fluids acting as an electrolyte. Implant materials used inside a human body are generally exposed to a harsh

aqueous environment containing various anions (Cl^-, HCO_3^-, HPO_4^{2-}), cations (Na^+, K^+, Ca^{2+}, Mg^{2+}), organic substances, and dissolved oxygen [76, 77]. Hence metallic implant materials are prone towards aqueous corrosion. The metallic components of the alloy are initially oxidized to their ionic forms and release a free electron. The dissolved oxygen presents in the aqueous environment then react with the water molecules and free electron to form hydroxyl ions. These hydroxyl anions then react with the metallic cations to form a corrosion product [52].

Corrosion resistance of the implants in the body fluid ended up the releasing of metal ions by the implants into the body. The released ions are caused allergic and toxic reactions which makes the implants as noncompatible materials [78, 79]. Development of implants with high corrosion resistance is emerged for the longevity of the material in the human system [45].

1.3.4 Surface characteristics

Implant surface characteristics is one of the implant design factor affecting the rate and extention of osteointegration. The process of osteointegration is now well known both histologically and at the cellular level [80-82]. When an implant material is inserted into the living tissue, an interface is created between the surface of the foreign implant material and surrounding tissues. The surrounding tissue consists of water molecules, oxygen, negative and positive ions, proteins and other biomolecules that will attack the implant surfaces and they may further trigger to build larger structures such as cells and cell membranes. On the other hand, the surfaces of a foreign material may consist of individual atoms, molecules or large polymeric structures. Hence the surface of an implant is a termination of extended, three-dimensional structure and thus generally represents broken bonds with higher surface energy. Because of thermodynamic and kinetic reasons, when implant surface comes in to the contact with the biological environment, it reacts immediately to form new bonds and compounds to lower the surface energy. The nature of implant surfaces plays a major role in thermodynamic process at implant-tissue interface. Therefore surface characteristics of implant materials such as chemistry, topography, roughness, wettability and energy may influence the cell interaction and consequently tissue integration [83, 52, 68].

1.3.4.1 Surface chemistry

Implant surface chemistry plays an important role in protein adsorption and subsequent cell adhesion. Although several studies have provided insights into the relationships between surface chemistry and protein adsorption, many of these experimental systems suffer either from a lack of surface homogeneity or uncharacterized surface properties. For instance, polymeric surfaces can undergo conformational rearrangements in response to environmental conditions and can exhibit differences in surface roughness and chemistry depending on processing or surface modifications [84, 85]. To address these limitations, recent work has focused on model substrates with well-controlled properties [86-88]. In particular, self-assembled monolayers (SAMs) of alkanethiols on gold have provided a useful model system to systematically investigate the effects of surface chemistry without altering other surface properties such as roughness. Recent studies using alkanethiol SAMs have demonstrated that surface chemistry can modulate cell adhesion, spreading and adhesion strength [89-91]. The same has been observed for titanium. For example, the surface oxide layer of titanium has many qualities regarded as important for promoting bone growth. This oxide layer of titanium can be manipulated chemically and there has been speculation whether the biological properties of the oxide surface may then be changed and even improved. The significance of titanium surface chemistry can be illustrated by the various cellular responses reported for different titanium alloys, different grades of c.p. titanium, and different bulk metals [92]. Specifically, chemical modification of titanium surfaces through their treatment in simulated body fluid, covalent attachment of biological molecules, changes in the surface ion content, and alkali soaking have all been reported to influence cellular responses (but to different degrees) [92]. An electrochemical method known as anodization or anodic oxidation is a well-established surface modification technique for titanium that produces protective layers. Anodization has been successfully used as a surface treatment for orthopedic implants and has some new advances recently reported to increase bone growth when possessing nanometer features [93]. Other strategies for improving the biocompatibility and osteogenic capacity of metal implants include surface modification with inorganic mineral coatings, particulates, or cements containing a diversity of calcium salts (mainly calcium phosphates, sulfates or carbonates) [94]. The idea behind all of these strategies is to make the

metal surface more acceptable to bone cells and, by doing so, trick the body into rapid integration of the implanted structure rather than fibrous encapsulation. An emerging area, still at the experimental stage to change chemistry to promote bone growth, is the use of photolithography to produce micro- and nano-fabricated surfaces. Such surfaces, made of silicon and titanium, incorporate intentional surface chemical and topographical features in the nano- and micrometer scales to provide greater opportunities to promote cell behavior [95, 96, 21].

1.3.4.2 Surface hydrophobicity (wettability)

Surface wettability is considered as a one of the important criteria that can control the biocompatibility of the implant materials due to its possible effect on protein adsorption followed by attachment of cells to the implant surface. The three most important factors that affect the wettability of the surface are its chemical composition, micro and nano structural topography and surface charge [52, 95, 97].

Contact angle measurements indicate whether the surface is hydrophilic and hydrophobic. If the contact angle is high (> 90^0) then the surface considered as a nonwetting or a hydrophobic surface. If the contact angle is small, then the surface is considered as wetting or a hydrophilic surface [98, 52, 99-101] (Figure 1.7).

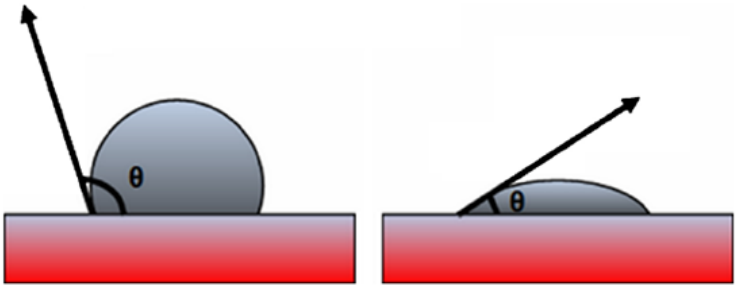

Figure 1.7: Schematic illustration of (a) a hydrophobic or non wetting surface (b) a hydrophilic or wetting surface [52].

In the literature, several studies have implied the interaction between different cell types or blood proteins and various solid substrates having different wettabilities to correlate the relationship between surface weattability and cell or blood compatibility. The surface of hexamethyldisiloxane were modeled to different degrees of wettability and thereby studied its effect on cell attachment, cell proliferation and cell morphology [52]. *Cai et al* investigated effect of titanium films shared the same surface chemistry but exhibited very different topographies on

protein adsorption and cellular growth [102]. On the other hand, *Webster et al.* demonstrated that the role of nano-topographies on different materials such as ceramics, polymer composites and metals on cellular response by increasing surface wettability. They also reported that adsorption of vitronectin and fibronectin which stimulates osteoblast adhesion on nanophase ceramics with greater wettability [103]. It is widely observed that cell adhesion and subsequent activity are generally better on hydrophilic surfaces [104, 105]. Therefore it is not surprising that materials for example titanium and hydroxyapatite with its hydrophilic character have high ability for osteointegration. Depending on all accumulated knowledge on surface wettability, the topographical features like roughness, energy and wettability modify cell behavior and alter the function of cells in the initial mechanism of osteointegration. *Feng et al* observed that, besides surface characteristics, the number of hydroxyl groups on implant surfaces influence the cell behavior [106, 97]. They also observed that the greater roughness, the larger surface energy and the higher number of hydroxyl groups, the greater number of adhered cells and cell activity.

1.3.4.3 Surface topography and roughness

It is well established that morphological features such as surface roughness and its topography can strongly affect the protein adsorption, cell attachment, cell proliferation, contact guidance, and differentiation. Hence, it controls the rate and quality of new tissue formation at the interface [52, 95, 81]. Surface roughness is a vastly studied subject by numerous investigators with the goal of enhanced performance factors of implants and it is commonly divided, depending on the dimension of the measured surface features, into macro-, micro- and nano-roughness. Typically, these different roughness features are related to distinct effects during wound healing and osseointegration [68].

Macro-roughness comprises features in the range of millimeters to tens of micrometers. This scale directly relates to implant geometry, with threaded screw and macro-porous surface treatments. The evidence exist that primary implant fixation and long-term mechanical stability can be improved by an appropriate macro-roughness. The underlying mechanism thereby is the mechanical interlocking between the macro-rough features of the implant surface and the surrounding bone profile [107, 108].

Micro-roughness is defined as being in the range of 1–10 mm. This range of roughness maximizes the interlocking between mineralized bone and implant surface. Specifically, compared with smooth surfaces, micron surface roughness on titanium substrates created by sandblasting, etching, machining and the use of micron-sized metal bead coatings has enhanced osteoblast functions such as adhesion, proliferation, production of alkaline phosphatase, and deposition of calcium-containing mineral [109]. Many of these techniques are currently being incorporated into the orthopedic marketplace. In fact, improved osteoinduction of titanium was observed on microporous structures compared with non-microporous titanium which did not induce bone formation at all [110]. Several studies have further suggested that other microstructural features (such as grain and particle size) promote osteoblast functions compared with smooth surfaces. However, the type of micro-roughness created in these studies does not match the roughness that osteoblasts are naturally accustomed to in the body. Since bone is composed of constituent nanostructures, it is clear that instead of formulating surfaces with micron roughness, emphasis should be placed on techniques that create nanometer roughness; that is, indeed, the role nanophase materials can play in universally increasing the efficacy of orthopedic implants [111, 21, 96, 97].

1.3.4.4 Surface porosity

Other design criteria to achieve successful implantation with best match the behavior of the bone is porous structure of implant materials. Implant material as mentioned above should be strong enough and durable to withstand the physiological loads placed upon it over the years. Suitable balance between strength and stiffness has to be found similarity with bone structure. One consideration to achieve this has been the development of materials that exhibit substantial surface or total bulk porosity in medical applications [112].

The fabrication of porous materials has been actively researched since 1943, when B. Sosnik attempted to introduce pores into aluminium by adding mercury to the melt. Numerous investigations into porous materials where subsequently initiated in the early 1970s involving porous ceramic, polymeric, and metallic materials, which showed in animal studies to be potential candidates for porous implants that would enable bone ingrowth [113-116]. Although ceramics portray excellent corrosion resistance, the general opinion is that porous ceramic structures, as they are available

today, cannot be employed as load bearing implants, due to their intrinsic brittleness. Likewise, porous polymeric systems cannot sustain the mechanical forces present in joint replacement surgery. This led researchers to focus on porous metals, based on orthopaedic metallic materials, as a consequence of their superior fracture and fatigue resistance characteristics, which are required for load-bearing applications.

A major problem concerning metallic implants in orthopaedic surgery is the mismatch of Young's modulus between bone (10–30 GPa) and bulk metallic materials (between 110 GPa for Ti and 230 GPa for Co–Cr alloys). Due to this mechanical mismatch, bone is insufficiently loaded and becomes stress shielded, which eventually leads to bone resorption. It has been suggested that when bone loss is excessive, it can compromise the long-term clinical performance of the prosthesis [117].

The clinical literature of the past 30 years records a variety of approaches to this end and several researchers have performed studies aimed at clarifying the fundamental aspects of interactions between porous metals and hard tissue. Porous materials in implantation are increasingly attracting the widespread interest of researchers as a method of reducing stiffness mismatches and achieving stable long-term fixation by means of full bone ingrowth and there have been a number of previous reviews on the many different porous coatings and fully porous matrices that have been developed [118, 119].

1.3.5 Biocompatibility

The materials used as implants are probable to be highly non toxic and should not cause any inflammatory or allergic reactions in the human body. The success of the biomaterials is mainly based on the biococompatibility of a material which can be defined the reaction of the human body to the implant [120]. The two main factors that influence the biocompatibility of a material, the one is the host response induced by the material and another one is the materials reponse or degradation induced by the environment around the implant. Depending on two main factors, materials can be subdivided into three different classes such as biotolerant, bioactive, and bioresorbable [45].

Table 1.2 Classification of biomaterials based on their interaction with its surrounding tissue [45].

Classification	Response	Examples	Effect
Biotolerant Materials	Formation of thin connective tissue capsules (0.1-10μm) and the capsule does not adhere to the implant surface	Polymer-poly tetra fluorethylene (PTFE), polymethyl metha acralyte(PMMA),Ti,Co-Cr, etc.	Rejection of the implant leading to failure of the implant
Bioactive Materials	Formation of bony tissue around the implant material and strongly integrates with the implant surface	Bioglass, synthetic calcium phosphate including hydroxyl apatite (HAP)	Acceptance of the implant leading to success of implantation
Bioreabsorbable Materials	Replaced by autologous tissue	Polylactic acid and polyglycolic polymers and processed bone grafts, composites of all tissue extracts or proteins and structural support system	Acceptance of the implant leading to success of implantation

The classification of biomaterials based on the reaction against to the human body is given in Table 1.2. Bioactive materials are highly preferred due to their high integration capacity with surrounding bone; however, biotolerant implants are available for production of implant materials. When implants are exposed to human tissues and fluids, several reactions take place between the host and the implant material. The acceptability of these materials by our system were determined by these reactions [83]. Resorbable biomaterials are another type of material that degrade gradually over a period of time and are replaced by the natural host tissue. This leads to a very thin or nonexistent interfacial thickness. There are various complications in the development of resorbable biomaterials such as maintenance of strength, stability of the interface during the degradation period, and matching resorption rates to the repair rates of the body. The concept of bioactive materials holds intermediate position in between resorbable and bioinert materials. All of the bioactive materials produce specific biological response and form an interfacial bond with adjacent tissue. Although they have wide ranges of bonding capacity with surrounding tissue, bonding time, strength, and mechanism is changeable form one

material type to another [121, 59]. There are two major issues with regard to biocompatibility. The one is thrombosis, which involves blood coagulation and adhesion of blood platelets to biomaterial surface, and the other second is the fibrous tissue encapsulation of biomaterials that are implanted in soft tissues.

1.4 Biomaterials Induced Biological Response at Implant-Tissue Interface

1.4.1 Material-host interactions

Scientists are continuously investigating novel materials which can promote desirable responses from surrounding cells for better osteointegration. There are two important factors to produce implant materials with high compability with the human body. The first one is correct chemistry that has a role to support or stimulate an appropriate host response and the second one is geometric structure of an appropriate scaffold. Ideal implant material should also interact with the host tissue and even promoting differentiation of osteogenic cells, rather than acting as passive stage for the performance of any itinerant cells. Implant material performance on cell response subsequently bone apposition is critical for rapid integration [95]. However, frequently implant materials are not preferentially compatible with bone cells, which is responsible for bone formation. They have tendency to promote the formation of undesirable soft connective tissue by other cells such as fibroblasts. Fibrous soft tissue has been shown improper fixation into surrounding tissue which leads implant failure. Excessive fibrous tissue formation hinders osteoblast/osteoclast activities and, thus, less new bones regeneration between an implant and juxtaposed bone results. Osteoblasts and osteoclasts form and resorb bone, respectively [92].

It is clear that to design better orthopedic implant materials, one needs to concentrate on cellular processes that lead to efficient new bone growth. Positive responses from osteoblasts, including increased initial adhesion, proliferation, and differentiation from non-calcium depositing to calcium depositing cells are essential. In addition, coordinated activities between osteoblasts and the bone–resorbing cells, osteoclasts, are needed to maintain healthy bone surrounding the implant. Poor communication between these cells will lead to necrotic (or dead) bone juxtaposed to the implant which is much weaker and will lead to fracture in the bone surrounding the implant. Due to the importance of these specific cellular events, understanding cellular

recognition of implant surfaces in order to create biomaterial surface properties that maximize initial cellular interactions leading to more bone formation is required [122].

A sequence and strongly interrelated events takes place at the implant surface after implantation of the material (Figure 1.8). Immediately after implantation, water molecules bind to the surface and form a water mono- or bilayer in nanoseconds. The arrangement of water molecules depends on the implant surface properties at the atomic scale. Blood proteins and tissue specific proteins adsorb and desorb to and from the surface [123]. This adsorption process is strongly dependent on the implant surface features, such as its physicochemical, biochemical and topographic characteristics. Inorganic, physicochemical stimuli, such as release of Ca^{2+} and PO_4^{-3} ions from calcium phosphates, can positively affect the cellular response. Implant surfaces that have protrusions, cavities, gullies, etc., on a micro- and/or nanoscale will induce biological interactions different from those with a flat surface. Indeed some studies provided evidence that in implant surface energy; surface chemical composition and topographical features influence the type and concentration of adsorbed proteins. For example, previous studies indicate that fibronectin preferentially adsorbs on calcium-phosphate coated bioactive glass compared with untreated bioactive glass and stoichiometric bioactive glass [124, 125]. Additionally, implants biochemically modified with biomolecules immobilized on the surface, such as growth factors or cell adhesion motifs, will induce certain cell responses in the physiological surrounding by specific cell signaling pathways. As a result, both the exact mixture of adsorbed proteins and their conformational state(s) are largely controlled by the implant surface. This surface specific adsorbed biofilm subsequently determines cell adhesion, since proteins act as contact for the attachment of cells. This is accomplished by means of integrins, which are specific transmembrane receptors that bind to adhesive proteins on the biomaterials surface and to components of the cytoskeleton through their extra- and intracellular domains, respectively. Moreover, it is now well known that osteoblasts preferentially adhere to specific amino acid sequences such as arginine- glycine-aspartic acid (RGD) and heparin sulfate binding regions in adsorbed proteins. Accordingly, how specific amino acid sequences are exposed in adsorbed proteins to associate with binding to

integrin receptors in cell membranes is critical to whether cell adhesion will occur on an implant surface [122, 96, 95].

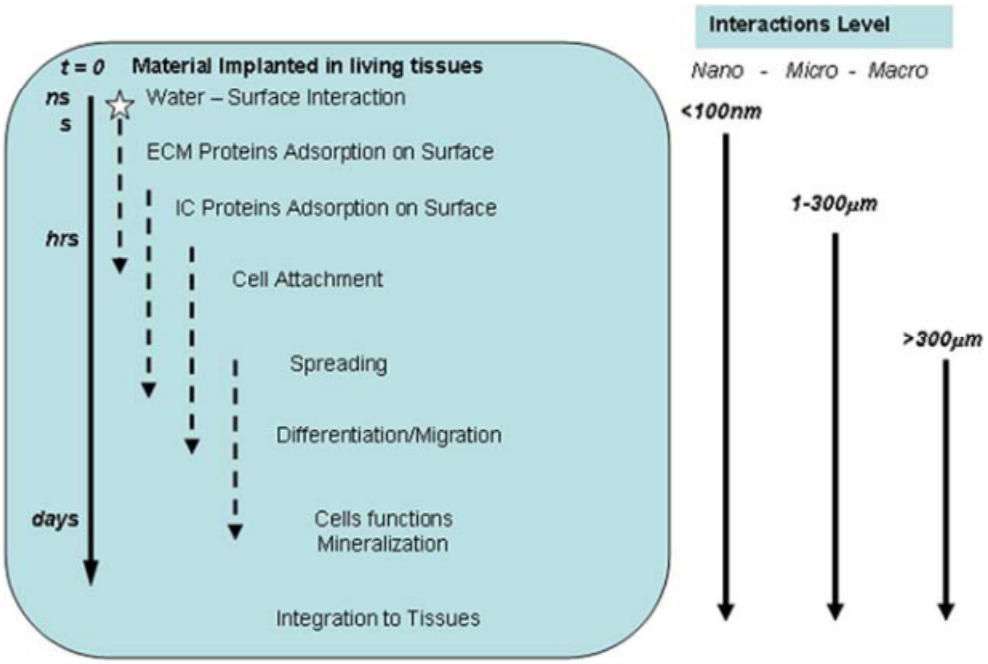

Figure 1.8: An example of biomaterial- tissue interactions, e.g., Implant- bone interactions [96].

In general, the biocompatibility of bone-replacing implant materials is closely related to osteoblast adhesion onto their surface. Osteoblast attachment, adhesion and spreading will influence the capacity of these cells to proliferate and to differentiate itself upon contact with the implant. These latter processes are quintessential for the establishment of a mechanically solid interface with complete fusion between the implant surface and bone tissue without any intervening fibrous tissue layer [126-128].

1.4.2 Cell-surface interactions

1.4.2.1 Protein adsorption

Proteins adsorb in different quantities, densities, conformations, and orientations depending on the chemical and physical characteristics of the surface. Although surface-protein interactions are not well understood, surface chemistry has been shown to play a fundamental role in protein adsorption [129]. Moreover, the properties of protein over-layers can be altered by underlying surface chemistry of a

material and this behavior has exciting implications for controlled biocompatibility [87, 130-132].

In here, we address the role of adsorbed proteins in directing cell responses to specific surface characteristics and materials. Proteins are highly surface active and thus exhibit high affinity for interfaces. Initial adsorption occurs rapidly, effectively preventing direct interactions between cells and implant materials. Adsorption may be promoted or opposed by a number of potential enthalpic and entropic changes within the surface- water protein system. Adsorption may be promoted or opposed by a number of potential enthalpic and entropic changes within surface-water-protein system. These changes can be summarized into three sections:

1. Dehydration of protein and surfaces
2. Redistribution of charged groups in the interface
3. Conformational changes in the protein molecule

The relative significance of each process depends on the nature of the protein, material surface and solvent [133, 87].

In complex biological components- surface interaction process, adsorption will increase with time and protein concentration in solution until at least the coating approaches monolayer coverage. The adsorption rate then decrease in relation to the number of available binding sites, becoming progressively more dependent on the protein-surface affinity. Such trends however are not necessarily indicative of adsorption behavior from mixed solutions, such as blood [92].

In implantation, after the initial hydration layer surrounds the material, blood proteins and other macromolecules (e.g., lipids and sugars) arrive at the surface. Since blood contains many hundreds of different proteins competition for the surface ensues. After a complex process of adsorption, desorption and surface rearrangement, wherein the protein layer composition changes dramatically over time, equilibrium is reached at the interface. It is generally accepted that the more abundant small proteins will adsorb first due to their rapid transport to the surface. Over time these are then replaced by larger proteins with a greater affinity towards the surface. The ‘surface enrichment’ of a protein from the ECM such as fibrinogen was first observed by Vroman and Adams and is generally termed the ‘Vroman effect’[134, 135]. The protein layer may then subsequently mediate cell attachment and progressively the material is integrated into the biological system.

Fundamentally, biomaterial responses are governed by the interaction of protein molecules on surfaces, involving both binding in the initial stage and subsequent unfolding. Residues pointing outwards into solution are available for surface interaction whereas those in the core of the protein are not. Unfolding, or denaturing of the protein would allow the internal amino acid residues to become accessible to the external environment thereby making them available to take part in external interactions. Protein deformation may be induced by interaction with a surface and is affected by several factors including electrostatic forces and entropic effects, hydrophobic interactions and conformational changes [133, 122, 96].

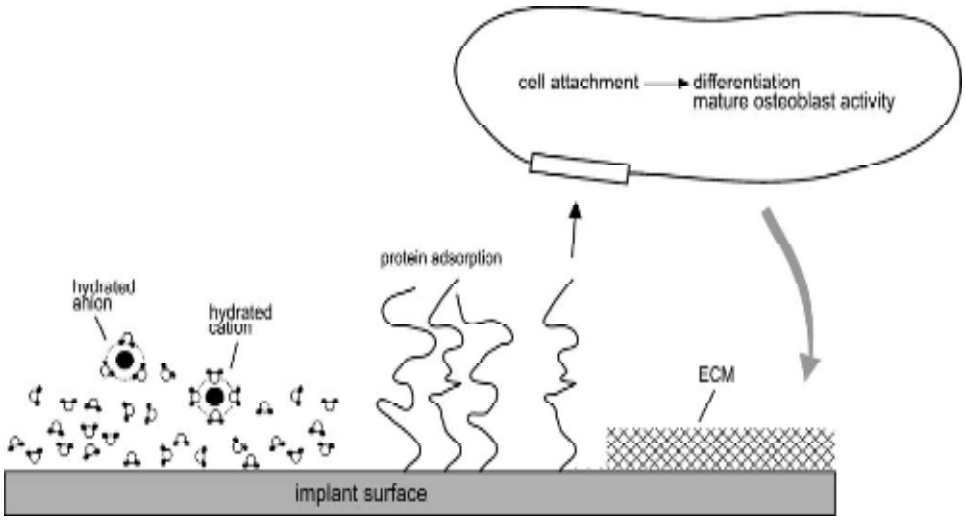

Figure 1.9: Schematic representation of events consecutively taking place at the titanium surface after implantation into living bone tissue. Water binds to the surface, followed by incorporation of hydrated ions, adsorption and desorption of proteins, eventually leading to cell attachment. After differentiation, mature osteoblasts produce the extracellular matrix (ECM) [122].

Dehydration of hydrophobic regions both on the substratum and on the external protein surface is favourable, which may cause the protein to deform to move its hydrophobic sections away from the aqueous environment (Figure 1.9 and Figure 1.10). Bonding between adsorbed neighbouring protein molecules can allow hydrophobic regions to remain shielded from the aqueous phase, due to the increase in flexibility of the polypeptide backbone brought about by loss of secondary structure. Van der Waals interactions, electrostatic interactions and hydrogen bonds can also form between proteins, provided they are enthalpically favourable. Model surfaces with varying functionalities have been used to assess protein adsorption rates and conformational stability upon adsorption. Proteins adsorb rapidly and

become deformed to a greater extent on surfaces with decreasing wettability, minimising hydrophobic contact with the aqueous phase as described above [132]. Likewise charged protein regions can interact with oppositely charged surfaces [136], although electrostatic effects are much weaker than hydroph obic effects when dealing with proteins adsorbing from an aqueous phase, due to complications arising from the charges being shielded by water molecules [137] and small ions [138]. Protein–surface interactions are very important factors when considering the adsorbed protein state. Initially protein molecules will adsorb giving the kinetic adsorption product, however, if the interaction is very high a deformation of the protein to afford an energetically more favourable thermodynamic adsorption product occurs.

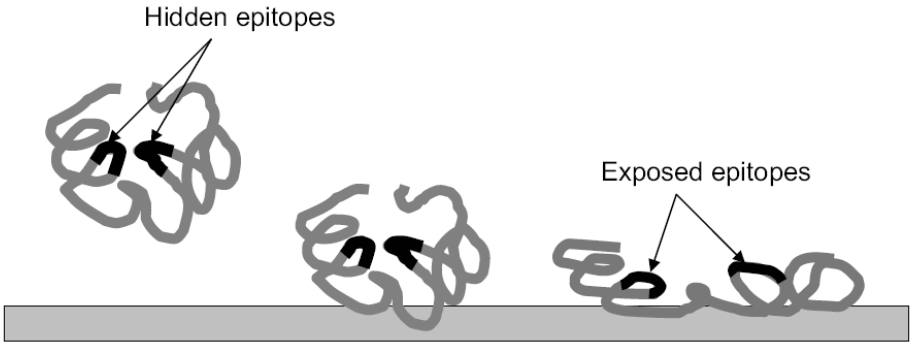

Figure 1.10: Schematic drawing to represent the protein-biomaterial interactions which often guide to conformational changes of adsorbed proteins and the subsequent disclosure of hidden proinflammatory epitopes [133].

This process, sometimes termed ‘relaxation’ occurs either directly on adsorption or some time thereafter, probably involving the protein spreading to increase its interaction with the surface and/or to decrease its interaction with the aqueous phase. Similarly, differing protein–surface interactions could force protein molecules to adopt specific orientations. As a result the protein may lose the specific structure required for activity, or functional sites may become obscured due to conformational/orientational rearrangements that hinder protein function [92, 96, 133].

1.4.2.2 Cell adhesion

In a physiological environment cell adhesion always follows protein adsorption. Cells are sensitive and responsive to the topography and surface chemistry of the material which they interact. Although cell-surface interaction may be affected by

several parameters, the interaction mechanism needs to be elucidated [129, 111, 92, 96, 83, 139].

Cells in their nature environment are anchored by discrete attachments to proteins in extracellular matrix. Osteoblastic cells (and various other cell types) in vitro have been shown to depend primarily on adsorbed vitronectin or fibronection for initial adhesion and spreading on implant material [140, 141]. Thus, the ability of materials to adsorb such proteins (in an active state) determines their ability to support cell adhesion and spreading [142, 143] and, hence, is an important aspect of their biocompatibility.

The primary interaction between cells and adhesion proteins occurs via integrins (heterodimeric receptors in the cell membrane), as demonstrated by the decrease in cell attachment observed when antibodies are introduced to prevent these interactions. Sinha *et. al.* conclude that differences in integrin expression observed on different materials may account for observed variations in cell attachment. Integrins are also involved in intracellular signaling and, thus, a diverse range of cell functions [144, 145]. Integrins bind specifically to an arginine-glycine- aspartic acid (RGD tripeptide) found in cell adhesive proteins such as fibronectin, vitronectin and laminin. Moreover, it is now well recognized that osteoblasts preferentially adhere to RGD in adsorbed proteins on implant surfaces. Accordingly, how specific amino acid sequences are exposed in adsorbed proteins to associate with binding to integrin receptors in cell membranes is critical to whether cell adhesion will occur on an implant surface (Figure 1.11).

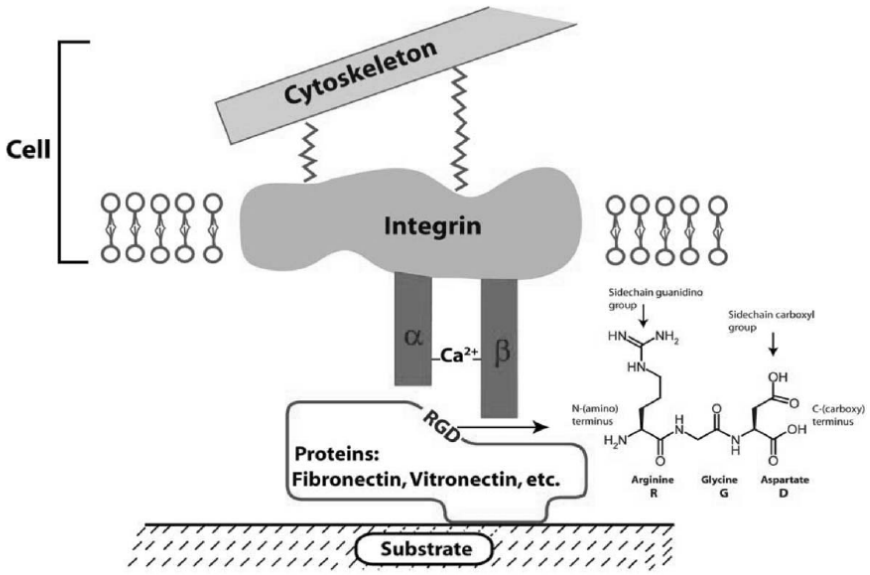

Figure 1.11: Initial protein interactions leading to cell recognition of implants [95].

Although the initial states of the surface, the cells, and the interface between them are critical, we should also consider the dynamic nature of the system. Cells may alter their environment and adhesion mechanism by secreting fibronectin, or by manipulating the extracellular matrix, as is discussed below. Furthermore, cells adapt to their environment. It has been demonstrated that nonadherent fibroblasts reduce production and/or secretion of fibronectin and the cell surface expression of its major receptor [146, 147]. Cells also adapt by changing the collection of integrins expressed, and their distribution, according to the ligands available and the differentiation state of the cells. Because of upregulation (and localization) of integrins when their preferred ligand is available, it is possible that differential integrin expression reflects distinct adsorption profiles characteristic of underlying surface properties. This may also account for differences observed in integrin expression in bone tissue [148, 146].

1.4.2.3 Cell morphology and motility

Cell spreading is a process related to adhesion and usually involves similar extracellular proteins. In addition to their effects on cell adhesion, proteins such as vitronectin and fibronectin are required for the formation of focal contacts and essential intracellular structures [149]. Massia *et. al.* [150] estimated that a ligand spacing of 140 nm or less was needed for these structures to form, although response

to ligand density may be altered by surface topography. The distribution of ligands on the substratum and the availability of the appropriate binding sites are thus important in cell adhesion, spreading, and subsequent functions[151]. In addition to adaptations relating to integrin expression and fibronectin production, a progressive change in the mechanism of anchorage is frequently observed as cells reorganize their cytoskeleton, and also the extracellular matrix to which they are anchored [152]. As cells spread, contractile forces apply tension to the extracellular matrix; these forces may be sufficient to remove adsorbed proteins from a biomaterial surface. Fibroblasts were thus able to remove fibronectin from a glass surface. Although this could potentially disrupt adhesion, it may assist in extracellular fibril assembly, suggesting that there is an upper limit to protein adsorption strength for normal cell activity to occur. Cell motility (including migration) also depends on the nature of adhesion to the substratum. Adhesive ligands are required for this and may provide a haptotactic signal, with a peak in migration being observed at certain intermediate ligand concentrations on the surface [153]. The ligand density corresponding to this peak is reduced with increasing strength of cell binding [154].However, migration rates and cell adhesion strength on various surfaces often show opposite trends [155, 156]. Webb *et al*. also showed an inverse relationship between cell migration and spreading [104]. Thus, it is apparent that maximal cell motility requires adhesion strength sufficient to maintain substratum contact, but not to the extent that release of contacts is inhibited.

14.2.4. Cell proliferation and differentiation

It is well established that cell adhesion and morphology influence subsequent activity such as proliferation and differentiation [157]. With respect to osteoblasts and adsorbed proteins, fibronectin (and its receptors) appears to become progressively more important as the cells differentiate [158]. Given that osteoblasts (and most other cells) produce their own fibronectin, this may reflect the deposition of an increasingly agreeable environment. Furthermore, Altankov *et.al.* propose that reorganization of surface-bound fibronectin is required for fibroblast proliferation [159]. Corresponding to the role of fibronectin, the β_1 integrin subunit (to which it frequently binds, particularly in the $\alpha_5\beta_1$ dimer) is predominant in the progression of precursor cells toward differentiated osteoblasts [160] and ligand binding by β_1 is

required for matrix mineralization[161]. The β_1 integrin is also involved in binding collagen and laminin.

The (not exclusively) vitronectin-binding $\alpha_V\beta_3$ integrin heterodimer also appears to be involved in mineralization. The $\alpha_V\beta_3$ integrin is also a key mediator of angiogenesis and osteoclast adhesion to extracellular matrix, suggesting a key role for its various ligands in bone repair and remodeling [162].

Although adhesion is clearly critical in osteoblast development, excessive adhesion strength may inhibit subsequent cell activities, as indicated above with regard to cell motility. Qiu *et al*. showed increased marrow stromal cell attachment on positively charged surfaces, but these cells also showed reduced spreading and differentiation [163]. This emphasizes that cell adhesion alone is not an adequate indicator of biocompatibility when a specific function is required.

Implant surfaces may also contribute to the proliferation and/or differentiation promoted by growth factors and other signaling molecules. Adsorbed proteins may provide binding sites for other molecules, mimicking storage in the extracellular matrix *in vivo*; for example, insulin-like growth factor II (IGF-II) is stored in bone as a complex with IGF-binding protein 5 (IGFBP-5), which in turn binds to bone matrix hydroxyapatite [164, 165]. Studies have exploited this concept to use vitronectin as a delivery vehicle for insulin-like growth factors [166].

1.5 Challenges at Implant–Tissue Interface

1.5.1 Osseointegration

A goal of current implantology research is to design devices that induce controlled, guided, and rapid healing. In addition to acceleration of normal wound healing phenomena, endosseous implants should result in formation of a characteristic interfacial layer and bone matrix with adequate biomechanical properties. To achieve these goals, however, a better understanding of events at the interface and of the effects biomaterials have on bone and bone cells is needed. Such knowledge is essential for developing strategies to optimally control osseointegration [167]. Osseointegration clearly belongs to the category of direct or primary healing. Originally, it was defined as direct bone deposition on the implant surfaces. In a

more comprehensive way, osseointegration is characterized as “a direct structural and functional connection between ordered, living bone and the surface of load bearing implant “ [168]. This term was initially defined by Branemark *et al.* Throughout bone to implant contact; specifically, the dynamic cellular and acellular processes at the interface at a micro- and nanoscale level are not fully elucidated [169]. Additionally, early aspects of the bone/biomaterial interaction in terms of seconds and minutes are not well known in the *in vivo* environment. Recent knowledge in both aspects of implant osseointegration is even more limited when the process of biomineral formation is under consideration. To gain insight into the state of mineralization at implant interfaces, the various levels of bone structure and physiology are considered and evaluated in light of the recent knowledge on implant osseointegration [170].

1.5.1.1 Prerequisites for osseointegration

Osseointegration shares many prerequisites with primary fracture healing, such as precise fitting (anatomical eduction), primary stability (stable fixation) and adequate loading during the healing period. In addition, it requires bioinert or bioactive material with desired surface properties that are attractive for bone deposition. The tissue response to a freshly installed implant greatly depends on the mechanical situation. As in direct fracture healing, it requires perfect stability if bone is expected to be formed. In a fracture, a stable fixation is obtained by exact adaptation and compression of the fragments. The primary stability of implants depends on their appropriate design and precise press fitting at surgery. Primary stability must counteract all forces that could create micromotion between the implant and the surrounding tissues or in other words, it should build up enough preload to compensate for functional load. It thus determines not only the size but also the direction of the forces that are considered to remain adequate. All these parameters must be specified, and this makes it understandable why immediate functional loading may be adequate for such systems as bar-connected screws, whereas others require a prolonged, unloaded healing period before a supraconstruction can be installed.

Direct bone healing, it occurs in defects, primary fracture healing and in osseointegration is activated by any lesion of the pre-existing bone matrix. When the matrix is exposed to extracellular fluid, noncollagenous proteins and growth factors

are set free and activate bone repair. Once activated, osseointegration follows a common stages first, incorporation by woven bone formation; second, adaptation of bone mass to load (lamellar and parallel-fibered bone deposition) and third, adaptation of bone structure to load [171, 172].

In the first stage, primitive type of bone or woven bone tissue characterized by a random, felt like orientation of its collagen fibrils, numerous, irregularly shaped osteocytes and low mineral density formed. It has an outstanding capacity. It grows by forming a scaffold of rods and plates and thus is able to spread out into the surrounding tissue at a relatively rapid rate. Woven bone is the ideal filling material for an open space and for the construction of the first bony bridges between bony walls and the implant surface. It usually starts growing from the surrounding bone towards the implant, except in narrow gaps, where it is simultaneously deposited upon the implant surface. Woven bone formation clearly dominates the scene within the first 4 to 6 weeks after surgery. Following woven bone formation stage, new bone formed towards either well known lamellar bone or parallel- fibered bone. Deposition of more mature bone on the initially formed scaffold results in reinforcement and often concentrates on the areas where major forces and transferred from the implant to the surrounding original bone. At the last stage of osseointegration is bone remodeling. This stage contributes to an adaptation of bone structure to load in two ways:

1. It improves bone quality by replacing pre-existing, necrotic bone and/or initially formed, more primitive woven bone with mature, viable lamellar bone.
2. It leads to a functional adaptation of the bone structure to load by changing the dimension and orientation of the supporting elements.

It has been mentioned already that bone remodeling continues throughout life and thus becomes important for the longevity of implants. Continuous replacement of old bone by new bone prevents accumulation of microdamage and fatigue as one possible cause of aseptic implant loosening [168, 170].

1.5.2 Bacterial infection

Bacterial infection at the site of implanted medical devices presents a serious ongoing problem in the biomedical area [173]. Infections associated with surgical

implants are generally aggressive and more cumbersome to manage, have a greater adverse impact on quality of life, result in primary cause of implant failure, excessive prolongation of hospital stays, and incur higher costs [174, 175]. They are very common various type of implants, including prosthetic heart valves, orthopedic implants, cardiac pacemakers, intravascular catheters, left ventricular assist devices, urinary catheters, vascular prostheses, ocular prostheses, cerebrospinal fluid shunts and contact lenses, and intrauterine contraceptive devices [176]. 2.6 million orthopedic implants inserted into humans annually in the United States, approximately 4.3% become infected. The annual infection rate for cardiovascular implants is even higher (7.4%). When considering all indwelling devices, the number of implant-associated infections approaches approximately 1 million per year [177, 173, 178].

At the cellular level, implant-associated infections are the result of bacterial adhesion to a biomaterial surface. Upon implantation, a competition exists between integration of the material into the surrounding tissue and adhesion of bacteria to the implant surface. For a successful implant, tissue integration occurs prior to appreciable bacterial adhesion, thereby preventing colonization at the implant. However, host defences are often not capable of preventing further colonization if bacterial adhesion occurs before tissue integration [179]. A 6 h post-implantation ‘‘decisive period’’ has been identified during which prevention of bacterial adhesion is critical to the long-term success of an implant [180]. Over this period, an implant is particularly susceptible to surface colonization. At extended periods, certain species of adhered bacteria are capable of forming a biofilm at the implant-tissue interface. Biofilms are remarkably resistant to both the immune response and systemic antibiotic therapies, and thus their development is the primary cause of implant-associated infection. The formation of a pathogenic biofilm ensues from the initial adhesion of bacteria to an implant surface. Thus, inhibiting bacterial adhesion is often regarded as the most critical step to preventing implant-associated infection [181, 173].

Implant infections or biofilm formation can be traced to several sources including the ambient atmosphere of the operating room, surgical equipment, clothing worn by medical professionals, resident bacteria on the patient’s skin, and bacteria already in the body [182]. Although sterilization and the use of aseptic techniques greatly reduces the levels of bacteria found in hospital settings, pathogenic microorganisms

are still found at the site of approximately 90% of all implants [183]. The most common pathogens that cause implant infections include Gram-positive *Staphylococcus aureus* and *Staphylococcus epidermidis,* which are responsible for up to 60% of all prosthetic hip implant infections since 1980 [182]. *S. aureus* infections proceed rapidly and are generally more severe than *S. epidermidis* infections. However, *S. epidermidis* has more accessibility as an opportunistic pathogen since it is found ubiquitously on the skin. Other bacteria that have been implicated in implant-associated infections include Gram-negative *Escherichia coli*, *Pseudomonas aeruginosa*, and those from the Proteus group (e.g., *P. mirabilis* and *P. vulgaris)* [182].

A pathogenic biofilm formation occurs in many steps which can also be categorized based on time dependent phases and formation of steps. The coating of surfaces with a layer consisting of proteins such as fibronectin, vitronectin, fibrinogen, albumin, and immunoglobulins, many of which serve as binding ligands to receptors on colonizing bacteria represents the initial step of biofilm formation (Fig.1.12a, Step 1). Following, bacteria, transported to the substratum (Fig.1.12a, Step 2), adhere through either a nonspecific or specific binding reaction (Step 3). These steps can be included in phase I (Figure 1.12b). Phase I also involves reversible cellular association with the surface over the first 1–2 h post-implantation. This nonspecific association is mediated through long (e.g., gravitational, van der waals, and electrostatic interactions) and short (e.g., hydrogen bonding, dipole–dipole, ionic, and hydrophobic interactions) range forces. If the forces are weak, bacteria may desorb into the liquid (Step 4). Once attached firmly to the substratum, bacteria begin cell-to-cell signal communications (Step 5) that may control growth, replication, plasmid conjugation, secretion of various virulence factors, and secretion of extracellular mucopolysaccharides, which can form a three-dimensional gelatinous matrix (Figure 1.12a, Steps 6, 7, and 8). These steps can be named phase II (Figure 1.12b). It begins approximately 2–3 h later and is characterized by stronger adhesion between the bacteria and the foreign material. Irreversible molecular bridging can settle down between compounds on the cell and substrate surfaces through the specific chemical reactions [184]. Both polysaccharides on and adhesin proteins within the bacterial membrane facilitate attachment to substrate surfaces. Beyond phase II, certain bacterial strains are capable of forming a biofilm if provided with an

appropriate supply of nutrients. During biofilm formation, bacteria secrete an exopolysaccharide layer that retains nutrients and protects the microorganisms from the immune response [173, 185, 186, 184].

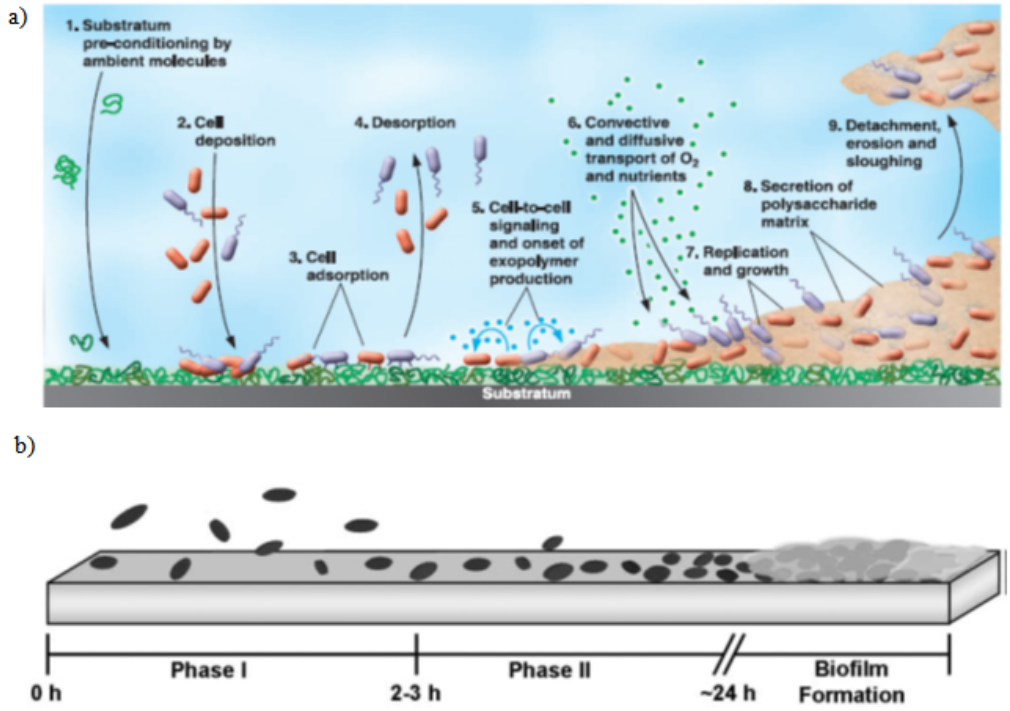

Figure1.12: a) Biofilm formation [176], b) Representation of bacterial adhesion to a biomaterial substrate. Phase I adhesion involves reversible cellular association with the surface. During Phase II, bacteria undergo irreversible molecular bridging with the substrate through cell surface adhesin compounds. After approximately 1d, certain bacterial species are capable of secreting a protective exopolysaccharide matrix (biofilm) that protects the adhered bacteria from host defences and systemically-administered antibiotics [173].

With the protective polysaccharide coating and sequestered nutrients, bacteria in biofilms exhibit extreme resistance to antibiotics. In some cases, it has been found that killing bacteria in a biofilm requires roughly 1000 times the antibiotic dose necessary to achieve the same results in a suspension of cells [187].

In the strategy for the prevention of infections, much has been done to improve the operating standards, minimize the possibility of contamination during surgery, reduce the establishment of infection by peri-operative antibiotic prophylaxis, and confine pathogenic strains by patient isolation [188, 189]. Along these directions further improvements can still be made, but little advancements in terms of decreased infection rates are being expected in return of this type of efforts [189]. As a

consequence, over the last 15 years, increasing attention has progressively been focused on the epidemiology and the pathogenesis of the infections, especially those associated to implant materials, in order to build knowledge and gain better control over this phenomenon. Many effort have been directed to investigate which are the most important etiologic agents involved, the pathogenetic mechanisms leading to microbial adhesion, colonization of implant surfaces, and evasion of the host defenses, the most crucial virulence factors, the nature and properties of microbial biofilms and, not last, the progressive alarming appearance of antibiotic resistant strains [190].

1.5.2.1 Main pathogen bacteria involved in implant Infections

Organization of bacteria in biofilm that cause implant infections is not random. It is quietly depending on implantation site and bacterial communication.

In orthopedics, it is well established that the vast majority of implant-related infections is due to Gram positive aerobes, *staphylococci* species in first place. Based on orthopedic clinical isolates, exclusively from infections associated to prosthetic implants (including these: artificial knees, hips, tendons and ligaments, fixation systems, and so on), about 16% of the infections are of polymicrobial origin. A very large proportion of all implant-related infections are caused by staphylococci (roughly four out of five), and two single staphylococcal species, respectively *Staphylococcus aureus* and *Staphylococcus epidermidis,* account together for two out of three infection isolates. They represent, in absolute, the main causative agents in orthopedics, while CoNS species other than *S. epidermidis*, and, especially among them, *Staphylococcus hominis* and *Staphylococcus haemolyticus*, contribute to an additional 13% of the infections (Figure 1. 13). In order of relevance in terms of prevalence then there follow *Pseudomonas aeruginosa and Enterococcus faecalis.*

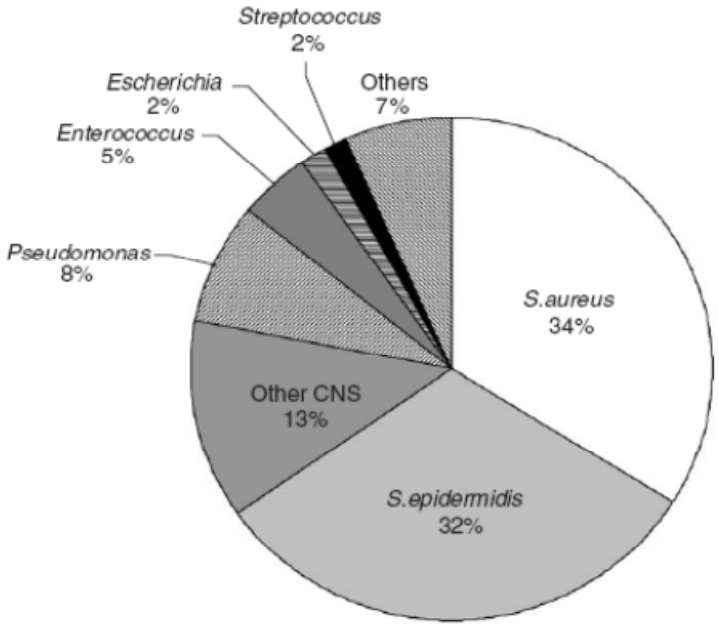

Figure 1.13: Frequency of main pathogenic species among orthopedic clinical isolates of implant-associated infections [190].

In other words, infections caused by all existing pathogenic microbial species except *staphylococci* represent together only a minority of implant infections, just about 22%. The *Staphylococcus* genus therefore acquires a huge importance in implant-related infections. It comprises important pathogenic species such as *S. aureus*, at times currently even deserving the denomination of ‘‘superbug’’[191], along with a broad number of typically saprophytic species capable to become harmful only when host defenses are significantly endangered. This holds a series of implications, the most important of which is that there are two main similar enemies belonging to the same group to defeat: *S. aureus* and *S. epidermidis*. Another one is that fully understanding the mechanisms underlying staphylococcal virulence and pathogenicity [192, 193] would provide unique clues to tackle the phenomenon of implant infection both on a prevention and on a treatment level, with significant numeric impact and vast clinical outcomes. As far as this is concerned, the comparison of the, at times subtle, differences between saprophytic CoNS species, and the more aggressive S. aureus can give important insights [194, 190].

In case of dental implant infections, it has been shown that there are specific associations among bacteria in dental biofilms. Socransky *et al.* examined over 13.000 subgingival plaque samples from 185 adult subjects and used cluster analysis

and community ordination techniques to demonstrate the presence of specific microbial groups within dental plaque (Figure 1.14) [195]. Six closely associated groups of bacterial species were recognized. These included the *Actinomyces*, a yellow complex consisting of members of the genus *Streptococcus*, a green complex consisting of *Capnocytophaga* species, *Actinobacillus actinomycetemcomitans* serotype a, *Eikenella corrodens* and *Campylobacter concisus* and a purple complex consisting of *Veillonella parvula* and *Actinomyces odontolyticus*. These groups of species are early colonizers of the tooth surface, and their growth usually precedes the multiplication of the predominantly gram negative orange and red complexes (Figure 1.14). Similar relationships have been demonstrated in *in vitro* studies examining interactions between different oral bacterial species. These studies of oral bacteria have indicated that cell-to-cell recognition is not random but that each strain has a defined set of coaggregation partners [196].

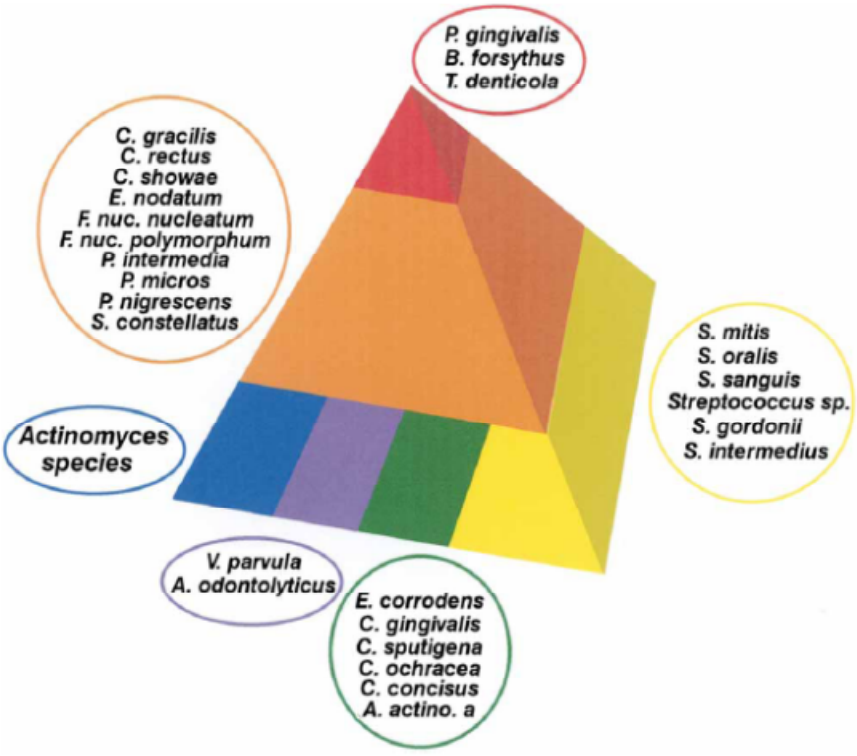

Figure 1.14: Diagram of the association among subgingival species [196].

1.6 Approaches for Implant-Tissue Integration

1.6.1 Implant surface modifications for better osseointegration

Variations in biological activity at the interface between materials and host tissue can be correlated with specific surface properties. Chemical composition, energy, roughness, and topography [197, 198] are all believed to help determine the activity of different cell lines, acting either separately or synergistically. The connections between the physico/chemical properties of surfaces and cellular responses are still not fully understood. Once they are elucidated, however, they will improve our understanding of fundamental biological processes. At the same time, the ability for tailoring surfaces to control cellular events and guide the cells along predetermined pathways will pave the way for the rational design of a new generation of biomaterials that can be integrated in the human body more effectively and beneficially. In the classical conception of conventional biologically, inert or biocompatible materials will gradually be replaced by a new generation of ‘‘smart’’ materials with intelligent surfaces able to interact decisively with the biological environment, and that may even initiate selective reactions in response to differential cues. Surface properties of materials can be modified on a range of scales by various techniques, [199, 200] with the common aim of collecting information to unravel the link between surface cues and cellular response. Straightforward surface treatments that have frequently been used to modify the behavior of biocompatible metals include polishing, grinding, blasting, and machining and chemical methods such as acid etching, alkali etching and anodization [201-203, 52]. Such mechanical methods, used either individually or in combination with other treatments, mainly cause the formation of different topographies with inhomogeneous micrometric features (Figure 1.15) [97]. These features have been demonstrated to have an impact on cellular activities and on osseointegration [69, 204, 205, 97, 206]. Another approach towards the creation of biologically active implants surface involves the application of an additional coating onto the implant surface by means of physicochemical and biochemical deposition techniques [207].

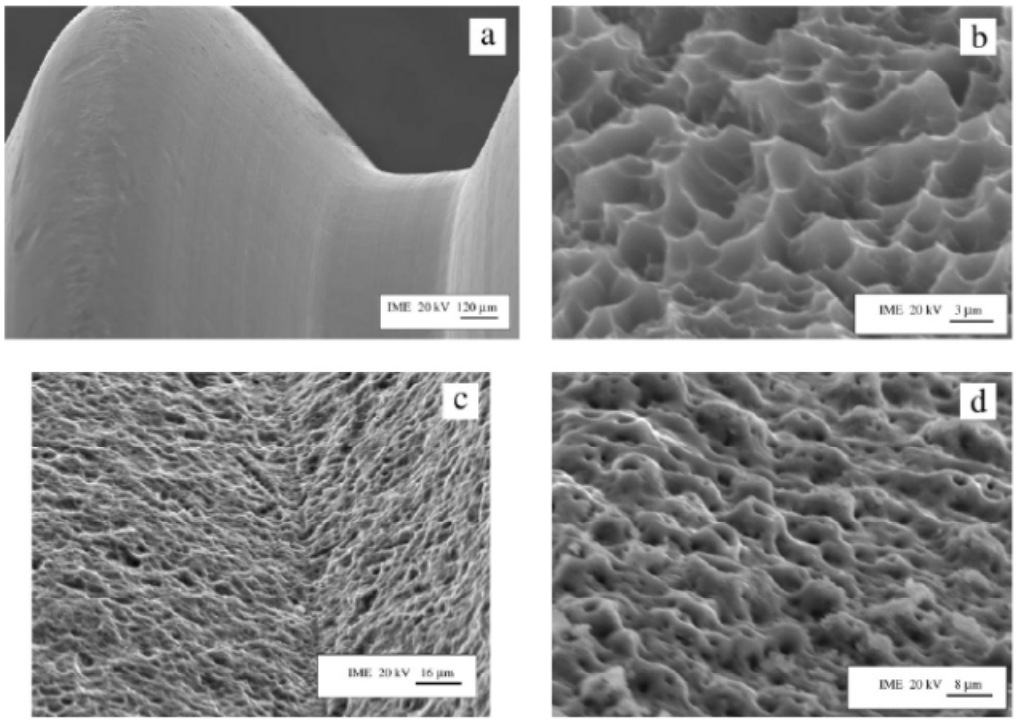

Figure 1.15: SEM micrographs of the dental implants surfaces. (A) machined, (B) acid etched, (C) sandblasted and (D) anodized [97].

1.6.1.1 Chemical surface modifications

Recent work has established that key biological processes, including protein adsorption, cell proliferation, and gene expression, can be controlled to some extent by using chemical methods to modify the surface properties of biocompatible materials [208]. The most popular and efficient ways to modify surfaces involve direct chemical modifications with acids and oxidants. Chemical treatments are attractive for large-scale manufacturing because they are simple and provide efficient and uniform access to all surfaces, even on multifaceted devices with complex 3D shapes such as dental screws and cardiovascular stents. In principle, chemical modifications leading to controlled surface functionalization can be also applied to other families of materials such as polymers [209], thus extending the scope of the technique. For example, it was reported that poly(lactic-coglycolic acid) can be nanostructured by chemical etching with NaOH, resulting in a material with novel surface features able to enhance the activity of various cell types [85, 32, 210]. Together, these characteristics make chemical treatments an advantageous and flexible way to modify biomaterials for commercial applications. Different chemical

treatments with acids, [211-213] bases and oxidants [214] have been used to create micrometer-scale and submicrometer-scale textures on surfaces (Figure 1.16) [207].

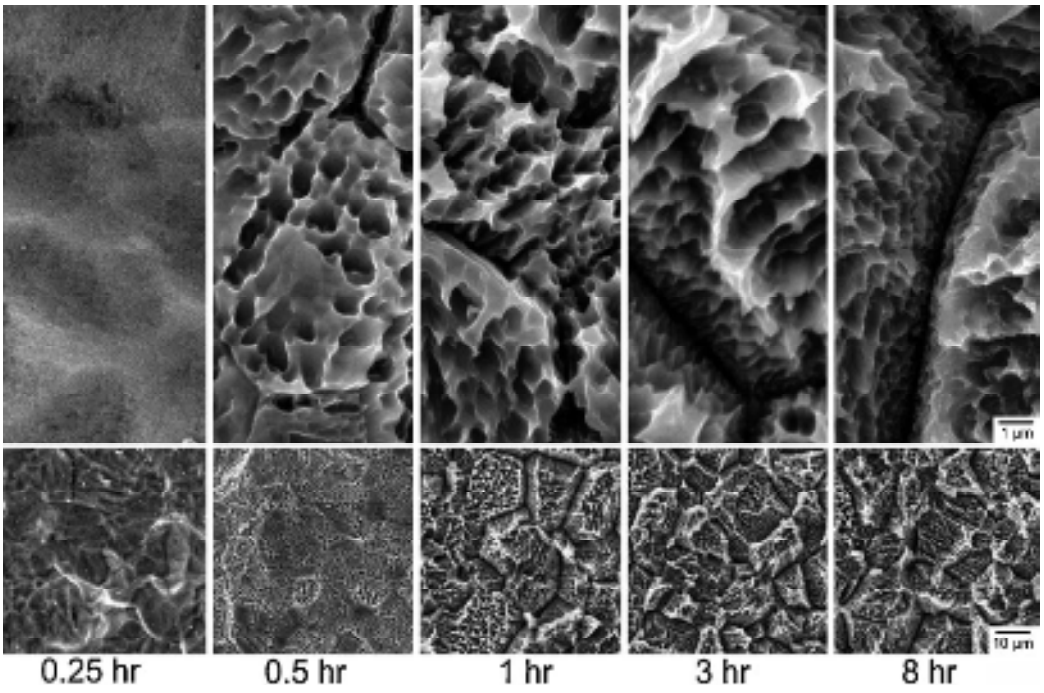

Figure 1.16: Scanning electron microscopy (SEM) images illustrating various microtextures achieved on Ti after etching in 48% H_2SO_4 at 60^0C for 0.25, 0.5, 1, 3, and 8 h. The upper row displays micrographs with higher magnification [207].

Such studies have revealed that chemically treated surfaces can enhance the adhesion and proliferation of osteogenic cells, precipitation of apatite, and the expression of bone-related genes and proteins [202, 215]. From these observations, surfaces that are hydrophilic, microrough, and porous appear to have beneficial effects on various biological phenomena.

Although chemical treatments have yielded a variety of microtextured implants with improved clinical outcomes, the demonstration in several laboratories that cell respond to nanofeatures has intensified the application of chemical treatments for nanostructuring biometals [71, 216]. A particularly effective method for nanostructuring titanium-based metals is electrochemical oxidation [217]. By adjusting parameters such as the nature of the electrolyte, voltage, and current

density, smooth Ti surfaces [218-220] were transformed into nanotubular tructures (Figure 1.17), with diameters less than 100 nm [207].

Biological studies carried out on these anodized Ti surfaces revealed a general increase of in vitro activity, measured by enhanced osteoblastic activit and mineral precipitation [221].

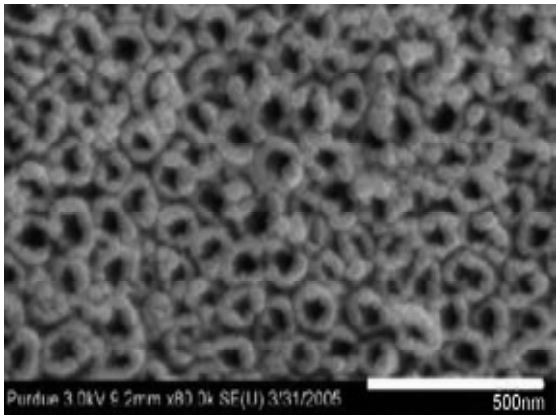

Figure 1.17: SEM image of nanotubular structures created by anodization of Ti [207].

Anodization creates nanoscale topographies, yet it also allows control over other physical properties such as pore size and the thickness of the oxide layer, [222] thus providing a way to conduct targeted experiments (e.g., varying only the dimension of surface features) to reveal how each of these parameters affects cellular behavior. A different chemical approach for modifying the surface of metals is based on the observation that etching with combinations of strong acids and oxidants can generate a micro and nanotopography. Mixtures of sulfuric acid (H_2SO_4) and hydrogen peroxide (H_2O_2) have been shown to reproducibly yield networks of nanometer-sized pits around 20 nm in diameter (Figure 1.18) on Ti [223, 224] , and Ti6Al4V alloy [225].

Surface morphology, wettability, nanoroughness, and the thickness of the TiO_2 overlayer can be controlled by adjusting the length of exposure to the etching solution. It is also possible to vary the density of OH groups on the surface, which is believed to influence cell activity [224]. Unlike other methods described so far for structuring surfaces, this chemical treatment of Ti and its alloys creates surfaces with distinctive discriminatory effects on different cell types.

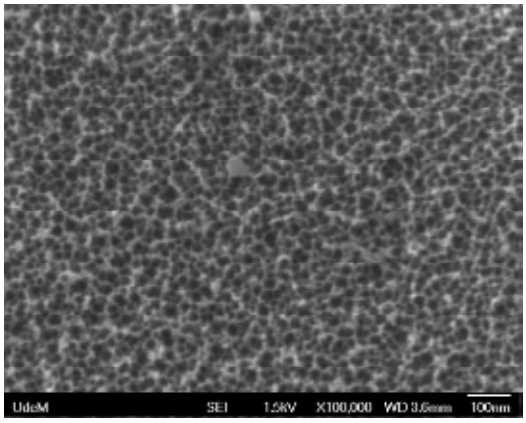

Figure 1.18: SEM image of the characteristic nanometric sponge-like structure that is achieved by treatment of Ti with H_2SO_4/H_2O_2 [207].

The properties of surfaces can also be modified at the nanometric level by using other processes such as sol–gel [226] and chemical vapor deposition (CVD) [227]. In vitro biological tests on materials coated in these ways have demonstrated that the novel surface features have beneficial effects on bone cell activities, including adhesion, spreading, and matrix mineralization. Chemical strategies have been efficiently exploited to create nanostructured coatings of materials that are not directly used in implantology. Coatings of nanostructured niobium oxide and diamond-like carbon, [228] when deposited by sol–gel or CVD on titanium and other substrates, have demonstrated significant bioactivity, thus providing additional avenues for improved biomaterials. In addition, alkali treatment of bulk niobium has resulted in the formation of nanometric fibers (Figure 1.17) that favor precipitation of apatite from simulated bodily fluids [229, 230].

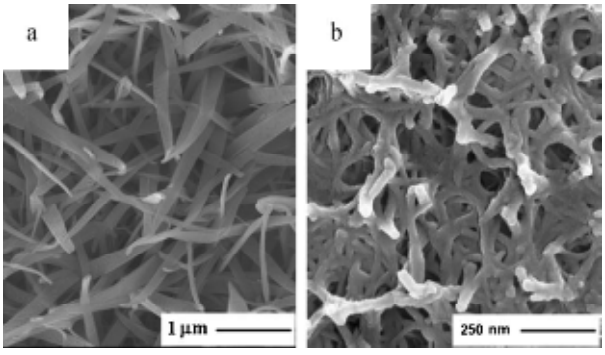

Figure 1.19: SEM images of rod-like structures resulting from the treatment of Nb with NaOH at a) 60^0C (diameter of the rods in the 100–300-nm range) and b) 80^0C (diameter of the rods in the 50–100-nm range) [207].

Electrochemical deposition makes it possible to create coatings comprised of wire like nanometric crystals of hydroxyapatite (Figure 1.18), which enhance bone remodeling and maturation [231] .Similarly, composite coatings of hydroxyapatite and multi-walled carbon nanotubes deposited on titanium have been achieved by electrophoretic deposition [207].

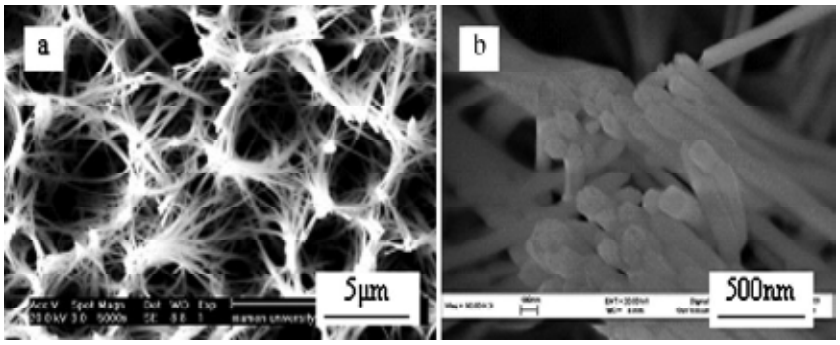

Figure 1.20: SEM images of an electrochemically deposited coating of calcium phosphate on smooth Ti. a) Microporous structure. b) Crystal grains on the nanometer scale [207].

1.6.1.2 Physical surface modifications

The vast majority of surface morphology modifications can be categorized under physical surface modifications that have been used to alter biomaterials and endow them with useful new properties, and such alterations have also shown to favor diverse biological processes [232, 233]. Electrostatic and plasma spray, as well as physical vapor deposition (PVD) techniques such as electron-beam evaporation, deposition and grit blasting can yield superficially deposited bioactive layers [52, 97, 234, 206]. The deposition of TiO_2 and hydroxyapatite in this way has been shown to enhance the activity of osteoblastic cells and to favor osseointegration in vivo [232, 235]. Although these methods generally result in modifications on the micrometer scale, such physical approaches can also be used to create nanostructures.

Laser-based approaches have been exploited to produce a coating of calcium phosphate on titanium and its alloys. Such coatings have been reported to have multiphase compositions ranging from the nano- to mesoscale [236] and to enhance in vitro osteogenic cell attachment, growth, and differentiation. A different approach based on compaction of metallic nanoparticles (Ti, Ti6Al4V, CrCoMo) has been successfully applied to produce nanostructured surfaces. The inherently higher

number of particle boundaries in materials prepared from nanoparticles was suggested as an explanation for the observed enhanced adhesion of osteoblastic cells [53]. Moreover, there was more deposition of calcium and phosphorus from simulated bodily fluid, which suggests that mineralization can also be enhanced by appropriate nanostructuring [237].

1.6.1.3 Biological surface modifications

In the last few years there has been a major shift in the design criteria for modern synthetic biomaterials. An understanding of cell and molecular biology had led biologists, chemists and material scientists to design biomaterials equipped with molecular cues mimicking certain aspects of structure or function of natural extra-cellular microenvironments. Hence biological surface modification is aimed at controlling cell and tissue response to an implant by immobilizing biomolecules representing such molecular cues on the surface of biomaterials. Adsorption, entrapment, and covalent attachment are the three mechanisms by which biomolecules are immobilized on the surface of a biomaterial [52].

Currently available organic coating approaches include (1) immobilization of ECM proteins (such as collagen) or peptide sequences as modulators for bone cell adhesion; (2) deposition of cell signaling agents (bone growth factors) to trigger new bone formation; (3) immobilization of DNA for structural reinforcement; (4) enzyme-modified titanium surfaces for enhanced bone mineralization [122].

Immobilization of ECM proteins or peptide sequences

Because of the crucial role of extracellular matrix components in osteoblast functions, extensive studies have been performed to functionalize titanium implant surfaces with elements of ECM proteins. Contact of cells with other cells and the surrounding ECM are mediated by cell adhesion receptors. The cell membrane receptor family of integrins is involved in cell adhesion to ECM proteins. These integrins bind to specific amino acid sequences within ECM molecules. In particular, the amino acid sequence arginine–glycine–aspartic (RGD) has been identified as a cell adhesion motif in many ECM proteins, including fibronectin, vitronectin, type I collagen, osteopontin and bone sialoprotein. Thus, by immobilizing ECM proteins or peptide sequences onto titanium implant materials, bio-functional surfaces are produced that bind adhesion receptors and promote cell adhesion. Additionally, the

ECM also takes an active part in regulating the cellular processes and responses, influencing not only adhesion, but also proliferation, migration, morphological change, gene expression and cell survival by intracellular signaling. As such, the biological acceptance of implants can be improved by modifying implant surfaces with ECM components, thereby mimicking the natural interface and influencing the response of osteoblastic cells.

Although surface immobilization of entire proteins, such as fibronectin and vitronectin, is demonstrated to be effective in enhancing cellular attachment [238], research has focused on the design of materials representing only short peptide fragments of ECM proteins. These peptide sequences can possess similar functionalities, for example, receptor specificity, binding affinity, and signaling of cell responses, compared to their native proteins.These sequences can be produced synthetically, allowing precise control over their chemical composition and avoiding issues related to concerns on proteins from animal sources. As compared to the long chain proteins, the short peptide sequences are generally more resistant to denaturizing agents [239]. Furthermore, an entire ECM protein tends to be randomly folded upon adsorption to the biomaterial surface, resulting in a less effective availability of the receptor-binding domains as compared to short peptides. The most commonly used peptide sequence for surface modification is cell adhesion motif RGD. Additionally, various other peptide sequences have been immobilized onto implant materials [240]. To provide a stable link, peptide sequences are usually covalently attached to the titanium surface, e.g. via functional groups like hydroxyl-, amino-, or carboxyl groups. RGD-functionalized materials are reported to improve early bone ingrowth and matrix mineralization in implanted constructs and to induce more bone contact to the implant [241].

Growth factor immobilization

Growth factors are proteins that serve as signaling molecule to induce an intracellular signal transduction system that produces a biological response. Once they release from an implant surface can increase the osteoblastic activity of the bone tissue. Bone regeneration around implants can be strongly enhanced by immobilizing growth factors such as bone morphogenetic protein (BMP), transforming growth factorbeta (TGF-β), fibroblast growth factor (FGF), platelet derived growth factor (PDGF), and insulin-like growth factor (IGF) to the titanium surface [242]. The most

common osteogenic growth factors used for biomedical purposes are the members of the TGF-β superfamily, including the BMP family. In particular BMP-2, BMP-7 and TGF-β1 are promising growth factors for enhanced bone formation around the implant [243]. Growth factors can be adsorbed or covalently bound to the titanium surface, but are commonly added to CaP or collagen-coated implants. Growth factors immobilized on titanium implants pre-coated with collagen or CaP were found to be more effective in inducing bone formation than growth factors bound to untreated titanium surfaces [244]. This may be due to a sustained delivery profile or a higher stability of the growth factor. Overall, loading implants with growth factors has shown to accelerate bone formation and to facilitate the bridging of small gaps between implant and surrounding bone. In summary, coating implants with locally acting growth factors can improve the remodelling process at the tissue–implant interface, and is therefore a promising option for establishing an improved integration of implants into healing bone [122].

Deoxyribonucleic acid (DNA) coatings

Another possibility for implant surface modifications is the generation of DNA-containing coatings. The structural properties of DNA show high potential for this unique biomolecule to be used as a biomaterial coating, regardless of its genetic information. DNA-based coatings improved the deposition of CaP, favorable for direct apposition of bone tissue to the implant surface. Furthermore, DNA-based coatings proved to be eligible for functionalization with biologically active growth factors, and hence can modulate cell response. These beneficial effects on cell and tissue response show potential for DNA-based surface modifications with respect to immunology, drug-delivery, and apposition of bone mineral [245, 246].

Enzyme coatings

A novel approach for surface modification utilizes enzyme-modified titanium surfaces to enhance bone mineralization along the implant surface. The enzyme alkaline phosphatase (ALP) is known to play an important role in the mineralization process of bone and cartilage. ALP appears to act both to increase the local concentration of inorganic phosphate (Pi), required for physiological mineralization of hard tissues, and to decrease the concentration of extracellular pyrophosphate (PPi), a potent inhibitor of mineralization. Under physiological conditions, ALP

coatings accelerated mineralization onto the titanium surface. These newly developed enzyme coatings seem promising for an early and improved implant fixation [247].

Ca-Phosphate coatings

Another surface modification of implant surfaces under bioactive coating is Calcium phosphate coatings (CaPs). They are often used in the biomedical field due to their similarity with the mineral phase present in bone and teeth. Hydroxyapatite, or more specifically carbonate apatite, is by far the most abundant inorganic phase in the human body. Carbonate apatite comprises a chemical composition closer to bone and dental enamel than that of hydroxyapatite. The relation between carbonate apatite and hydroxyapatite is important, because carbonate increases the chemical reactivity of apatites. This occurs by an increase of the solubility of the product and rate of dissolution in acids, and by reducing the thermal stability. Since carbonate is known as an effective crystal growth inhibitor, carbonate apatite consists of smaller crystals than hydroxyapatite [52, 121].

Calcium phosphate (CaP) ceramics are known for their bioactive properties. Generally, bioactive materials interact with surrounding bone, resulting into the formation of a chemical bond to this tissue ("bone-bonding"). CaP ceramics are too brittle for use as bulk material under loaded conditions, which makes that CaP ceramics are frequently applied as coatings onto the surface of metallic implant materials in order to combine the mechanical strength of metals with the excellent biological properties of CaP ceramics. Following utilization of CaP coatings for orthopaedic and dental implants, numerous reports have been published about the osteoconductive properties of CaP-coated implants (osteoconduction refers to the ability of a biomaterial to support the growth of bone over its surface). These CaP coatings are described to induce an increased bone-to-implant contact, to improve the implant fixation, and to facilitate the bridging of small gaps between implant and surrounding bone [248, 124, 122].

CaP-organic coatings

Since bone is composed of an organic matrix strengthened by an inorganic CaP phase, research during the last decade composite coatings made of both biomolecules have therefore generated a great deal of interest for implant surface modifications. Due to potential capability of CaPs, Ca-P coatings are the most popularmethod that is used to loading therapeutic and bioactive agents in. This allows diffusion of the respective agent(s) into the coating after processing. The degree and type of bonding of these agents largely depends on the composition, microstructure and properties of the finished coating products. For example, a nanoporous biomimetic apatite coating adsorbs more serum proteins than the dense plasma-sprayed hydroxyapatite coating. The development of a biomimetic coating approach has made it possible to incorporate therapeutic agents directly into the Ca-P coating. The molecules of interest dissolved in the calcifying solution can be adsorbed or incorporated into the forming Ca-P coating during the coating process. The most applicable embedded molecules into Ca-P coatings as carriers are several proteins and therapeutic agents, including albumin, collogen, BMPs, bisphosphonates, antibiotics and amelogenin [249, 52, 121].

Amelogenins and their incorporation in Ca-P coatings

The use of naturally occurring matrix proteins that regulate mineral crystal growth holds promise as one way to biologically regulate bone formation. Amelogenin proteins, the principal components of the developing dental enamel extracellular matrix, have been postulated to facilitate the elongated and oriented growth of the carbonated apatite crystals during enamel formation [249].

Thus, amelogenin, the predominant protein components of secretory stage in tooth enamel, have been using as a good candidate to fabricate biomimetic coating implant materials. Furthermore, they have potential signal transduction functions during tooth and bone development and can promote the adhesion of several cell type. Based on potential signaling the effect of amelogenin and its ability to promote cell adhesion, control apatite crystal morphology and organization can be good candidate for biomimetic coating that would not only improve the implant integration but also promote bone tissue engineering [250].

1.6.2 Strategies to prevent implant infections

Implant-associated infection is still one of the most serious complications in implant surgeries due to the existence of immune depression in the peri-implant area. Many approaches with understanding of pathogenesis of implant-associated infections have been applied to prevent implant infections. In this section, current strategies such as systemic and local antibiotic treatment, nonfouling surfaces, utilization of antimicrobial agents and peptides have been explained with advantages and disadvantages for implant infection treatment.

1.6.2.1 Antibiotic treatment

One of the most applied conventional treatments to prevent implant associated infection is antibiotics which are chemical compounds that inhibit or abolish the growth of microorganisms, such as bacteria, fungi or protozoans. The main goal of treating various types of infections should be reduce the bacterial load in the wound to a level at which wound healing processes can take place. Conventional systemic delivery of antibiotics entails poor penetration into ischemic and necrotic tissue and can cause systemic toxicity with associated renal and liver complications, which result in a need for hospitalization for monitoring. Alternative local delivery of antibiotics by either topical administration or by a delivery device may enable the maintenance of a high local antibiotic concentration for an extended duration of release without exceeding systemic toxicity [251, 252]. Hence, controlled release of antibiotics from the implant or medical devices shows many advantages over systemic treatments, such as increasing the local dosage of antibiotics, as well avoiding systemic side effects [178, 253, 175, 177].

For nondegradable implants, such as central venous catheters, urinary catheters and stents, surface coating is doubtless a simple method, which can maintain the bulk properties of the implants as well as increase the antibacterial ability of the surface. Owing to the structure of antibiotics, which normally have a molecular weight of less than 1000, direct coating through solvent dipping is obviously not suitable. The retention of drugs on the surface is limited and the release rate cannot be controlled. However, many antibiotics are synthetically designed as anionic derivatives with carboxylate, phosphate or sulfate substitutes [254]. Thus, the immobilization of antibiotics on the surface can be facilitated by an electrostatic force. Besides

immobilization of antibiotics onto implant surfaces, an alternative method is to first blend the antibiotics into the coating materials and then coat the mixture on the surface. The options for the coating materials include biodegradable or non-degradable polymers. For the nondegradable polymer coating, normally polyurethane [255-257], the release of the antibiotics is entirely through diffusion.

The release profile can be also controlled through the coating strategy. For example, another thin layer can be coated on the top of the layer loaded with antibiotics, thus providing a barrier to restrict the fast initial burst of the release [258]. Controlled release can also be approached through creating a coating with a concentration gradient of loaded antibiotics; for example, with a higher concentration in the inner layer and a lower concentration in the outer layer. Biodegradable polymer coating is also applicable [259-261]. The release of antibiotics is not only through diffusion, but also influenced by the degradation rate and mechanism of the coating. FDA-approved biodegradable polymers include PLA, PGA, PLGA, polyanhydride, and so on. All of these show great potential as matrixes for the release of antibiotics [262, 263].

Antibiotics are also incorporated into non-degradable PMMA bone cement and beads for prophylaxis and treatment of total joint arthroplasty infection, treatment of chronic osteomyelitis and prophylaxis of infections in open fracture repair [264]. Although these have been put into clinic application, the release of most antibiotics from the PMMA cements or beads are far from satisfactory [265, 266]. For example, for gentamicin, less than 50% was observed to be released from implants after 4 weeks, and no continuous release was found after that, which may be due to the solid, glassy, non-swelling properties of the PMMA matrix. Thus the antibiotic-loaded biodegradable implants show great potential [267-270]. Unlike PMMA, biodegradable implants degrade over time, eliminating the need for a second surgery to take them out, and thereby preventing the possibility of re-infection during second surgery. Moreover, the loaded antibiotics can be totally released out of the implants once they degrade. The degradation rate can be tuned through the selection of the biodegradable chemical structure and through building up a concentration gradient in the implants.

Antibiotics are also combined with bioactive ceramics as a coating for metal implants. The utilization of a bioactive ceramic coating containing hydroxyapatite

(HA), calcium phosphate and other osteo-conductive materials as antibiotic carriers offers the added value of providing the physiochemical environment and structural scaffold required for bone-implant integration. In vitro release of antibiotics from hydroxyapetite coated implants has been reported for chlorhexidine, vancomycin, gentamicin, tobramycin and several other antibiotics [252, 271].

In all application of antibiotic treatment, the main concern with all of these antibiotics is the development of resistant bacteria. Many important pathogens, *S. aureus* in first line among them, have long been recognized to exhibit always more alarming levels of antibiotic resistance [272, 273]. Moreover, bacteria forming biofilms on prosthetic surfaces are per se particularly resistant to antimicrobials and tend to survive to aggressive chemotherapy even in the absence of specific antibiotic resistance factors. In consideration of this, it may result clear how important is to survey the presence of antibiotic resistant strains at clinical setting, not uniquely with the scope to decide the patient treatment regimen [190].

The mechanisms of resistance to antibiotics in bacterial biofilms are beginning to be elucidated [274]. Figure 1.21 shows three main hypotheses. The first hypothesis is the possibility of slow or incomplete penetration of the antibiotic into the biofilm. Measurements of antibiotic penetration into biofilms in vitro have shown that some antibiotics readily permeate bacterial biofilms [275]. There is no generic barrier to the diffusion of solutes the size of antibiotics through the biofilm matrix, which is mostly water [276].

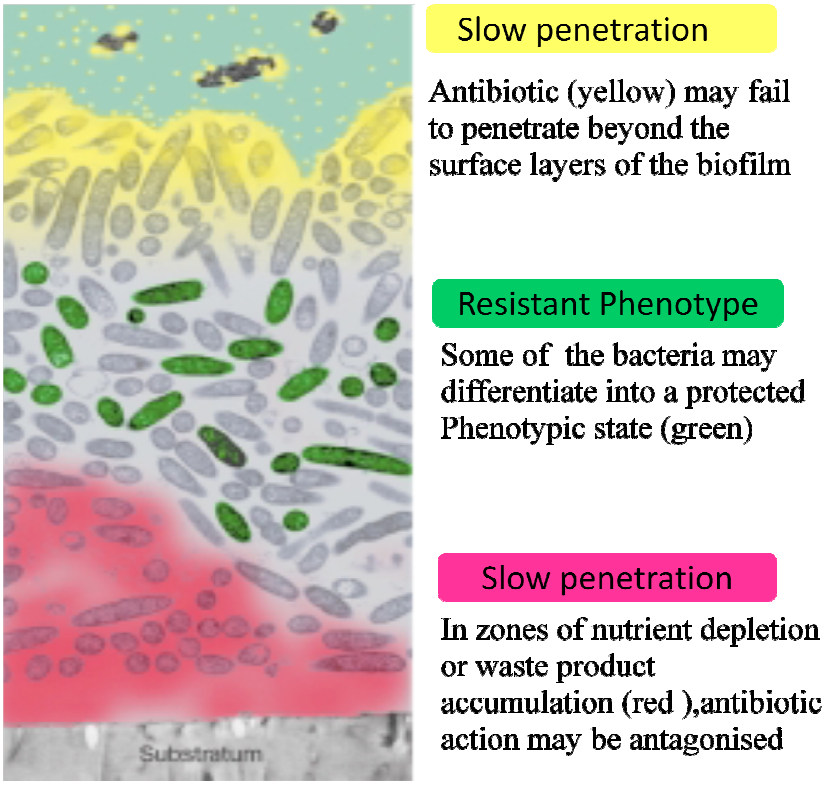

Figure 1.21: Three hypotheses for mechanisms of antibiotic resistance in biofilms [181].

The second hypothesis depends on an altered chemical microenvironment within the biofilm. Microscale gradients in nutrient concentrations are a well known feature of biofilms. Findings from studies with miniature electrodes have shown that oxygen can be completely consumed in the surface layers of a biofilm, leading to anaerobic niches in the deep layers of the biofilm [277]. Concentration gradients in metabolic products mirror those of the substrates. Local accumulation of acidic waste products might lead to pH differences greater than between the bulk fluid and the biofilm interior, [278] which could directly antagonise the action of an antibiotic.

A third and still speculative mechanism of antibiotic resistance is that a subpopulation of micro-organisms in a biofilm forms a unique, and highly protected, phenotypic state-a cell differentiation similar to spore formation. This hypothesis is lent support by findings from studies that show resistance in newly formed biofilms, even though they are too thin to pose a barrier to the penetration of either an antimicrobial agent or metabolic substrates. Additionally, most bacteria in the biofilm, but not all, are rapidly killed by antibiotics [279]. Survivors, which might consist of 1% or less of the original population, persist despite continued exposure to

the antibiotic. The hypothesis of a spore-like state entered into by some of the bacteria in a biofilm provides a powerful, and generic, explanation for the reduced susceptibility of biofilms to antibiotics and disinfectants of widely different chemistries [181].

In addition these mechanism steps, a number of studies have reported the existence of a strong association between genomic DNA mobile elements termed transposons and important virulence factors as well as most of the genes for the resistance to anti-microbials. The importance of this association relies on movement of transposons across the microbial population, transferring clusters of genes, crucial to the ability of bacteria to do harm and to survive to medical treatments, not only among strains of the same species, originating new dangerous clones, but even across different species [190, 280].

1.6.2.2 Antimicrobial agents

An attractive alternative to using antibiotics would be to use an antiseptic, such as chlorhexidine or quaternary ammonia compounds, since antiseptics tend to have broad spectrum activity against Gram-positive and Gram-negative bacteria. Chlorhexidine is commonly used in surgical scrub, hand wash, and to clean wounds, but has been used in association with external fixator pins [281], polymeric coatings on titanium [282], and other indwelling implants [283, 284]. There are disadvantages reported for using chlorhexidine in association with implants, including the toxicity of the antiseptic to host cells. In vitro, chlorhexidine diacetate has been reported to be lethal to fibroblasts [285], probably because chlorhexidine diacetate lyses the host cell membranes in the same way as it does bacterial cell membranes. Hypersensitive reactions are also known to occur when patients are exposed to chlorhexidine diacetate [286, 287]. A second disadvantage is that chlorhexidine diacetate resistance has been observed in various staphylococci and Gram-negative bacteria, particularly with antibiotic-resistant bacteria [288]. Quaternary ammonia compounds (QAC) has also been studied for use, through covalent binding of the antimicrobial directly onto the implant surface [289]. QAC works by disrupting the cell membrane of both Gram-positive and Gram-negative bacteria [290].

Other alternative method is silver ion- and silver nitrate-based coatings on implants, since silver is known to have broad spectrum antibacterial properties. Silver-based

coatings have been studied in association with polymer andmetal implants, particularly on external fixation pins [291, 292]. Coating stainless steel pins with silver has been found to decrease the adhesion and colonization of *S. aureus, S. epidermidis, E. coli,* and *P. aeruginosa* around the coated implant [293, 294]. However, there are reports that silver is toxic to host cells, causing severe inflammatory responses [295]. Due to the toxicity of silver, "NanoSilver", which is a new form of silver consisting of silver particles (5−50 nm), has been tested and in vitro results have shown that it was effective against several type of bacteria and have indicated that it is not cytotoxic due to its higher porosity and active surface [294].

Another possible solution to the development is to use lysostaphin instead of conventional antibiotics. Lysostaphin is an antibacterial enzyme that cleaves pentaglycine bridges in the cell wall of staphylococci. A study by *Wu et al* [296] found that applying lysostaphin to *S. aureus* and *S. epidermidis* biofilms not only killed the bacteria, but also disrupted the extracellular polysaccharide matrix surrounding the bacteria [262].

1.6.2.3 Nonfouling surfaces

An important step in preventing infections is to inhibit the adhesion of proteins, biomolecules, and bacteria onto the implant surfaces. PEO or PEG and its derivatives represent a class of hydrophilic polymers that can be used to create anti-adhesive surfaces [26, 262, 297, 298, 178]. These hydrophilic polymers have highly dynamic chain structures that, when locating on surfaces, present large exclusion volumes in an aqueous environment (such as in circulation) by retaining a surrounding hydrous layer, thereby repelling the adhesion of molecular species [299], cells [300], and bacteria from the surfaces.

PEO or PEG type of polymers can be introduced onto surfaces via physical or chemical approaches. Using physical approaches, PEG is coated onto material surfaces by direct deposition such as dipping. However, PEG layer formed by physical approaches is unstable in an aqueous environment due to the good solubility of PEG in water and poor wettability with the surface. Alternatively, PEG may be chemically linked to surfaces by crosslinking or grafting. PEG can be crosslinked by argon radio frequency (RF)-plasma after spin coating on a stainless steel (SS) surface

[301] or by using dicumyl peroxide (DCP) as a crosslinking agent on the surface of a polyurethane-containing PEO segment [302]. The crosslinked PEG surface was shown to have decreased bacterial adhesion. PEG with a functional end group can be chemically grafted onto the substrate surface, such as polyurethane, glass, silicon and poly(ethylene terephthalate). The coating density and PEO chain length greatly influence the antibacterial ability. When the density of PEO is high enough, the molecules are forced to stretch out and form a layer called "molecular brush". Generally speaking, higher coating density and longer PEO chain length attain better anti-bacterial ability [178] .

Various derivatives of PEG have been testing their effectiveness against different bacteria type, osteoblast, fibroblast. For example, cell adhesion and spreading of osteoblast and fibroblast on metal oxide surfaces coated with PLL-*g*-PEG is strongly reduced in comparison to uncoated oxide surfaces [303]. *In vitro* PLL-*g*-PEG coatings are also effective at inhibiting *S. aureus*, *S. epidermidis*, *P. aeruginosa* and *Streptococcus mutans* [297, 304, 303, 305]. A biofunctionalized version of PLL-*g*-PEG copolymer with the cell-adhesive peptide Arg−Gly−Asp (RGD) motif has been synthesized and used to induce specific attachment of fibroblasts and osteoblasts to surfaces [306, 303]. The RGD motif is present in proteins such as fibronectin, vitronectin and fibrinogen. It is known to interact specifically with a number of integrin cell receptors, while being resistant to the adsorption of non-specific biomolecules. The advantage of this coating is that it enhances fibroblasts and osteoblasts, but remains inhibitory to *S. aureus*, *S. epidermidis*, *P. aeruginosa*, and *Streptococcus mutans* adhesion. Such surfaces (PLL-*g*-PEG and PLL-*g*-PEG/RGD) are believed to have potential as implant coatings, but they currently need improvement in the coating adhesion strength to the implant surface [262].

1.6.2.4 Antimicrobial peptides

A novel class of peptides, the antimicrobial peptides (AMPs), has received considerable attention over the last few decades due to their potential use as therapeutic treatments. AMPs are an evolutinary conserved constituent of the innate immune response and have been found in all walks of life including insects, plants, and animals [307-310]. Due to the wide distribution and characteristics of AMPs, it is difficult to categorize them except broadly on the basis of their secondary stucture

and aminoacid composition. The fundemental structural principle underlying all classes is the ability of the molecule to adapt a shape based on hydrophobic and cationic amino acid spatial organization (Figure 1.22) [309].

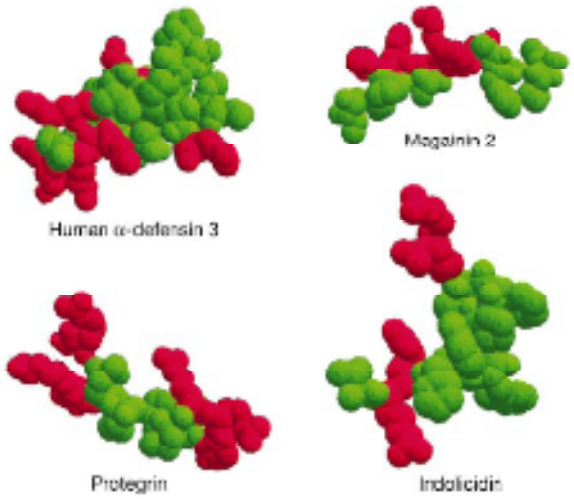

Figure 1.22: Clustering of cationic and hydrophobic amino acids into distinct domains in several antimicrobial peptides of different structural classes. This `amphipathic' design is evident in many, but not all, antimicrobial peptides. Red, basic (positively charged) amino acids; green, hydrophobic (`oily') amino acids. Other amino acids are not shown. Magainin is depicted in its a-helical configuration [309].

Depending on structural features, they have been divided into four major classes: β-sheet, α-helical, loop, and extended peptides. Of these classes, β-sheet and α-helical appear to be the most common in nature [307]. Several idealized peptides have been synthesized since the explosive interest in the class of peptides as a therapeutic target [311, 312]. AMP characteristics and their antimicrobial peptide activity and specificity against wide specturum of organisms are influenced by the size, sequence, charge, conformation and structure, hydrophobicity, and ampipathicity of the peptide [308].

The precise mechanism of action for matimicrobial peptides has not been understood yet. Nevertheless, most AMPs are believed to target the negatively charged cell membrane of bacteria, (and possibily the embedded lipids bearing phospholipid head-groups), and mediate killing by membrane disruption or pore formation [309, 307, 308]. For some AMPs an intracellular target has been proposed that may be the sole mechanism of action of the peptide, or may work synergistically with membrane disruption [307].

According to described variety of mechanisms on antimicrobial peptide activity, these peptides have targeted clearly the difference in design of membranes of microbes and multicellular animals. Bacterial membrane are organized in leaflet of lipid bilayer. The surface exposed to the outer world is heavily populated by lipids with negatively charged phosholipid headgroups. In contrast, the outer leaflet of the membranes of plants and animals is copmposed of principally of lipids with no net charge; most of the lipids with negatively charged headgroups are segregated into the inner leaflet, facing the cytoplasm (Fig. 1.23) [309].

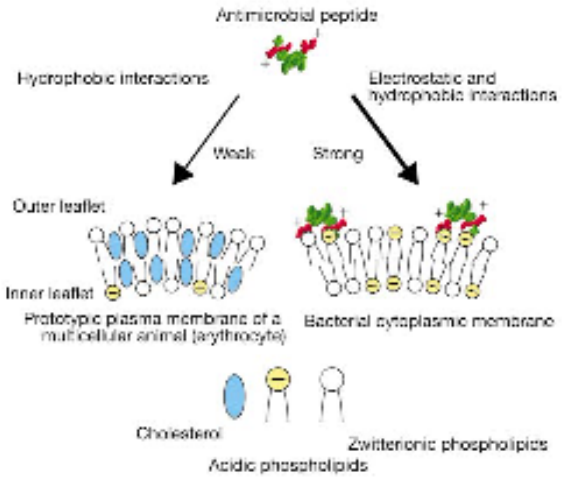

Figure 1.23: The membrane target of antimicrobial peptides of multicellular organisms and the basis of specificity [309].

A model that explains the activity of most antimicrobial peptides is the Shai-Matsuzaki-Huang (SMH) model (Figure 1.24). The model proposes the interaction of the peptide with the membrane, followed by displacement of lipids, alteration of membrane structure, and in certain cases entry of the peptide into the interior of the target cell. The presence of cholesterol in the target membrane in general reduces the activity of antimicrobial peptides, due either to stabilization of the lipid bilayer or to interactions between cholesterol and the peptide. Similarly, it is believed that increasing ionic strength, which in general reduces the activity of most antimicrobial peptides, does so in part by weakening the electrostatic charge interactions required for the initial interaction [309].

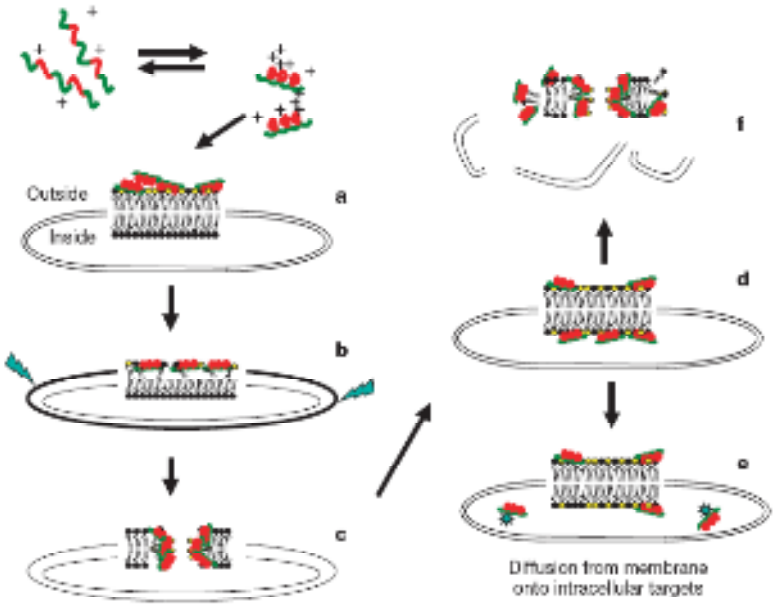

Figure 1.24: The Shai-Matsuzaki-Huang model of the mechanism of action of an antimicrobial peptide. An alpha-helical peptide is depicted. a, Carpeting of the outer leaflet with peptides. b, Integration of the peptide into the membrane and thinning of the outer leaflet. The surface area of the outer leaflet expands relative to the inner leaflet, resulting in strain within the bilayer (jagged arrows). c, Phase transition and `wormhole' formation. Transient pores form at this stage. d, Transport of lipids and peptides into the inner leaflet. e, Diffusion of peptides onto intracellular targets (in some cases). f, Collapse of the membrane into fragments and physical disruption of the target cell's membrane. Lipids with yellow headgroups are acidic, or negatively charged. Lipids with black headgroups have no net charge [309].

Many hypotheses have been presented on the actual mechanism of antimicrobial peptide to kill the microbes which include: fatal depolarization of the normally energized bacterial membrane; the creation of physical holes that cause cellular contents to leak out; the activation of deadly processes such as induction of hydrolases that degrade the cell wall; the scrambling of the usual distribution of lipids between the leaflets of the bilayer, resulting in disturbance of membrane functions; and the damaging of critical intracellular targets after internalization of the peptide [313, 314].

AMPs are an exciting class of antibiotics because they are effective against a broad range of microorganisms [315-318], including multidrug resistant bacteria, can work independently or synergistically with classical antibiotics, neutralize endotoxin, and

are active in animal models [307]. The ability of AMPs to inhibit and/or kill multidrug resistant bacteria increase their importance as a therapuetic agent, as there is a high need for new treatment options against such epidemeological pathogens. Another advantage of AMPs is their ability to work synergestically with classical antibiotics, possibly facilitating access of antibiotics to the infection site, and thus providing an avenue for a more aggressive treatment approach against biofilms.

The use of AMPs in therapeutical approaches is vast underway. Appendini *et. al.* covalently liked an AMP onto the surface of polystyrene resin beads that had polyethyleneglycol (PEG) grafted onto them and found it to be microcidal against several microorganisms [317]. Etienne *et al* developed a way to insert an AMP into polyelectrolyte multilayer films that was reported to effectively inhibit *Micrococcus luteus* and *Escherichia coli* D22 when 10 antimicrobial peptide layers were applied [318]. Kwakman *et.al.* locally administered an AMP along the site of insertion of a catheter in a murine model and found the peptide to have a broad *in vivo* potentency against microorganisms and reduced inflammed tissue [319]. The list goes on with exciting new applications of AMPs being published frequently; for a review of AMPs as therapeutics see Guliane *et al.* (2007).

During the past two decades it has become evident that increasing bacterial drug resistance has created an urgent need for new classes of antibiotics. Even if a superbug epidemic has not yet hit and the panel of traditional antibiotics can still manage drug resistant pathogens, at the moment, AMPs seem to represent one of the most promising future strategies for defeating this threat. This statement is well represented by the fact that AMPs are subject to an increasing number of academic studies. At industrial level, several companies worldwide are focused on the development of AMPs with several molecules both at the preclinical and clinical stage. This demonstrates that despite the first clinical trials failing (Pexiganan and Iseganan), there is still a lot of general optimism for their use in future clinical practice. Some of the challenges facing the development of peptidic drugs have already been overcome, starting from the industrial production of T-20 peptide (Fuzeon) at the multi-ton scale production, incredibly boosting the production of new peptides on a large scale with beneficial effects on the cost of all starting materials. Other challenges are common to other class of molecules that may be defined as innovative. Several strategies have been devised to optimize AMPs with promising

activity, ranging from inclusion of non-natural aminoacids and a new method applicable to high-throughput screening to multimerization of linear sequences. Even if we cannot exclude the fact that resistance may evolve whenever bacterial populations are consistently exposed to elevated levels of AMPs, this concern should not discourage their further study and development; instead, they may help us to rationalize their use in future, for example preventing the big mistake made in the past of distribution of large amounts of antibiotics, and thereby minimizing the emergence of resistant organisms [307-309, 312, 313, 310].

1.7 Biomolecule Immobilization Approaches to Functionalize Implant Surfaces

Biological surface modifications are one of the emerged fields to overcome limitations for implant–tissue integration. In the previous sections, the role of immobilized various biomolecules on implant surfaces for successful integration were explained in detail. In this following section, principles of immobilization techniques for biofunctionalization of implant surfaces will be mentioned. The major principle of immobilization increased stability and functionality of biomolecules. However, activity of biomolecules can be reduced due to the random orientation and structural deformation during the attachment. In fact, the immobilization techniques shouldn`t effect conformation and function of the molecule to fully retain the biological activity [320]. Physical and chemical immobilizations are two major techniques for biomolecule functionalization of implants.

1.7.1 Physical immobilization

Physical immobilization or adsorption is a very simple immobilization method performed under mild conditions, and therefore hardly disruptive to the biomolecules. However, by dipping titanium implants into a solution of proteins, biomolecule linkage is highly dependent on experimental parameters such as pH, temperature and solvent. Basically adsorption occurs at surfaces via intermolecular forces, mainly ionic bonds and hydrophobic and polar interactions. Mostly, the resulting layer is to be heterogeneous and randomly oriented, since each molecule may have different optimum conformation to minimize the repulsive forces from the surface and previously attached protein, during the adsorption [320]. However,

it should be also noted that the physical adsorption of proteins constitutes the first step of chemical immobilization involving covalent bonding of proteins at the surface as a second step.

During protein adsorption at a surface, the net free energy change must be negative, that may be caused from enthalpic or entropic origins. For example, many proteins undergo conformational changes and generally, their ordered structural content is decreased at the adsorption process. This fact yields an entropic gain and may act as an adsorption-driving force [321]. From an enthalpic point of view, the adsorption driving force may be originated from the interactions between the protein and the surface. The most important ones are van der Waals, hydrophobic, electrostatic interactions and hydrogen bonding [320, 321].

Surface properties of the inorganic materials directly affect the physical attachment of protein; also surface modification may be needed to increase the protein adsorption. The surface hydrophobicity is one of the surface properties that one can control over a wide range. Furthermore, hydrophobic interactions between the solid surface and the protein would be expected to be more favorable comparing to hydrophilic interactions in terms of protein adsorption. This is also frequently, but not always, observed experimentally [321, 322]. As an example, the preferential adsorption of fibrinogen at a hydrophobicity gradient surface was demonstrated by Elwing *et al.*

Electrostatic interactions between the inorganic surface and the protein may also enhance the protein adsorption. For example, the adsorption of bovine pancrease ribonuclease at a (hydrophobic) negatively charged polystyrene surface was found to be high at both above and below the protein isoelectric point. This indicates us there is interplay among hydrophobic and electrostatic interactions.

For the proteins undergoing large conformational changes on adsorption, *e.g.* BSA, nonelectrostatic driving forces considerably take roles. Hence, the adsorption usually does not follow the electrostatic interactions. Moreover, the adsorption is governed also by other effects, such as van der Waals and hydrophobic interactions [323].

Especially in biomedical applications, PEG derivatives are mostly used reagents in the literature to prevent the protein adsorption at a solid surface [324, 325]. If the PEG chains are sufficiently long and molecule density is high enough at the surface,

PEG modified surfaces display very low protein adsorption. The main reason of the efficient repulsive characteristics of the PEG layer is two-fold [326, 324]. Firstly, dense and thick layer of the PEG derivatives maintain a strong streic hinderance for the proteins [326]. Secondly, the adsorption driving forces are absent. For example, since the typical PEG-layers are uncharged, electrostatic interactions are insufficient for the protein attachment [326]. Also, PEG molecules can interact with the water molecules, preventing van der Waals interactions between the surface and the protein [30]. Under these conditions, it is really hard for a protein to attach to the PEG-modified surface unless it can penetrate through the PEG layer and reach the bare surface.

In adsorption, surface loading is very low compared to methods as covalent coupling. In addition, biomolecules desorb from the surface in an uncontrolled manner. Using the approach of physical entrapment of biomolecules, the biomolecule is retained by a barrier but not chemically bound to it. Therefore, this technique is extremely mild and universal for any biomolecule. However, barriers are often fragile, and tearing or eroding can cause loss of biomolecules. Besides, this method is mostly used to biosensor applications [327]. For the delivering of biomolecules to the implant interface, biomolecules are incorporated into coatings made of materials such as poly(D,L-lactide) (PDLLA), ethylene vinyl acetate (EVAc) and collagen [328, 329]. In this way, biomolecule release from the implant surface can be controlled, which makes it an attractive approach for the immobilization of bone growth factors.

1.7.2 Chemical immobilization

Covalent attachment is widely used for the immobilization of peptides, enzymes and adhesive proteins onto implant surfaces, even though this approach is more complicated and time consuming than other immobilization methods. Major limitations of this methodology, especially when immobilize the proteins, include the loss of protein mobility on the surface which is directly effected by possible repsentation of unfamiliar protein conformation on the surface. Other drawbacks of this technique, remains of toxic monomer residue on the surface may cause biocompatibility problems in the area of implantation. Issues in task of chemical immobilization can be addressed by physical adsorption techniques, which usually involve dip coating a material to form a film with desired properties on the surface. While physical adsorption may help reduce toxic monomer residues, issues while

binding between the materials and immobilized molecules mainly retain as an unsolved problem which is directly caused by the instability of the molecules on the surface [133].

Due to the limatations in chemical and physical modification, self-assembled monolayers (SAMs) were developed as a method to control the density and conformation of a single or multiple specific functional groups on a surface precisely [330]. The general process of producing SAMs requires two major steps. Firstly, the bulk material surface needs to be activated by SAMs, then graft polymerize onto the activated surface. At the end of the two major steps, flat and chemically well defined surfaces can be provided through the SAMs [331]. Additional benefits of applying SAMs are obtaining closely packed, well-ordered functionalities near thermodynamic equilibrium on the surface.

SAMs tend to provide functionalities with control over pattern and densities. Selection of terminal group can also provide a site for further functionalization of the coated surface. Surface functionality via SAMs have been used to investigate *in vitro* cell responses and *in vivo* inflammatory and foreign body responses of implanted biomaterials [332] as well as many other processes, giving insight into how a particular functional group effects a particular process. However, application of SAMs are limited the type of materials. The most common materials that SAMs easily funtionalize its surface is gold and silver. These surfaces can be derivatized into reactive groups, such as amino groups or aldehyde groups [234].

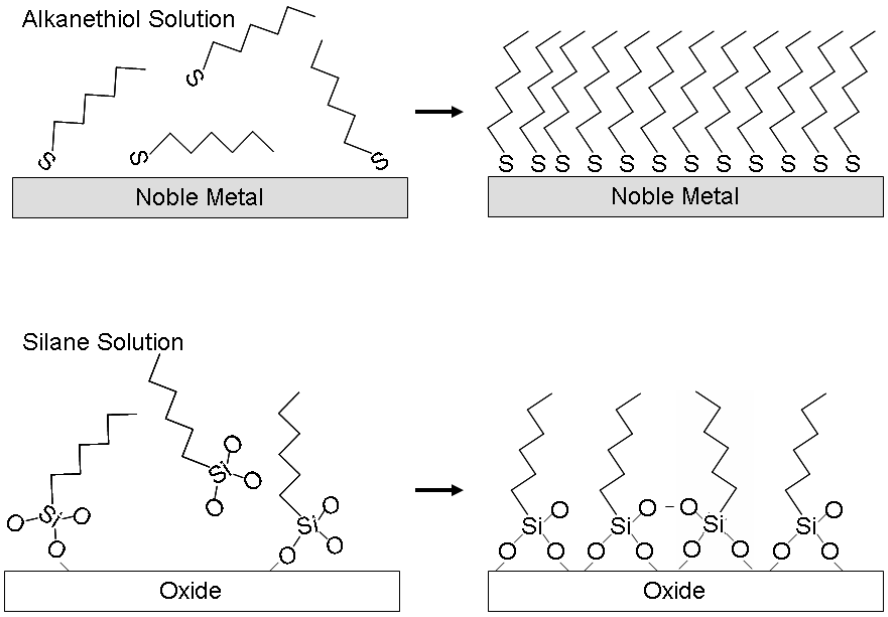

Figure 1.25: Standard approaches for creating SAMs on noble metal and oxide surfaces using alkanethiol and silane chemistry [331].

1.8 Genetically Engineered Peptides for Inorganics (GEPI) in Bionanotechnology

In recent years, genetically engineered peptides for inorganics (GEPIs) is remarkable in various application areas taking advantage of molecular biomimetics where different disciplines such as material science and molecular biology are utilized to understand the interactions between materials and biomolecules by taking lessons from the nature [16, 4].

Molecular biomimetics is the application of methods and systems found in nature to the study, design and engineer materials. The biological world has long been a source of inspiration for engineering design. The popularity of designs that mimic natural systems is due, in large part, to advantages in performance.

In the past, drawing ideas from nature was limited to macroscopic engineering problems [5]. Advances in analytical techniques over the past several decades have opened the door to understanding the materials' structure and properties at the molecular level and have provided a better understanding of the potential of the nanotechnology. However, the realization of the full potential of nanotechnological systems has so far been limited due to the difficulties in their synthesis and subsequent assembly into useful functional structures and devices. Biological

materials, on the other hand, are highly organized from the molecular to the nano- and macro scales, often in a hierarchical manner, with complex nano-architectures [333, 334]. One key aspect of this process is the participation of biomacromolecules such as glycoproteins and phosphoproteins. Therefore the next-generation biomimetic engineering systems should include proteins in synthesis, assembly or function [5, 335, 17].

The interaction of proteins with inorganic surfaces is a fundamental process, which has great impact on biotechnological and biomedical applications such as biomaterial design, biosensing, biominerilization, and tissue engineering. Especially, specific interactions between proteins and inorganics promise new application areas in the field of nano- and bionanotechnology. In biological organisms proteins controls the formation of different hard tissues like tooth, bone and many other hard tissues occurring in different organisms. Bionanotechnological applications focuses on utilizing proteins in order to create multifunctional nanomaterials, self assembled supramolecular structures that could be applicable in the fields of nanomedicine (drug delivery, cancer probing, implantation), nanoelectronics, nanophotonics, nano- and microelectromechanical systems (NEMS/MEMS) [16, 336, 337, 4, 338]. Integration with protein functionality and materials science can offer a new way for explosive growth in medical implants research area.

Our overarching aim has stem from the various inherent capabilities of GEPIs. The aspect is to develop biomimetic implant materials using GEPIs. This includes creating biocompatible and/or non-fouling surfaces for implant material applications using the molecular recognition and binding capabilities of GEPIs and creating biomimetic restorative materials and cell free tissue engineering systems using the morphogenic and synthetic capabilities of GEPIs.

1.8.1 Biocombinatorial selection of GEPIs

Progress in development of combinatorial selection techniques created a major tool for a myriad of biotechnological applications including antigen-antibody, peptide-ligand interactions, and drug and vaccine development [339]. Phage display [340] and cell surface display [341-343] are two well-adapted techniques based on screening of peptides against to target. The basic principles of each technique rely on the link between phenotype and genotype of the organism. DNA sequence of random

peptides is inserted into genome of organisms where they will express within the context of proteins localized on the surface of phage or the cell. Random peptides as a chemic protein display in lipoprotein, flagellar protein of cell or major or minor coat protein of phage [344, 340, 345].

Recently, adaptation of these techniques in the area of molecular biomimetics with isolation of peptides that are specific inorganic materials opens up new avenues for the design and utilization of multifunctional molecular systems with the wide range of applications, from tissue engineering, and biosensors to nanomedicine [9, 346-349].

The first example of identifying peptide that bind to inorganic surface was shown by *S. Brown*. The peptides were selected against to Fe_2O_3 substrate by using cell surface display technique [350]. Afterwards, Belcher and coworkers utilized the phage display technique for the first time in the selection of semioconductor materials [351]. These initiative works was example for utilization of combinatorial biology techniques to select and identify sequences that have high affinity to other materials systematically.

By applying two major techniques, short amino-acid sequences peptides have been selected to various materials including noble metals (Au, Pd, Pt, Ag) [352-355, 4, 356, 357], oxides (Al_2O_3, SiO_2, ZnO, Cu_2O, TiO_2) [358-360, 4, 16, 361-364], semiconductors (GaN, ZnS, CdS, GaAs) [351, 365, 366], minerals [367-370] polymers [371], zeolites [372] and carbon nanotubes [373]. *In vitro* selection of GEPIs are carried out by biopanning step where the library of phage or cell clones, displaying a vast population of randomized peptides on their surfaces, exposed to desired inorganic material as target (Figure 1.23). Following the binding step, the unbound clones are washed away and the bound one eluted by physical or chemical methods [368]. Subsequently, amplification step was carried out to increase population of bound clones. Generally, the biopanning cycle is repeated, usually 3-5 times to enrich the population of clones that have affinity to desired surface. In the final step, selected individual clones isolated and their DNA sequence was identified [374, 4, 9, 368].

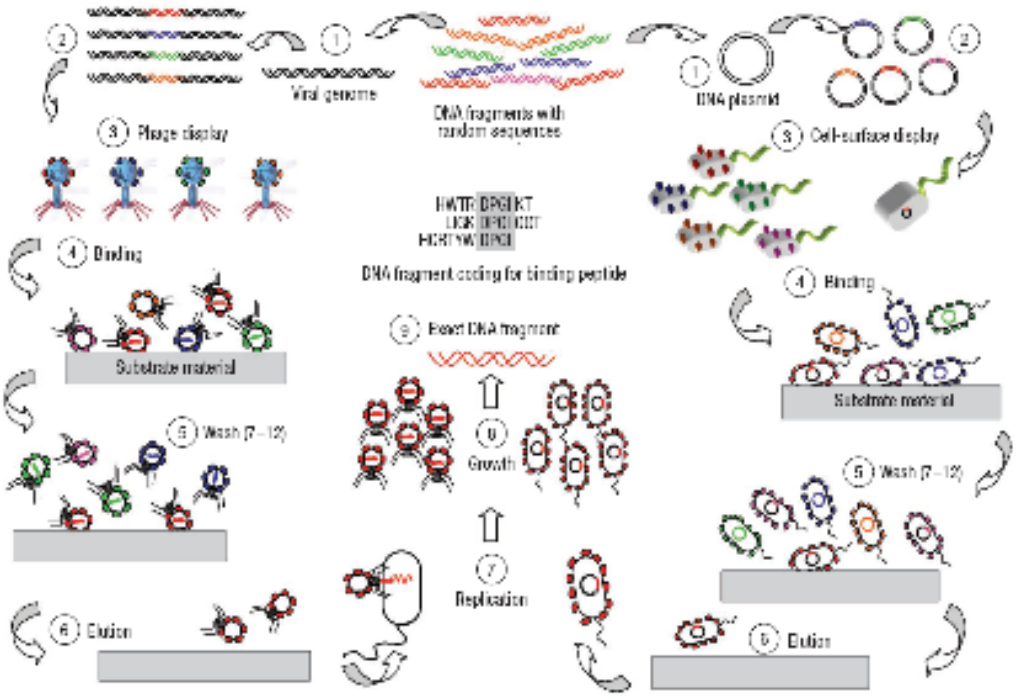

Figure 1.26: Schematic diagram for phage and cell-surface display techniques [16].

Although cell or phage display is two successfully adapted selection techniques so far, one has advantages and disadvantages rely on different criteria over the other. For example, cell surface display has greater efficiency, in generating peptide sequences due to simply amplification and replication of genomic DNA process, than phage display. Besides, there is a still need improvement in the selection of peptides since solid materials are quite different from protenacous ligands for which the combinatorial selection techniques were originally developed [16, 348, 375, 349]. Solvent conditions in biopanning, which may have intrinsic effects on surface modifications need to be taken consideration. In addition, display technologies are also limited the form of solid substrate. For instance, in case of cell surface display; any centrifugal force used in biopanning step could disrupt and shear off the flagella form the cells and result in loss of tightly bound clones from the pool. Therefore, utilization of cell surface for selection of peptides against to inorganic powders and nanostructures are not feasible [368, 9].

In general, a consensus binding motive is common in protein-protein interactions [345, 340, 343]. However, to obtain clear binding sequence in case of inorganic-peptide interaction is difficult. This probably reflects the heterogeneity of inorganic

surfaces and occurrence of possible binding mechanisms [16, 348]. Consequently, further binding analysis is required in selection of material specific peptides. Generally, in a biopanning experiment, 50 clones characterize with different methods developed Sarikaya group to indicate degree of binding strength. In our group, initial peptide binding characterization has been performed using semi-quantitative methods such as direct colony counting while peptide displayed on cell or surface coverage of phage on inorganic surface by fluorescence microscopy to assess the affinity levels of individual clones. The affinities of the clones are sorted from "strong" to "weak" based on the number of bound cells or the surface coverage ratio The FM technique also enables characterization of binding specificities of selected clones which are tested on various different inorganic solid surfaces. Further quantitative characterization methods such as quartz crystal microbalance (QCM), surface plasma resonance spectroscopy (SPR) and atomic force microscopy (AFM) have been applied to understand binding strength and assembly of peptides on inorganic surfaces [376, 377]. In our approach, set of peptide sequence of experimentally selected clones from an initial random library is referred to as the first generation peptides. This first generation of peptides can be further engineered by computational approaches incorporating bioinformatics to produce second and higher generation of more functional peptides [360, 378].

1.8.2 Theoretical design and molecular binding characterization of GEPIs

With the accumulating knowledge on the utility of GEPI in nanotechnology and bionanotechnology, there is a need for improvement in the selection of peptides with better affinity and material selectivity. First generation of peptides are restricted the size of library that is not enough to cover all possibilities to obtain the best sequence through directed evolution [375]. Therefore various molecular tailoring strategies such as site directed mutagenesis, bioinformatics and molecular conformations will offer way to improve peptide affinity and specificity to inorganic surfaces. Examples were shown the effect of molecular restrictions on peptide affinity by utilizing various surfaces such as Pt, Au, TiO_2, and SiO_2 [356, 354, 359, 379]. Besides, some studies were accomplished based on use of multiple repeats of peptides and site-specific changes of amino acids within the sequence to understand peptide binding domain and affinity correlation [353, 380-383].

In addition to genetic tailoring strategies, computational studies may introduce novel perspectives for the design of new peptides bearing improved affinity as well as material-specificity. A successful strategy for the design of GEPI was developed by Sarikaya and his co-workers. The basic principle in this strategy based on degree of sequence similarity among the selected peptides [360].

The interaction between and solids that already exists in nature has been studied to understand the molecular recognition as well as binding mechanism of the proteins in biomineralization, fabrication of hybrid materials, directed assembly of functional materials [384-386]. These studies indicated that the proteins in the nature that exhibit similar functions also have aa sequence similarity to each other [387]. According to this observation, Sarikaya Group proposed theory that peptide, have an ability to recognize one surface, should hold sequence similarity [360]. To examine this theory, protein sequence alignment is one the tool to detect key functional residues inferring the evolutionary history of protein families. Based on this knowledge, different sequences were aligned using optimization procedure to find out the most possible relative arrangement of the sequences [388-390]. To align sequences, a scoring matrix is used to obtain the score that can consider as a measure of the similarity between sequences. Sarikaya group developed methodology combining sequence alignment techniques to produce unique material –specific scoring matrices through bioinformatics tool [360, 349]. The method starts sequence selection based on experimentally selected, characterized and categorized inorganic binding peptides into three groups; strong, moderate and weak for specific materials. The sequence alignment methods [388] and the standard scoring matrices [389] are applied to the experimentally selected sequences to generate a new material-specific sequence scoring matrix that can determine the aa pattern among the strong with a certain score. To design new peptides with higher affinity, the resultant sequence scoring matrix that is specific to certain material is applied to millions of aa sequence that are generated by computer and similarity score for each generated peptide is calculated. Among them, the peptides with highest or lowest similarity score are define as “strongest” or “weakest”, respectively, comparing to experimentally selected strong binders [360]. The first successful example was shown to generate new quartz-binding sequences. As described above, with the combination of different sequence alignment techniques, they produce material-specific scoring matrices

using the experimentally observed sequence similarities of quartz binders (Figure 1.27 (lower)). From these matrices, they randomly generated new quartz-binding sequences. Thereafter, they have chosen six strong (high-scored) and four weak (low-scored) predicted quartz binders and tested their binding affinities to quartz. Experimental results were in consistency with the predicted results. As a consequence, second generation GEPI sequences were acquired by using the existing knowledge of the first generation GEPI sequences [360].

A detailed understanding of peptide recognition and assembly process is required to develop better tailoring strategies for novel peptides with enhanced binding and specificity capabilities. There are various techniques that open windows to understand binding mechanism. The most applicable quantitative methods are QCM and SPR which allow us to monitor adsorption and desorption process of peptides providing molecular binding kinetic parameters [356, 354, 359, 381, 379]. In addition these techniques, a better knowledge mechanism(s) of the quantitative adsorption may become possible through high resolution surface microscopy (e.g AFM, STM), molecular spectroscopy (X-ray photoelectron spectroscopy (XPS), time of flight secondary ion mass spectroscopy (TOF-SIMS, fourier transform infrared spectroscopy) [391, 392] Since the molecular conformation of the peptides is a key for understanding the binding mechanism on the inorganic surface, solid and liquid state of nuclear magnetic resonance (NMR) spectroscopy can provide quantitative information on molecular conformations of peptides but the contribution of solid-NMR method is limited due to the interface coming from the solid surface [393]. Due to NMR limitations, utilization of circular dichroism (CD) is another way to understand the effect of secondary structure on peptide adsorption.

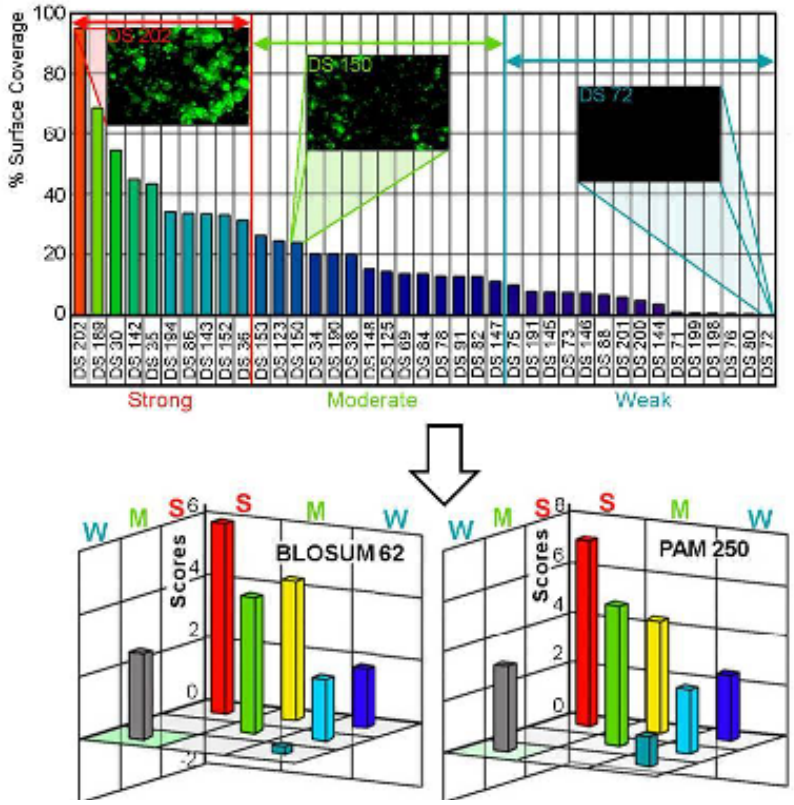

Figure 1.27: Design of second generation GEPI using bioinformatic approach. Experimentally selected and categorized peptide sequences (upper) are used to calculate similarity scoring matrices (lower) [360].

Combination of SPR, QCM and CD measurements is useful to understand structure-molecular conformations relations on adsorption behavior of inorganic binding peptides [356, 354]. Additionally, atomic force microscopy (AFM) is powerful technique to gain insights into assembly and diffusion of the peptide on solid surface. Collective utilization of these techniques will open way for a better understanding of GEPI-inorganic interactions. On the other hand, the knowledge obtained from experimental studies should be supported with theoretical models to see whole picture of GEPI-inogranic interactions. Molecular simulation studies especially molecular dynamics (MD) simulations is very promising to reveal information about structural behavior of GEPI on solid surfaces [394-396]. Oren *et al.* was performed noticeable study in this area. They observed that out that platinum binding septapeptides conform into multiple protrusions, referred as *polypods*, which spatially match with the crystallographic metal surface [378]. Recently, similar match of surface and GEPI orientation was observed by So *et. al.* for another GEPI, namely a gold binding peptide $3rGBP_1$. In that work, molecular simulation and

geometrical docking studies were coupled with experimental AFM observations resulting in integrated information [397].

It is difficult to answer all fundamental questions by only utilizing current techniques; however advances in molecular spectroscopic techniques and analytical approach including combination of appropriate methods will provide more quantitative information on peptide assembly. As the knowledge on the peptide recognition and assembly processes increases, novel peptides with tailored binding and higher material-specificity will be designed for the control of solid-peptide interface, leading to fabrication of new hybrid materials [375].

1.8.3 Current and Potential Applications of GEPIs in Bionanotechnology

What functions make GEPIs as an useful tools for bionanotechnology? Among the myriad functions allocated to natural proteins/peptides, some of those that become a focus in bionanotachnology are specific recognition, biomineralization, self-assembly and self-organization [398, 374, 399, 349, 347, 400]. In the broadest sense of expression, specific recognition is the foundation of all biological phenomena, while biomineralization, self assembly and self organization reflect specific recognition between proteins/peptides and themselves or other molecules. Due to GEPIs` material selectivity and self assembly properties, they can be utilized as molecular linkers, assemblers and erectors in targeted immobilization [401-409], as synthesizers and nano-organizers in fabrication of inorganic materials [362, 367, 410-412, 357, 413]. They have also advantage to enhance their applicability with desired functionality in nanoscale when inserted into permissive sites of several biomacromolecules (proteins, enzymes, viruses etc.) applying genetic engineering techniques [414-416, 352].

On the other hand, GEPI can provide a new platform for high performance of implants and hard tissue engineering via immobilization of biomolecules with controlled attachment and assembly on solid surfaces [417, 418, 400]. In this section, only three examples will be demonstrated to give basic perspective for promising potential of GEPI in implantation and hard tissue engineering. In the first example, capability of GEPIs as a synthesizer in biomineralization process will be given. Biomineralization has been attracted attention in the field of bio-nanotechnology because firstly, biomineralization reactions proceed under mild

conditions than conventional industrial methods and secondly, the hard tissues obtained through biomineralization often have elaborately designed nanostructures. The unique morphological, structural, and functional properties of inorganic materials synthesized by biological organisms have been controlled towards proteins. This phenomenon has led to development of biomimetic approaches for utilization in designing and engineering of functional materials. The traditional approach involves extracting and purifying proteins from organism of interest and utilizing them for in vitro material synthesis [419-421]. Although there are exciting examples, performing biomineralization using isolated proteins is limited because of the difficulties involved in extraction and purification of these proteins from biological systems. Another approach is prediction of functional sequence by using computational methods called as *de novo* design, based on identified protein sequence proved role in biomineralization. Usually, there may be a large number of proteins with various temporal and spatial distribution involved in a given biological mineralization process. Practical biomineralization through extracted proteins or *de novo* designed peptide sequence remains elusive due to impractical identification of all proteins and their sequence. GEPIs offer unique and a more practical approach in biomineralization. Given that the GEPIs recognize and bind to solid materials, there may also be inherent capability within the sequences to influence fabrication process of these inorganic solids as well. Gungormus *et. al.* was shown exploring the possibility of HA-binding peptides to regulate calcium phosphate formation in vitro. They found that a strong- binding peptide HABP1 affects formation of calcium phosphate mineral in several aspects (Figure 1. 28). The addition of HABP1 slowed the rate of initial mineralization, resulting in the formation of much larger plate-like particles compared to control samples (weak binding peptide, HABP2 and no peptide containing solutions) and increased the rate of transformation of the amorphous phase to the crystalline phase [367]. This conversion may involve interactions of HABP1with the amorphous mineral surface, which in turn stabilizes the crystal structure by lowering the surface energy, therefore resulting in a growth- dominated mineralization pathway.

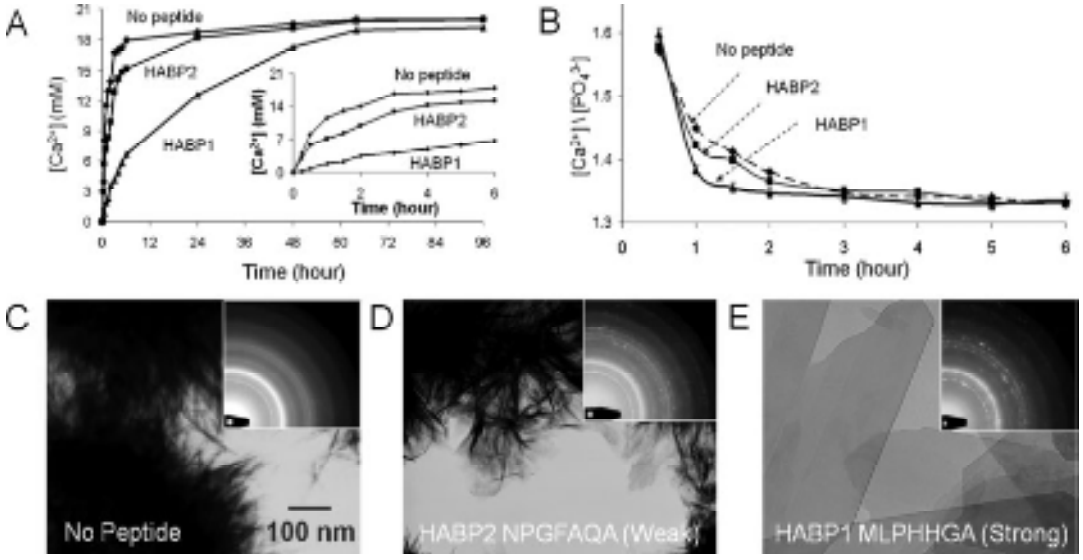

Figure 1.28: (A) Rate of Ca2+ consumption in the presence of peptides; inset: the consumption rate during the first 6 h. (B) Ca/P ratio of the mineral phase at different time points. The final morphology of the minerals after 96 hours of mineralization in the presence of (C) no peptide, (D) weak binding control peptide and (e) strong binding peptide, HABP1 [367].

The second example is related capability of GEPIs in a variety of immobilization applications uniquely suited for modifications of biomaterial surfaces. Several articles have already been published demonstrating bioactive or bioinert surfaces via peptide linkers on a number of materials [422, 371]. Another example was presented by Sarikaya and his group present. Four different materials (gold, platinum, glass and titanium) as a proof of concept substrate were used to show applicability of GEPIs in implant surface modifications. Gold and platinum were chosen because of ideal chemical stability for bioinert applications in implantation that are in direct contact with blood. Two different peptide linkers (3RGBP1 and PtBP1) were used to functionalize these surfaces with PEG anti-fouling polymer. Two step-targeted assembly processes in which the peptides are first immobilized on the surface and then chemically conjugated with the activated polymer by Schiff- base chemistry (Figure 1.29B) were employed. The surfaces that are able to resist cell adhesion were obtained as well as those formed by oligo (ethyleneglycol) thiol SAM on gold (Figure 1.30A). In the same study, bioactive surface modifications were achieved with immobilization of RGD integrin- binding sequence on glass surface via QBP1 (glass binding peptide) and titanium surface TiBP1 (titanium binding peptide).

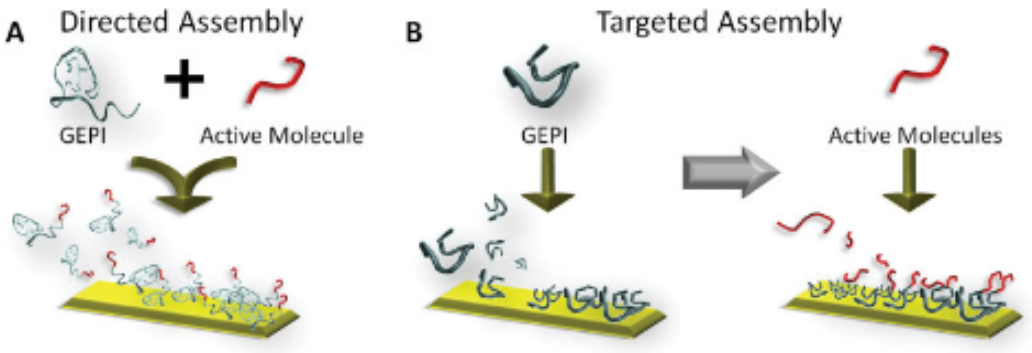

Figure 1.29: (A) Directed assembly—GEPI is conjugated with the active molecule before immobilization on the substrate. (B) Targeted assembly—GEPI is immobilized on the substrate alone then conjugated with the active molecule by secondary means, such as Schiff base chemistry [346].

This modification is accomplished through single step directed assembly process (Figure 1.29A). The resulting samples increase adhesion and spreading of the cells, exhibiting increase only when both parts of the construct are present (Figure 1.30B and C). Although employing GEPIs as linkers in biomaterial applications are significant, the path to clinical application has not been covered yet. Understanding the mechanism of binding in a number of peptide-solid systems may allow the design of new sequences that combine different functional domains.

Immobilization of cytokines on the implat surface via peptide linker was given as a third example. Shiba and his group proposed a similar approach that we described in previous examples for immobilizing cytokines on material surfaces. In this method, material binding artificial peptide is used to mediate reversible interaction between the cytokine and material surface. In their experimental design, they embedded the minTBP-1 motif such that the proteins could be used to coat a Ti surface with crystals of calcium phosphate. Some of the proteins created in that experiment contained multiple copies of minTBP-1 in their sequences. Among them, they focused on #56, which contains three copies of minTBP-1, and used it as a Ti-binding protein in the present experiment. As controls, we also used #55 and #69, neither of which contain a minTBP-1 motif, but the amino acid composition of #55 is more hydrophobic than that of #69. In Figure 1.31 shows the each contructs mineralization efficiency on the surface of titanium via alkanine phosphatase activity.

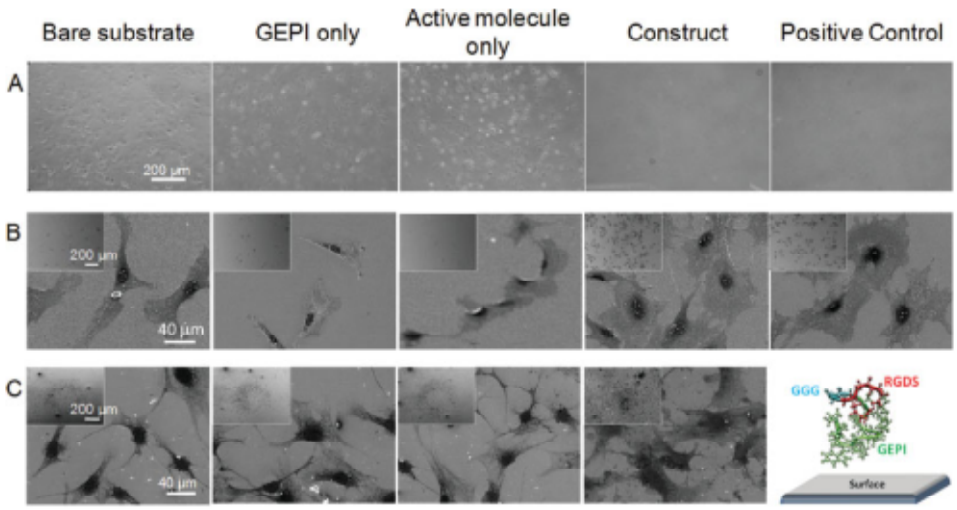

Figure 1.30: (A) Light optical microscopy images of NIH3T3 fibroblast cells ($3x10^5$ cells, 1.5 hrs, 200X) on gold substrate modified with GEPI-PEG conjugate; (B) Scanning electron microscopy (SEM) images of NIH3T3 (5 3 103 cells, 24 hrs) on glass substrate modified with GEPI-RGD conjugate; (C) SEM images of NIH3T3 ($8x10^4$ cells, 24 hrs) on titanium surface modified with GEPI-RGD conjugate [346].

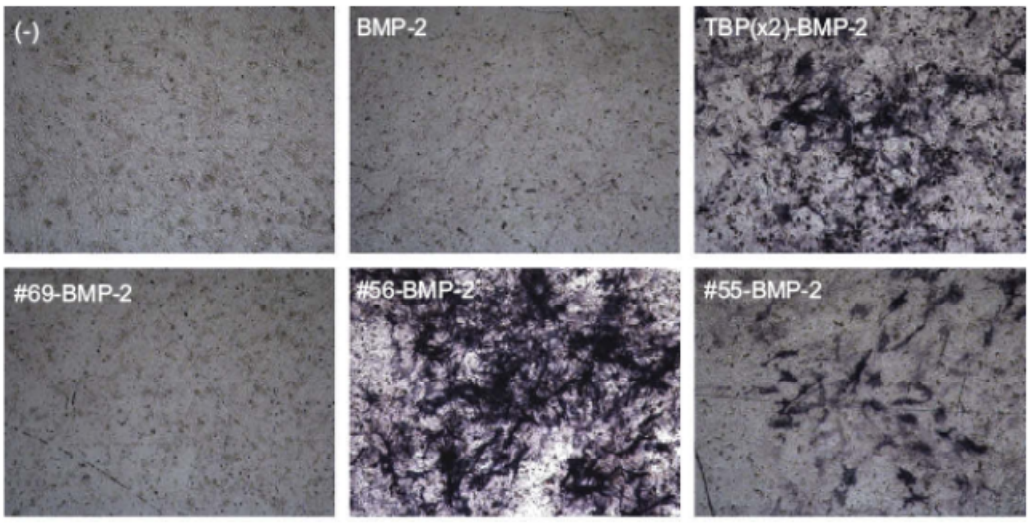

Figure 1.31: ALP activity was assessed by staining with BCIP/NBT [407].

All examples indicate us GEPIs enormous potential in wide range applications especially they can provide the ways for genetic control on bimeralization, funtionilization of implant surfaces with diffrenet purposes in tissue restoration and regeneration.

2. MATERIALS AND METHODS

2.1. Combinatorial Selection Methods

2.1.1. Cell surface display selection

2.1.1.1. Target material preparation

cp Grade 4 and cp Grade 1 titanium implant surfaces were kindly gifted Gronowicz *et.al.* 0.78 cm^2 round implant disks were cleaned before performing any experiments. Disks were first soaked in 1% SDS for overnight and then sonicated for 1 hour. Following, they were washed in double distilled water several times before and after passivation in 30% nitric acid for 1 hour, and then sterilized 15 min under ultraviolet light for both sides to achieve sterility prior to any cell experiments.

2.1.1.2. FliTRx random peptide display library

FliTrx Library (Invitrogen, K1125-01) was used for selection of titanium binding peptides. The library was designed displaying peptides on the surface of *E. coli* using the major bacterial flagellar protein (FliC) and thioredoxin A (TrxA) diverse library of random dodecapeptides was inserted into the active site loop of thioredoxin, which is itself inserted into the dispensable region of the flagellin gene (fliC). Construction of library in the thioredoxin active site loop constrains the N- and C- terminal ends of the peptide resulting in a well-defined structural context. The Flitrx library has an estimated diversity of $1.77x10^8$ different random dodecamer sequences. The peptide fusion construct is expressed from the bactreriophage lambda major leftward promoter (P_L). When induced, the fusion protein Flitrx is exported and assembled into flagella on the bacterial cell surface, allowing display of constrained peptide. The figure below shows schematically how the peptide library is constructed and displayed (Figure 2.1).

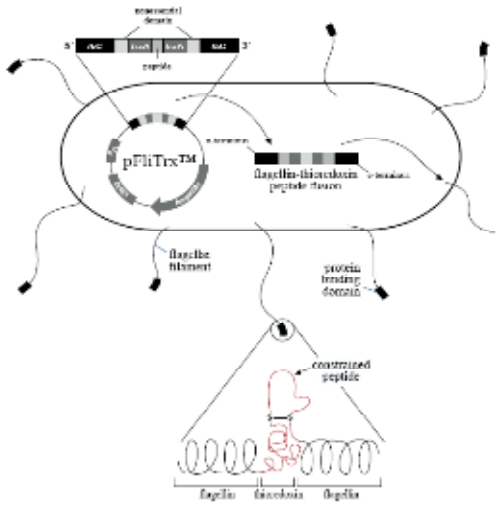

Figure 2.1: Schematic of library construction and displayed peptide on the surface of E. *coli* [354].

2.1.1.3. Cell surface display

Before applying basic panning procedure for selection of titanium binding peptides, one vial of the FliTrx peptide library were grown in 50 mL IMC media (1XM9 Salts, 0.2% casamino acids, 0.5% glucose, 1mM $MgCl_2$) containing 50 μg/mL carbenicillin (no tryptophan) with shaking (225-250 rpm) for 15 hours (overnight) at 25°C until reach OD_{600} = ~3 to proceed panning experiment. Then, number of cells in the culture were determined by measuring optical density at 600 nm (1 OD_{600} = ~1 x 10^9 cells for a 1 mL sample). Following, FliTrx Library expression was induced by adding 1 x 10^{10} cells (~3 ml) of the overnight culture into 50 mL IMC Medium containing (50 μg/mL carbenicillin and 100 μg/mL tryptophan). Induced culture was grown at 25°C with shaking (225-250 rpm) for 6 hours. Meanwhile, titanium target in a sterile petri dish was incuabated with freshly prepared blocking sloution (IMC media, 150 mM NaCl, 1% BSA, 1% α-methyl mannoside) for 1 hr with gently agitation (50 rpm) at room temperature. At the end of the induction period, 10 mL induced library in IMC containing 1% BSA, 150 mM NaCl, 1% α-methyl mannoside were exposed to titanium surface after decanting blocking solution from the surface and incubated with gently agitation at 50 rpm for 1min at room temperature. Subsequently, the surface and induced library was let to interaction for 1 more hour without any agitation. Following, titanium target was washed 5X times using IMC media containing 1% α-methyl mannoside. After 5 washing steps, adhering bacterial

cells were sheared off by vortexing for 3 min; released cells were then grown overnight in IMC media at 25°C and shaking at 225 rpm. At the end of incubation, Glycerol stocks (20%) of the grown cells (4 mL) were prepared. 1 x 10^{10} cells (~3 mL) were induced in 50 mL IMC Medium containing (50 µg/mL carbenicillin and 100 µg/mL tryptophan) to continue for the next round. After each selection round, serial dilutions of overnight cultures were plated onto RMG plates (RM media: 1XM9 Salts, 2% casamino acids, 1% glycerol, 1 mM $MgCl_2$, 50 µg/mL carbenicillin and 1.5% agar) and incubated overnight at 30°C for positive clone selection. (Figure 2.2)

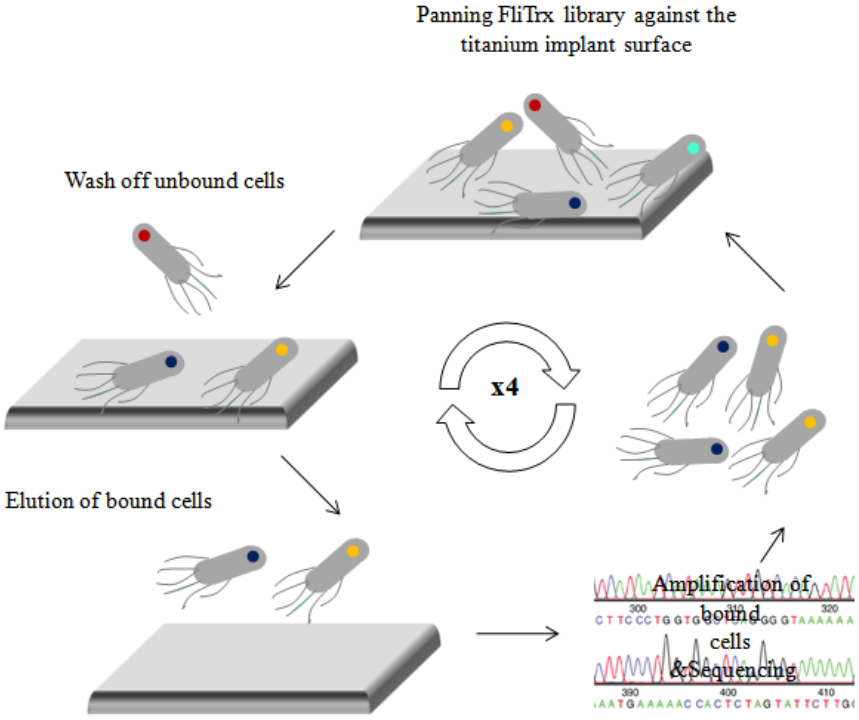

Figure 2.2: Schematic representation of selection of titanium binding peptides by cell surface display.

For DNA isolation, individual colonies were grown overnight at 30°C with shaking at 225 rpm in RM media. Plasmid DNA was isolated using Miniprep Spin Kit (Qiagene, USA). Nucleotide sequences of positive clones were determined using an automated DNA sequencer (ABI Prism 310 Genetic Analyzer, Perkin-Elmer Life Sciences, USA) using BigDye 3.1 terminator kit (Applied Biosystems, USA) and 5'-TAACCCAGCTTCAATTGAGG-3' and/or 5'-ACAGTGCACCCACTTTGG-3' designed primers (Invitrogen, USA).

2.1.1.4 Initial binding characterization of selected clones via fluorescence microscopy

Fluorescence microscopy characterization was applied to investigate binding affinity of selected titanium binding clones. Firstly, titanium substrates were prepared by directly coating 25 nm thick titanium layer on both sides of glass slides using a GATAN Precision Etching Coating System (GATAN, Inc., USA). Then the coated substrates were quickly cleaned by ultrasonication first in 1:1 acetone: methanol, then isopropanol and lastly in water. The substrates were used immediately after sputtering and cleaning procedure. Meanwhile, each selected individual clones were first grown in RM media (1XM9 Salts, 2% casamino acids, 1% glycerol, 1 mM $MgCl_2$, 50 μg/mL carbenicillin) 16-24 hours at 30^0C, shaking 225 rpm.

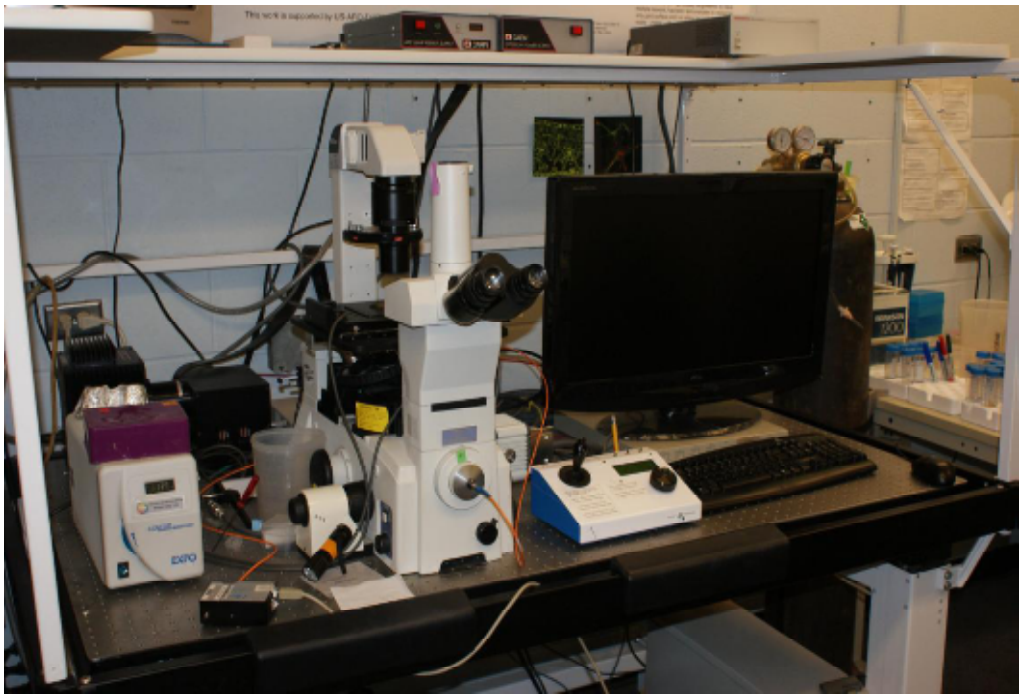

Figure 2.3: The optical microscope dedicated for fluorescence and dark field imaging.

Next, cells were induced in IMC media (50 μg/mL carbenicillin and 100 μg/mL tryptophan) for 6-16 hours at 37^0C shaking 225 rpm until mid-log phase (OD_{600nm}= 0.4). 1ml aliquots of induced-cell clones were labeled with 500 μL (2.5 μM in DI water) nucleic-acid fluorescent dye SYTO9 (Molecular Probes, USA) for 20 min by gently mixing. Labeled cells were incubated with a 12 mm diameter titanium surface for 20 min with rotating in the dark. Following, substrates were washed with DI

water two times, bound cells were visualized on the titanium surface using a Nikon Eclipse TE-2000U Florescent Microscope (with Hamamatsu ORCA-ER cooled CCD camera) (Figure 2.3) using a FITC filter (exciter 460-500, dichroic 505, emitter 510-560) (Figure 2.3) and METAMORPH Software (Universal Imaging, USA) Number of cell on the titanium surface was counted by using METAMORPH Software. As a negative control, *E.coli* GI826 (Invitrogen, 50-0091) plasmid-free cells were also grown in same conditions as described above except adding any carbenicillin in specified media and used for FM. All measurements were carried out in triplicate experiments; this led to the identification of three binding groups - strong, moderate and weak (Figure 2.4.).

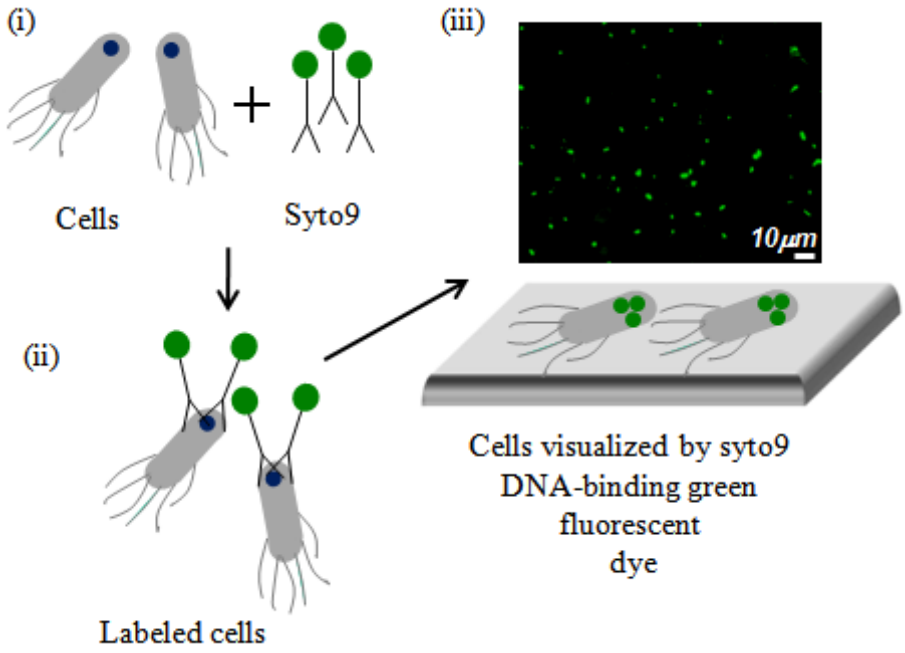

Figure 2.4: Initial binding characterization of titanium binding peptides via fluorescence microscopy.

2.2 Solid State Peptide Synthesis

An automated solid-phase peptide synthesizer (CS336X, CS-Bio Inc., Menlo Park, USA, Figure 2.5) was utilized to synthesize GEPIs through Fmoc-chemistry. In this approach, modified amino acids (Chempep, USA), where N-terminus and side chain of amino acids were protected by a Fmoc group and an appropriate protecting group, respectively, were used. In the reaction vessel, the Wang resin (Novabiochem, USA) pre-loaded with F-moc protected first amino acid was treated with 20% piperidine in

DMF to remove the Fmoc group, which was monitored by UV-absorbance at 301 nm. The incoming amino acid separately activated with HBTU (Sigma Aldrich, USA) in DMF was transferred into the vessel and incubated with the resin for 45 min. After washing the resin with DMF, the same protocol was applied for addition of the next amino acids. Following the synthesis, the peptide-resin conjugate was applied to the cocktail containing 90:5:3:2 TFA:thioanisole:EDT:anisole under nitrogen for 3 h to remove peptide from the resin as well as blocking agents from the side chains of the peptide. The peptide solution was then filtered to separate the resin and the peptide. The cleaved peptide was precipitated in cold ether followed by lyophilization (Virtis Benchtop K, SP Industries, Inc, USA) to get crude product. The purification was carried out by HPLC (Waters, USA) using C-18 column (Gemini, USA) under reverse-phase conditions (see Figure 2.6). Firstly, lyophilized peptide powder was dissolved in ~25/75 % (v/v) Acetonitrile:DI water mixture and injected into HPLC. At the column, isocratic gradient of Acetonitrile was maintained for 2 min and then 60 linear gradient of DI water with 1%/min for analytical (at a rate of 1 ml/min) and 0.5%/min for semi-prep scales (at a rate of 10 ml/min) was employed. Each peak monitored by the UV detector at 280 nm and 215 nm was collected and characterized by MALDI-TOF mass spectrometry with reflectron (RETOF-MS) on an Autoflex II (Bruker Daltonics, USA) mass spectrometer located in Department of Medicinal Chemistry at University of Washington. Synthesized peptides were listed in Table 2.1. The MW and pI parameters for each peptide were calculated through ExPASy Proteomics Server.

Figure 2.5: Image of CS-Bio peptide synthesizer.

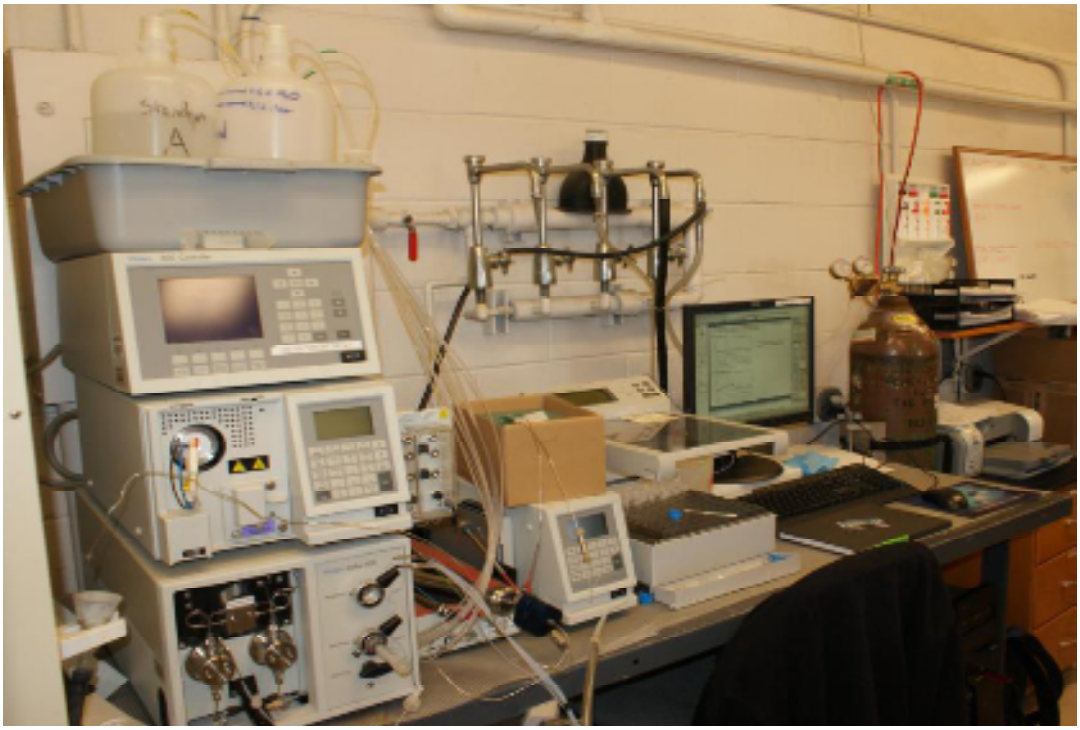

Figure 2.6: Image of Waters HPLC.

Table 2.1: Sequence, MW, pI and net charge of synthesized peptides.

Name	Sequence	MW (g/mol)	pI	Net Charge at pH 7.4
TiBP1	RPRENRGRERGL	1495.67	11.82	+
TiBP2	SRPNGYGGSESS	1197.18	5.72	0
TiBP60	VGRVTSPRPQGR	1309.49	12.3	+
TiBP1-RGDS	RPRENRGRERGL GGGRGDS	2082.23	11.70	+
TiBP2-RGDS	SRPNGYGGSESS GGGRGDS	1783.75	5.79	+
RGDS	RGDS	433.42	5.84	+
TiBP1-AMP	RPRENRGRERGLGGG LKLLKKLLKLLKKL	3341.14	11.85	+
TiBP2-AMP	SRPNGYGGSESSGGG LKLLKKLLKLLKKL	3042.66	10.39	+
AMP	LKLLKKLLKLLKKL	1692.34	10.70	+
TiBP2-cHABP1	SRPNGYGGSESS GGGCMLPHHGAC	2318.5	6.65	0
TiBP2-ADP5	Under Patent Pending	3815.99	6.48	0
TiBP2-ADP7	Under Patent Pending	5995.64	7.08	0
cHABP1	CMLPHHGAC	968	6.90	0
ADP5	Under Patent Pending	2465.6	7.16	0
ADP7	Under Patent Pending	4645.3	7.28	0

2.3 Molecular Structure and Modeling Methods

2.3.1 Circular dichroism spectroscopy (CD)

A solution containing 30 μM peptide, 100 mM Tris-HCl at pH 7.4 and various amounts of 2, 2, 2-trifluoroethanol (99.8% purity) was prepared for circular dichroic analysis. The spectrum, which is the average of 8 scans from 185 – 260 nm with a 0.5 nm/s scan rate, was collected at 20 ° C using an AVIV Stopped Flow 202SF CD Spectropolarimeter. The averaged spectrum, which was then subtracted with the appropriate buffer background, was smoothened using the Savitzky-Golay algorithm. A section of the smoothened spectrum (from 190 – 240 nm) was compared to the five component reference spectra [(1) a helix, (2) b sheet, (3) b turn, Type-I, (4) b turn, Type-II, and (5) random coil] compiled by Reed, *et al.* using a constrained least-squares fit [423]. Note that the standard spectra do not consider any aromatic nor disulfide dichroic contributions. This is appropriate because the analyzed peptides do not contain significant non-structural features. (TiBP2 contains only one peptide with an aromatic residue, Y.) The secondary structure estimates are reported as the fractional weight ± the standard deviation. All spectral smoothing and secondary structure estimation were executed using commercial graphing software (IGOR Pro. 6.0). The CD machine was carefully calibrated using (1S)-(+)-10-camphorsulfonic acid (Aldrich, 99%). Ellipticity is reported as mean residue ellipticity, q M (deg cm^2 $dmol^{-1}$).

2.3.2 Molecular modeling

Six different peptides (TiBP1, TiBP2, TiBP60, AMP, TiBP1-AMP, TiBP2-AMP as in Table 2.1) were modeled to determine molecular conformation of peptides. To model peptides, we built linear forms using the HyperChem's molecular modeling software (Hyperchem 7.5, USA). The energy minimization of these peptides was carried out under implicit solvent conditions using the conformational analysis program. The conformational search module finds the minimum-energy structures by varying the chosen dihedral angles. To perform energy minimization, it changes dihedral angles randomly and creates new initial structures. In each round of energy minimization, unique low-energy conformations are stored, and high-energy and duplicate structures are discarded. Using the conformational search module, we found 1000 different local minima on the potential energy surface, and we chose the

lowest one as the global minimum or the lowest-energy conformation [424, 378] Then, the lowest energy conformations are solvated with TIP3P water explicitly; and finally the overall system is energy minimized using the Polak-Ribiere conjugate gradient method until convergence of the gradient (0.01 kJ/mol) was reached using the CHARMM 27 force field [425]. The final configurations and the corresponding Ramachandran Plots were generated using the VMD (Visual Molecular Dynamics) software.

2.4 Quantitative Peptide Binding Characterization Methods

2.4.1 Quartz crystal microbalance (QCM)

In QCM-D systems the peptides or protein were flown through the flow cell onto the quartz crystal system. The mass loaded onto the quartz crystal was followed in real time. During the analysis of adsorbed layer of GEPI, dissipation change during the adsorption of the peptides was also monitored. The mechanic properties were followed as the change in the dissipation of the adsorbed layer and layers. The operating principle of the QCM-D system is represented in Figure 2.7

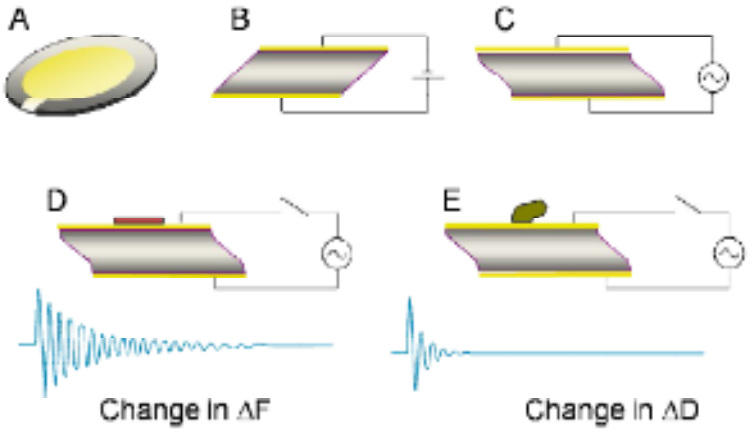

Figure 2.7: (A) The quartz crystal used in the QCM-D. (B) Applying of the direct current to the crystal (C) Applying alternative current to the quartz crystal (D) The change in the frequency upon adsorption of a layer onto the quartz crystal. (E) The change in the dissipation upon adsorption of a viscoelastic layer on to the quartz crystal (reproduced form the user guide of QCM-D apparatus, Q-Sense AB, Sweden) [382].

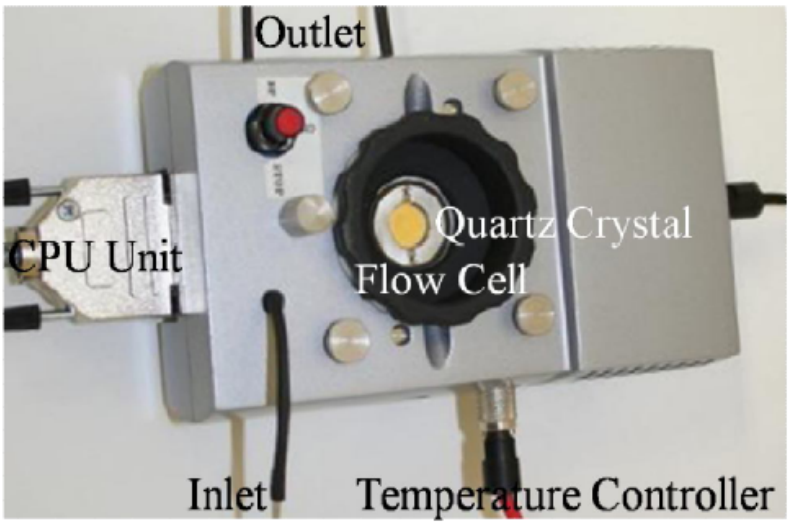

Figure 2.8: The picture of the Quartz Crystal System. The temperature of the QCMD system is controlled with Peltier embedded systems coupled with a temperature controller.

In this study, QCM-D was used to determine quantitative peptide binding affinity to solid surfaces. We monitored the interaction between inorganic surfaces and peptides (as listed in Table 2.1) using titanium, silica, gold and hydroxapaptite surfaces. The photograph of the QCM-D system in our lab is shown in Figure 2.8.

2.4.1.1 Quantification of peptide binding affinity via QCM

First, to quantify binding strength of peptides on titanium surface, five-megahertz quartz crystals (Q-Sense) were coated with 25nm of titanium via physical vapor deposition. Commercial SiO_x and hydroxapatite (HA) crystals (Q-Sense) were used to analyze peptide binding affinity on other surfaces. In the beginning of experiment, the crystals were placed in a KSV QCM-D Z500 parallel flow system, which monitors frequency change over time. PBS buffer were flown through the flow cell until the surface reach the steady state. Meanwhile, peptides were diluted in PBS buffer at various concentrations and introduced to the crystal surface by a flow cell. The flow was stopped and the peptides were allowed to bind to the surface until reaching equilibrium. Each concentration was flowed several times avoid depletion of the peptide in the flow cell. Binding was observed by the frequency shift, which is directly related to the wet mass of the adsorbed peptide. To determine the dissociation constant (K_d) of each peptide on titanium, the equilibrium frequency shift caused by peptide binding was measured at several concentrations. These values

were then fit using the Langmuir adsorption model. Initially, peptide concentrations of 0.1 to 2 μM and 2 μM to 15 μM were used for all binders. These concentrations were then adjusted as necessary to be in a similar range as the K_d value of each peptide. After testing, titanium and SiO_x surfaces were cleaned using a surfactant solution (1% SDS, 1N NaOH), HA surfaces were kept and cleaned in ethanol solution overnight, and all surfaces were ozone cleaned for 15 minutes before reuse.

2.4.1.2 *In vitro* monitoring for peptide-mediated mineralization via QCM

To determine the kinetics of hydroxyapatite mineralization and formation, QCM measurements were carried out. Firstly, titanium surface was equilibrated with PBS solution until reach steady state. Then 10 μM, 1 mL Peptide (TiBP2-cHABP1, TiBP2-ADP5, TiBP2-ADP7, TiBP2, ADP5, ADP7, cHABP1) solution that is dissolved in PBS was injected to the flow cell three times in 10 min time interval. Once the bifunctional peptide was observed to bind to the titanium substrate, a calcium-phosphate solution was introduced into the flow cell as a mixture (1:1 ratio) of 4.8 mM calcium chloride and 2.8 mM potassium phosphate. By using QCM, formation of Hydroxylapatite on top of the bifunctional peptide layer was monitored 24 hours. Then the substrate was gently washed with deionized water and was dried with pressurized nitrogen gas to ensure that any unbound hydroxyapatite minerals were removed. Following peptide mediated mineralized film were characterized under SEM and TEM.

2.5 Material Surface Characterization Methods

2.5.1 Scanning electron microscopy (SEM)

SEM was used first to determine surface morphology and chemistry of cp Grade1, cp Grade4 and titanium foil surfaces. Then bacteria, osteoblast and fibroblast adhered titanium surfaces was monitored under SEM. The last peptide–mediated hydroxyapaptite mineralization on titanium surfaces were characterized by applying SEM. All experiments were carried out and scanned under JSM-7000F (JEOL, Japan) coupled with the attachments for Energy-dispersive X-ray (EDX) spectroscopy (Figure 2.9).

Figure 2.9: JEOL JSM-7000F Scanning Electron Microscope with EDX detector.

In case of determination surface properties of cp Grade1, cp Grade4 and titanium foils, samples were directly mounted onto aluminum cylinder using carbon tape. Images and EDS spectra were taken at 9 keV using a LaB_6 filament. EDS spectra were collected for 100 seconds at approximately 1500 counts per second (cps). In case of monitoring cell- adhered titanium and hydroxapatite mineralized surfaces, the samples were coated with thin layer of platinum and then directly placed on the aluminum mouth.

2.5.2 Atomic force microscopy (AFM)

Surface morphology and roughness of cp Grade1 and cp Grade4 titanium implant surfaces were obtained by using AFM. Root mean square roughness (R_{rms}) of cleaned implant disks and topographic features were examined by using a Nanoscope III/MMAFM system (Veeco Instruments, Inc., Santa Barabra, CA). (Figure 2.10) Scans of 30 μm by 60 μm were made in contact mode using standard SiN contact mode AFM tips. R_{rms} values were calculated from these scans using the onboard software.

Figure 2.10: The image of the Atomic Force Microscope in the chamber for acoustic and mechanical isolation.

2.5.3 Transmission Electron Microscopy (TEM)

Philips EM420 TEM (Figure 2.11) was used to observe crystal structure or X-ray pattern of peptide mediated–hydroxapatite mineralized surfaces. Prior to characterization, nanoparticles were rinsed with DI water to remove the salt and then drop-coated on copper TEM grid coated with carbon film (Ted Pella, USA). Excess of the nanoparticle solution was removed using tissue paper and then the grid was allowed to dry under vacuum. 100 kV were used as accelerating voltage. The projection of the nanoparticles was printed on photographic negatives (Kodak, USA) that were then developed in the dark room.

Figure 2.11: Philips EM420 Transmission Electron Microscope.

2.6 Preparation of PDMS Stamps for µCP

2.6.1 Master preparation

The silicon wafer was prepared through cleaning procedure in which the wafer was sonicated in acetone for 5 min, then incubated in methanol for a min, and, lastly, dried under stream of nitrogen. The cleaned substrate was spin-coated with negative photoresist, SU-8 2035 (Microchem, USA) through two subsequent steps; 500 rpm for 5 sec and 3000 rpm for 45 sec. Photoresist-coated wafer was incubated for 3 min on hotplate that was set to 65^0C, and then kept for 6 min following ramping up to 95^0C. Soft-baked wafer was then exposed to UV light (λ= 365 nm) for 20 sec through a photomask where the micropatterns were printed on. For the post exposure baking, UV-exposed wafer was kept at 65^0C for 1 min and then at 95^0C for 6 min on hotplate. Micropatterns produced on the photoresist were developed through incubating the photoresist coated silicon wafer in SU-8 200 developer (Microchem, USA) for 5 min. Finally, the wafer (master) was incubated at 200^0C for hard baking.

2.6.2 PDMS stamp preparation

A small petri dish with one droplet of tridecafluoro-1,1,2,2-tetrahydrooctyl)-1-trichlorosilane was placed into the bottom of the desiccator whereas the master was located at upper part of it. Desiccator was closed and left for 30 min under vacuum. This treatment step makes the master surface hydrophobic so that the PDMS sticking on the master is avoided. The modification can be controlled by putting a drop of water on the master to see if the droplet is formed. If it is formed, master is ready to use. CAUTION: the silane molecule is toxic and the fume hood is necessary.

Viscous pre-polymer and the curing agent (Sylgard 184 Elastomer kit, Dow Corning, USA) were mixed with ratio of 10:1 (w/w) and poured onto the treated master. Following degassing for removing the formed air bubbles, the viscous mixture spread on the master was cured at 70°C for overnight. The PDMS and master were separated and the elastomer stamp was cut into the smaller pieces. The stamps were then washed several times with ethanol and dried with nitrogen before use.

2.7 Cytotoxicity Assays for Peptide Functionalized Titanium Surfaces

2.7.1 Cell culture maintenance

MC3T3-E1 preosteoblast (ATCC, CRL-2593™) and NIH3T3 (ATCC, CRL-1658™) were cultured in Minimum Essential Medium (MEM) Alpha Medium (Gibco, 12561) supplemented with 10% fetal bovine serum (Gibco, 16250), 2mM glutamine (Gibco, 25030-164) and 1% antibiotic solution (Gibco, 15140). Cells were incubated at 37°C in 5% CO_2 for one week. After one week, cells were enzymatically detached from the surface of the petri-dish using 0.25% trypsin-EDTA solution (Gibco, 25200) and precipitated by centrifugation (2000 rpm for 5min). Following, certain number of cells was used to proceed further experiments.

2.7.2 Cell viability (MTT assay)

First, peptides (TiBP1 and TiBP2) were dissolved and diluted to 200 μM in 1X PBS (Gibco, 14200). Then, 750 μL each peptide solution was incubated with sterilized cp Grade1 and Grade4 implant surfaces and as a positive control, each type of implant surfaces were also incubated 1X PBS for 4 hours at 37°C in 5% CO_2. Following incubation with the various solutions, all samples were washed two times in 1X PBS

to remove unbound peptides. $8x10^5$ cells/mL (2 mL) cells in 12-well plates were exposed to samples and as a negative control in other wells. The cultures were maintained in serum-free Minimum Essential Medium (MEM) Alpha Medium with 1% antibiotic solution at 37°C in 5% CO_2 and incubated for 24 hours. Following incubation time, 200 µL media was removed from each well, 200 µL of an MTT (Sigma M5655) solution (5 mg/mL) (1:10 ratio) was added into each well and incubated 3 hours. At the end of incubation time, purple formazan crystals were observed under inverted microscope. All implant surfaces were transferred into clean wells and formazan crystals were dissolved and incubated with 1.5 mL DMSO and 0.1 M Glycine, NaCl pH 10.5 (10:1) ratio for 5 min. Absorbance of converted dye was measured at a wavelength of 570 nm with background subtraction at 630-690 nm. Relative cell viability (%) was calculated based on bare titanium surfaces for each group.

2.7.3 Cell adhesion and spreading

In this section, cp Grade4, cp Grade1 titanium implant surfaces and glass coated titanium were functionalized with peptides (TiBP1, TiBP2, TiBP1-RGDS, TiBP2-RGDS, RGDS) as described above. Following each peptide modified surfaces were inoculated with 10^4 cells in 1 mL serum free media for 2 hours at 37^oC and 5% CO_2. Following the 2 hours incubation, the cells were fixed in 500 µL of 2% glutaraldehyde (Ted Pella, USA) solution in PBS for 20 minutes at room temperature and dehydrated with a series of increasing ethanol solutions. (10-30-60-90-100% ethanol, 10 minutes in each). The implant disks were then rinsed twice with PBS. Previously prepared methanolic stock solution of Alexa Fluor488-Phalloidin (Invitrogen Co., U.S.A.) was diluted 200 times in water to obtain an approximately 33 nM working solution. 500 µL of the final working solution was added on top of each sample and kept at room temperature protected from light for 20 minutes. The samples where then rinsed twice with distilled water and dried under N_2, then observed using a TE 300L microscope (Nikon, Japan). Metamorph (Universal Imaging, USA) and Image J Software (NIH) were used to analyze number of cell, cell spreading and circularity factor.

2.8 Antimicrobial Assays for Peptide Functionalized Titanium Surfaces

2.8.1 Bacterial maintenance and culturing

Three bacteria - *Escherichia coli* ATCC® 25922™, *Streptococcus mutans* ATCC® 25175™, and *Staphylococcus epidermidis* ATCC® 29886™ - were used in the present study. All bacteria were cultured according to ATCC® protocol using the following media: Tripticase Soy Broth (TSB) for *E. coli*, Brain Heart Infusion (BHI) Broth (Sigma Aldrich, 53286) for *S. mutans*, and Nutrient Broth (NB) (Difco, 0003) for *S. epidermidis*. For all three bacterial species, the bacterial pellet obtained from ATCC was rehydrated in 0.5 mL of the above specified media, and several drops of the suspension were immediately placed and streaked on an agar slant of the specified media. The agar was then incubated aerobically at 37°C for 24 hours (and in the presence of 5% CO_2 in the case of *S. mutans*). *S. mutans* overnight cultures were made by aseptically transferring a single-colony forming unit into 10mL of BHI, followed by aerobic incubation at 37°C in the presence of 5% CO_2 for 16 hours under static conditions. Overnight cultures of *S. epidermidis* and *E. coli* were made by aseptically transferring a single-colony forming unit into 10 mL of NB or TSB (respectively), followed by aerobic incubation at 37°C with constant agitation (200 rpm) for 16 hours.

2.8.2 In solution antimicrobial activity of TiBP-AMP conjugates

The in-solution antimicrobial activities of the peptides were analyzed against *S. mutans, S. epidermidis,* and *E. coli* spectrophotometrically. For each bacteria species, peptide solutions (AMP, TiBP1-GGG-AMP, and TiBP2-GGG-AMP) were added in specified media to reach final concentrations of 10 μM-200 μM, and inoculated with the bacteria to a final concentration of 10^7 cells/mL. Bacterial growth at 37°C was monitored over the course of 24 hours by optical density measurements at 600 nm on a Tecan Safire Spectrophotometer No. I 112 913. For each experiment, a positive control consisting of solely 10^7 cells/mL of bacteria in the specified media, and a negative control consisting of solely media was monitored as well. Additionally, bacterial growth of the three bacteria in the presence of TiBP1 and TiBP2 was monitored to determine if the titanium-binding peptides exhibited any antimicrobial effects.

2.8.3 Titanium substrate preparation and peptide immobilization

0.5 mm thick, 99% titanium foil (AlfaAesar, 43677) was cut into 1 cm x 1 cm squares. The titanium substrates were cleaned by sonicating them for 15 minutes each in a 1:1 acetone:methanol mixture, then isopropyl alcohol, and finally de-ionized water. Following all bacterial-adhesion experiments, substrates were first soaked overnight in a 1:1 mixture of 20% bleach: 70% ethanol before being cleaned by the above regimen. Cleaned $1cm^2$ titanium foil substrates were transferred into a pre-sterilized 24-well plate. The substrates were then sterilized under UV light for 15 minutes on each side. Substrates were subsequently incubated aerobically at 37˚C under constant agitation (200 rpm) with 500 µL of 1X PBS (positive control), AMP, TiBP1-GGG-AMP, or TiBP2-GGG-AMP solutions for 4 hours. (200 µM peptide solutions were used for *S. mutans* experiments, while 50 µM peptide solutions were used for *S. epidermidis* and *E. coli* experiments as these were determined to be the minimal inhibitory concentrations for each of the bacteria. Following the 4 hours of incubation with peptides, the peptide solutions were removed from each well. 1 mL of sterile 1X PBS was then added to each well, pipetted up-and-down twice, and removed from the well. A second 1 mL of sterile 1X PBS was then added to each well, pipette up-and-down once, and removed from the well. Using sterile forceps, each titanium substrate was moved to a clean well, free of any peptides.

2.8.4 Mid-log culture and preparation of 10^8 cells/mL cell suspension

To proceed with bacterial adhesion experiments, overnight cultures for each bacteria were prepared as described above. Bacteria from the overnight cultures were used to inoculate fresh media to a final concentration of 10^7 cells/mL. Cultures were then incubated in the same manner as the overnight cultures were (see *bacterial maintenance and culturing*), until they reached the mid-log phase as determined by optical density measurement at 600nm. (*S. mutans* O.D.≈0.4, *S. epidermidis* O.D.≈0.25, and *E. coli* O.D.≈1.0.) Cultures were then centrifuged at 4000 rpm for 5 minutes in a Sorvall® RC 5B Plus Centrifuge. The supernatant was removed and the bacterial pellet was re-suspended in 500 µL of specified media. This suspension was then transferred to a 2 mL centrifuge tube and centrifuged at 5500 rpm for 3 minutes in a Fischer Scientific accuSpin™ Micro Centrifuge. The supernatant was carefully removed and the bacterial pellet was re-suspended in sterile 1X PBS to a

final concentration of 10^8 cells/mL. Then, 1mL of the 10^8 cells/mL cell suspension was added to each well containing a peptide-modified titanium substrate, and incubated for 2 hours. For *S. mutans* experiments, incubation was carried out aerobically at 37°C in the presence of 5% CO_2 under static conditions; for *S. epidermidis* and *E. coli* experiments, incubation was carried out aerobically at 37°C under constant agitation (200 rpm). After 2 hours incubation, first the bacterial suspension was removed and the surfaces were washed two times with 1 mL of 1X PBS by pipetting.

2.8.5 Fixation of adhered bacteria to peptide-modified titanium surfaces

Cells adhering to Titanium substrates were fixed with 500 µL of 2% Glutaldehyde (in 50 mM Tris Buffer, pH 7.4) for 30 minutes, followed by dehydration in a series of increasing alcohol baths. (50% ethanol for 10 minutes, 70% ethanol for 10 minutes, 90% ethanol for 10 minutes, followed by a 1mL wash with 100% ethanol.)

2.8.6 Micro-contact printing of TiBP1-AMP with *S. mutans*

To establish the dramatic effects of TiBP1-GGG-AMP, the peptide was stamped onto a clean titanium-substrate in a manner previously described. The patterned side of the polydimethylsiloxane (PDMS) stamp was incubated in 200 µM of TiBP1-GGG-AMP for 5 minutes and then the peptide solution was removed by pipette from the surface of the stamp. The stamp was dried with inert gas, followed by a brief washing with 1X PBS. The titanium substrate was then applied to the surface of the stamp and pressed using force for 10 seconds and left on the stamp for 1 minute. Then the substrate was removed from the stamp, washed twice with 1X PBS and was then subjected to the above procedures (except the incubation with peptides) for *S. mutans* only.

2.8.7 Visualization and quantification of bacterial adhesion on GEPI-modified titanium substrates

500 µL of 5 µM SYTO 9 dye was added onto bacteria adhered and fixed titanium surfaces, protected from light, and incubated for 20 minutes. Substrates were then washed 3 times with 1 mL of 1X PBS by pipetting the PBS up-and-down two times. Substrates were then secured onto a clean microscope slide and viewed under a Nikon Eclipse TE2000-U Fluorescent Microscope. Five random images of each

surface were taken and analyzed for percent surface coverage using Meta Morph (Version 6.r6) software. Two independent analyses were conducted and averaged for each image. For each substrate, the averaged value for each of the five images were averaged together and subjected to statistical analysis.

2.9 Statistical Analysis

One way Anova Test was used to determine the significant difference $p<0.05$ between the samples.

3. RESULTS AND DISCUSSION

3.1 Selection and Characterization of Titanium Binding Peptides (TiBPs) as a Molecular Linker

3.1.1 Biocombinatorial selection and characterization of TiBPs

Biocombinatorial methods such as phage and cell surface display have been widely used to identify peptide sequence with high affinity and specificity for inorganics. In here, we first applied cell surface display technique [341] onto cp Grade 4 titanium dental implant [426] to select TiBPs as a potential molecular linker for titanium implant surface functionalization. Then, detail peptide characterization were performed in the frame of binding affinity, specificity and peptide structure that will allow us precise control on utilization of peptide as a potential molecular linker for implant surface functionalization. In the cell surface display selection, after four successive rounds of biopanning, 60 random clones with equal distribution from each round were selected and subjected to sequence analysis. Among peptide sequence, consensus binding motive wasn`t obtained as in general protein-protein interaction. To identify clear consensus binding motive is difficult in selection of inorganic binding peptides because of inorganic surface heterogeneity [9]. Consequently, further binding analysis via fluorescence microscopy (FM) was applied to assess the affinity levels of individual clones semi-quantitatively. In this method, binding affinity levels for each clone was achieved by incubating the selected clones with a titanium surface, followed by staining with Syto9 dye. The Syto 9 dye, which binds to nucleic acids, allowed for the visualization and quantification of bound clones; the bound cells expressing titanium-binding sequences were visualized as fairly uniformly distributed bright green rods on a dark background, as opposed to GI826 plasmid free control cells, which did not adhere to the titanium substrate (Figure 3.1).

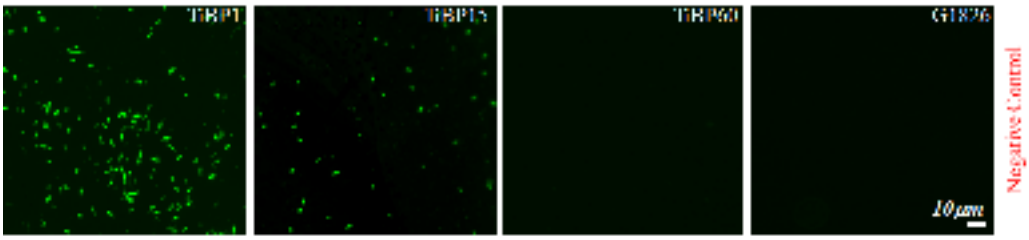

Figure 3.1: Florescence microscopy images of titanium binding peptides with various binding affinities.

The binding affinity of selected titanium-binding clones was estimated by enumerating adhered cells in three random regions in triplicate experiments. This led to categorization of binders into three different groups: strong, moderate and weak binders (Figure 3.2).

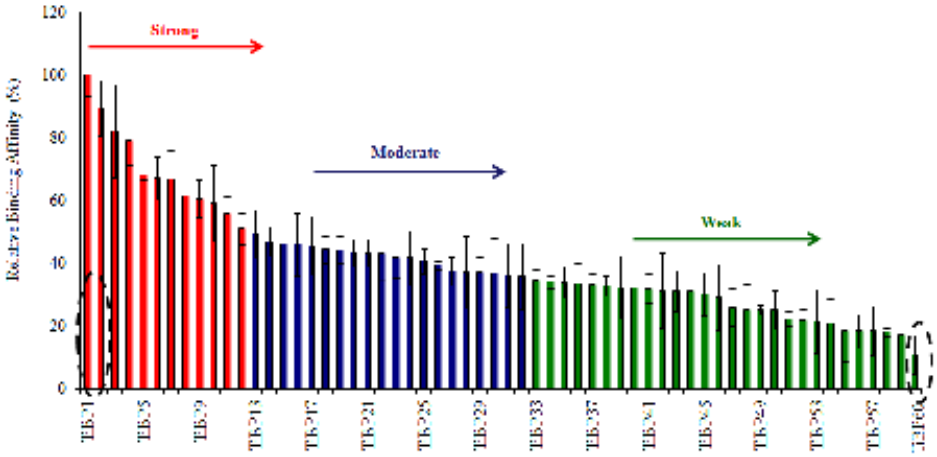

Figure 3.2: Categorization of titanium binding clones via fluorescence microscopy.

Following this categorization, to determine the role of amino acid distribution on binding affinity of clones on titanium surface, we compared the observed amino acid distribution among strong and weak binder groups of selected TiBPs with the native (unpanned) library to calculate the relative abundances of amino acids among them. Based on amino acid distribution analysis of the TiBPs, expression level of polar amino acids (Ser, Asn), and basic (Arg) amino acids were noticeable (Figure 3.3).

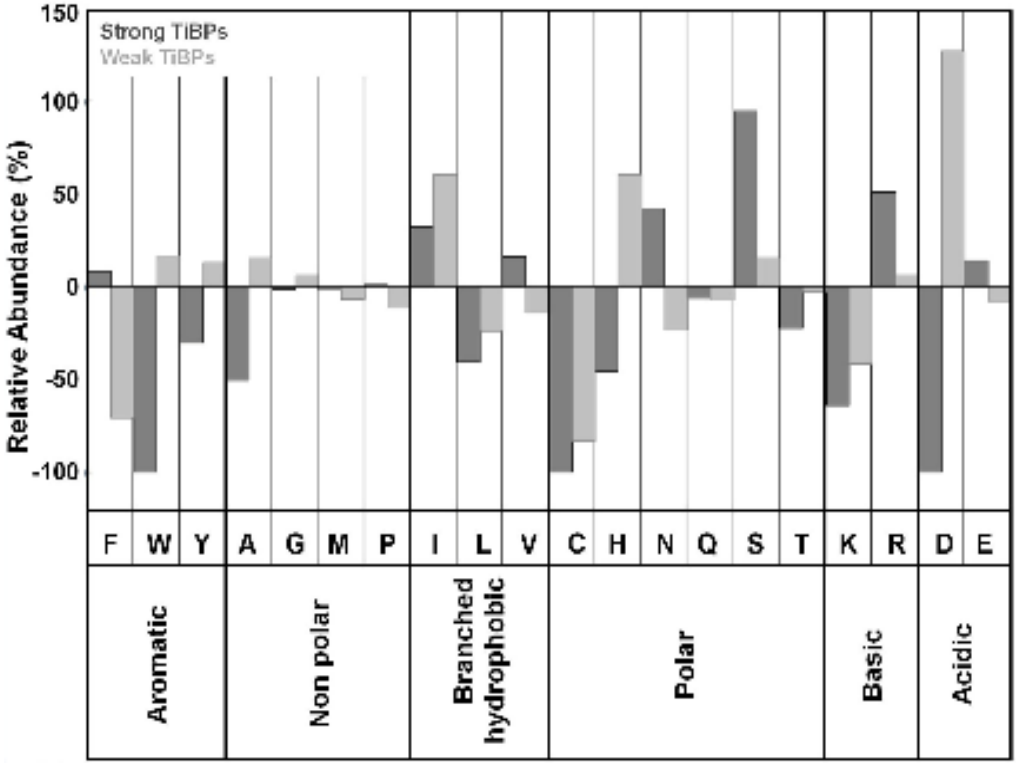

Figure 3.3: Relative abundance of amino acids in strong and weak binding groups of titanium binding peptides.

Physico-chemical properties of both inorganic surfaces and peptides need to investigate to bring approaches on peptide recognition and binding on solid surfaces. Especially, the role of amino acid composition versus amino acid sequence order and the role of peptide net charge versus local charge distribution have been studying to understand binding mechanism of peptides to desired surface. Number of studies in the literature has been focus on probing interactions peptides and metal, metal-oxide and mineral surfaces based on amino acid type and position relations. For example, mineral (e.g hydroxapatite) binding sequences are rich in acidic residues (aspartate, glutamate and serine) resulting in a net negative charge that promotes binding to positively charged calcium at apatite crystal faces. Hydroxyl rich and cysteine residues present in metal (e.g gold) binding sequences. In metal-oxide (e.g titanium and silica) binders case, peptides enriched with charged and polar amino acid residues (Lys, Arg, His, Asp and Glu) have high affinity to most of the negatively charged metal–oxide surfaces, because of their positive charge in an aqueous environment at neutral pH [380, 359, 381].

In this study, amino acid distribution among strong binders indicate us different trend from literature. Expression level of Ser is remarkable compare to His, Lys and Arg expression that have role peptide binding on metal–oxide. Besides, expression levels of Asp and Glu are similar to previous studies (Figure 3.3). Although there is general categorization for amino acid type in binding sequences to metal, metal-oxide and mineral surfaces, to understand and indicate clear contribution of each residue based on their effect on peptide net charge and local charge distribution is challenging. There are key limitations factors such as target surface properties, selection technique and solution pH to reveal this difference. In the literature, there are a number of peptides that were selected utilizing phage display against different forms and various sizes of titanium oxide powders, such as anatase, titania and titanium particles [359, 411, 380]. Features of phage and cell surface library and their adapted protocols are a constraint in terms of their design criteria based on different amino acid distribution percentage, peptide generation efficiency, and random sequence diversity. Consequently, to draw conclusion about peptide binding affinity to metal oxide surfaces in the frame of this parameter is difficult so different critical design parameters should also be evaluated.

In here, to refine peptide binding affinity to titanium and other implantable (e.g Silica and HA) surfaces and to show peptide capability as a molecular linker more in detail, we chose three peptides, TiBP1 and TiBP2 have very similar high titanium binding affinity with their distinct physicochemical properties; TiBP60 has the lowest affinity exhibiting similar physicochemical properties with TiBP1 (Table 3.1) based on initial FM characterization. The first reason for choosing these sequences is that evaluation of their adsorption behavior on titanium surface by combining their molecular structure. The second reason is that analyzing binding affinity and selectivity properties of TiBP1 and TiBP2 on other implantable surfaces such as silica and HA to indicate their potential capability as a molecular linker. The third is that to show the difference in physicochemical properties of TiBP1 and TiBP2 may allow us flexibility to control their efficient immobilization on implant surfaces while conjugating them with biomolecules.

Table 3.1: Amino acid sequence and physicochemical properties of TiBP1, TiBP2 and TiBP60.

Peptide Name	AA Sequence	MW	pI	Charge
TiBP1	RPRENRGRERGL	1495.67	11.82	+3
TiBP2	SRPNGYGGSESS	1197.18	5.72	0
TiBP60	VGRVTSPRPQGR	1309.49	12.3	+3

3.1.2 Conformational properties of TiBPs

Molecular conformation is one of the challenging design parameter to understand peptide binding behavior to desired surface. Its challenge comes from a number of polypeptides which interact with inorganic solids exhibit some degree of intrinsic disorder or unfolded structure. [383, 427, 354, 367, 428, 429] In addition, it has been shown that folding propensity, or the ability of an unfolded polypeptide sequence to fold into an ordered structure, is another molecular characteristic that distinguishes functionally different inorganic binding protein sequences from one another [367, 428] From this, we first synthesized TiBPs by solid phase synthesis and then investigated two properties : First, we assayed for the presence of ordered or disordered structure within each sequence, and second, we determined the folding propensity of each sequence in the presence and absence of the structure-stabilizing solvent, 2, 2, 2-trifluoroethanol (TFE). As shown in Figure 3.4, at 0% TFE in aqueous media each peptide exhibits a strong (-) ellipticity band representing the pi – pi* transition[428, 423] For TiBP1 and TiBP2 this band is centered near 198 nm and is characteristic of random coil conformation in equilibrium with other secondary structures such as alpha-helix and beta turn that are featured in these sequences (Table 3.2) [428, 354, 423, 367, 429] The presence of beta turn structures may arise from the Arg, Gly and Ser residues in TiBP1 and TiBP2 that would promote turn or loop-like regions in either sequence [428, 430, 431]. In addition, TiBP2 possesses a second, slightly (+) ellipticity band centered near 218 nm, representing the n-pi* transition. Under the same conditions the TiBP60 peptide sample features a pi-pi* band centered near 200 nm and this reflects a shift away from random coil

conformation towards other secondary structures. As shown in Table 3.2, TiBP60 possess more beta strand structure and reduced beta Type II content compared to either TiBP1 or TiBP2 and this may be due to the presence of a extended beta strand forming tetramer sequence cluster, -PRPQ-, [432] located near the middle of the TiBP60 sequence.

Table 3.2: Secondary structure classifications of TiBP1, TiBP2 and TiBP60.

		TiBP1	TiBP2	TiBP60
Alpha helix	% 0 TFE	0	0	0
	% 75 TFE	0.02 ± 0.01	0	0.01 ± 0.004
Beta sheet	% 0 TFE	0	0	0.26 ± 0.03
	% 75 TFE	0.07 ± 0.03	0.06 ± 0.04	0.22 ± 0.02
Beta turn Type I	% 0 TFE	0.13 ± 0.03	0.12 ± 0.03	0.04 ± 0.02
	% 75 TFE	0.11 ± 0.02	0.13 ± 0.03	0.08 ± 0.01
Beta turn Type II	% 0 TFE	0.30 ± 0.07	0.37 ± 0.07	0.13 ± 0.04
	% 75 TFE	0.30 ± 0.05	0.35 ± 0.06	0.21 ± 0.03
Random coil	% 0 TFE	0.57 ± 0.08	0.51 ± 0.07	0.57 ± 0.04
	% 75 TFE	0.50 ± 0.05	0.47 ± 0.07	0.48 ± 0.03

Thus, this tetramer sequence may be inducing a more linear, extended beta strand-like region within TiBP60 that is not found in the random coil/beta turn structures of TiBP1 or TiBP2. From this data, we conclude that each TiBP peptide exhibits intrinsic disorder, with TiBP1 and TiBP2 adopting a combination of coil, turn, or loop structures in solution, whereas TiBP60 adopts a more linear conformation under the same conditions. With the addition of TFE, we note that for each peptide the pi-pi* transition ellipticity band is reduced in intensity as a function of TFE addition and undergoes a 7-8 nm red shift in absorption wavelength. This red shift is indicative of a shift in secondary structure population away from random coil towards other secondary structures, and thus like other intrinsically disordered inorganic binding sequences each TiBP peptide undergoes some degree of

conformational reordering in the presence of TFE. This is reflected in Table 3.1, where the percentage of random coil structure is observed to decrease for each peptide at 75% v/v TFE as compared to 0% v/v TFE.

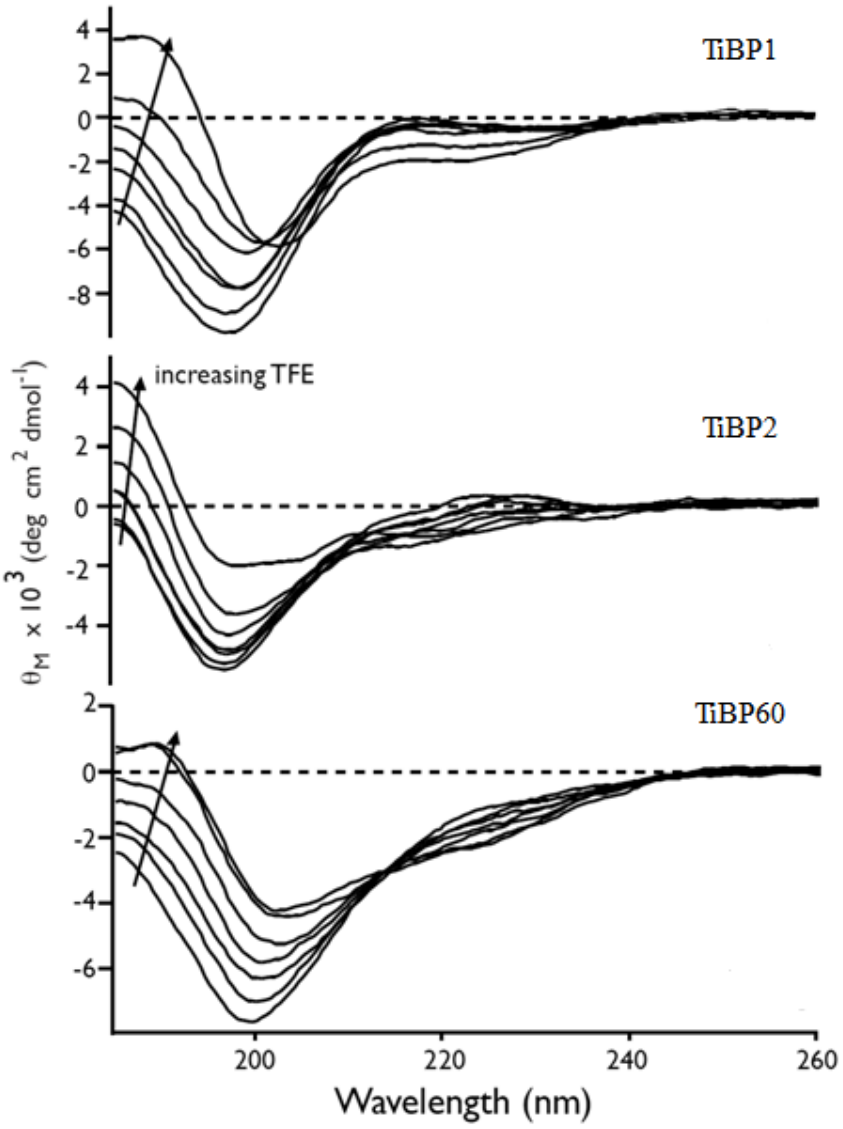

Figure 3.4: CD spectra of 30 μM TiBPs (TiBP1, TiBP2, TiBP60) in the presence of varying volume percentages of TFE in 100 μM Tris–HCl, pH 7.4. Arrow indicates increasing sample TFE concentration (0, 10, 20, 30, 40, 50, 75 %).

In addition, we note that TiBP60 exhibits an isochromic transition point [423] centered at 215 nm, and this is not observed for either TiBP1 or TiBP2. We infer from this transition point that the conformational transition for TiBP60 differs from that of TiBP1 and TiBP2, and we believe that this difference may arise from the

presence of the extended -PRPQ- sequence in TiBP60. These observed differences in conformational transition may play a role in the ability of these sequences to adapt to titanium surfaces. The structural models of the three different titanium-binding peptides, two of them strong (TiBP1 and TiBP2) and one of them weak (TiBP60), have been obtained using CHARMM force field parameters for the peptide and TIP3P parameters for the solvent. All three peptides mainly have turn and random coil conformations, lacking regular secondary structure elements such as an alpha helix or beta sheet (Fig. 3.5).

This finding is in accord with the CD analysis and indicates that all three peptides exhibit some degree of intrinsic disorder or unfolded structure.[383, 427, 354, 367, 428, 429] The plots in Figure 3.5 shows the structure of the peptides in water, which is omitted for clarity, and reflects the CD experiments in the absence of the structure-stabilizing solvent (TFE). These plots indicate that, TiBP1 and TiBP2 have slightly more compact structures than TiBP60, which may explain the differences in conformational transition studied via CD experiments in TFE conditions.

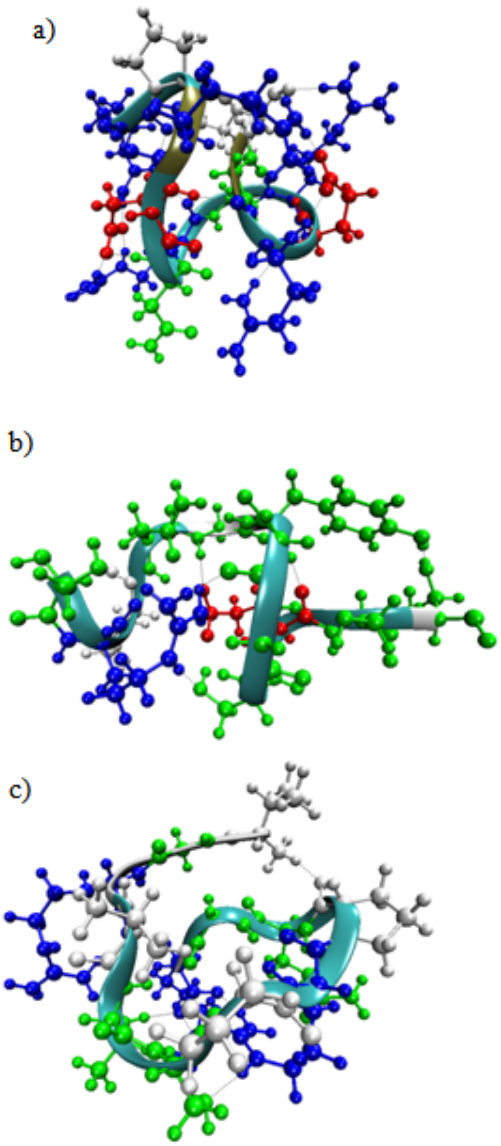

Figure 3.5: a) Overlapped ribbon and CPK models of the predicted structures of the (a) TiBP1, (b) TiBP2 and (c) TiBP60. The residues are colored according to residue type (Basic: blue, Acidic: red, Polar: green, Nonpolar: gray). The backbone is colored according to secondary structure (Turn: cyan, Random Coil: Gray, Isolated Bridge: Tan). *Water is omitted for clarity.*

3.1.3 Adsorption behavior of TiBPs on titanium and other implantable surfaces

Understanding the exact nature of peptide binding mechanism on solid surfaces has been elusive for practical applications. Various peptides that can mediate cell adhesion were adsorbed or covalently attached onto biomaterial surfaces. However, these cell adhesive sequences were not designed based on preferential affinity towards a specific material. Weakly attached molecules can be redistributed by cells

attempting to attach the surface. In this case, effective formation of focal adhesion that influences cell attachment will not occur. This demonstrates that the need to design a peptide including both material specific and cell adhesive domains. To investigate adsorption behavior of peptide on titanium surfaces provides us not only adjusting initial peptide concentration required to promote cell adhesion but also evaluation of molecular structure and peptide binding mechanism relations.

In here, we tested the adsorption behavior of TiBP1, TiBP2 and TiBP60 quantitatively via QCM on titanium-coated quartz crystals. Frequency shift (ΔF) data from QCM was used to determine the dissociation constants (K_d) for each peptide. K_d values represent the concentration necessary to achieve 50% surface coverage on a given surface. Thus the lower the K_d value the stronger the peptide binds to that surface. The K_d values were calculated by fitting data to Langmuir's adsorption model. This was done using the following relationship:

$$-\Delta F = \Delta F_{max} C/(C + K_d) \quad \textbf{3.1}$$

where ΔF_{max} is the frequency shift when the surface is saturated and C is the concentration of the bulk solution. The unknown constants ΔF_{max} and K_d were fit to the data using a least squared regression. The dissociation constant is also related to the free energy of adsorption by the following relationship:

$$\Delta G_{ads} = RT \ln(K_d) \quad \textbf{3.2}$$

The TiBP1, TiBP2 and TiBP60 showed vast difference in their binding affinity. In the case of TiBP1 and 2, shown to be a strong binder in FM analysis, the peptide saturated the surface at relatively low concentrations (Figure 3.6), yielding K_d values of 0.90 μM and 018 μM, respectively in Table 3.3. Both of these peptides can be characterized as strong binders from these K_d values when compared to other titanium binding peptides in the literature [380].

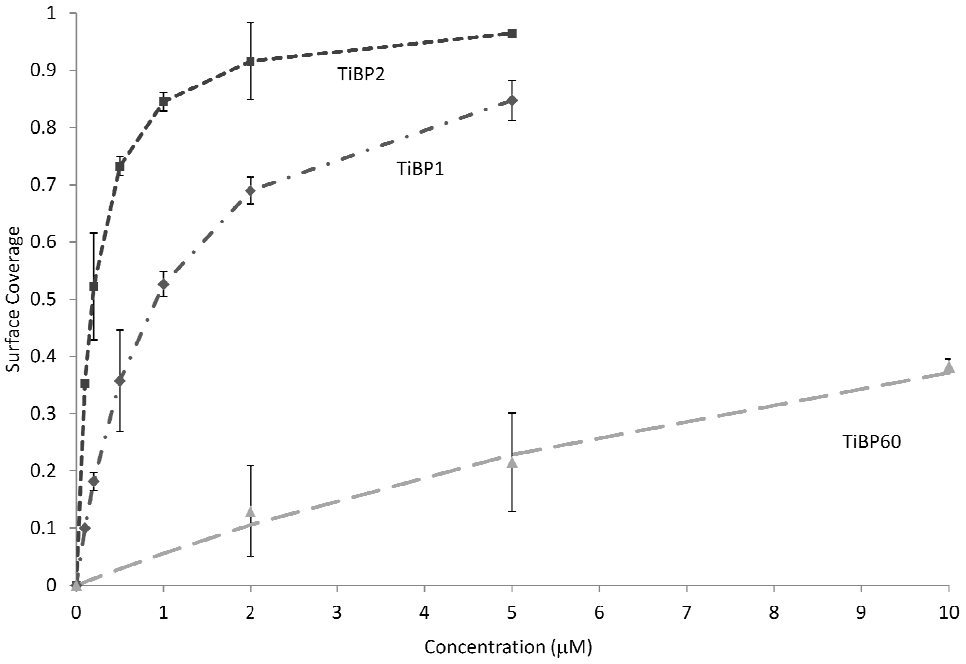

Figure 3.6: Surface coverage of TiBP1, TiBP2 and TiBP60 on titanium via QCM.

On the other hand, TiBP60 showed much weaker binding on titanium with 14.76 μM K_d value (Figure 3.6 and Table 3.3), confirming FM results. TiBP60 requires an approximately one hundred times higher concentration in solution to achieve the same surface coverage as TiBP2 (Figure 3.6 and Table 3.3). There is a significant difference in binding strength between the strong binding peptides. TiBP2 showing five times lower K_d value than TiBP1.

Table 3.3: Observed K_d and ΔG values of TiBP1, TiBP2 and TiBP60.

	QCM Analysis	
Peptide Name	**K_D (μM)**	**ΔG (kcal/mol)**
TiBP1	0.90 ± 0.12	-8.25 ± 0.08
TiBP2	0.18 ± 0.03	-9.19 ± 0.11
TiBP60	14.76 ± 2.74	-6.59 ± 0.12

The reason of this difference in K_d could be the cause of various parameters between the two peptides that we mentioned above. TiBP2 has high binding affinity with its hydroxyl (Ser) rich amino acid content and with its neutral charge. Although TiBP1 and TiBP60 have high Arg content with their net positive charge, their binding strength is an order of magnitude different than each other. The thermodynamic effect of this difference is not so significant, as shown in the ΔG_{ads} values in Fig. 4b. In case of TiBP60, it has higher binding energy (-6.59 ± 0.12 kcal/mol) compared to TiBP1 and TiBP2 respectively (-8.25 ± 0.08, -9.19±0.11 kcal/mol). In the literature, the assumption on peptide binding adsorption basically relies on oxide layer and charged group interactions. Identified peptides possessed strong enrichment in histidine residues, hydroxyl-containing residues and with high cationic charge [411, 358]. However, The trend on adsorption behavior of TiBPs indicate us, it is not only results of electrostatic interactions, hydrogen, hydrophobic, dipole or combination of these forces but also more complex binding mechanism involved in peptide inorganic interactions beyond simple binding affinity, amino acid content and peptide net charge correlation. The observed differences in their binding affinity may be attributed to the similarities in their molecular architecture so conformational transition may play a critical role in the ability of these sequences to adapt to titanium surfaces.

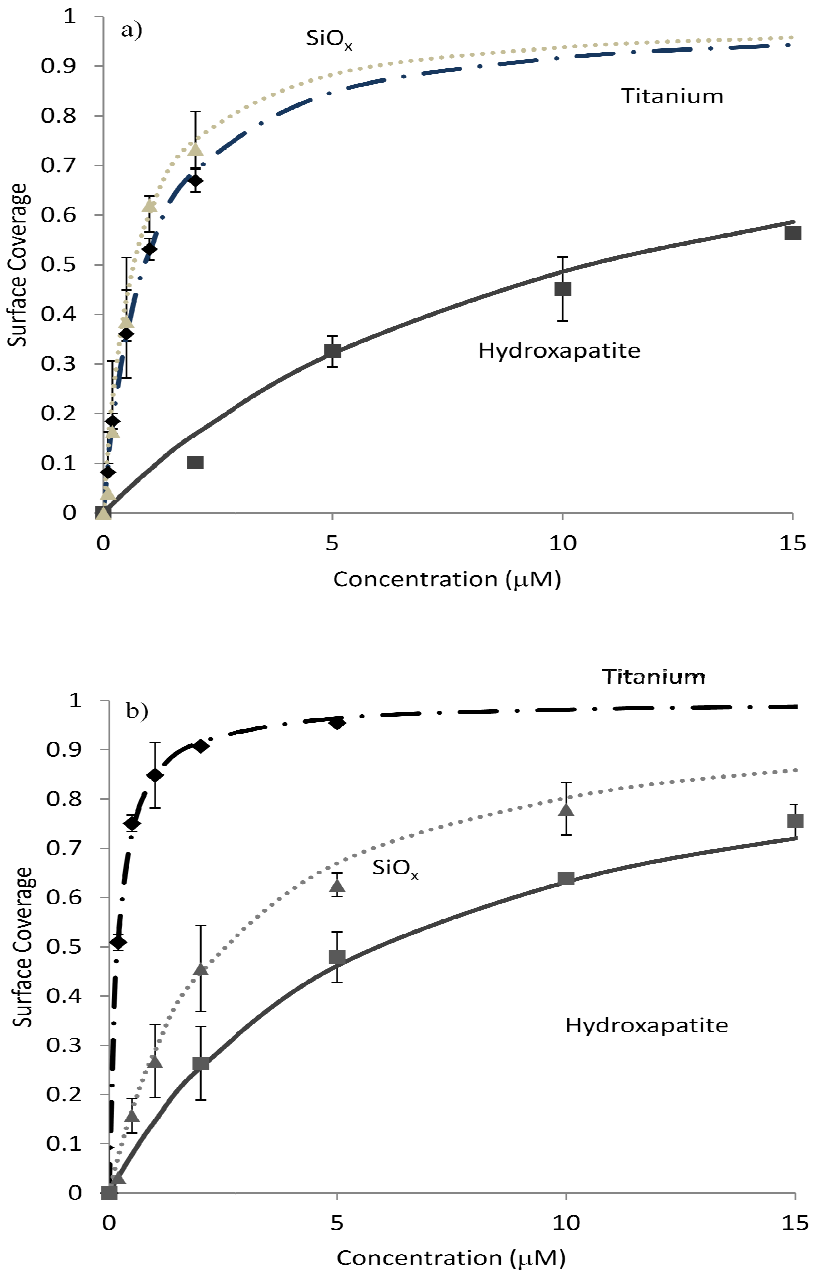

Figure 3.7: Surface Coverage and K_D (μM) of TiBPs on various implantable surfaces (SiO_x and Hydroxapatite). a) TiBP1 (b) TiBP2.

On the other hand, to explain material selectivity of any inorganic binding peptides based on only their adsorption behavior on particular surface is difficult through the effect of many unknown parameters. However, it is imperative to fully characterize peptide specificity onto substrate material to understand its applicability boundary in implantation. Consequently, we evaluated adsorption behavior of TiBPs on two different implantable materials to indicate their material selectivity as a molecular

tool for any implant surface modifications. Silica was chosen as suitable material to demonstrate proof of concept due to the applicability of glass and glass-based materials as coating substrate for implants and its widespread use in cell culture experiments as control group because of its hydrophilic surface character in comparison of new implant surface modifications efficiency. HA is also preferable material for implant coating due to its similarity with the mineral phase in bone and teeth.

To evaluate material selectivity, each peptide on two substrates was tested five different selected concentrations ranging from 0.1 μM through 2 μM and 5 μM to 15 μM via QCM. The calculated surface coverage values relative to peptide concentrations for each peptide on two surfaces were shown in Figure 3.7. TiBP1 displays fairly high affinity with 0.90 μM K_d value to silica surface as well as titanium in Figure 3.7a and Table 3.4. TiBP2 exhibits 10 fold low K_d value (2.46 μM) to silica surfaces compare to its binding affinity to titanium surface (0.18 μM) as in Figure 3.7b and Table 3.4.

While evaluating peptide adsorption on other metal-oxide (silica) surface for TiBP1 and TiBP2 depending on the role of charged group interaction, we may speculate that TiBP1 may bind to silica and titanium as two native oxide surfaces because of its high number of cationic charged groups; however TiBP2 has low affinity to silica comparable to titanium with its net neutral charge.In HA case, TiBP1 and TiBP2 shows low binding affinity with low K_d values (10.57 μM and 5.8 μM) respectively as in Figure 3.7 and Table 3.4. For practical applications to utilize peptides as multi-purpose molecular linkers, TiBP1 generally tend to high affinity to both titanium and silica surfaces while it has no affinity to HA. TiBP2 has more distinctive material selectivity properties on among silica, titanium and HA surfaces.

Although analysis of their binding affinity and selectivity properties can required for their possible application, an appropriate cellular response to peptide–functionalized surfaces should also be evaluated. Therefore, we first examined effect of TiBPs in term of cytotoxicity, cell adhesion and spreading on two different dental implants (cp Grade 1 and cp Grade 4) with their various surface topography and similar in composition. Then their conjugates with RGD as a cell adhesive motive were

designed to show capability of TiBPs as molecular linker for bioactive surface modification of implants.

Table 3.4: QCM analysis of TiBP1and TiBP2 on SiO_x and Hydroxapatite.

	TiBP1		**TiBP2**	
Various Surfaces	K_D (μM)	ΔG (kcal/mol)	K_D (μM)	ΔG (kcal/mol)
On Titanium	0.90 ± 0.12	-8.25 ± 0.08	0.18 ± 0.03	-9.19 ± 0.11
On Silica	0.66 ± 0.13	-8.40 ± 0.11	2.46 ± 0.29	-7.64 ± 0.7
On Hydroxapatite	10.57± 0.08	-6.90 ± 0.06	5.80 ± 0.30	-6.74 ± 0.7

3.1.4 Surface topography of cp Grade 4 and cp Grade 1 titanium dental implant materials

The biocompatibility of biomaterials is closely related to cellular functions particularly cell viability and adhesion in early stage of cell-surface interactions [197]. This interaction is limited and depended on surface characteristics of materials such as topography, chemistry, surface energy. Both material composition and surface morphology influence protein adsorption and the resulting cell adhesion and proliferation. On the other hand, adsorption behavior of TiBPs may also be affected surface roughness properties. Due to the possible role of surface morphology for appropriate cellular response and peptide adsorption, we first examined the surface roughness of cp Grade 4 and cp Grade 1 titanium dental implants by applying AFM. The results revealed that the cp grade 4 surface was relatively smoother than cp grade 1 surface. The R_{rms} values were 170 nm with a peak to valley range of 1.6 μm and 300 nm with peak to valley range of 2.6 μm, respectively for cp grade 4 and grade 1 surfaces. A depiction of the difference surface groove depth is shown in by the 30 μm by 30 μm cut-out of the AFM scans in 3D view in Fig 3.8 a and b.

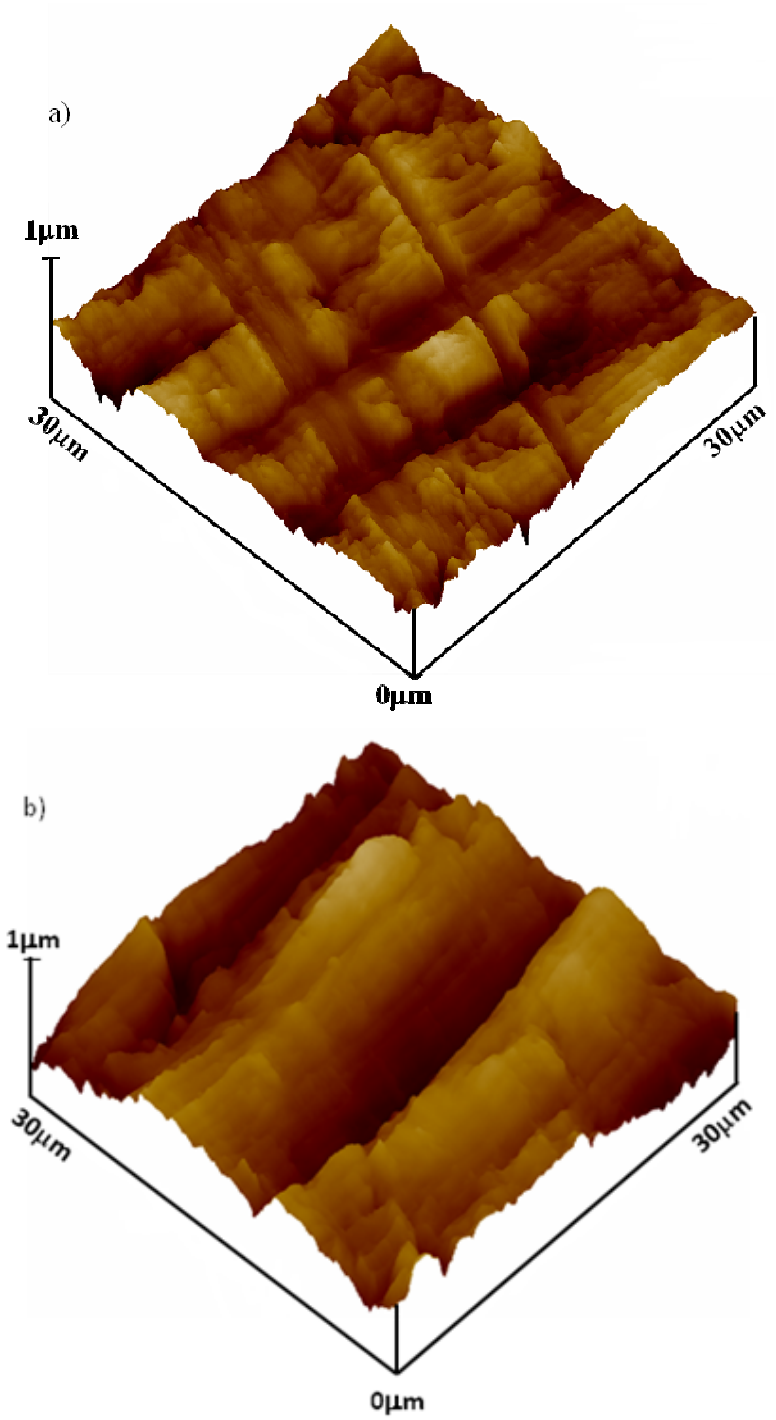

Figure 3.8: AFM scans in 3D view with the 30 µm by 30 µm cut-out (a) cp Grade 4 (b) cp Grade 1.

In SEM images, we also showed the general view of surface properties. Grade 1 clearly has deeper grooves than Grade 4. Larger SEM scans revealed that the groove patterns are similar between the two grades of Ti disk with Grade 4 having a smoother surface (Figure 3.9 a).

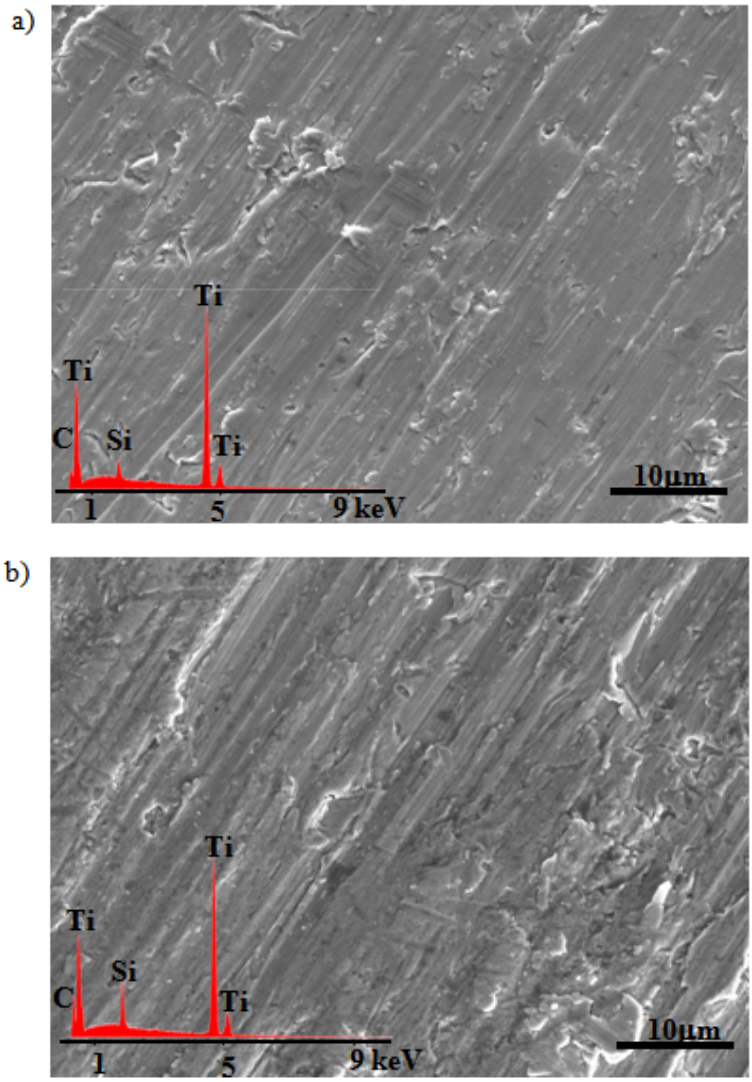

Figure 3.9: SEM scans titanium implant surfaces (a) cp Grade 4 (b) cp Grade 1. The inset represents EDS spectra of each surfaces.

EDS spectra revealed an interesting surface chemistry. Grade 1 was found to carry 4 wt % of Si compared to 2 wt % in that of Grade 4 (see spectra in insets of Figure 3.9 b). The detected Si was likely due to surface contamination resulted from roughening process which typically involve grinding and/or sand blasting using Si based media. The higher Si content in Grade 1 was likely due to a more intense surface roughening treatment than that of cp Grade 4.

3.1.5 Cell viability (MTT assay)

It was required that to test cytotoxicity properties of TiBPs before performing any conjugation with biomolecules to utilize as a molecular linker. In here we first tested cell viability on peptide-functionalized two dental implant surfaces (cp Grade4 and cp Grade1) with MTT assay to evaluate changes in cell viability and growth inhibition. Following peptide self assembly on two implant surfaces, MC3T3-E1 cells were exposed to peptide modified surfaces to proceed MTT assay (Figure 3.10).

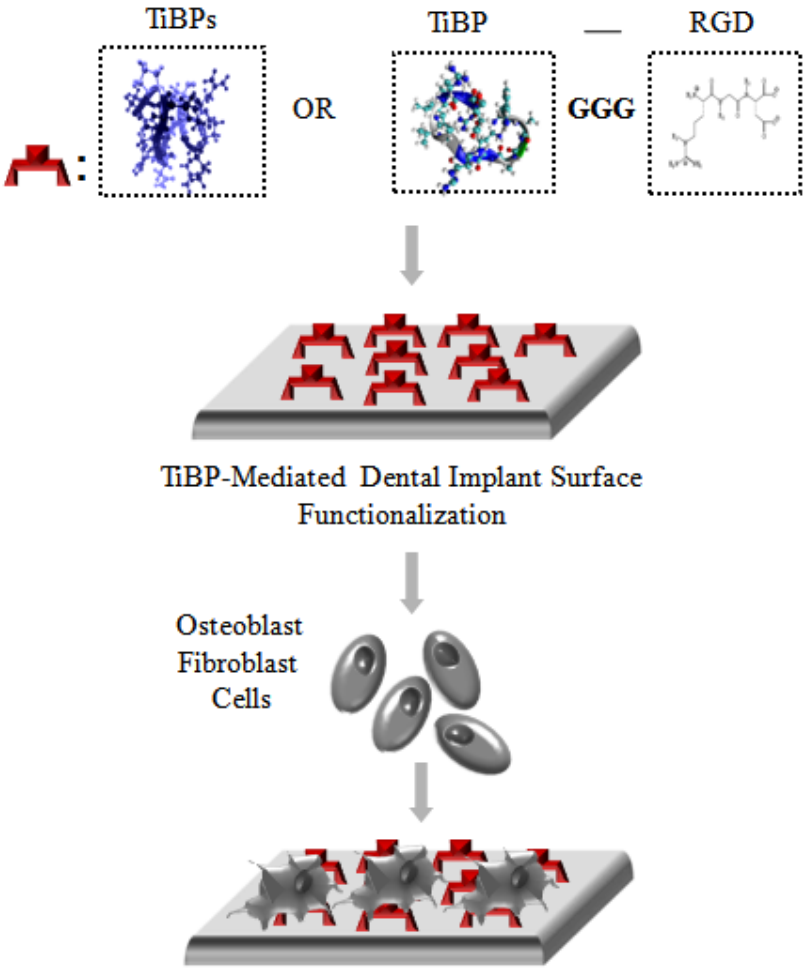

Figure 3.10: Schematic representation of peptide functionalized dental implant surface.

The results of experiment demonstrate that cell viability and growth have not been affected in the presence of TiBP1 and TiBP2 modified surfaces compare to control groups (Figure 3.11 and 3.12).

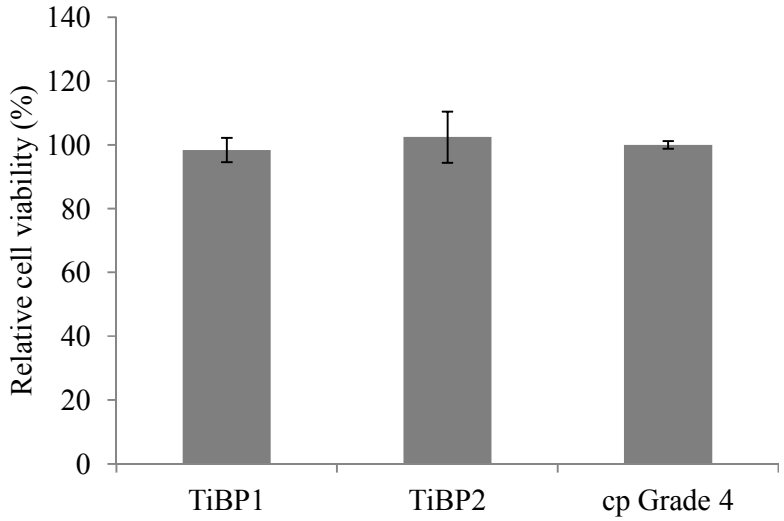

Figure 3.11: TiBP1 and TiBP2 functionalized cp Grade 4 titanium implant surface.

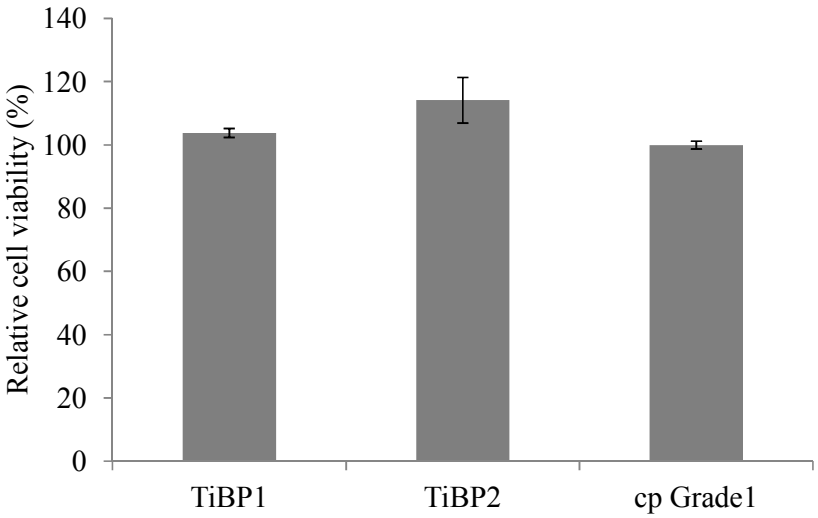

Figure 3.12: TiBP1 and TiBP2 functionalized cp Grade 1 titanium implant surface.

In this part of this work, detailed selection and characterization in terms of binding affinity, specificity, molecular structure and cytotoxicty were accomplished. Firstly, selection of TiBPs against cp Grade 4 titanium implant surface to generate set of sequences that could offer a route for implant surface functionalization as a molecular linker were reported. Following, three TiBPs (TiBP1, 2 and 60) were identified based on initial fluorescence microscopy (FM) characterization for further investigations. Two (TiBP1 and TiBP2) that exhibited high affinity, one (TiBP60) with lowest binding affinity to titanium were subjected to determine their quantitative binding characteristics on titanium with the contribution of primary and

secondary structural properties. We were also interested in learning material selectivity properties of TiBP1 and TiBP2 on various implantable surfaces such as silica and HA via QCM due to requirement of new molecular linkers with their recognition and specificity capabilities in implantation. Then, we attempt to show cellular response against TiBPs (TiBP1 and TiBP2) functionalized surfaces via MTT assay.

3.2. TiBPs as a Molecular Linker for Bioactive Implant Surface Functionalization

3.2.1. Biocompatibility of TiBPs functionalized titanium dental implant surface

Following fully characterization of TiBPs, we aimed to show the effect of peptide-functionalized dental implant surfaces on cell adhesion. MC3T3-E1 cells were exposed to peptide functionalized cp Grade1 and Garde4 surfaces including positive control groups. After 2 hours incubation, the cytoskeleton of MC3T3-E1 was visualized with phalloidin labeling under FM.

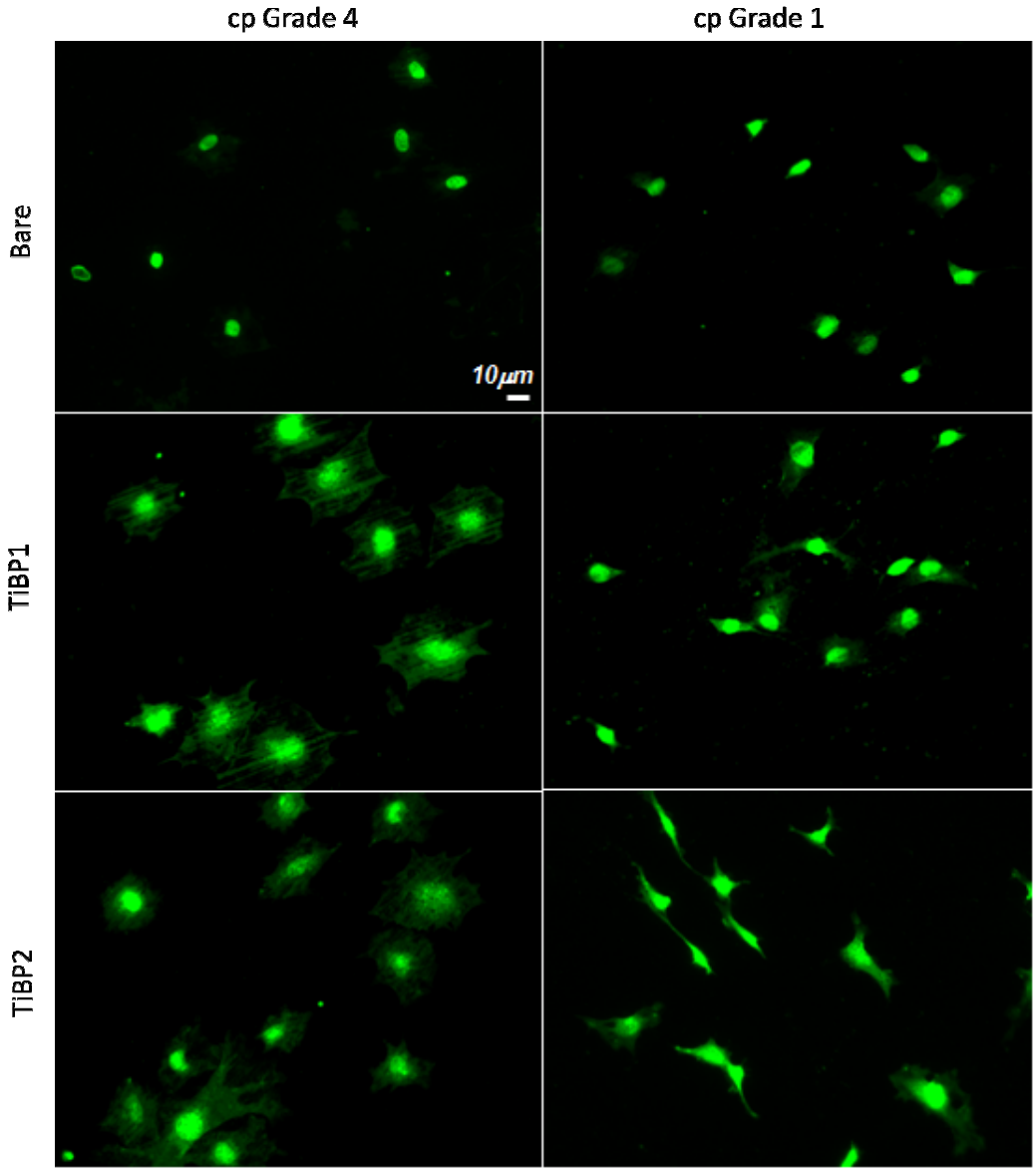

Figure 3.13: FM micrographs of phalloidin stained MC3T3-E1 cells on cp Grade 4 and Grade 1 titanium implant surfaces.

To test effect of peptide on cell adhesion and spreading, FM images were processed with Image J soft ware (NIH) by using at least three different images from one experiment. The results were plotted after repeating the experiments three times. At 2 hours, in control groups, the number of cells on both surfaces was not significantly different than each other (Figure 3.13, first line). However cells had begun to spread on cp Grade1 and Grade 4 surfaces (Figure 3.13, first line). Significantly, more cells had spread on cp grade 4 than grade1. The cells on cp Grade1 were more elongated

and on Grade 4 surfaces flattened. In case of TiBP functionalized cp Grade 4 surfaces, the number of cells on control and peptide-functionalized surfaces was very similar (Figure 3.14) conversely, the spreading of cells are on peptide functionalized surfaces significantly different than control group. A slight increase in the cell spreading was observed on the cp Grade 4 titanium surfaces modified with TiBP1 and TiBP2 (Figure 3.15). In case of TiBP functionalized cp Grade 1 surfaces, there are no significant chances cell number and spreading among control and peptide-functionalized surfaces. The difference in cell behavior among two peptide modified dental implant surfaces can be related surface roughness. Although cp Grade 4 surface smoother than cp Grade 1, cells like especially peptide functionalized cp Grade4 surfaces.

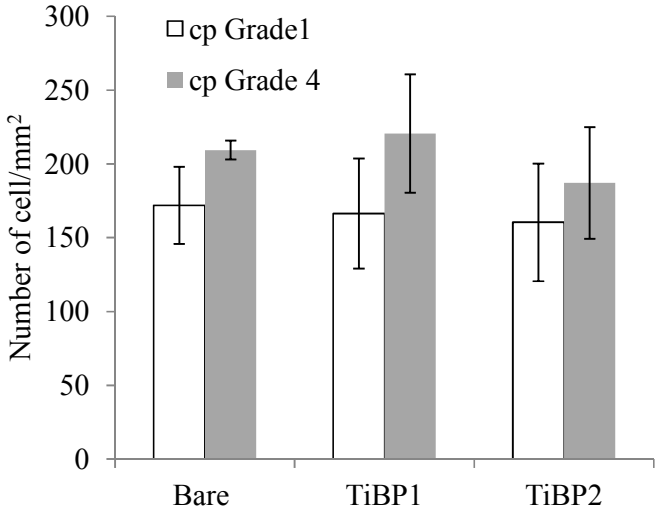

Figure 3.14: The number of adhered MC3T3-E1 cells per mm^2 in serum free conditions on two titanium implant surfaces.

Surface roughness may have an effect on not only cell attachment and spreading, but also peptide binding. Effect of surface nano or micro topography on peptide binding mechanism or peptide functionality on the surface and effect of peptide binding on surface physcochemical properties needs to investigate.

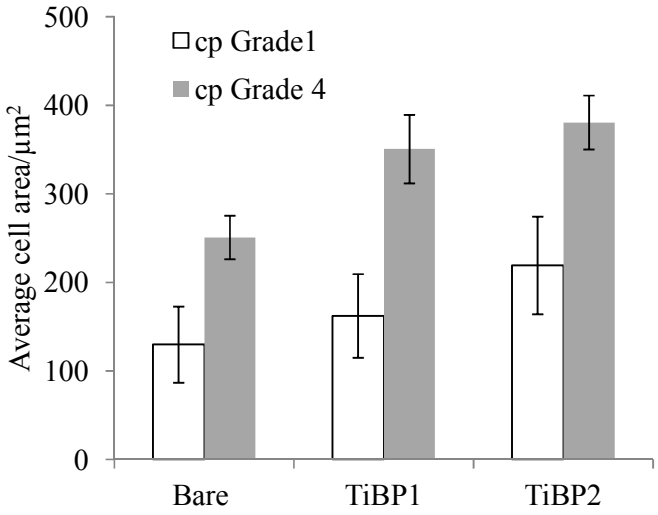

Figure 3.15: Average cell spreading per μm^2 on TiBP1 and TiBP2 functionalized cp Grade1 and cp Grade4 titanium dental implant surfaces.

3.2.2 TiBP-RGDS mediated bioactive surface modifications

The RGD sequence is by far the most effective and most often employed peptide sequence for stimulated cell adhesion on synthetic surfaces. This is based upon its widespread distribution and use throughout the organism, its ability to address more than one cell adhesion receptor, and its biological impact on cell anchoring, behavior and survival. The process of integrin mediated cell adhesion comprises a cascade of four different partly overlapping events: cell attachment, cell spreading, organization of actin cytoskeleton, and formation of focal adhesions. This cascade also effect further cell differentiation and proliferation which are important steps for implant-tissue integration. In here, bi-functional peptide was designed in conjugation with titanium binding peptide (TiBP) and integrin binding domain RGD via GGG flexible linker for bioactive surface modifications. Bi-functional peptide effect on cell viability, adhesion and spreading were examined on cp Grade 4 titanium implant surfaces and titanium coated glass surfaces in the presence of osteoblast and fibroblast. Firstly, the efficiency of bi-functional peptides (TiBP1-RGDS and TiBP2-RGDS) on cell adhesion and spreading were shown on cp Grade 4 titanium dental implant surface including one negative (bare surface), one positive control (RGDS) in the presence of MC3T3-E1which show and an RGD-dependent adhesion through integrins. There is a 1.5 fold difference in case of adhered cell number among bi-functional peptide treated cp Grade4 surfaces and negative (bare), positive

control group (RGDS) as shown in FM micrographs and plotted graph (Figure 3.16 and Figure 3.17). There is a significant difference in cell spreading data among two bi-functional peptide behaviors as shown in Figure 3.18. TiBP1-RGDS has ~ 2.5 fold higher spreading then the others. The difference may reveal because of various reasons. The one is structural conformation of peptide may allow us exposing of RGDS domain more freely with resulting effect of cell adhesion and spreading. The other one is peptide charge and hydrophilicity may affect surface chemistry that can alter cell behavior.

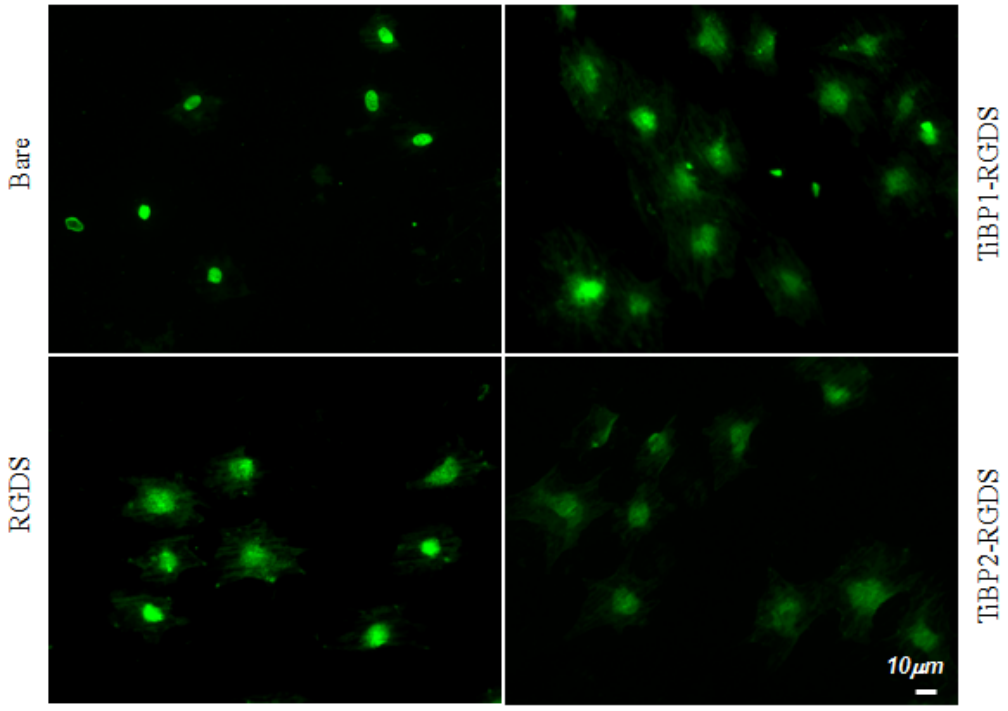

Figure 3.16: FM micrographs of phalloidin stained MC3T3-E1 cells on RGDS, TiBP1-RGDS and TiBP2-RGDS functionalized cp Grade 4 titanium dental implant surfaces.

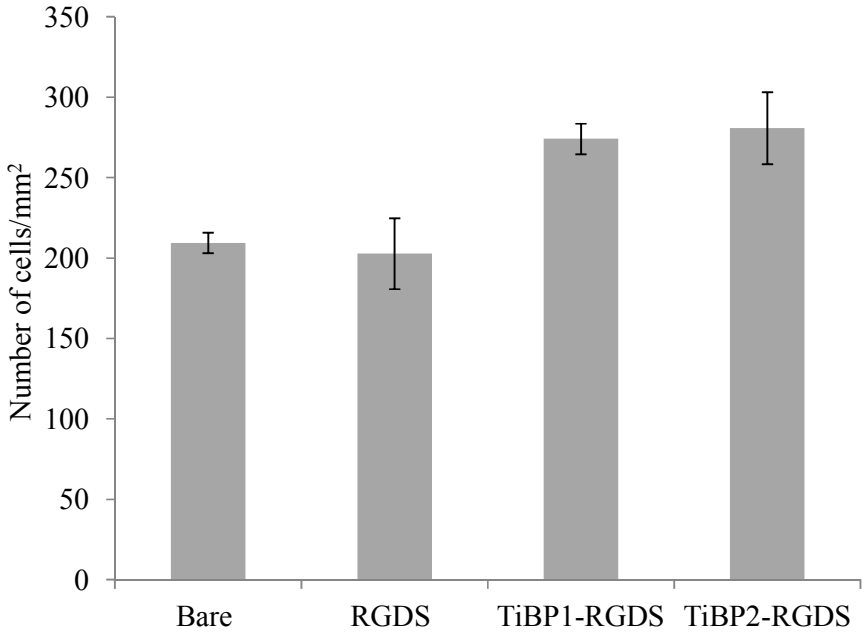

Figure 3.17: The number of adhered MC3T3-E1 cells per mm^2 in serum free conditions on peptide functionalized cp Grade 4 titanium dental implant surfaces.

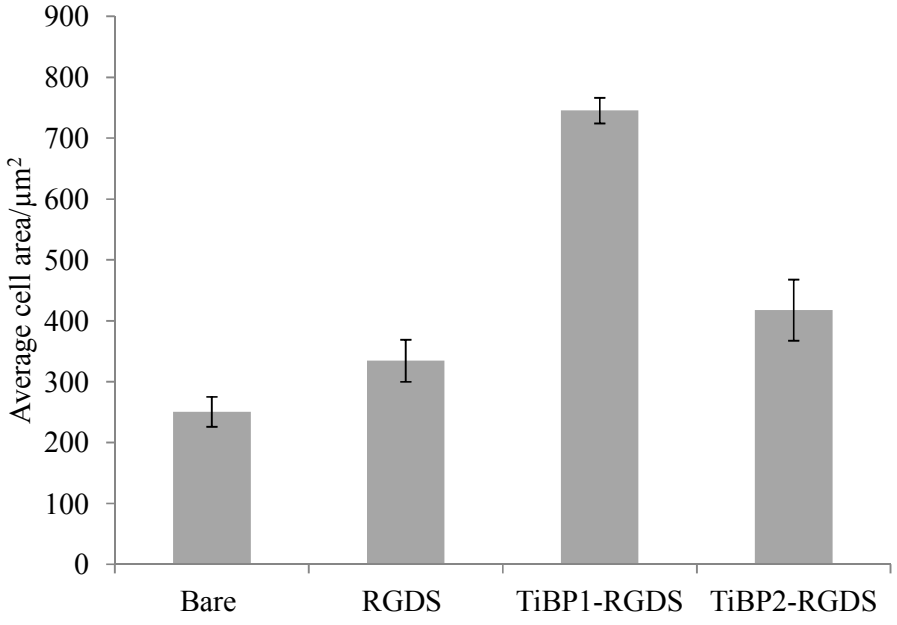

Figure 3.18: Average cell spreading per μm^2on peptide functionalized cp Grade 4 titanium dental implant surfaces.

In this experimental set up, depending on previous results with cp Grade 4 titanium dental implant surface, titanium coated glass substrate due to its different surface

roughness, NIH3T3 mouse fibroblast and only TiBP1-RGDS substrate were used to examine peptide effect on cell adhesion and spreading with varied parameters. Thus, in case of titanium coated glass surface, adhesion of the NIH3T3 cells on titanium surfaces modified with RGD chimeric peptides were increased by 3.5 to 5 fold compared to unmodified negative controls (Figure 3.19 and 3.20). No significant change was observed in the adhesion on the surfaces incubated with RGD alone. Conversely, a slight increase in the adhesion was observed on the surfaces modified with TiBP1 alone.

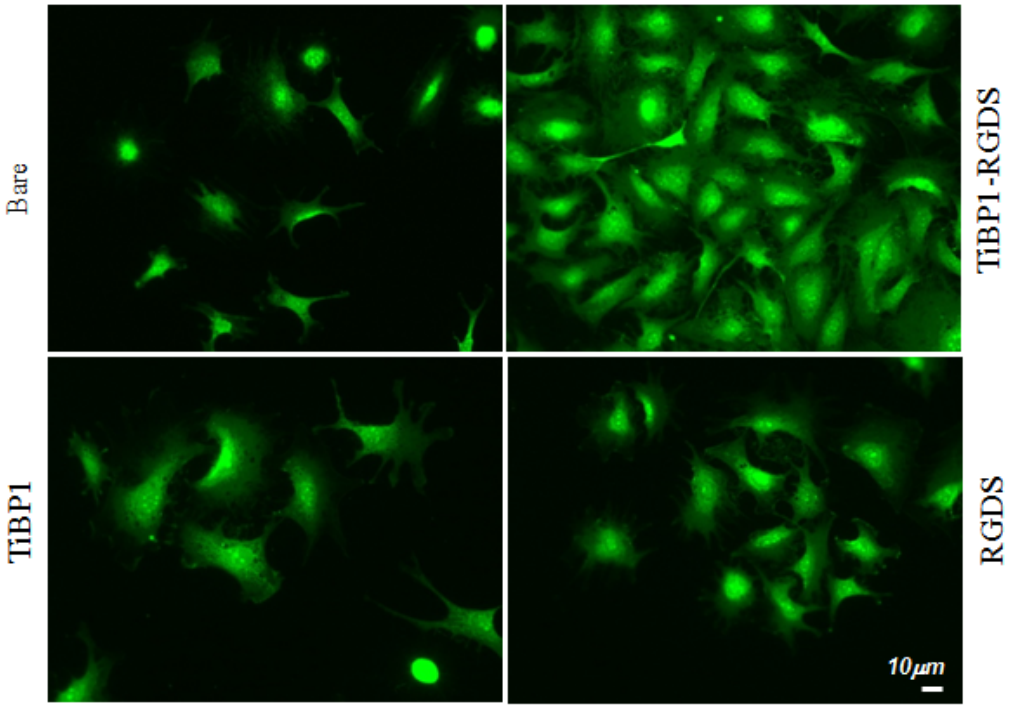

Figure 3.19: FM micrographs of phalloidin stained NIH3T3 cells on titanium coated glass surfaces.

Although within the margin of error, this effect may be due to the inherent chemical properties of the peptides. Consequently, when amphiphilic molecules on the cell membrane, such as proteins, interact with the non-polar residues, an increase in non-specific adsorption on the surface may be observed. To test whether the RGD chimeric peptides results in any enhancement of the cell viability, cell spreading was evaluated in addition to the cell adhesion. An increase about 1.6 fold in the cell spreading was observed on both materials modified with chimeric RGD peptides compared to bare surfaces (Figure 3.21).

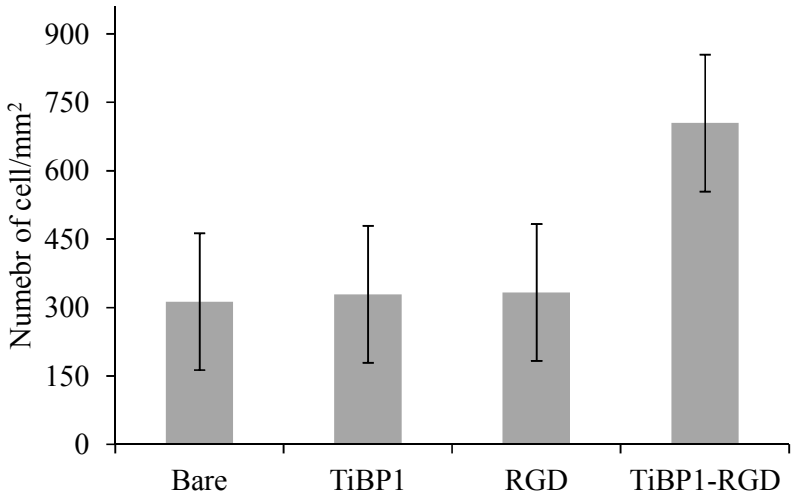

Figure 3.20: The number of adhered NIH3T3 cells per mm^2 in serum free conditions on peptide functionalized titanium coated glass surfaces.

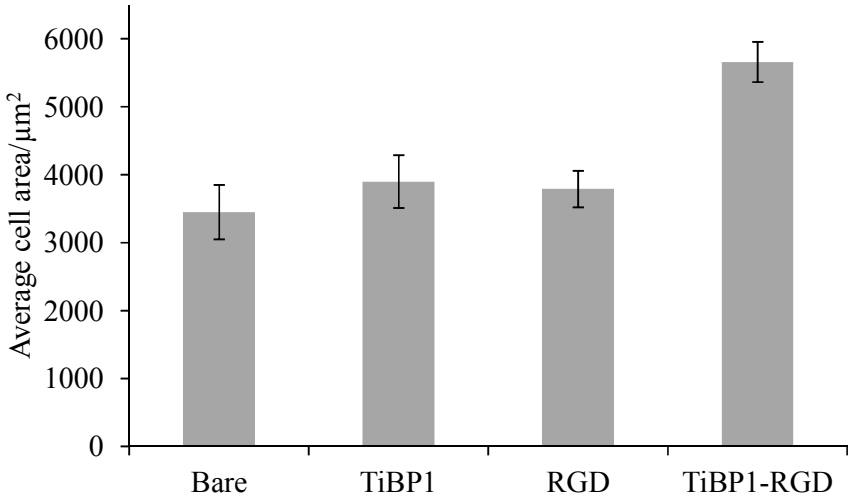

Figure 3.21: Average cell spreading per μm^2 on peptide functionalized titanium coated glass substrate.

A similar increase was observed on fibronectin modified surfaces. The results indicate that the presence of both material binding and RGD domains in the designed bi-functional molecular construct is necessary to promote cell adhesion and spreading.

In this part of dissertation, the utility and versatility of TiBPs for controlling cell-surface interactions through immobilization of functional molecules on various

implant surfaces especially on titanium were demonstrated. We also identify basic design criteria for the choice of the most suitable peptides for specific potential applications. Directed assembly, on the other hand, is preferred for the immobilization of small molecules *via* synthesizing a single chimeric molecule with bi-functional domains. Our results demonstrated that the engineered peptide-based surface modification is an adaptable platform to meet the specific requirements that may arise due to the inherent properties of the materials used for a particular application, the need of the use variety of functional molecules to be conjugated, and the molecular characteristics of the solid-binding peptides themselves. Single-step surface modification using solid-binding peptides conjugated to desired medically relevant molecules may prove to be a robust, biocompatible approach in the functionalization of complex devices in clinical applications.

3.3 GEPI Mediated Antimicrobial Titanium Implant Surface Modifications

Implant-associated infections are a primary cause of early implant failures. Such infections have been difficult to treat due to the unique (and complex) biomicroenvironment inside the human body. The success of implants depends not only on the bone–implant integration, but also on the presence of a sterile environment around the implant that will prevent bacterial infection. The generally prescribed oral antibiotics, e.g., for dental implants, are not always effective in combating implant-associated infections for a variety of reasons including the inability to reach the infection site in bone tissue, and an increase in bacterial resistance. A novel class of peptides, the antimicrobial peptides (AMPs), is useful for their utility as therapeutic agents mainly because of the difficulty for microorganisms to develop resistance towards them.

In the present study, we use a novel bi-functional peptide based approach for implant surface functionalization. Specifically, we use Titanium-binding peptides that have been selected using biocombinatorial approach, via a flagella display method, and well characterized in binding and material selectivity properties. The selected AMP was chosen for its broad range of activity against both gram-positive and gram-negative bacteria, including but not limited to *E. coli* [316], *K. pneumonia*, *S. aureus*, and *B. subtilis*, and its demonstrated ability to remain bacteriacidal when covalently bound to a water-insoluble resin [315, 316].

3.3.1 Designing of TiBP-AMP bi-functional conjugates

In the current study, two set of bi-functional peptides were designed and synthesized based on three parameters including structural, charge and binding affinity on titanium surface. In design of bi-functional peptide; firstly, each domain activity should retained and then desired activity should be revealed by utilizing other domain capability. Depending on targeted goal, we first evaluated peptide retained binding affinity to titanium surface. Following, the effect of other parameters on the antimicrobial activity and selectivity was analyzed by combination with CD, molecular modeling and biological studies. These parameters affect antimicrobial potency and spectrum of peptides.

Many of the antimicrobial peptides characterized to date display a net positive charge, ranging from +2 to +9, and may contain highly defined cationic domain(s). Cationicity is undoubtedly important for the initial electrostatic attraction of antimicrobial peptides to negatively charged phospholipid membranes of bacteria and other microorganisms, and mutual electro affinity likely confers selective antimicrobial targeting relative to host tissues. Besides their cationic properties, three-dimensional topology of peptides appears predominant and peptides have been categorized accordingly. The two largest groups are the α-helical and β-sheet peptides, whereas the majority of remaining peptides can be classified as those that are enriched in one or more amino acid residues [e.g., proline-arginine or tryptophan-rich].

According to charge and structural properties, the first designed bi-functional peptide, AMP with α helical and +6 cationic charge were combined TiBP1 with +3 cationic charge, Arg rich peptide and close α helical structure via GGG flexible linker. For the second one, the same AMP was conjugated with TiBP2 with net neutral charge.

Designed bi-functional peptides and AMP with their physicochemical properties were listed in Table 3.5.

Table 3.5: Sequence, MW, pI and net charge of TiBP-AMP bi-functional peptides

Peptide Name	Sequence	MW	pI	Charge
AMP	LKLLKKLLKLLKKL	1692.34	10.70	+6
TiBP1-GGG-AMP	RPRENRGRERGL GGGLKLLKKLLKLLKKL	3341.14	11.85	+9
TiBP2-GGG-AMP	SRPNGYGGSESSGGG LKLLKKLLKLLKKL	3042.66	10.39	+6

3.3.2 Adsorption behavior of TiBP-AMP bi-functional peptides on titanium

One of the goals of this study was determine whether the binding abilities of antimicrobial peptides to titanium surfaces were enhanced by conjugation with titanium binding peptides. Before testing our approach applicability on implant surfaces as a candidate for prevention of implant infections, we first evaluated adsorption behavior of AMP and bi-functional conjugates to titanium surface.

Frequency shift data obtained by QCM analysis was converted to wet mass data and fit to a Langmuir adsorption model in order to obtain K_D values for AMP, TiBP1-GGG-AMP, and TiBP2-GGG-AMP. The two bifunctional peptides were found to have stronger binding affinities to titanium than the AMP alone (Table 3.6). TiBP1-GGG-AMP exhibits a 2.85-fold higher K_D value than AMP, while TiBP2-GGG-AMP exhibits a 1.5-fold higher K_D value than AMP. TiBP1-GGG-AMP has the strongest binding affinity of the three peptides, exhibiting a 1.85-fold higher K_D value than TiBP2-GGG-AMP.

Table 3.6: Binding affinity analysis of AMP and TiBP-AMP bi-functional peptides on titanium via QCM.

	QCM Analysis	
Peptide Name	**K_D (μM)**	**ΔG (kcal/mol)**
AMP	0.40 ± 0.04	-8.78 ± 0.22
TiBP1-GGG-AMP	0.14 ± 0.06	-9.00 ± 0.35
TiBP2-GGG-AMP	0.26 ± 0.06	-9.01 ± 0.11

3.3.3 Conformational properties of TiBP-AMP bi-functional peptides

Peptide secondary structure was evaluated to understand one of the design parameter affect AMP activity and TiBP binding affinity. CD experiments were carried out only in PBS buffer to mimic the environment for active peptide. This finding is in accord with the CD analysis and indicates that all three peptides exhibit some degree of intrinsic disorder or unfolded structure [383, 427, 354, 367, 428, 429] or all of the peptides negligible secondary structure. However, structural difference can also observe among peptides structure (Figure 3.22). In case of AMP and TiBP1-GGG-AMP, alpha helical content and β turns are more distinct. Besides, the increase was observed on terms of alpha helical content in case of TiBP1-GGG-AMP. There is no observed difference for alpha helical content among AMP and TiBP2-GGG-AMP (Table 3.7).

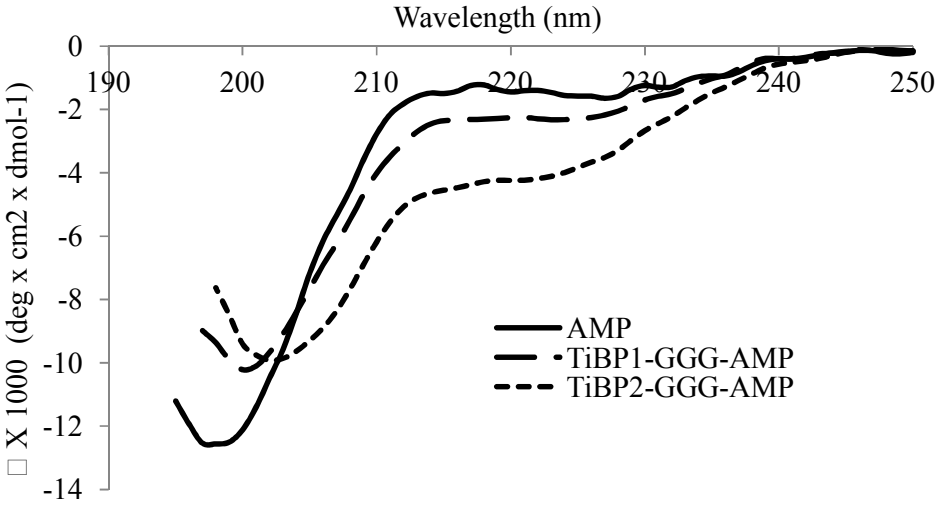

Figure 3.22: CD Spectra of 50 μM AMP, TiBP1-GGG-AMP and TiBP2-GGG-AMP bi-functional peptides in the presence PBS.

Table 3.7: Secondary structure classifications of AMP, TiBP1-AMP, TiBP2-AMP.

	AMP	TiBP1-GGG-AMP	TiBP2-GGG-AMP
Alpha helix	0.165 ± 0.01	0.35 ± 0.03	0.18 ± 0.01
Beta Sheet	0.140 ± 0.01	0.08 ± 0.01	0.12 ± 0.01
Beta Turn	0.241 ± 0.15	0.21 ± 0.02	0.27 ± 0.02
Random coil	0.455 ± 0.02	0.36 ± 0.03	0.42 ± 0.03

The finding in CD analysis is also correlated modeling studies. The plots in Figure 3.23 show the structure of peptide in water. These plots indicate that AMP has distinct alpha helical structure that can affect its antimicrobial activity. We see alpha helical structure in case of TiBP1-GGG-AMP bi-functional peptide. Peptide structure of TiBP1 may also affect occurrence or dominancy of alpha helical structure in bi-functional peptide. In case of TiBP2-GGG-AMP, we can`t observe extended alpha helical structure because of TiBP2 more distinct unfolded structural properties.

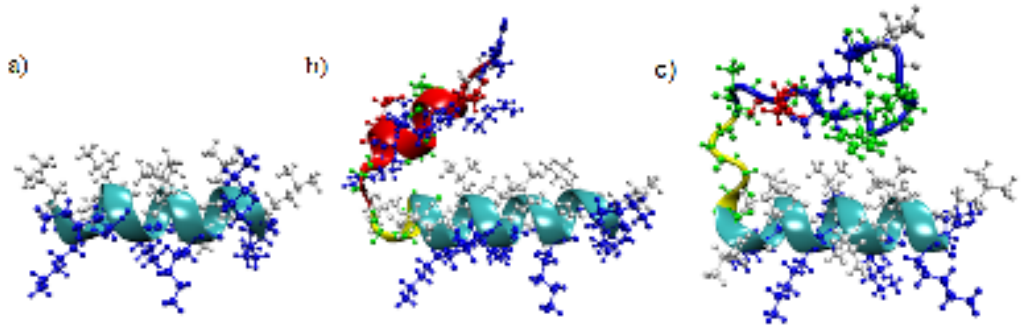

Figure 3.23: Models of the predicted structures of the a) AMP, b) TiBP1-GGG-AMP, c) TiBP2-GGG-AMP.

3.3.4 In solution antimicrobial activity of TiBP-AMP bi-functional peptides

In this section, the efficiency of TiBP-AMP bi-functional peptides in solution was evaluated *in vitro* against three bacteria S. *mutans*, *S. epidermidis*, and *E. coli*. which are common for oral and orthopedic implants, and the growth was analyzed in solution by optical density measurement. To observe the minimum inhibitory concentration of peptides to prevent for *S.mutans* growth at least 8 hours, the experiment were conducted including positive *(S. mutans* only*)* and negative control (only AMP) in the presence of various concentrations (10-100 μM) at different time points (Figure 3.24 a, b, c, d). In case of 10 μM peptide concentration in solution between 0 to 8 hours, nice growth were observed in the presence of all bi-functional peptides including positive and negative control (Figure 3.24a). The peptide concentration were increased until 25 μM, there was no growth until 10 hours in the presence of AMP where until 4 hours in the presence of TiBP1-GGG-AMP. No antimicrobial effect was observed in case of TiBP2-GGG-AMP at 25 μM concentration. We continued to gradually increase the peptide concentration until reach minimum inhibitory concentration for two bi-functional peptides (Figure 3.24b). Thus at 50 μM peptide concentration, we observed very similar trend for peptide antimicrobial behavior in case of 25 μM peptide concentration. (Figure 3.24c). The increase in peptide concentration wasn`t enough to prevent bacterial growth, in case of 100 μM, there was no growth until 12 hours in the presence of AMP, until 8 hours in the presence of TiBP1-GGG-AMP (Figure 3.24d).There wasn`t significant difference in growth in case of TiBP2-GGG-AMP. Although antimicrobial properties of TiBP2-GGG-AMP is not as good as TiBP1-GGG-AMP, sharp increase wasn`t observed in the *S.mutans* growth in the presence of TiBP2-

GGG-AMP. However, there is a sharp increase in the growth curve after certain hour in case of TiBP1-GGG-AMP and AMP. This result may reveal that, TiBP2-GGG-AMP may suppress the growth in some extent but its efficiency is not as good as TiBP1-GGG-AMP and the trend in antimicrobial behavior for AMP and TiBP1-GGG-AMP is very similar each other.

The same experimental set up was utilized against to other two bacteria that already described (*S. epidermidis and E.coli*). In case of *S. epidermidis,* 10 μM was chosen as initial peptide concentration, AMP was very efficient to preventing bacterial growth until 12 hours, following very slow growth were obtained. In the presence of TiBP1-AMP and TiBP2-GGG-AMP, there was no growth until 12 hours, following there is a sharp growth that reach same growth with positive control at the end of 24 hours period (Figure 3.25a). Again the peptide concentration was increased to 25 μM. In case of TiBP1-GGG-AMP and TiBP2-GGG-AMP, there was very slow growth at the end of 24 hours (Figure 3.25b).

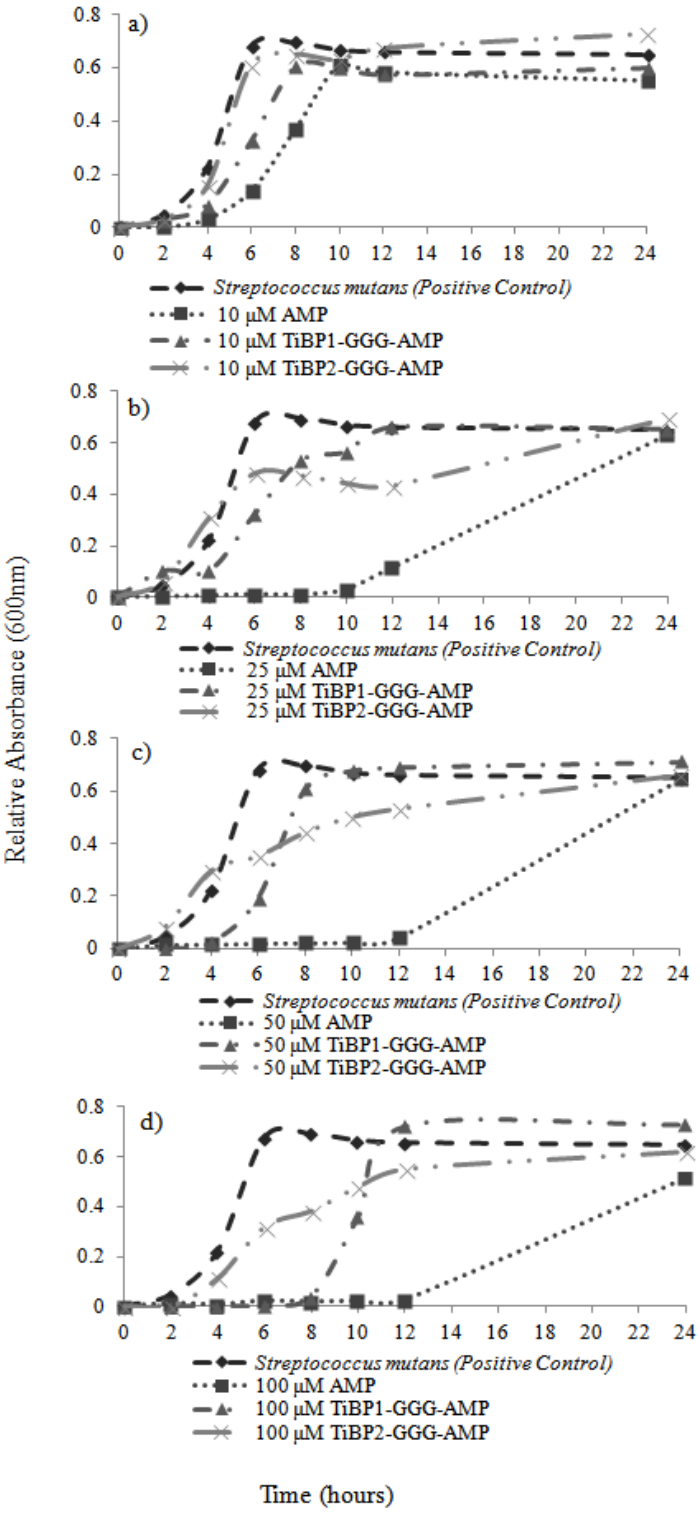

Figure 3.24: In solution antimicrobial activity of bi-functional peptides (TiBP1-AMP, TiBP2-AMP) in the presence of gradually increased peptide concentrations a) 10 µM, b) 25 µM c) 50 µM, d) 100 µM including positive (only *S. mutans*), negative control (only AMP).

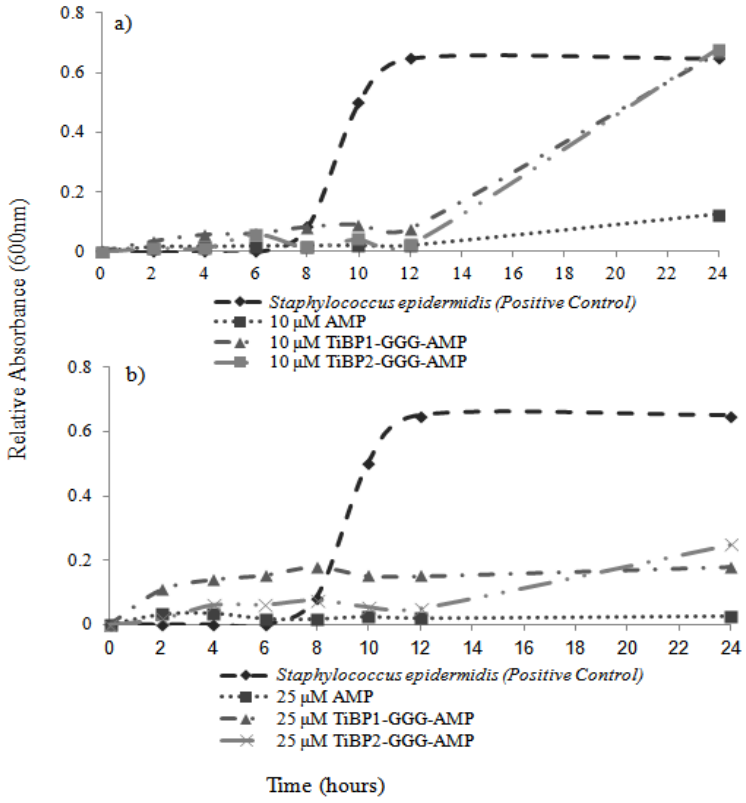

Figure 3.25: In solution antimicrobial activity of bi-functional peptides (TiBP1-GGG-AMP, TiBP2-GGG-AMP) in the presence of gradually increased peptide concentrations a) 10 µM, b) 25 µM including positive (only *S. epidermidis*), and negative control (only AMP).

The antimicrobial efficiency of two bi-functional peptides was tested against to *E.coli* as an example of gram negative bacteria in the presence of various concentrations as performed for other bacteria types. At 10 µM, there was no growth in the presence of AMP at the end of 24 hours, where 8 hours for TiBP1-GGG-AMP and 4 hours for TiBP2-GGG-AMP. In case of 25 µM, both of bi-functional peptide antimicrobial efficiency was longer until approximately 12 hours. The trend their antimicrobial behavior of two bi-functional peptides was similar to *S.mutans* case.

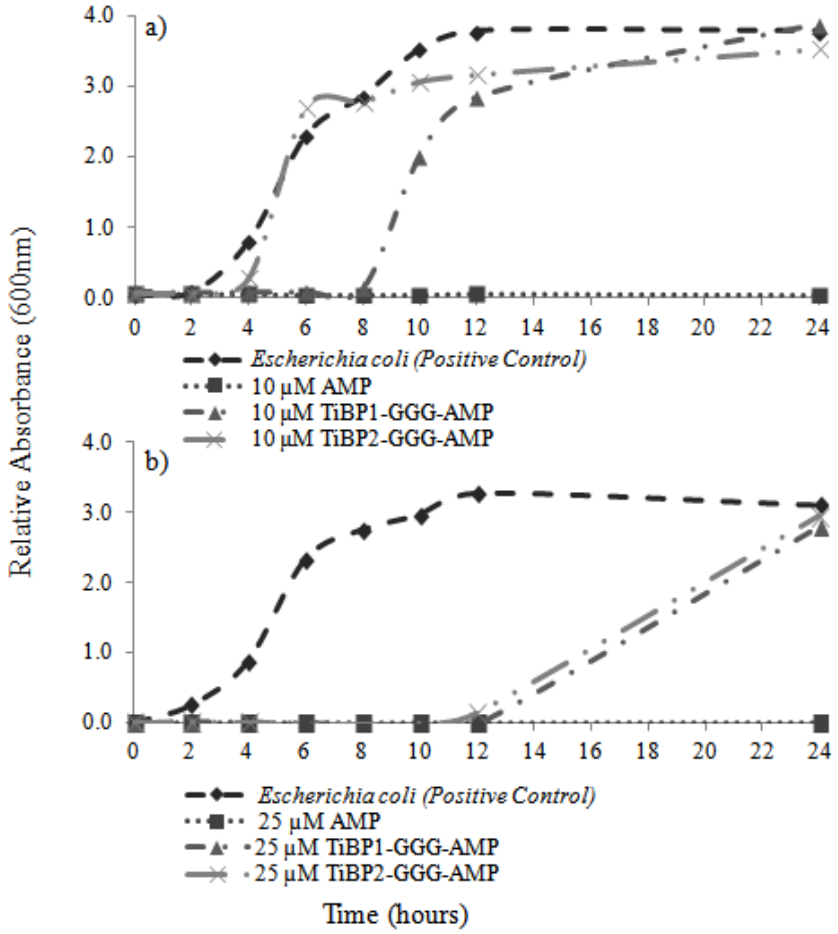

Figure 3.26: In solution antimicrobial activity of bi-functional peptides (TiBP1-GGG-AMP, TiBP2-GGG-AMP) in the presence of gradually increased peptide concentrations a) 10 µM, b) 25 µM including positive (only *E. coli*) and negative control (only AMP).

In solution antimicrobial activity results of two bi-functional peptides revealed that high peptide concentration were required and efficiency of TiBP1-GGG-AMP is higher than TiBP2-GGG-AMP against to *S.mutans.* In the presence of *S. epidermidis,* the trend in the antimicrobial behavior of two bi-functional peptides is very similar which is different than *S.mutans* case. At 4X lower peptide concentrations than in case of *S. mutans* is required to get the same antimicrobial activity. In case of *E.coli*, there is a difference antimicrobial behavior of two bi-functional peptides which is similar to *S. mutans* case. Although the trend is similar, required peptide concentration is 4X lower as same as in case of *S. epidermidis.*

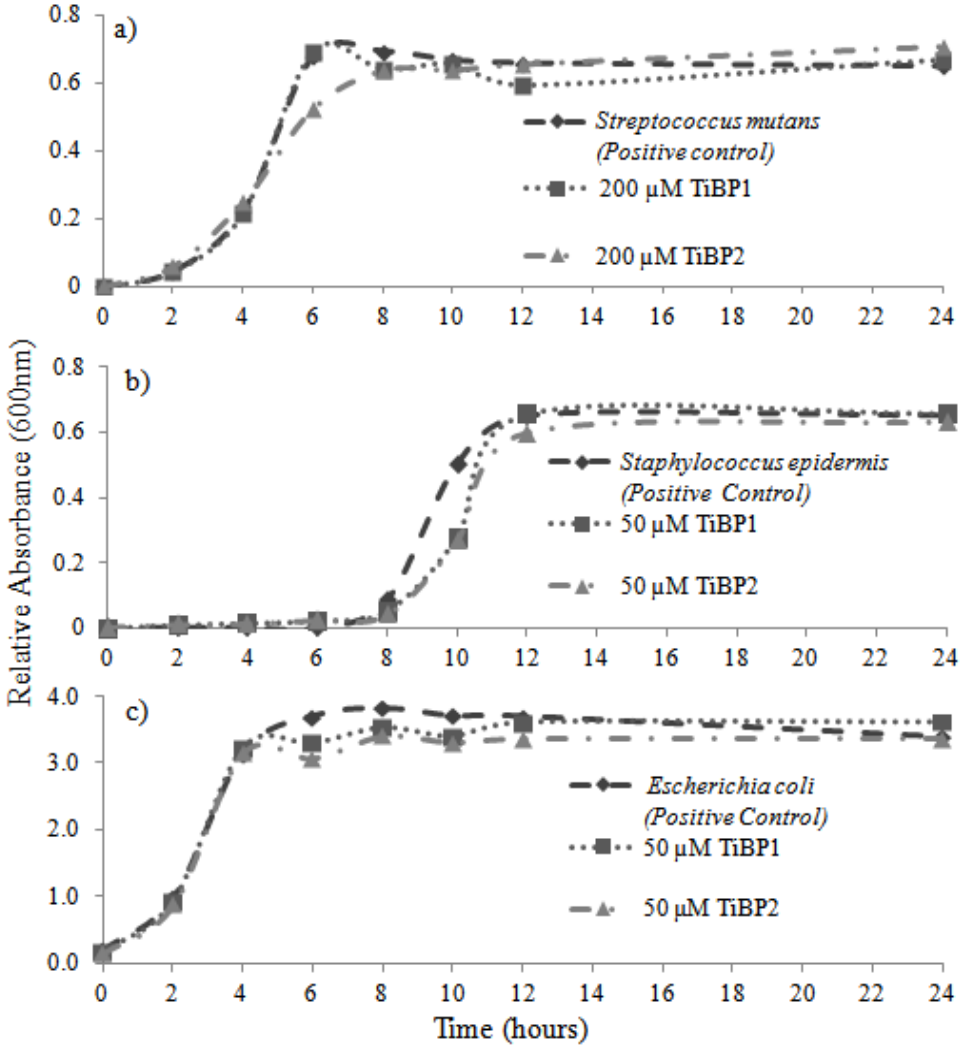

Figure 3.27: Minimum growth inhibition concentration of AMP, TiBP1-GGG-AMP, TiBP2-GGG-AMP in the presence of various bacteria type a) *Streptococcus mutans*, b) *Staphylococcus epidermidis*, c) *Escherichia coli*.

Following, bi-functional peptides antimicrobial activity including was tested in presence of various concentrations against all there bacteria types. The "minimum working-concentration," as determined by stability of the peptides for at least 8 hours after the bacteria had entered the mid-log phase, was found to be 200 µM for *S. mutans*, 50 µM for *S. epidermidis* and 50 µM for *E. coli*.

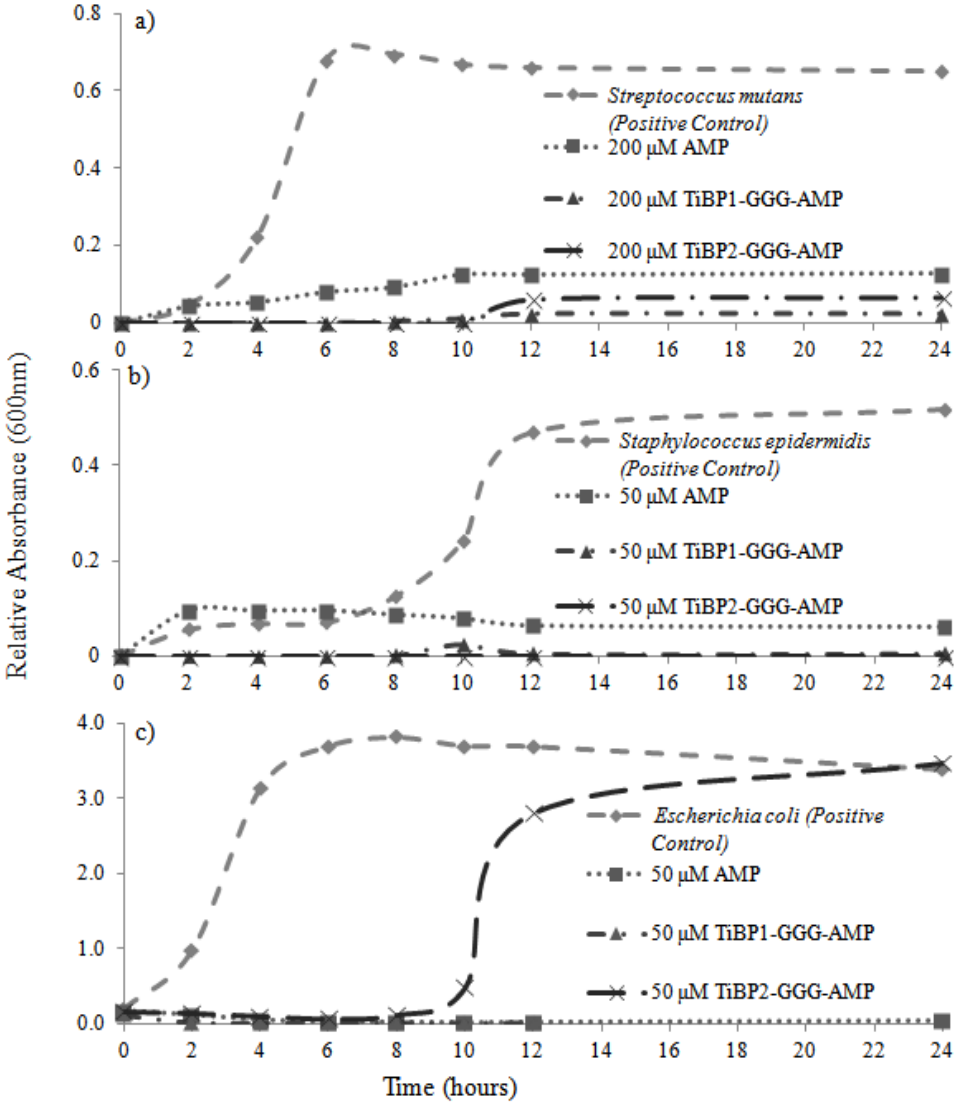

Figure 3.28: In solution antimicrobial activity of TiBP1 and TiBP2 at minimum inhibitory concentration of their bi-functional conjugates against a) *Streptococcus mutans,* b) *Staphylococcus epidermidis,* c) *Escherichia coli*.

Afterwards, all in solution experiments to find out antimicrobial activity of bi-functional peptide, the only antimicrobial activity of TiBP1 and TiBP2 in the presence of *E.coli, S.epidermidis and S.mutans* were tested as a second negative control (Figure 3.28). In these experiments, required peptide concentration was chosen rely on the minimum inhibitory concentration. 200 µM for *S.mutans* (Figure 3.28a), 50 µM for *S. epidermidis* (Figure 3.28b) and 50 µM for *E.coli* (Figure 3.28c) was used in these experiments.

3.3.5 On the surface antimicrobial activity of TiBP-AMP bi-functional peptides

After determining best working concentrations for each bacteria. Peptide antimicrobial efficacy was tested on the titanium surface. Certain concentration of peptides for bacteria type depending on our in-solution activity results were self assembled to titanium surface and incubated 4 hours at 37^0C with agitation and the end of the incubation period, surface was washed two times to remove excess amount of peptide. Meanwhile, each bacterium was grown until their mid-log phase and 10^8 cells/mL from mid-log phase were exposed to peptide modified titanium surface an incubated 2 hours. At the end of the incubation time, cells are fixed and labeled with Syto 9 and visualized under fluoresce microscopy. Based on FM results, the amount of adhered bacteria on the bare titanium surface among three bacteria is significantly different than each other (Figure 3.29, first row). In case of *S.mutans*, the difference in adhered bacteria on peptide functionalized surface is significant. Especially, there is ~45 fold difference among TiBP1-GGG-AMP modified titanium surface and positive control (bare titanium) where ~20X difference with negative control (only AMP) (Figure 3.29, left column and Figure 3.30 a). On the surface antimicrobial activity of TiBP2-GGG-AMP was not as high as TiBP1-GGG-AMP however it's higher than negative control. The difference in surface coverage ratio among TiBP2-GGG-AMP modified surface and negative control is ~2 fold where ~4 fold difference with positive control (Figure 3.30a). In the presence of *S. epidermidis*, the similar 2 fold decrease in bacterial adhesion as in *S. mutans* was observed among positive control (bare titanium) and negative control (AMP). However, on the surface antimicrobial behavior of TiBP1-GGG-AMP and TiBP2-GGG-AMP was very similar in case of *S. epidermidis.* The efficiency of TiBP2-GGG-AMP is higher against to *S.epidermidis* than *S.mutans* (Figure 3.29 middle column and Figure 3.30b). In case of *E.coli,* AMP was very efficient to prevent bacterial adhesion on titanium surface. The difference in surface coverage ratio among AMP and TiBP1-GGG-AMP is very low. Although TiBP2-GGG-AMP had a significant decrease on cell adhesion compare to positive control, the difference rely on surface coverage ratio is not higher than AMP (negative control) (Figure 3.29 left column and Figure 3.30c).

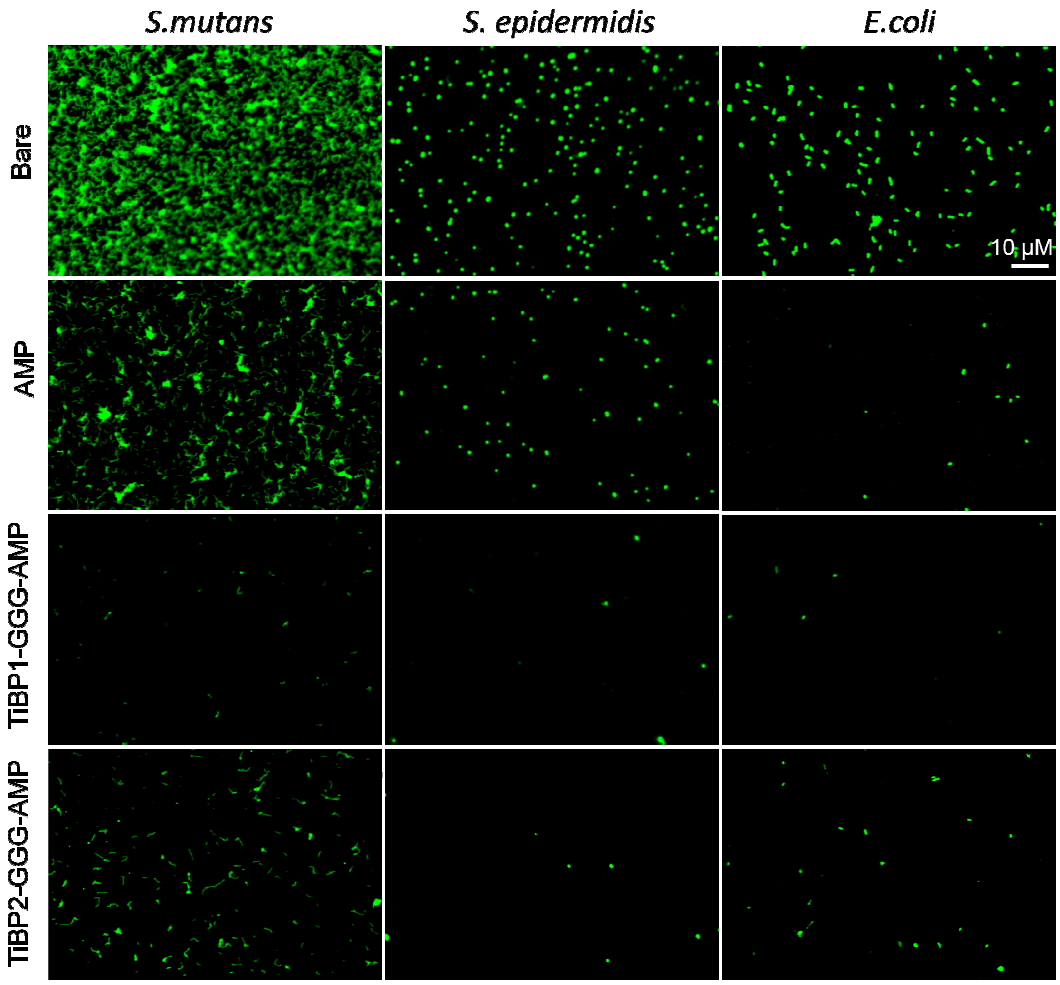

Figure 3.29: Bacterial adhesion on AMP, TiBP1-GGG-AMP and TiBP2-GGG-AMP peptide modified titanium surfaces against *Streptococcus mutans* (left column), *Staphylococcus epidermidis* (middle column), *Escherichia coli* (right column).

In summary, in case of three bacteria, bare titanium was found to have significantly more bacterial adhesion on average than titanium treated with TiBP1-GGG-AMP, TiBP2-GGG-AMP, or AMP. Surfaces modified with our bi-functional peptides were found to significantly reduce bacterial adhesion against all three bacteria when compared to adhesion on pristine titanium and AMP. Substrates modified with TiBP2-GGG-AMP were found to have less bacterial adhesion on average than substrates modified with AMP when incubated with *S. mutans* and *S. epidermidis*; however, they were interestingly found to have more bacterial adhesion on average than substrates modified with AMP when incubated with *E. coli*. Surfaces modified

with TiBP1-GGG-AMP were found to reduce bacterial adhesion of *S. mutans* and *E. coli* better than surfaces modified with TiBP2-GGG-AMP.

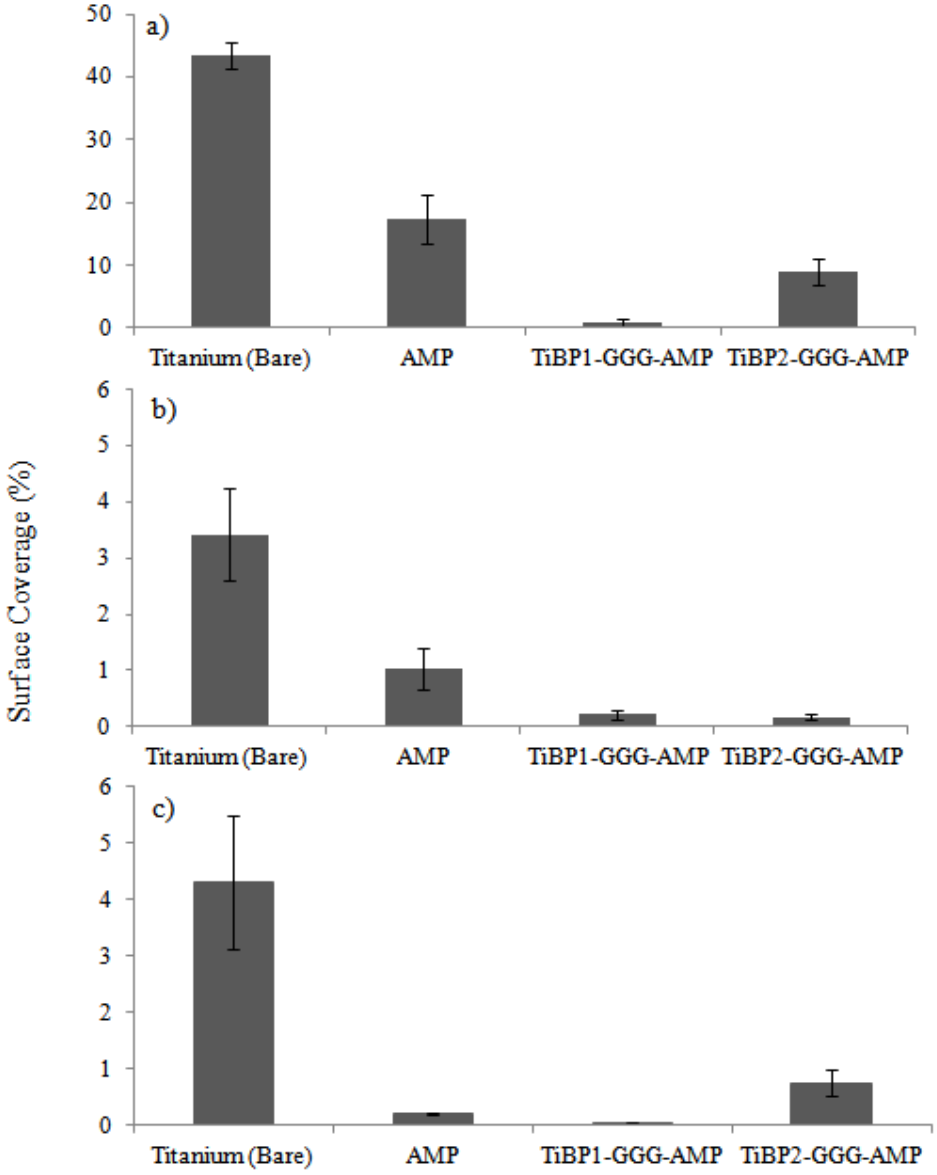

Figure 3.30: Surface coverage analysis on AMP, TiBP1-GGG-AMP and TiBP2-GGG-AMP peptide modified titanium surfaces against a) *Streptococcus mutans,* b) *Staphylococcus epidermidis,* c) *Escherichia coli*

3.3.6 Micro-contact printing of TiBP1-AMP on titanium surface

To examine the striking difference in bacterial adhesion between pristine titanium and titanium treated with TiBP1-GGG-AMP, PDMS Stamping of TiBP1-GGG-AMP was performed against to *S.mutans (*Figure 3.31).

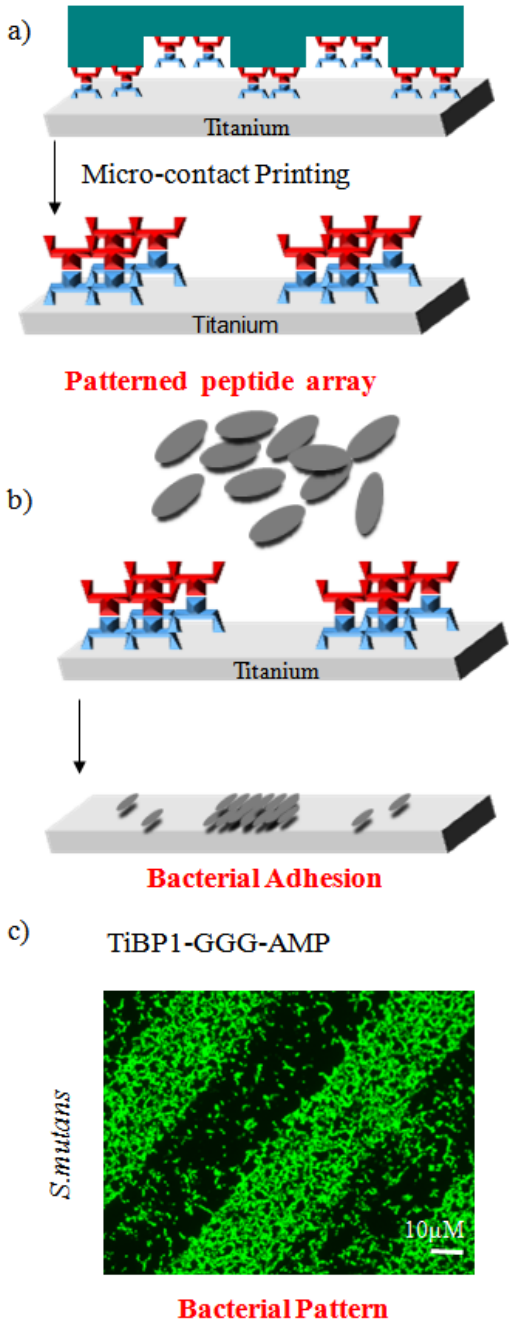

Figure 3.31: a) Schematic representation for PDMS patterning of TiBP1-GGG-AMP on titanium. b) Adhesion of *S.mutans* (10^8 cell/mL) from log-phase on peptide modified surfaces after 2 hours incubation. c) FM images of Syto9 labeled *S.mutans* on patterned peptide array.

Depending on all experimental findings, AMP efficiency is higher especially higher against to *E.coli* as a gram negative bacterium than gram positive bacteria examples such as *S.mutans* and *S.epidermidis*. Different mechanisms were hypothesized to understand the mode of action of cationic antimicrobial peptides on gram positive

and gram negative bacteria. The general principle of this mechanism is relying on the bacterial membrane structure and properties. In general, the bacterial membranes are rich in the acidic phospholipids. Especially, the outer surface of Gram negative bacteria contains lots of negatively charged lipopolysaccharides (LPS). Therefore the net positive charge of the antimicrobial peptides facilitates their perturbing activity towards bacterial membrane. Although electrostatic interactions between cationic peptide and negatively charged bacterial cell envelope components are important, there is not always a direct correlation between LPS and antimicrobial activity. In comparison, gram positive bacteria lack an outer membrane of LPS, however their cell envelopes are enriched in negatively charged teichoic and teichuronic acids. This charge also increases sensitivity to killing the bacteria by positively charged antimicrobial peptides. Some of the studies also report efficiency of antimicrobial peptides on gram positive and gram negative bacteria by considering the kinetics of membrane permeabilization and of bacterial inactivation. Rely on their results; gram negative bacteria have faster permeabilization and killing kinetics respect to gram positive bacteria and this also confirm the conclusion of previous studies that double membrane of this gram negative bacterium is a less efficient barrier than the single membrane and thick peptidoglycan layer of the gram-positive species. This study is also revealed that chosen AMP is more efficient on *E.coli* in solution and on the surface antimicrobial activity than *S.mutans* and *S.epidermidis*. All in solution activity cases; AMP is the most efficient antimicrobial activity at constant concentration with the other bi-functional counterparts. However, bi-functional peptides have more improved antimicrobial activity on the surface in case of three bacteria. Among two bi-functional peptides, TiBP1-GGG-AMP is the most efficient one against three bacteria. AMP has less antimicrobial activity against gram positive S.mutans both in solution and on the surface. TiBP1-GGG-AMP has especially improved activity on the surface. The similar trend was shown in case of *S.epidermidis.* However, the ratio among the all positive, negative and bi-functional ones is not high as in case of *S.mutans.* The AMP modified surface has a high resistance against to *E.coli.* The difference in bacterial resistance is not significant in the presence of bi-functional conjugates. These results may rely on bi-functional peptide design criteria. Especially, its efficiency can also be related two important parameters, the one is increased charge and the other one is structural properties.TiBP1-GGG-AMP has +9 cationic charge which is increased positive

charge. Its molecular model reveals that it has turns that similar to alpha helical structure of AMP. Although TiBP2-GGG-AMP has the same +6 charge with AMP, it has more unfolded structure than AMP. This unfolded structure may affect its antimicrobial efficiency. Although we compare the structure, charge and functionality relations depending on comparison in solution, on the surface antimicrobial activity and in solution structural properties, the exact peptide conformation on the titanium surface is not known. There are not only mechanism interplay related to antimicrobial peptide activity against to three bacteria species but also peptide binding mechanism on titanium surface including sequence, structure and charge parameters.

3.4. *In situ* Mineralization of Hydroxapatite Films on Titanium Surface via Bi-functional Peptide

The formation of hydroxyapatite layers is an important process in biological organisms, which possess complex catalytic systems for mineralizing, absorbing and repairing hard tissues. These processes have drawn interest from the research community, where the ability to mimic the control shown in biological systems would represent a significant advancement processing technology. The key area of interest is the formation of thin films to facilitate the osseointegration of structural implants and the regeneration of damaged hard tissues [433, 434, 107]. Thin films of hydroxyapatite have been formed on titanium and other implant material surfaces using a variety of chemical and physical methods including among others, spontaneous formation in electrolyte solutions [435, 436], electrochemical methods [437], sol-gel methods [438], plasma-spray coating [439], and hybrid methods [440]. These studies aim to attach the film of hydroxyapatite to the implant and control the morphology. Biological approaches have also been used, especially with the use of natural proteins such as amelogenin for the control of HaP nucleation and morphology [441, 442]. Genetically engineered peptides (GEPIs) selected through combinatorial approaches, have also been used to control the formation of HaP [367]. A study by Gungomus *et al*. has shown the ability of these peptides to not only control growth rates but also crystal structure. In this case crystals were formed in aqueous solution at room temperature and neutral pH. Besides GEPIs efficacy in controlling mineralization processes, they also have the added advantage of being

easily modified to add additional functionalities. This includes being attached to larger proteins sequences of with other peptide sequences, creating multifuncional molecules. Here we utilize these attributes of GEPIs to mineralize an attached HAP layer on a titanium surface, using previously selected TiBPs and designed ADPs peptide sequences [367].

In the following section in this part of dissertation; first, designing strategy of ADPs, then binding and biomineralization characteristic of ADPs were explained briefly. Afterwards, designed and synthesized bi-functional peptide with conjunction of TiBP2-ADP in a single peptide chain was used to examine their mineralization capability. The resulting bi-functional peptide TiBP2-ADP (various types) was characterized both for its ability to bind to titanium and mineralize hydroxyapatite. The binding and mineralization process was monitored in real-time using quartz crystal microbalance (QCM). Both peptide adsorption and HAP film formation cause a mass change that is easily detected via QCM. Mineralization was run in solution with several concentrations of calcium and phosphate ions to examine the mineralization kinetics. The resulting film was characterized via electron microscopy. A series of control experiments verify the significance of the findings.

3.4.1. Bioinformatics design of peptides derived from natural proteins:

Amelogenin case study

The peptides used in biomimetic materials formation are selected using combinatorial biology techniques based on the developments during last two decades. Although the nature of peptide-inorganic interaction is not yet well understood, many short peptide sequences specific to metals, oxides and semiconductorshave been discovered as potential utility for future engineering materials and have been used in the proof-of-principle synthesis, morphogenesis and assembly studies.

In nature, proteins that perform functions similar to each other usually have similar sequences due to biochemical, biophysical and evolutionary constraints [387]. Founded on this observation, Oren *et al.* showed that the inorganic binding peptides, generated by *in vivo* selection, recognizing same material have alike sequences, much as evolutionarily related proteins do [360]. To use in this bioinformatics-based approach we showed a way to derive novel sequence similarity scoring matrices

which capture the relationships within the strong binders while differentiating them from the weak-binding peptides for a given material system. A scoring matrix is used to obtain the score for aligning two amino acids (match or mismatch) in an alignment of two protein sequences, and the overall score can be considered as a measure of the similarity between sequences.

We have selected amelogenin as a proof of concept study. Amelogenin is a protein found in developing tooth enamel. The function of amelogenin is believed to be interacting with the developing tooth mineral and organizing enamel rods during tooth development [443-445]. Despite the obvious importance of the amelogenin during the teeth development, the function of the protein and its cleavage fragments is not completely understood. It has been shown that the amelogenin is a modular protein having domains and cleavage products with multiple functionalities [446, 447]. Therefore, it is important to be able to identify what functionalities the certain domains of amelogenin may carry. We hypothesize the amelogenin may have sequence similarities with the phage display [367] selected HABPs, much as evolutionarily related proteins do. To test this hypothesis, two similarity scoring matrices (HAPI and HAPII) were generated using two different sets of HABPs (7 and 12 a.a. long) selected by phage display. Once the scoring matrices were created, we compared amelogenin sequence with the two sets of experimentally selected hydroxyapatite binding peptides using the appropriate scoring matrices and detected high similarity regions for both sets. Then we have chosen the 4 regions with the highest similarity as the putative functional regions and 3 regions with the lowest similarity as control groups. The sequences and the positions of the ADPs are depicted in Figure 3.32. This allowed us to compare putative functional regions of the amelogenin with the predicted structure of the protein. Based on the previously predicted structures, we have shown that the regions predicted to have the highest similarity scores are water accessible and may have to ability to interact with the HA mineral and modify the nucleation and growth during enamel formation. These putative functional regions were named as Amelogenin derived peptides (ADPs). All the ADPs were then synthesized and their binding and mineralization properties were investigated.

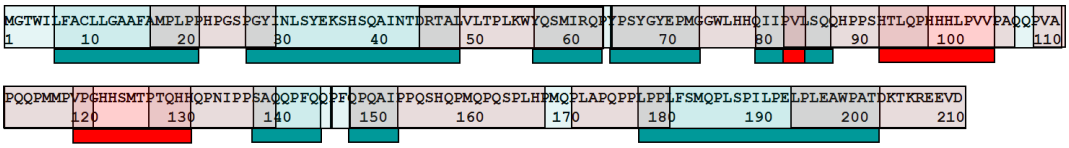

Figure 3.32: Mouse amelogenin sequence (P63277|AMELX_MOUSE) and predicted high (red) and low (teal) similarity sequence domains [448].

3.4.1.1 Binding characterization of ADPs

The binding affinity of the peptides on hydroxyapatite was determined via quartz crystal microbalance (QCM). Lyophilized peptides were diluted in a phosphate-carbonate buffer at concentrations ranging from 0.1 μM to 50 μM. The peptide solutions were introduced to the surface of a hydroxyapatite-coated quartz crystal, and the resonance frequency was allowed to equilibrate. As the decrease in resonance frequency is directly related to the mass of peptide on the surface, the net frequency shift at different concentrations was used to determine the dissociation constant (K_D) of each peptide. The K_D values were determined using the relationship $-\Delta F = \Delta F_{max} C/(C+K_D)$, where Fmax is the maximum frequency shift at surface saturation, and C is the concentration. The hydroxyapatite-coated crystals were rinsed with ethanol then cleaned in an ozone chamber between uses as prescribed by the manufacturer. K_D is an equilibrium constant that represents the concentration necessary to achieve fifty percent surface coverage. These values can vary over many orders of magnitude. The results obtained from the QCM analysis showed that the prediction of binding strength was accurate for the amelogenin derived peptides. The peptides that were predicted to have a high binding affinity (ADP1, ADP2, ADP4 and ADP7) had a relatively strong K_D value on the order of 1 μM. In fact, the binding affinities of the strong ADPs were higher than the experimentally selected HABP1. Likewise, the peptides predicted to have low binding affinity (ADP3, ADP5, ADP6) resulted in K_d values varying from 5-14 μM, which was comparable with the experimentally selected weak binding peptide HABP2. The relative binding affinities derived from the K_d values are shown were indicated us ADP5 has high binding affinity, ADP7 has very low binding affinity to HA surface. The binding affinity analyses show that the similarity scoring matrices work pretty well for the binding affinities [448]. However, binding affinity is not always correlated with biomineralization activity. To test the relationship between the binding affinity and

the mineralization activity, kinetics and morphological analyses were performed as described in the previous section.

3.4.1.2 Biomineralization characteristics of ADPs

To investigate the effects of the ADPs on calcium phosphate mineralization, an alkaline phosphatase (AP) based mineralization model was used. Ca^{+2} consumption was monitored for 24 hours and noted that complete conversion of Ca^{+2} ions had occurred for all cases. However, varying conversion rates were observed in presence of different peptides. Ca^{+2} consumptions were observed for the first 90 minutes. We noted that the majority of the weak binders exhibited similar reaction kinetics to that of mineralization without peptide while majority of the strong binders exhibited faster kinetics. Namely, kinetics of two of the three weak binders were similar to that of no peptide case, with reaction constants for the first 60 minutes of $-3.3x10^{-3}$/min, $-3.4x10^{-3}$/min and $-3.3x10^{-3}$/min for ADP3 (weak), ADP6 (weak) and no peptide, respectively. In addition, three of the four strong binders exhibited faster kinetics compared to that of no peptide case, with reaction constants of $-5.1x10^{-3}$/min, $-5.0x10^{-3}$/min and $-4.9x10^{-3}$/min for ADP1, ADP2 and ADP4, respectively. However, One strong (ADP7) and one weak (ADP5) binders were exhibited opposite kinetic trends, in which ADP7 (strong) exhibited the slowest kinetics ($-9x10^{-4}$/min) and ADP5 (weak) exhibited the fastest ($-6.7x10^{-3}$/min). The reaction kinetic in the presence of amelogenin, the protein which ADP's were derived from, was relatively fast compared to that of no peptide reaction with a rate constant of $-5.2x10^{-3}$/min [448].

Microstructural analyses were performed by SEM and TEM. Samples at 24 hours revealed that mineralization reactions exhibiting similar kinetics showed a high correlation in crystal morphology. For example, as shown in Figure 3.33, reactions in the presence of strong binders, ADP1, ADP2, and HABP1 where reactions were relatively fast compared to no peptide, yielded minerals with similar structural morphology. In particular, microstructure in all three cases revealed spherulites of ~3-5 μm diameter crystal plate of ~200 nm wide fully populating their surfaces. On the other hand, reactions in the presence of weak binders ADP3, ADP6 and no peptide yielded minerals that formed in spherulites but with no apparent plate-like structures on their surfaces. However, we noted that in the case of strong binding

ADP7, where reaction kinetics was the slowest, the microstructure was similar to that of full amelogenin with needle like crystals forming bundle like structures. Interestingly, minerals formed in the presence of ADP5 exhibited very different crystal morphologies. There were no spherulites, only plate-like crystals that were larger than that of other minerals 10 fold.

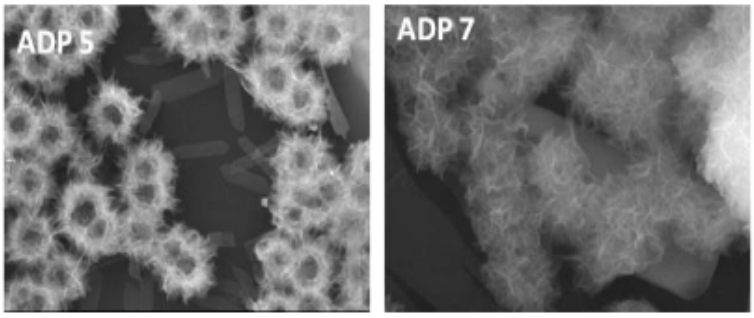

Figure 3.33: SEM micrographs of the minerals formed by the ADPs. The morphologies ADP5 and ADP7 yielded [448].

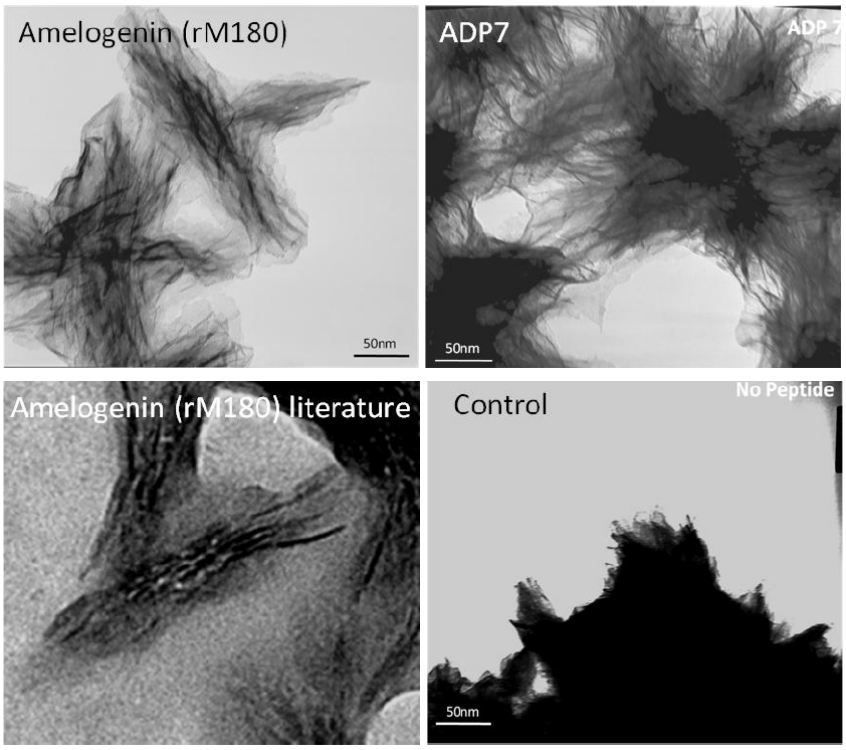

Figure 3.34: TEM micrographs of the minerals formed by ADP7 and the full length recombinant amelogenin, and a literature [449] comparison to a mineral formed by the same full length amelogenin. The control mineral was formed in the presence of no peptide [448].

The significant morphological differences suggest that the final phase of the resulting mineral might be different as well. The plate like structures and the spherulites are the characteristic morphologies of OCP observed in similar experimental conditions. However, the needle-like morphologies obtained from amelogenin and the ADP7 are characteristic with HA formed in wet-precipitation reactions.

Mineralization characterizations, on the other hand, have shown that some of the ADPs emulate the function of the full amelogenin in different aspects. Amelogenin has shown high binding affinity to HA, resulted in HA crystals forming the characteristic bundle structures and has resulted in high mineralization rate. ADP7 has shown very high binding affinity to HA, higher than the amelogenin and formed minerals with very similar morphology to those formed by amelogenin. However, ADP7 failed to emulate the high mineralization kinetics observed in the full amelogenin. ADP5, on the other hand, resulted in mineralization kinetics very similar to the full amelogenin but failed to reproduce the mineral phase and morphology observed in the full amelogenin. This data indicate that the ADP5 and ADP7 might be two different functional domains on the amelogenin, ADP5 being the region controlling the mineralization kinetics and ADP7 being the region controlling the binding, morphology and the mineral phase (Figure 3.34).

3.4.2. Designing of TiBP-ADP(s) bi-functional conjugates for hydroxyapatite mineralization on titanium

One of the major characteristics of inorganic binding peptides is their ability to mineralize materials from solution as mentioned in previous section. This has been an area of interest in several studies that have assessed the effects of peptides on the biomineralization of such materials as gold, silver, silica, HAp and others. This phenomenon represents a major area of future applications of GEPIs, making them not only material linkers and modifiers, but also material synthesizers. Thus far, GEPIs have been used to form films [450], nanoparticles [357, 355, 343] and nanorods [451] as well as multiple-material hybrids [452, 453]. Despite the interest the area this phenomenon is yet poorly understood. This lack of understanding is due to the fact that the mineralization process can be affected by peptides in a number of ways that cannot easily be observed. Peptides can be responsible for ion binding, chemical reduction of ions (in the case of metals), stabilization of nuclei, surface

energy modification, or steric hindrance of crystal growth, or some combination of these factors. Depending on described features of GEPIs with the examples, the goal was to design multifunctional construct or bi-functional peptide carrying with TiBPs` molecular linker and ADPs` mineralization capability for HA mineralization on titanium surface.

In here, first detailed binding affinity characterization experiment was performed on both titanium and hydroxyapatite surfaces via QCM for each domain of bi-functional peptide (i.e. TiBP2, ADP5 and ADP7 on titanium and HA) to do possible best design with their affinity comparison. In designed peptides, two domains were combined with GGG flexible linker and synthesized from C terminus to N terminus (ADP to TiBP). Following, each individual domain binding affinity were examined. Figure 17 represents K_d values of ADP5, ADP7, TiBP2 on titanium and hydroxyapatite. ADP5 has low affinity with more than 50 μM K_d value to HA surface where ADP7 has relatively high binding affinity with 10x lower K_d value. In case of titanium surface, ADP5 has high binding affinity to titanium surface with 0.5 μM K_d value where ADP7 has relatively low binding affinity with 5X lower K_d value. For titanium binding peptides, TiBP2 is reported previous sections as a best binder were chosen for linker domain in bi-functional peptides. It has also really low binding affinity to HA surface (Figure 3.35).

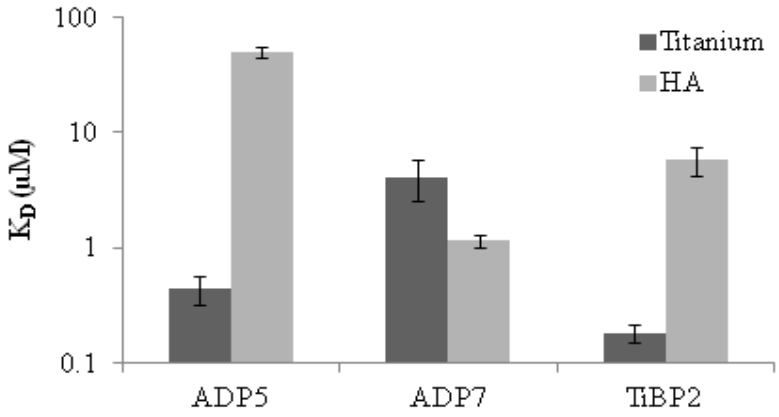

Figure 3.35: Binding affinity of TiBP2, ADP5 and ADP7on titanium and HA respectively.

3.4.3 Adsorption behavior of TiBP-ADP(s) bi-functional peptides on titanium

Following testing binding affinity and selectivity properties of peptides for each target material (titanium and hydroxyapatite), binding affinity of designed bi-functional peptide were tested on titanium surface first. As indicated in Figure 3.36, TiBP2-ADP7 has high surface coverage at low concentrations compared to TiBP2-ADP5. There is a 7.3 fold difference among their K_D values as shown in Table 3.7. Although binding affinity levels of two bi-functional peptides are different then each other, both of them are good binders. Binding affinity of TiBP2-ADP7 is almost as same as TiBP2.

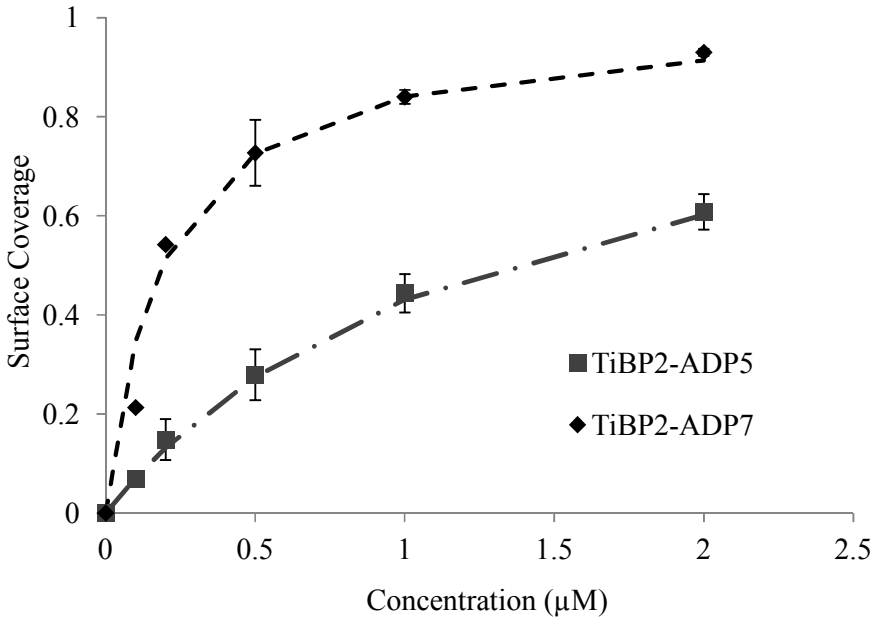

Figure 3.36: Surface Coverage of TiBP2-ADP5 and TiBP2-ADP7 on Titanium Surface

Table 3.8 K_D (µM) values of TiBP2-ADP5 and TiBP2-ADP7 on titanium.

Peptide Name	K_D (µM)
TiBP1-ADP5	1.32 ± 0.22
TiBP2-ADP7	0.18 ± 0.02

3.4.4 Kinetics of bi-functional peptides facilitated biomineralization

QCM experiments were run to show the kinetics of mineral formation induced by different immobilized peptide films. Peptides were first allowed to adsorb to the titanium surface at 10 μM. Once the signal stabilized a supersaturated calcium-phosphate buffer was introduced. The solution was then left for up to three days to mineralize. In the cases of TiBP2-ADP5 and ADP5 mineralization began almost immediately, with the rate of mineralization increasing exponentially until reaching an approximately linear growth rate after around four hours. TiBP2-ADP7 also leads to short term mineralization; however, there were several hours of incubation before the mineralization rate began increasing exponentially. TiBP2-ADP7 also stabilized with a significantly slower growth rate than the ADP5-based peptides. The other peptides, TiBP2 and ADP7, did not cause any mineralization during the first 24 hours. Nothing mineralized on the bare Ti surface during a three day test (Figure 3.37).

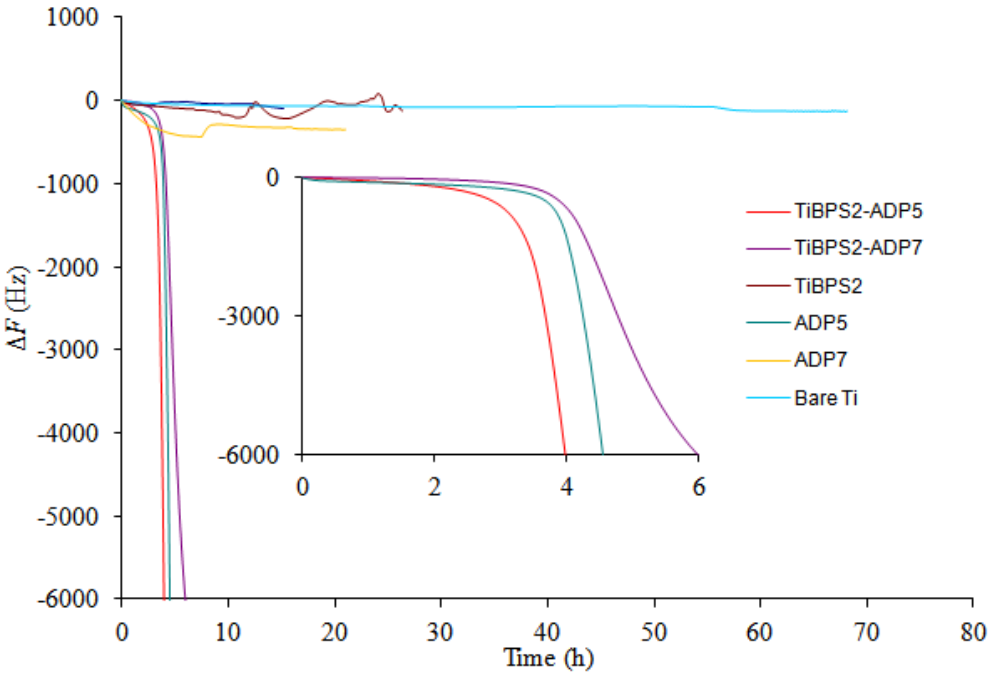

Figure 3.37: In situ monitoring of bi-functional peptide mediated $Ca_5(PO_4)_3OH$ mineralization via QCM.

3.4.5 Mineralization characteristics of bi-functional peptides on titanium

Following, the kinetics of mineralization were monitored via QCM. The effect of the peptide on the structure of the mineralized film was monitored using SEM first and

then TEM. Titanium surfaces showing no mineralization in QCM were indistinguishable from control bare titanium substrates. Two bi-functional peptides that did show significant mineralization all had very similar structures to the HAP film (Figure 3.38). No mineralization was observed in case of no peptide, ADP5, ADP7 and TiBP2. Among them, mineralization and binding behavior of ADP5 is significant with variety of contrast examples. It has low binding affinity to HA surface where high binding affinity to titanium surface. Its mineralization capability in solution was significantly different than on titanium surface. It also shows us there is no correlation between binding strength and mineralization capability of peptides. Their behavior can also be affected depending on occurrence of mineralization reaction in the solution or on the surface. This data also may reveal that changes in molecular conformation of peptides in solution and on the surface may alter the mineralization process. In case of ADP7, it has really high binding affinity to HA surface where binding affinity to titanium surface low. It can form HA like structure in solution however any mineral formed on the surface of the titanium. In case of bi-functional peptides, they both form mineral with similar structure. TEM (Figure 3.41) data was also indicate us formed mineral structure is very similar to HA crystals.

In conclusion, there are several possible mechanisms for an immobilized peptide films have in influencing the nucleation and growth of a mineralizing film. These include binding the relevant ions, leading to a local increase in the concentration; and, perhaps most likely, by reducing the surface energy of calcium-phosphate nuclei. Since the peptides are immobilized on the titanium surface and there is a very low concentration of peptide in solution, we can only expect that the once the peptide is covered with HAp they should no longer have any effect on the way the HAp film evolves. This was shown to be the case in both QCM and SEM data. These results isolate the peptides ability as nucleating agents, and show the peptides' ability to form a HAp film in situ, without the need of any surface modification of the titanium. The results are also revealed that peptide mineralization behavior can be different in solution and on the surface.

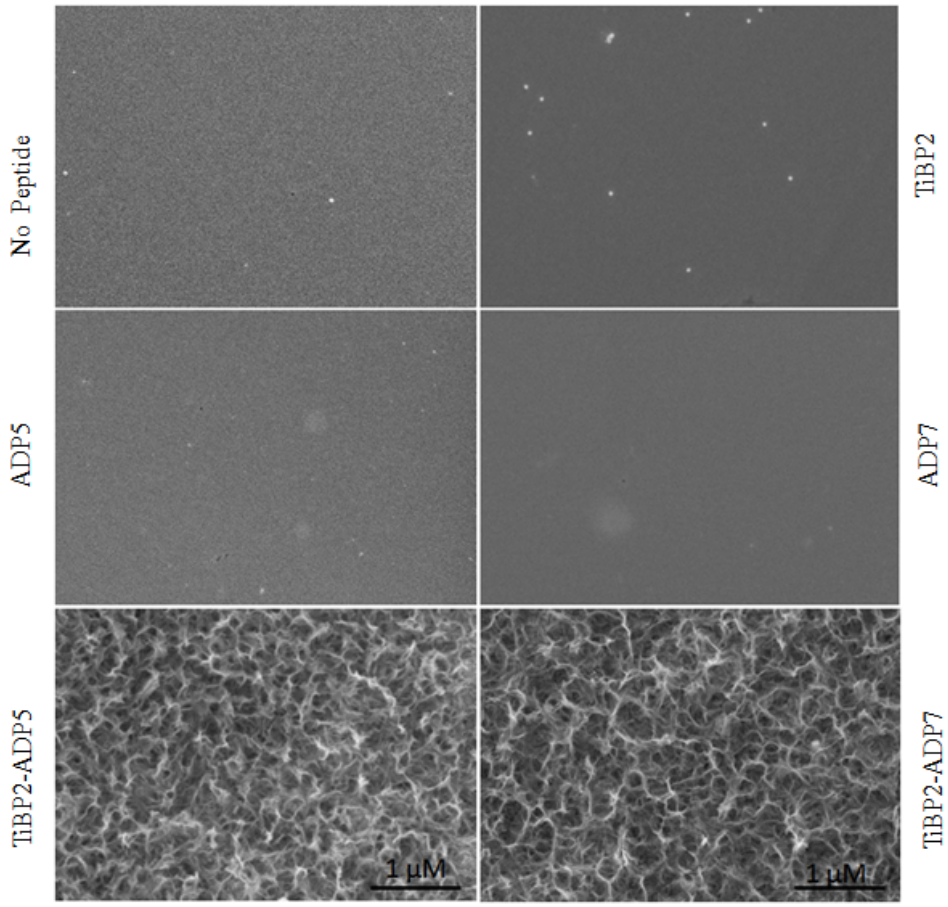

Figure 3.38: SEM micrographs of minerals formed by bi-functional peptides (TiBP2-ADP5, TiBP2-ADP7) including positive and negative controls.

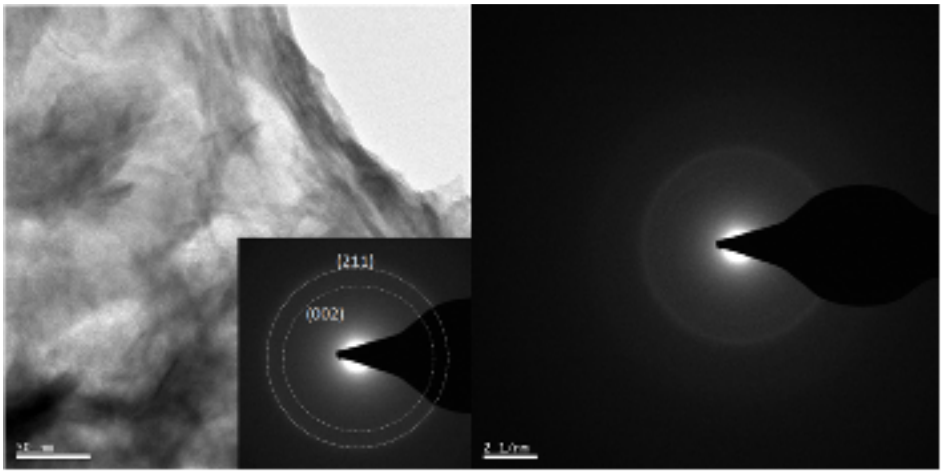

Figure 3.39: TEM images of the minerals formed in the presence of TiBP2-ADP5. The inset is the corresponding selected area diffraction patterns of the minerals.

4. CONCLUSION

Nanotechnology has revolutionized many fields of science including fabrication and characterization of various nanostructures. In general, it is experiencing a rapid growth period with major advances arriving quickly. According to these advances are applied in the biomedical field in numerous diverse ways. Especially, remarkable recognition capabilities of biomolecules when combined with the unique properties of nanomaterials can lead to novel implant materials with significantly improved performances. Nature also provides abundant examples of materials and systems with a rich variety of interconnections among materials and biomlecules. The joining of biology in the implementation of nanotechnology to design, engineer materials help scientist for realization of nanobiotechnology. Due to control of all interfaces between materials and tissues by proteins and peptides in biology, molecular biomimetics bring approaches into engineering and technological systems by utilizing peptides. Based on potentials of peptides, GEPIs as a field of molecular biomimetics may serve a platform for achieving the goal of efficient ways for design and fabrication of complex materials with multiple functionalities. They can act as fundamental building blocks in nanoinorganic assembly for electronics and photonics application. They can couple with solid substrates to open new routes in the development of advanced biosensors for pathogen detection, drug screening, bioseparations systems and diagnostics in medicine (e.g. cancer therapeutics). GEPI have short amino acid sequences with material selective binding and self assembling properties can also be good candidate as a molecular linker for functionalization of material surfaces. Once selected by combinatorial biology techniques, they can be further tailored to enhance/modify their binding ability and multifunctionality. The multifunctionality could be introduced either two or more material binding peptides to create novel ways of making dissimilar materials and coupling material binding properties with other bio-functional molecules to modify surfaces with improved properties for particular goal.

In the scope of this dissertation, the remarkable findings on multifunctional features of GEPIs to improve implant material properties with different examples were demonstrated. In the following examples, controlling cell-surface interactions were demonstrated either designing bioactive, antimicrobial surfaces or inducing mineral formation on titanium surface towards peptide-based biomolecule immobilization.

In the first part, selection and detailed characterization of TiBPs in terms of binding affinity, specificity, molecular structure and cytotoxicty were shown. Selection of TiBPs against cp Grade 4 titanium implant surface via cell surface display to generate set of sequences that could offer a route for implant surface functionalization as a molecular linker were reported. Following, three TiBPs (TiBP1, 2 and 60) were identified based on initial fluorescence microscopy (FM) characterization for further investigations. Two (TiBP1 and TiBP2) that exhibited high affinity, one (TiBP60) with lowest binding affinity to titanium were subjected to determine their quantitative binding characteristics on titanium with the contribution of primary and secondary structural properties. We were also interested in learning material selectivity properties of TiBP1 and TiBP2 on various implantable surfaces such as silica and HA via QCM due to requirement of new molecular linkers with their recognition and specificity capabilities in implantation. Then, we attempt to show cellular response against TiBPs (TiBP1 and TiBP2) functionalized surfaces via MTT assay. The findings rely on remarkable high binding affinity, material selectivity, cytotoxicity features with distinct physicochemical properties of the two TiBPs (TiBP1 and TiBPs) was a potential candidate to tailor their capabilities conjugation with other functional molecules for implant surface modifications.

In the second section, to address the utility and versatility of TiBPs for controlling cell-surface interactions through immobilization of functional molecules on various implant surfaces especially on titanium, bi-functional peptide was designed in conjugation with two titanium binding peptides (TiBP1 and TiBP2) and integrin binding domain RGD via GGG flexible linker for bioactive surface modifications. Their effects on cell viability, adhesion and spreading were examined on cp Grade 4 titanium implant surfaces and titanium coated glass surfaces in the presence of osteoblast and fibroblast. Our results demonstrated that peptide-based surface modification is an adaptable platform to meet the specific requirements to design bioactive surfaces enhancing with cell adhesion and spreading. This also indicate us

single-step surface modification using solid-binding peptides conjugated to desired medically relevant molecules may prove to be a robust, biocompatible approach in the functionalization of complex devices in clinical applications.

In the third section, we offer a way for development of biomaterial surfaces that capable of preventing bacterial infection towards peptide-based surface functionalization. We have created two bi-functional peptides composed of a genetically engineered peptide for inorganics (GEPI) motif and an antimicrobial peptide (AMP) motif; these bi-functional peptides rely on the titanium-binding properties of the GEPI to preferentially bind to the biomaterial, freely exposing the AMP motif to combat invading bacteria. The efficacy of our bi-functional peptides (TiBP1-AMP and TiBP2-AMP) were evaluated both in-solution and on the surface of titanium against *Streptococcus mutans, Staphylococcus epidermidis,* and *Escherichia coli.* Surfaces modified with our bi-functional peptides were found to significantly reduce bacterial adhesion against all three bacteria when compared to adhesion on bare titanium. The results of the presented work indicate that surface modification with conjugated molecules consisting of antimicrobial and titanium binding peptides is a promising approach to prevent bacterial infection on implant surfaces. Although antimicrobial properties of peptide modified implant surfaces were shown against to three different bacteria (*S.mutans, S.epidermidis and E.coli*), various peptide can be also designed against to broad range of bacteria by utilizing sequence, structure and charge relations of AMPs and material binding peptides. It should be noted that controlled binding and release of biomolecules to implant surfaces are critical in the development of intelligent implant materials. Detail studies are necessary to clarify the underlying mechanism of antimicrobial activity in such conjugated peptides and determine the stability of adsorbed peptides in the presence of body fluids.

In the last section, molecular linkers and synthesizers capabilities of GEPIs were demonstrated. Depending on described features of GEPIs, the goal was to design multifunctional construct or bi-functional peptide carrying with TiBPs` molecular linker and ADPs` mineralization capability for HA mineralization on titanium surface. Real time monitoring of the $CaPO_4$ biomineralization were successfully achieved on the surface of titanium via QCM. The mineral morphology and crystal structure were examined with TEM and SEM. This part of work indicates that GEPI

may provide the ways for genetic control on biomineralization from tissue restoration to regeneration.

In conclusion, GEPIs are smart molecules selected using combinatorial biology protocols such as phage and cell surface display and subsequently characterized by different qualitative and semi quantitative methods *e.g.* AFM, QCM, SPR and FM. Their binding affinity and material selectivity properties can also be improved by efficacy of the bioinformatics approach. The overall results indicate in here, GEPI has potential to become more attractive in implant applications not only molecular linker but also synthesizer capability. Their high binding affinity, specificity and recognition capability for desired surface that allow precise control density, functionality, accessibility of biomolecules offers an alternative immobilization methods for biological surface modification of implants.

REFERENCES

[1] **Whitesides, G. M.** (2005). Nanoscience, nanotechnology, and chemistry, *Small, **1***, 172-179.

[2] **Lieber, C. M.** (2001). Building with nanotechnology, *Chemical & Engineering News, **79***, 146-146.

[3] **Lieber, C. M.** (2003). Nanoscale science and technology: Building a big future from small things, *Mrs Bulletin, **28***, 486-491.

[4] **Sarikaya, M., Tamerler, C., Schwartz, D. T. & Baneyx, F. O.** (2004). Materials assembly and formation using engineered polypeptides, *Annual Review of Materials Research, **34***, 373-408.

[5] **Ball, P.** (2001). Life's lessons in design, *Nature, **409***, 413-416.

[6] **Weiner, S., Addadi, L. & Wagner, H. D.** (2000). Materials design in biology, *Materials Science & Engineering C-Biomimetic and Supramolecular Systems, **11***, 1-8.

[7] **Tran, N. & Webster, T. J.** (2009). Nanotechnology for bone materials, *Wiley Interdisciplinary Reviews-Nanomedicine and Nanobiotechnology, **1***, 336-351.

[8] **Zhang, L. J. & Webster, T. J.** (2009). Nanotechnology and nanomaterials: Promises for improved tissue regeneration, *Nano Today, **4***, 66-80.

[9] **Tamerler, C., Khatayevich, D., Gungormus, M., Kacar, T., Oren, E. E., Hnilova, M. & Sarikaya, M.** Molecular biomimetics: Gepi-based biological routes to technology, *Biopolymers, **94***, 78-94.

[10] **Weiner, S. & Wagner, H. D.** (1998). The material bone: Structure mechanical function relations, *Annual Review of Materials Science, **28***, 271-298.

[11] **Weiner, S., Traub, W. & Wagner, H. D.** (1999). Lamellar bone: Structure-function relations, *Journal of Structural Biology, **126***, 241-255.

[12] **Laurencin, C. T., Kumbar, S. G. & Nukavarapu, S. P.** (2009). Nanotechnology and orthopedics: A personal perspective, *Wiley Interdisciplinary Reviews-Nanomedicine and Nanobiotechnology, **1***, 6-10.

[13] **Christenson, E. M., Anseth, K. S., Van Den Beucken, L., Chan, C. K., Ercan, B., Jansen, J. A., Laurencin, C. T., Li, W. J., Murugan, R., Nair, L. S., Ramakrishna, S., Tuan, R. S., Webster, T. J. & Mikos, A. G.** (2007). Nanobiomaterial applications in orthopedics, *Journal of Orthopaedic Research, **25***, 11-22.

[14] **Liu, H. & Webster, T. J.** (2007). Nanomedicine for implants: A review of studies and necessary experimental tools, *Biomaterials, **28***, 354-369.

[15] **Whitesides, G. M. & Wong, A. P.** (2006). The intersection of biology and materials science, *Mrs Bulletin, **31***, 19-27.

[16] **Sarikaya, M., Tamerler, C., Jen, A. K. Y., Schulten, K. & Baneyx, F.** (2003). Molecular biomimetics: Nanotechnology through biology, *Nature Materials, **2***, 577-585.

[17] **Seeman, N. C. & Belcher, A. M.** (2002). Emulating biology: Building nanostructures from the bottom up, *Proceedings of the National Academy of Sciences of the United States of America, **99***, 6451-6455.

[18] **Webster, T. J., Siegel, R. W. & Bizios, R.** (1999). Osteoblast adhesion on nanophase ceramics, *Biomaterials, **20***, 1221-1227.

[19] **Qin, X. Y., Kim, J. G. & Lee, J. S.** (1999). Synthesis and magnetic properties of nanostructured gamma-ni-fe alloys, *Nanostructured Materials, **11***, 259-270.

[20] **Webster, T. J., Ergun, C., Doremus, R. H., Siegel, R. W. & Bizios, R.** (2000). Enhanced functions of osteoblasts on nanophase ceramics, *Biomaterials, **21***, 1803-1810.

[21] **Sato, M. & Webster, T. J.** (2004). Nanobiotechnology: Implications for the future of nanotechnology in orthopedic applications, *Expert Review of Medical Devices, **1***, 105-114.

[22] **Vasir, J. K., Reddy, M. K. & Labhasetwar, V. D.** (2005). Nanosystems in drug targeting: Opportunities and challenges, *Current Nanoscience, **1***, 47-64.

[23] **Engel, E., Michiardi, A., Navarro, M., Lacroix, D. & Planell, J. A.** (2008). Nanotechnology in regenerative medicine: The materials side, *Trends in Biotechnology, **26***, 39-47.

[24] **Ferrari, M.** (2005). Cancer nanotechnology: Opportunities and challenges, *Nature Reviews Cancer, **5***, 161-171.

[25] **Hasirci, V., Vrana, E., Zorlutuna, P., Ndreu, A., Yilgor, P., Basmanav, F. B. & Aydin, E.** (2006). Nanobiomaterials: A review of the existing science and technology, and new approaches, *Journal of Biomaterials Science-Polymer Edition, **17***, 1241-1268.

[26] **Ratner, B. D. & Bryant, S. J.** (2004). Biomaterials: Where we have been and where we are going, *Annual Review of Biomedical Engineering, **6***, 41-75.

[27] **Palin, E., Liu, H. N. & Webster, T. J.** (2005). Mimicking the nanofeatures of bone increases bone-forming cell adhesion and proliferation, *Nanotechnology, **16***, 1828-1835.

[28] **Ergun, C., Liu, H. N., Webster, T. J., Olcay, E., Yilmaz, S. & Sahin, F. C.** (2008). Increased osteoblast adhesion on nanoparticulate calcium phosphates with higher ca/p ratios, *Journal of Biomedical Materials Research Part A, **85A***, 236-241.

[29] **Yao, C., Slamovich, E. B. & Webster, T. J.** (2008). Enhanced osteoblast functions on anodized titanium with nanotube-like structures, *Journal of Biomedical Materials Research Part A, **85A***, 157-166.

[30] **Stupp, S. I.** Self-assembly and biomaterials, *Nano Letters, **10***, 4783-4786.

[31] **Kay, S., Thapa, A., Haberstroh, K. M. & Webster, T. J.** (2002). Nanostructured polymer/nanophase ceramic composites enhance osteoblast and chondrocyte adhesion, *Tissue Engineering, **8***, 753-761.

[32] **Park, G. E., Pattison, M. A., Park, K. & Webster, T. J.** (2005). Accelerated chondrocyte functions on naoh-treated plga scaffolds, *Biomaterials, **26***, 3075-3082.

[33] **Savaiano, J. K. & Webster, T. J.** (2004). Altered responses of chondrocytes to nanophase plga/nanophase titania composites, *Biomaterials, **25***, 1205-1213.

[34] **Miller, D. C., Haberstroh, K. M. & Webster, T. J.** (2007). Plga nanometer surface features manipulate fibronectin interactions for improved vascular cell adhesion, *Journal of Biomedical Materials Research Part A, **81A***, 678-684.

[35] **Lu, J., Rao, M. P., Macdonald, N. C., Khang, D. & Webster, T. J.** (2008). Improved endothelial cell adhesion and proliferation on patterned titanium surfaces with rationally designed, micrometer to nanometer features, *Acta Biomaterialia, **4***, 192-201.

[36] **Choudhary, S., Haberstroh, K. M. & Webster, T. J.** (2007). Enhanced functions of vascular cells on nanostructured ti for improved stent applications, *Tissue Engineering, **13***, 1421-1430.

[37] **Miller, D. C., Haberstroh, K. M. & Webster, T. J.** (2005). Mechanism(s) of increased vascular cell adhesion on nanostructured poly(lactic-co-glycolic acid) films, *Journal of Biomedical Materials Research Part A, **73A***, 476-484.

[38] **Mccann-Brown, J. A., Webster, T. J. & Haberstroh, K. M.** (2007). Vascular cells respond to endothelial cell flow- and pressure-released soluble proteins, *Chemical Engineering Communications,* ***194***, 309-321.

[39] **Khang, D., Kim, S. Y., Liu-Snyder, P., Palmore, G. T. R., Durbin, S. M. & Webster, T. J.** (2007). Enhanced fibronectin adsorption on carbon nanotube/poly(carbonate) urethane: Independent role of surface nano-roughness and associated surface energy, *Biomaterials,* ***28***, 4756-4768.

[40] **Khang, D., Sato, M., Price, R. L., Ribbe, A. E. & Webster, T. J.** (2006). Selective adhesion and mineral deposition by osteoblasts on carbon nanofiber patterns, *International Journal of Nanomedicine,* ***1***, 65-72.

[41] **Webster, T. J., Waid, M. C., Mckenzie, J. L., Price, R. L. & Ejiofor, J. U.** (2004). Nano-biotechnology: Carbon nanofibres as improved neural and orthopaedic implants, *Nanotechnology,* ***15***, 48-54.

[42] **Elias, K. L., Price, R. L. & Webster, T. J.** (2002). Enhanced functions of osteoblasts on nanometer diameter carbon fibers, *Biomaterials,* ***23***, 3279-3287.

[43] **Chun, A. L., Moralez, J. G., Webster, T. J. & Fenniri, H.** (2005). Helical rosette nanotubes: A biomimetic coating for orthopedics?, *Biomaterials,* ***26***, 7304-7309.

[44] **Khang, D., Carpenter, J., Chun, Y. W., Pareta, R. & Webster, T. J.** Nanotechnology for regenerative medicine, *Biomedical Microdevices,* ***12***, 575-587.

[45] **Geetha, M., Singh, A. K., Asokamani, R. & Gogia, A. K.** (2009). Ti based biomaterials, the ultimate choice for orthopaedic implants - a review, *Progress in Materials Science,* ***54***, 397-425.

[46] **Katti, K. S.** (2004). Biomaterials in total joint replacement, *Colloids and Surfaces B-Biointerfaces,* ***39***, 133-142.

[47] **Barrere, F., Mahmood, T. A., De Groot, K. & Van Blitterswijk, C. A.** (2008). Advanced biomaterials for skeletal tissue regeneration: Instructive and smart functions, *Materials Science & Engineering R-Reports,* ***59***, 38-71.

[48] **Kasemo, B.** (1998). Biological surface science, *Current Opinion in Solid State & Materials Science,* ***3***, 451-459.

[49] **Olivier, V., Faucheux, N. & Hardouin, P.** (2004). Biomaterial challenges and approaches to stem cell use in bone reconstructive surgery, *Drug Discovery Today,* ***9***, 803-811.

[50] **Green, D., Walsh, D., Mann, S. & Oreffo, R. O. C.** (2002). The potential of biomimesis in bone tissue engineering: Lessons from the design and synthesis of invertebrate skeletons, *Bone,* ***30***, 810-815.

[51] **Kroese-Deutman, H. C., Van Den Dolder, J., Spauwen, P. H. M. & Jansen, J. A.** (2005). Influence of rgd-loaded titanium implants on bone formation in vivo, *Tissue Engineering, **11***, 1867-1875.

[52] **Paital, S. R. & Dahotre, N. B.** (2009). Calcium phosphate coatings for bio-implant applications: Materials, performance factors, and methodologies, *Materials Science & Engineering R-Reports, **66***, 1-70.

[53] **Webster, T. J. & Ejiofor, J. U.** (2004). Increased osteoblast adhesion on nanophase metals: Ti, ti6al4v, and cocrmo, *Biomaterials, **25***, 4731-4739.

[54] **Frauchiger, V. M., Schlottig, F., Gasser, B. & Textor, M.** (2004). Anodic plasma-chemical treatment of cp titanium surfaces for biomedical applications, *Biomaterials, **25***, 593-606.

[55] **Akahori, T. & Niinomi, M.** (1998). Fracture characteristics of fatigued ti-6al-4v eli as an implant material, *Materials Science and Engineering a-Structural Materials Properties Microstructure and Processing, **243***, 237-243.

[56] **Scharnweber, D., Beutner, R., Rossler, S. & Worch, H.** (2002). Electrochemical behavior of titanium-based materials - are there relations to biocompatibility?, *Journal of Materials Science-Materials in Medicine, **13***, 1215-1220.

[57] **Bruni, S., Martinesi, M., Stio, M., Treves, C., Bacci, T. & Borgioli, F.** (2005). Effects of surface treatment of ti-6al-4v titanium alloy on biocompatibility in cultured human umbilical vein endothelial cells, *Acta Biomaterialia, **1***, 223-234.

[58] **Gotman, I.** (1997). Characteristics of metals used in implants, *Journal of Endourology, **11***, 383-389.

[59] **Hench, L. L.** (1991). Bioceramics - from concept to clinic, *Journal of the American Ceramic Society, **74***, 1487-1510.

[60] **Hench, L. L. & Wilson, J.** (1991). Bioceramics, *Mrs Bulletin, **16***, 62-74.

[61] **Cao, W. P. & Hench, L. L.** (1996). Bioactive materials, *Ceramics International, **22***, 493-507.

[62] **Agrawal, C. M.** (1998). Reconstructing the human body using biomaterials, *Jom-Journal of the Minerals Metals & Materials Society, **50***, 31-35.

[63] **Hasirci, V., Lewandrowski, K., Gresser, J. D., Wise, D. L. & Trantolo, D. J.** (2001). Versatility of biodegradable biopolymers: Degradability and an in vivo application, *Journal of Biotechnology, **86***, 135-150.

[64] **Wang, M.** (2003). Developing bioactive composite materials for tissue replacement, *Biomaterials, **24***, 2133-2151.

[65] **Liu, L. S., Thompson, A. Y., Heidaran, M. A., Poser, J. W. & Spiro, R. C.** (1999). An osteoconductive collagen hyaluronate matrix for bone regeneration, *Biomaterials, **20***, 1097-1108.

[66] **Ber, S., Kose, G. T. & Hasirci, V.** (2005). Bone tissue engineering on patterned collagen films: An in vitro study, *Biomaterials, **26***, 1977-1986.

[67] **Kose, G. T., Korkusuz, F., Ozkul, A., Soysal, Y., Ozdemir, T., Yildiz, C. & Hasirci, V.** (2005). Tissue engineered cartilage on collagen and phbv matrices, *Biomaterials, **26***, 5187-5197.

[68] **Junker, R., Dimakis, A., Thoneick, M. & Jansen, J. A.** (2009). Effects of implant surface coatings and composition on bone integration: A systematic review, *Clinical Oral Implants Research, **20***, 185-206.

[69] **Le Guehennec, L., Soueidan, A., Layrolle, P. & Amouriq, Y.** (2007). Surface treatments of titanium dental implants for rapid osseointegration, *Dental Materials, **23***, 844-854.

[70] **Steinemann, S. G.** (1998). Titanium - the material of choice?, *Periodontology 2000, **17***, 7-21.

[71] **Buser, D., Broggini, N., Wieland, M., Schenk, R. K., Denzer, A. J., Cochran, D. L., Hoffmann, B., Lussi, A. & Steinemann, S. G.** (2004). Enhanced bone apposition to a chemically modified sla titanium surface, *Journal of Dental Research, **83***, 529-533.

[72] **Rupp, F., Scheideler, L., Olshanska, N., De Wild, M., Wieland, M. & Geis-Gerstorfer, J.** (2006). Enhancing surface free energy and hydrophilicity through chemical modification of microstructured titanium implant surfaces, *Journal of Biomedical Materials Research Part A, **76A***, 323-334.

[73] **Zhao, G., Schwartz, Z., Wieland, M., Rupp, F., Geis-Gerstorfer, J., Cochran, D. L. & Boyan, B. D.** (2005). High surface energy enhances cell response to titanium substrate microstructure, *Journal of Biomedical Materials Research Part A, **74A***, 49-58.

[74] **Katz, J. L.** (1980). Anisotropy of youngs modulus bone - reply, *Nature, **288***, 196-196.

[75] **Sumner, D. R., Turner, T. M., Igloria, R., Urban, R. M. & Galante, J. O.** (1998). Functional adaptation and ingrowth of bone vary as a function of hip implant stiffness, *Journal of Biomechanics, **31***, 909-917.

[76] **Mudali, U. K., Sridhar, T. M. & Raj, B.** (2003). Corrosion of bio implants, *Sadhana-Academy Proceedings in Engineering Sciences, **28***, 601-637.

[77] **Pourbaix, M.** (1984). Electrochemical corrosion of metallic biomaterials, *Biomaterials, **5***, 122-134.

[78] **Hallab, N. J., Anderson, S., Caicedo, M., Brasher, A., Mikecz, K. & Jacobs, J. J.** (2005). Effects of soluble metals on human peri-implant cells, *Journal of Biomedical Materials Research Part A, **74A***, 124-140.

[79] **Sargeant, A. & Goswami, T.** (2006). Hip implants: Paper v. Physiological effects, *Materials & Design, **27***, 287-307.

[80] **Sigurgeirsdottir, E., Abron, A. & Cooper, L. F.** (1998). Immunohistochemical analysis of cp titanium implant integration using preembedding fracture technique, *Journal of Dental Research, **77***, 1333-1333.

[81] **Mendonca, G., Mendonca, D. B. S., Aragao, F. J. L. & Cooper, L. F.** (2008). Advancing dental implant surface technology - from micron- to nanotopography, *Biomaterials, **29***, 3822-3835.

[82] **Cooper, L. F.** (1998). Biologic determinants of bone formation for osseointegration: Clues for future clinical improvements, *Journal of Prosthetic Dentistry, **80***, 439-449.

[83] **Kieswetter, K., Schwartz, Z., Dean, D. D. & Boyan, B. D.** (1996). The role of implant surface characteristics in the healing of bone, *Critical Reviews in Oral Biology & Medicine, 7*, 329-345.

[84] **Pattison, M. A., Wurster, S., Webster, T. J. & Haberstroh, K. M.** (2005). Three-dimensional, nano-structured plga scaffolds for bladder tissue replacement applications, *Biomaterials, **26***, 2491-2500.

[85] **Miller, D. C., Thapa, A., Haberstroh, K. M. & Webster, T. J.** (2004). Endothelial and vascular smooth muscle cell function on poly(lactic-co-glycolic acid) with nano-structured surface features, *Biomaterials, **25***, 53-61.

[86] **Wertz, C. F. & Santore, M. M.** (2001). Effect of surface hydrophobicity on adsorption and relaxation kinetics of albumin and fibrinogen: Single-species and competitive behavior, *Langmuir, **17***, 3006-3016.

[87] **Roach, P., Farrar, D. & Perry, C. C.** (2005). Interpretation of protein adsorption: Surface-induced conformational changes, *Journal of the American Chemical Society, **127***, 8168-8173.

[88] **Kozlova, N. & Santore, M. M.** (2006). Manipulation of micrometer-scale adhesion by tuning nanometer-scale surface features, *Langmuir, **22***, 1135-1142.

[89] **Franco, M., Nealey, P. F., Campbell, S., Teixeira, A. I. & Murphy, C. J.** (2000). Adhesion and proliferation of corneal epithelial cells on self-assembled monolayers, *Journal of Biomedical Materials Research, **52***, 261-269.

[90] **Kennedy, S. B., Washburn, N. R., Simon, C. G. & Amis, E. J.** (2006). Combinatorial screen of the effect of surface energy on fibronectin-

mediated osteoblast adhesion, spreading and proliferation, *Biomaterials, **27***, 3817-3824.

[91] **Hersel, U., Dahmen, C. & Kessler, H.** (2003). Rgd modified polymers: Biomaterials for stimulated cell adhesion and beyond, *Biomaterials, **24***, 4385-4415.

[92] **Wilson, C. J., Clegg, R. E., Leavesley, D. I. & Pearcy, M. J.** (2005). Mediation of biomaterial-cell interactions by adsorbed proteins: A review, *Tissue Engineering, **11***, 1-18.

[93] **Gong, D., Grimes, C. A., Varghese, O. K., Hu, W. C., Singh, R. S., Chen, Z. & Dickey, E. C.** (2001). Titanium oxide nanotube arrays prepared by anodic oxidation, *Journal of Materials Research, **16***, 3331-3334.

[94] **Ellingsen, J. E., Thomsen, P. & Lyngstadaas, S. P.** (2006). Advances in dental implant materials and tissue regeneration, *Periodontology 2000, **41***, 136-156.

[95] **Balasundaram, G. & Webster, T. J.** (2006). A perspective on nanophase materials for orthopedic implant applications, *Journal of Materials Chemistry, **16***, 3737-3745.

[96] **Roach, P., Eglin, D., Rohde, K. & Perry, C. C.** (2007). Modern biomaterials: A review-bulk properties and implications of surface modifications, *Journal of Materials Science-Materials in Medicine, **18***, 1263-1277.

[97] **Elias, C. N., Oshida, Y., Lima, J. H. C. & Muller, C. A.** (2008). Relationship between surface properties (roughness, wettability and morphology) of titanium and dental implant removal torque, *Journal of the Mechanical Behavior of Biomedical Materials, **1***, 234-242.

[98] **Decker, E. L., Frank, B., Suo, Y. & Garoff, S.** (1999). Physics of contact angle measurement, *Colloids and Surfaces a-Physicochemical and Engineering Aspects, **156***, 177-189.

[99] **Takei, Y. G., Aoki, T., Sanui, K., Ogata, N., Sakurai, Y. & Okano, T.** (1994). Dynamic contact-angle measurement of temperature-responsive surface-properties for poly(n-isopropylacrylamide) grafted surfaces, *Macromolecules, **27***, 6163-6166.

[100] **Meiron, T. S., Marmur, A. & Saguy, I. S.** (2004). Contact angle measurement on rough surfaces, *Journal of Colloid and Interface Science, **274***, 637-644.

[101] **Yasuda, T., Okuno, T. & Yasuda, H.** (1994). Contact-angle of water on polymer surfaces, *Langmuir, **10***, 2435-2439.

[102] **Cai, K., Hu, Y. & Jandt, K. D.** (2007). Surface engineering of titanium thin films with silk fibroin via layer-by-layer technique and its effects on osteoblast growth behavior, *Journal of Biomedical Materials Research Part A, **82A***, 927-935.

[103] **Webster, T. J., Ergun, C., Doremus, R. H., Siegel, R. W. & Bizios, R.** (2000). Specific proteins mediate enhanced osteoblast adhesion on nanophase ceramics, *Journal of Biomedical Materials Research,* ***51***, 475-483.

[104] **Webb, K., Hlady, V. & Tresco, P. A.** (2000). Relationships among cell attachment, spreading, cytoskeletal organization, and migration rate for anchorage-dependent cells on model surfaces, *Journal of Biomedical Materials Research,* ***49***, 362-368.

[105] **Takebe, J., Itoh, S., Okada, J. & Ishibashi, K.** (2000). Anodic oxidation and hydrothermal treatment of titanium results in a surface that causes increased attachment and altered cytoskeletal morphology of rat bone marrow stromal cells in vitro, *Journal of Biomedical Materials Research,* ***51***, 398-407.

[106] **Feng, B., Weng, J., Yang, B. C., Qu, S. X. & Zhang, X. D.** (2003). Characterization of surface oxide films on titanium and adhesion of osteoblast, *Biomaterials,* ***24***, 4663-4670.

[107] **Buser, D., Schenk, R. K., Steinemann, S., Fiorellini, J. P., Fox, C. H. & Stich, H.** (1991). Influence of surface characteristics on bone integration of titanium implants - a histomorphometric study in miniature pigs, *Journal of Biomedical Materials Research,* ***25***, 889-902.

[108] **Gotfredsen, K., Wennerberg, A., Johansson, C., Skovgaard, L. T. & Hjortinghansen, E.** (1995). Anchorage of tio2-blasted, ha-coated, and machined implants - an experimental-study with rabbits, *Journal of Biomedical Materials Research,* ***29***, 1223-1231.

[109] **Anselme, K., Bigerelle, M., Noel, B., Iost, A. & Hardouin, P.** (2002). Effect of grooved titanium substratum on human osteoblastic cell growth, *Journal of Biomedical Materials Research,* ***60***, 529-540.

[110] **Fujibayashi, S., Neo, M., Kim, H. M., Kokubo, T. & Nakamura, T.** (2004) Osteoinduction of bioactive titanium metal, in: M. A. Barbosa, F. J. Monteiro, R. Correia & B. Leon (Eds) *Bioceramics 16.* (vol. 254-2), 953-956.

[111] **Boyan, B. D., Lohmann, C. H., Dean, D. D., Sylvia, V. L., Cochran, D. L. & Schwartz, Z.** (2001). Mechanisms involved in osteoblast response to implant surface morphology, *Annual Review of Materials Research,* ***31***, 357-371.

[112] **Ryan, G., Pandit, A. & Apatsidis, D. P.** (2006). Fabrication methods of porous metals for use in orthopaedic applications, *Biomaterials,* ***27***, 2651-2670.

[113] **Weber, J. N. & White, E. W.** (1972). Carbon-metal graded composites for permanent osseous attachment of non-porous metals, *Materials Research Bulletin,* ***7***, 1005-&.

[114] **Klawitte.Jj** (1974). Porous aluminum-oxide biomaterial, *American Ceramic Society Bulletin, **53***, 384-384.

[115] **Sauer, B. W., Weinstei.Am, Klawitte.Jj, Hulbert, S. F., Leonard, R. B. & Bagwell, J. G.** (1974). Role of porous polymeric materials in prosthesis attachment, *Journal of Biomedical Materials Research, **8***, 145-153.

[116] **White, E. W., Weber, J. N., Roy, D. M., Owen, E. L., Chiroff, R. T. & White, R. A.** (1975). Replamineform porous biomaterials for hard tissue implant applications, *Journal of Biomedical Materials Research, **9***, 23-27.

[117] **Kroger, H., Venesmaa, P., Jurvelin, J., Miettinen, H., Suomalainen, O. & Alhava, E.** (1998). Bone density at the proximal femur after total hip arthroplasty, *Clinical Orthopaedics and Related Research,* 66-74.

[118] **Kienapfel, H., Sprey, C., Wilke, A. & Griss, P.** (1999). Implant fixation by bone ingrowth, *Journal of Arthroplasty, **14***, 355-368.

[119] **Bauer, T. W. & Schils, J.** (1999). The pathology of total joint arthroplasty i. Mechanisms of implant fixation, *Skeletal Radiology, **28***, 423-432.

[120] **Williams, D. F.** (2008). On the mechanisms of biocompatibility, *Biomaterials, **29***, 2941-2953.

[121] **Narayanan, R., Seshadri, S. K., Kwon, T. Y. & Kim, K. H.** (2008). Calcium phosphate-based coatings on titanium and its alloys, *Journal of Biomedical Materials Research Part B-Applied Biomaterials, **85B***, 279-299.

[122] **De Jonge, L. T., Leeuwenburgh, S. C. G., Wolke, J. G. C. & Jansen, J. A.** (2008). Organic-inorganic surface modifications for titanium implant surfaces, *Pharmaceutical Research, **25***, 2357-2369.

[123] **Vroman, L., Adams, A. L. & Klings, M.** (1971). Interactions among human blood proteins at interfaces, *Federation Proceedings, **30***, 1494-&.

[124] **Hench, L. L.** (1998). Bioactive materials: The potential for tissue regeneration, *Journal of Biomedical Materials Research, **41***, 511-518.

[125] **Hench, L. L.** (1998). Bioceramics, a clinical success, *American Ceramic Society Bulletin, **77***, 67-74.

[126] **Anselme, K., Noel, B. & Hardouin, P.** (1999). Human osteoblast adhesion on titanium alloy, stainless steel, glass and plastic substrates with same surface topography, *Journal of Materials Science-Materials in Medicine, **10***, 815-819.

[127] **Keller, J. C., Collins, J. G., Niederauer, G. G. & Mcgee, T. D.** (1997). In vitro attachment of osteoblast-like cells to osteoceramic materials, *Dental Materials, **13***, 62-68.

[128] **Zinger, O., Anselme, K., Denzer, A., Habersetzer, P., Wieland, M., Jeanfils, J., Hardouin, P. & Landolt, D.** (2004). Time-dependent morphology and adhesion of osteoblastic cells on titanium model surfaces featuring scale-resolved topography, *Biomaterials, **25***, 2695-2711.

[129] **Mrksich, M.** (2000). A surface chemistry approach to studying cell adhesion, *Chemical Society Reviews, **29***, 267-273.

[130] **Taborelli, M., Eng, L., Descouts, P., Ranieri, J. P., Bellamkonda, R. & Aebischer, P.** (1995). Bovine serum-albumin conformation on methyl and amine functionalized surfaces compared by scanning force microscopy, *Journal of Biomedical Materials Research, **29***, 707-714.

[131] **Lenk, T. J., Horbett, T. A., Ratner, B. D. & Chittur, K. K.** (1991). Infrared spectroscopic studies of time-dependent changes in fibrinogen adsorbed to polyurethanes, *Langmuir, 7*, 1755-1764.

[132] **Pitt, W. G. & Cooper, S. L.** (1988). Albumin adsorption on alkyl chain derivatized polyurethanes .1. The effect of c-18 alkylation, *Journal of Biomedical Materials Research, **22***, 359-382.

[133] **Thevenot, P., Hu, W. J. & Tang, L. P.** (2008). Surface chemistry influences implant biocompatibility, *Current Topics in Medicinal Chemistry, **8***, 270-280.

[134] **Vroman, L. & Adams, A. L.** (1969). Effect of heparin on reactions at aminated polymer - blood interfaces, *Journal of Colloid and Interface Science, **31***, 188-&.

[135] **Zucker, M. B. & Vroman, L.** (1969). Platelet adhesion induced by fibrinogen adsorbed onto glass, *Proceedings of the Society for Experimental Biology and Medicine, **131***, 318-&.

[136] **Gergely, C., Bahi, S., Szalontai, B., Flores, H., Schaaf, P., Voegel, J. C. & Cuisinier, F. J. G.** (2004). Human serum albumin self-assembly on weak polyelectrolyte multilayer films structurally modified by ph changes, *Langmuir, **20***, 5575-5582.

[137] **Hanein, D., Geiger, B. & Addadi, L.** (1993). Fibronectin adsorption to surfaces of hydrated crystals - an analysis of the importance of bound water in protein substrate interactions, *Langmuir, **9***, 1058-1065.

[138] **Haynes, C. A., Sliwinsky, E. & Norde, W.** (1994). Structural and electrostatic properties of globular-proteins at a polystyrene water interface, *Journal of Colloid and Interface Science, **164***, 394-409.

[139] **Jager, M., Zilkens, C., Zanger, K. & Krauspe, R.** (2007). Significance of nano- and microtopography for cell-surface interactions in orthopaedic implants, *Journal of Biomedicine and Biotechnology*.

[140] **Howlett, C. R., Evans, M. D. M., Walsh, W. R., Johnson, G. & Steele, J. G.** (1994). Mechanism of initial attachment of cells derived from human bone to commonly used prosthetic materials during cell-culture, *Biomaterials, **15***, 213-222.

[141] **Kilpadi, K. L., Chang, P. L. & Bellis, S. L.** (2001). Hydroxylapatite binds more serum proteins, purified integrins, and osteoblast precursor cells than titanium or steel, *Journal of Biomedical Materials Research, **57***, 258-267.

[142] **Steele, J. G., Dalton, B. A., Johnson, G. & Underwood, P. A.** (1993). Polystyrene chemistry affects vitronectin activity - an explanation for cell attachment to tissue-culture polystyrene but not to unmodified polystyrene, *Journal of Biomedical Materials Research, **27***, 927-940.

[143] **Steele, J. G., Dalton, B. A., Johnson, G. & Underwood, P. A.** (1995). Adsorption of fibronectin and vitronectin onto primaria(tm) and tissue-culture polystyrene and relationship to the mechanism of initial attachment of human vein endothelial-cells and bhk-21 fibroblasts, *Biomaterials, **16***, 1057-1067.

[144] **Sinha, R. K. & Tuan, R. S.** (1996). Regulation of human osteoblast integrin expression by orthopedic implant materials, *Bone, **18***, 451-457.

[145] **Damsky, C. H. & Ilic, D.** (2002). Integrin signaling: It's where the action is, *Current Opinion in Cell Biology, **14***, 594-602.

[146] **Dalton, S. L., Scharf, E., Briesewitz, R., Marcantonio, E. E. & Assoian, R. K.** (1995). Cell-adhesion to extracellular-matrix regulates the life-cycle of integrins, *Molecular Biology of the Cell, **6***, 1781-1791.

[147] **Singer, Ii, Scott, S., Kawka, D. W., Kazazis, D. M., Gailit, J. & Ruoslahti, E.** (1988). Cell-surface distribution of fibronectin and vitronectin receptors depends on substrate composition and extracellular-matrix accumulation, *Journal of Cell Biology, **106***, 2171-2182.

[148] **Bagambisa, F. B., Kappert, H. F. & Schilli, W.** (1994). Cellular and molecular biological events at the implant interface, *Journal of Cranio-Maxillofacial Surgery, **22***, 12-17.

[149] **Schneider, G. & Burridge, K.** (1994). Formation of focal adhesions by osteoblasts adhering to different substrata, *Experimental Cell Research, **214***, 264-269.

[150] **Massia, S. P. & Hubbell, J. A.** (1991). An rgd spacing of 440nm is sufficient for integrin alpha-v-beta-3-mediated fibroblast spreading and 140nm for focal contact and stress fiber formation, *Journal of Cell Biology, **114***, 1089-1100.

[151] **Ranucci, C. S. & Moghe, P. V.** (2001). Substrate microtopography can enhance cell adhesive and migratory responsiveness to matrix ligand density, *Journal of Biomedical Materials Research, **54***, 149-161.

[152] **Grinnell, F.** (1986). Focal adhesion sites and the removal of substratum-bound fibronectin, *Journal of Cell Biology,* ***103***, 2697-2706.

[153] **Dimilla, P. A., Stone, J. A., Quinn, J. A., Albelda, S. M. & Lauffenburger, D. A.** (1993). Maximal migration of human smooth-muscle cells on fibronectin and type-iv collagen occurs at an intermediate attachment strength, *Journal of Cell Biology,* ***122***, 729-737.

[154] **Huttenlocher, A., Ginsberg, M. H. & Horwitz, A. F.** (1996). Modulation of cell migration by integrin-mediated cytoskeletal linkages and ligand-binding affinity, *Journal of Cell Biology,* ***134***, 1551-1562.

[155] **Dee, K. C., Andersen, T. T. & Bizios, R.** (1999). Osteoblast population migration characteristics on substrates modified with immobilized adhesive peptides, *Biomaterials,* ***20***, 221-227.

[156] **Okumura, A., Goto, M., Goto, T., Yoshinari, M., Masuko, S., Katsuki, T. & Tanaka, T.** (2001). Substrate affects the initial attachment and subsequent behavior of human osteoblastic cells (saos-2), *Biomaterials,* ***22***, 2263-2271.

[157] **Ingber, D. E.** (2003). Tensegrity ii. How structural networks influence cellular information processing networks, *Journal of Cell Science,* ***116***, 1397-1408.

[158] **Globus, R. K., Doty, S. B., Lull, J. C., Holmuhamedov, E., Humphries, M. J. & Damsky, C. H.** (1998). Fibronectin is a survival factor for differentiated osteoblasts, *Journal of Cell Science,* ***111***, 1385-1393.

[159] **Altankov, G. & Groth, T.** (1994). Reorganization of substratum-bound fibronectin on hydrophilic and hydrophobic materials is related to biocompatibility, *Journal of Materials Science-Materials in Medicine,* ***5***, 732-737.

[160] **Stephansson, S. N., Byers, B. A. & Garcia, A. J.** (2002). Enhanced expression of the osteoblastic phenotype on substrates that modulate fibronectin conformation and integrin receptor binding, *Biomaterials,* ***23***, 2527-2534.

[161] **Moursi, A. M., Globus, R. K. & Damsky, C. H.** (1997). Interactions between integrin receptors and fibronectin are required for calvarial osteoblast differentiation in vitro, *Journal of Cell Science,* ***110***, 2187-2196.

[162] **Horton, M. A.** (1997). The alpha v beta 3 integrin "vitronectin receptor", *International Journal of Biochemistry & Cell Biology,* ***29***, 721-725.

[163] **Qiu, Q., Sayer, M., Kawaja, M., Shen, X. & Davies, J. E.** (1998). Attachment, morphology, and protein expression of rat marrow stromal cells cultured on charged substrate surfaces, *Journal of Biomedical Materials Research,* ***42***, 117-127.

[164] **Bautista, C. M., Baylink, D. J. & Mohan, S.** (1991). Isolation of a novel insulin-like growth-factor (igf) binding-protein from human bone - a potential candidate for fixing igf-ii in human bone, *Biochemical and Biophysical Research Communications, **176***, 756-763.

[165] **Linkhart, T. A., Mohan, S. & Baylink, D. J.** (1996). Growth factors for bone growth and repair: Igf, tgf beta and bmp, *Bone, **19***, S1-S12.

[166] **Upton, Z., Webb, H., Hale, K., Yandell, C. A., Mcmurtry, J. P., Francis, G. L. & Ballard, F. J.** (1999). Identification of vitronectin as a novel insulin-like growth factor-ii binding protein, *Endocrinology, **140***, 2928-2931.

[167] **Puleo, D. A. & Nanci, A.** (1999). Understanding and controlling the bone-implant interface, *Biomaterials, **20***, 2311-2321.

[168] **Schenk, R. K. & Buser, D.** (1998). Osseointegration: A reality, *Periodontology 2000, **17***, 22-35.

[169] **Branemark, P. I., Adell, R., Albrektsson, T., Lekholm, U., Lundkvist, S. & Rockler, B.** (1983). Osseointegrated titanium fixtures in the treatment of edentulousness, *Biomaterials, **4***, 25-28.

[170] **Joos, U., Wiesmann, H. P., Szuwart, T. & Meyer, U.** (2006). Mineralization at the interface of implants, *International Journal of Oral and Maxillofacial Surgery, **35***, 783-790.

[171] **Cochran, D. L., Schenk, R. K., Lussi, A., Higginbottom, F. L. & Buser, D.** (1998). Bone response to unloaded and loaded titanium implants with a sandblasted and acid-etched surface: A histometric study in the canine mandible, *Journal of Biomedical Materials Research, **40***, 1-11.

[172] **Ericsson, I., Randow, K., Glantz, P. O., Lindhe, J. & Nilner, K.** (1994). Clinical and radiographical features of submerged and nonsubmerged titanium implants, *Clinical Oral Implants Research, **5***, 185-189.

[173] **Hetrick, E. M. & Schoenfisch, M. H.** (2006). Reducing implant-related infections: Active release strategies, *Chemical Society Reviews, **35***, 780-789.

[174] **Arciola, C. R., Alvi, F. I., An, Y. H., Campoccia, D. & Montanaro, L.** (2005). Implant infection and infection resistant materials: A mini review, *International Journal of Artificial Organs, **28***, 1119-1125.

[175] **Darouiche, R. O.** (2003). Antimicrobial approaches for preventing infections associated with surgical implants, *Clinical Infectious Diseases, **36***, 1284-1289.

[176] **Bryers, J. D. & Ratner, B. D.** (2004). Bioinspired implant materials befuddle bacteria, *Asm News, **70***, 232-237.

[177] **Trampuz, A. & Zimmerli, W.** (2006). Antimicrobial agents in orthopaedic surgery - prophylaxis and treatment, *Drugs,* ***66***, 1089-1105.

[178] **Qiu, Y., Zhang, N., An, Y. H. & Wen, X.** (2007). Biomaterial strategies to reduce implant-associated infections, *International Journal of Artificial Organs,* ***30***, 828-841.

[179] **Gristina, A. G.** (1987). Biomaterial-centered infection - microbial adhesion versus tissue integration, *Science,* ***237***, 1588-1595.

[180] **Poelstra, K. A., Barekzi, N. A., Rediske, A. M., Felts, A. G., Slunt, J. B. & Grainger, D. W.** (2002). Prophylactic treatment of gram-positive and gram-negative abdominal implant infections using locally delivered polyclonal antibodies, *Journal of Biomedical Materials Research,* ***60***, 206-215.

[181] **Stewart, P. S. & Costerton, J. W.** (2001). Antibiotic resistance of bacteria in biofilms, *Lancet,* ***358***, 135-138.

[182] **An, Y. H. & Friedman, R. J.** (1996). Prevention of sepsis in total joint arthroplasty, *Journal of Hospital Infection,* ***33***, 93-108.

[183] **Nablo, B. J., Rothrock, A. R. & Schoenfisch, M. H.** (2005). Nitric oxide-releasing sol-gels as antibacterial coatings for orthopedic implants, *Biomaterials,* ***26***, 917-924.

[184] **An, Y. H. & Friedman, R. J.** (1998). Concise review of mechanisms of bacterial adhesion to biomaterial surfaces, *Journal of Biomedical Materials Research,* ***43***, 338-348.

[185] **Bryers, J. D.** (2008). Medical biofilms, *Biotechnology and Bioengineering,* ***100***, 1-18.

[186] **Dunne, W. M.** (2002). Bacterial adhesion: Seen any good biofilms lately?, *Clinical Microbiology Reviews,* ***15***, 155-+.

[187] **Smith, A. W.** (2005). Biofilms and antibiotic therapy: Is there a role for combating bacterial resistance by the use of novel drug delivery systems?, *Advanced Drug Delivery Reviews,* ***57***, 1539-1550.

[188] **Sanderson, P. J.** (1991). Infection in orthopedic implants, *Journal of Hospital Infection,* ***18***, 367-375.

[189] **Lentino, J. R.** (2003). Prosthetic joint infections: Bane of orthopedists, challenge for infectious disease specialists, *Clinical Infectious Diseases,* ***36***, 1157-1161.

[190] **Campoccia, D., Montanaro, L. & Arciola, C. R.** (2006). The significance of infection related to orthopedic devices and issues of antibiotic resistance, *Biomaterials,* ***27***, 2331-2339.

[191] **Foster, T. J.** (2004). The staphylococcus aureus "Superbug", *Journal of Clinical Investigation, **114***, 1693-1696.

[192] **Lowe, A. M., Beattie, D. T. & Deresiewicz, R. L.** (1998). Identification of novel staphylococcal virulence genes by in vivo expression technology, *Molecular Microbiology, **27***, 967-976.

[193] **Gu, J., Li, H., Li, M., Vuong, C., Otto, M., Wen, Y. & Gao, Q.** (2005). Bacterial insertion sequence is256 as a potential molecular marker to discriminate invasive strains from commensal strains of staphylococcus epidermidis, *Journal of Hospital Infection, **61***, 342-348.

[194] **Von Eiff, C., Peters, G. & Heilmann, C.** (2002). Pathogenesis of infections due to coagulase-negative staphylococci, *Lancet Infectious Diseases, **2***, 677-685.

[195] **Socransky, S. S., Haffajee, A. D., Cugini, M. A., Smith, C. & Kent, R. L.** (1998). Microbial complexes in subgingival plaque, *Journal of Clinical Periodontology, **25***, 134-144.

[196] **Socransky, S. S. & Haffajee, A. D.** (2002). Dental biofilms: Difficult therapeutic targets, *Periodontology 2000, **28***, 12-55.

[197] **Anselme, K.** (2000). Osteoblast adhesion on biomaterials, *Biomaterials, **21***, 667-681.

[198] **Albrektsson, T. & Wennerberg, A.** (2004). Oral implant surfaces: Part 1 - review focusing on topographic and chemical properties of different surfaces and in vivo responses to them, *International Journal of Prosthodontics, **17***, 536-543.

[199] **Bagno, A. & Di Bello, C.** (2004). Surface treatments and roughness properties of ti-based biomaterials, *Journal of Materials Science-Materials in Medicine, **15***, 935-949.

[200] **Barbucci, R., Pasqui, D., Wirsen, A., Affrossman, S., Curtis, A. & Tetta, C.** (2003). Micro and nano-structured surfaces, *Journal of Materials Science-Materials in Medicine, **14***, 721-725.

[201] **Guizzardi, S., Galli, C., Martini, D., Belletti, S., Tinti, A., Raspanti, M., Taddei, P., Ruggeri, A. & Scandroglio, R.** (2004). Different titanium surface treatment influences human mandibular osteoblast response, *Journal of Periodontology, **75***, 273-282.

[202] **Anselme, K. & Bigerelle, M.** (2005). Topography effects of pure titanium substrates on human osteoblast long-term adhesion, *Acta Biomaterialia, **1***, 211-222.

[203] **Bigerelle, M., Anselme, K., Noel, B., Ruderman, I., Hardouin, P. & Iost, A.** (2002). Improvement in the morphology of ti-based surfaces: A new

process to increase in vitro human osteoblast response, *Biomaterials,* ***23***, 1563-1577.

[204] **Aparicio, C., Manero, J. M., Conde, F., Pegueroles, M., Planell, J. A., Vallet-Regi, M. & Gil, F. J.** (2007). Acceleration of apatite nucleation on microrough bioactive titanium for bone-replacing implants, *Journal of Biomedical Materials Research Part A,* ***82A***, 521-529.

[205] **Schliephake, H. & Scharnweber, D.** (2008). Chemical and biological functionalization of titanium for dental implants, *Journal of Materials Chemistry,* ***18***, 2404-2414.

[206] **Stanford, C. M.** (2008). Surface modifications of dental implants, *Australian Dental Journal,* ***53***, S26-S33.

[207] **Variola, F., Vetrone, F., Richert, L., Jedrzejowski, P., Yi, J. H., Zalzal, S., Clair, S., Sarkissian, A., Perepichka, D. F., Wuest, J. D., Rosei, F. & Nanci, A.** (2009). Improving biocompatibitity of implantable metals by nanoscale modification of surfaces: An overview of strategies, fabrication methods, and challenges, *Small,* ***5***, 996-1006.

[208] **Lim, J. Y. & Donahue, H. J.** (2007). Cell sensing and response to micro- and nanostructured surfaces produced by chemical and topographic patterning, *Tissue Engineering,* ***13***, 1879-1891.

[209] **Potter, W., Kalil, R. E. & Kao, W. J.** (2008). Biomimetic material systems for neural progenitor cell-based therapy, *Frontiers in Bioscience,* ***13***, 806-821.

[210] **Thapa, A., Miller, D. C., Webster, T. J. & Haberstroh, K. M.** (2003). Nano-structured polymers enhance bladder smooth muscle cell function, *Biomaterials,* ***24***, 2915-2926.

[211] **Ban, S., Iwaya, Y., Kono, H. & Sato, H.** (2006). Surface modification of titanium by etching in concentrated sulfuric acid, *Dental Materials,* ***22***, 1115-1120.

[212] **Sader, M. S., Balduino, A., Soares, G. D. & Borojevic, R.** (2005). Effect of three distinct treatments of titanium surface on osteoblast attachment, proliferation, and differentiation, *Clinical Oral Implants Research,* ***16***, 667-675.

[213] **Takemoto, M., Fujibayashi, S., Neo, M., Suzuki, J., Matsushita, T., Kokubo, T. & Nakamura, T.** (2006). Osteoinductive porous titanium implants: Effect of sodium removal by dilute hcl treatment, *Biomaterials,* ***27***, 2682-2691.

[214] **Macdonald, D. E., Rapuano, B. E., Deo, N., Stranick, M., Somasundaran, P. & Boskey, A. L.** (2004). Thermal and chemical modification of titanium-aluminum-vanadium implant materials: Effects on surface

properties, glycoprotein adsorption, and mg63 cell attachment, *Biomaterials,* ***25***, 3135-3146.

[215] **Vanzillotta, P. S., Sader, M. S., Bastos, I. N. & Soares, G. D.** (2006). Improvement of in vitro titanium bioactivity by three different surface treatments, *Dental Materials,* ***22***, 275-282.

[216] **Chiesa, R., Giavaresi, G., Fini, M., Sandrini, E., Giordano, C., Bianchi, A. & Giardino, R.** (2007). In vitro and in vivo performance of a novel surface treatment to enhance osseointegration of endosseous implants, *Oral Surgery Oral Medicine Oral Pathology Oral Radiology and Endodontology,* ***103***, 745-756.

[217] **Yao, C. & Webster, T. J.** (2006). Anodization: A promising nano-modification technique of titanium implants for orthopedic applications, *Journal of Nanoscience and Nanotechnology,* ***6***, 2682-2692.

[218] **Choi, J. W., Heo, S. J., Koak, J. Y., Kim, S. K., Lim, Y. J., Kim, S. H. & Lee, J. B.** (2006). Biological responses of anodized titanium implants under different current voltages, *Journal of Oral Rehabilitation,* ***33***, 889-897.

[219] **Das, K., Bose, S. & Bandyopadhyay, A.** (2007). Surface modifications and cell-materials interactions with anodized ti, *Acta Biomaterialia,* ***3***, 573-585.

[220] **Sul, Y. T.** (2003). The significance of the surface properties of oxidized titanium to the bone response: Special emphasis on potential biochemical bonding of oxidized titanium implant, *Biomaterials,* ***24***, 3893-3907.

[221] **Oh, S. H., Finones, R. R., Daraio, C., Chen, L. H. & Jin, S. H.** (2005). Growth of nano-scale hydroxyapatite using chemically treated titanium oxide nanotubes, *Biomaterials,* ***26***, 4938-4943.

[222] **Oh, H. J., Lee, J. H., Jeong, Y., Kim, Y. J. & Chi, C. S.** (2005). Microstructural characterization of biomedical titanium oxide film fabricated by electrochemical method, *Surface & Coatings Technology,* ***198***, 247-252.

[223] **Nanci, A., Wuest, J. D., Peru, L., Brunet, P., Sharma, V., Zalzal, S. & Mckee, M. D.** (1998). Chemical modification of titanium surfaces for covalent attachment of biological molecules, *Journal of Biomedical Materials Research,* ***40***, 324-335.

[224] **Yi, J. H., Bernard, C., Variola, F., Zalzal, S. F., Wuest, J. D., Rosei, F. & Nanci, A.** (2006). Characterization of a bioactive nanotextured surface created by controlled chemical oxidation of titanium, *Surface Science,* ***600***, 4613-4621.

[225] **Variola, F., Yi, J. H., Richert, L., Wuest, J. D., Rosei, F. & Nanci, A.** (2008). Tailoring the surface properties of ti6al4v by controlled chemical oxidation, *Biomaterials,* ***29***, 1285-1298.

[226] **Eisenbarth, E., Velten, D. & Breme, J.** (2007). Biomimetic implant coatings, *Biomolecular Engineering,* ***24***, 27-32.

[227] **Popescu, S., Demetrescu, I., Sarantopoulos, C., Gleizes, A. N. & Iordachescu, D.** (2007). The biocompatibility of titanium in a buffer solution: Compared effects of a thin film of tio2 deposited by mocvd and of collagen deposited from a gel, *Journal of Materials Science-Materials in Medicine,* ***18***, 2075-2083.

[228] **Roy, R. K. & Lee, K. R.** (2007). Biomedical applications of diamond-like carbon coatings: A review, *Journal of Biomedical Materials Research Part B-Applied Biomaterials,* ***83B***, 72-84.

[229] **Wang, X. J., Li, Y. C., Lin, J. G., Yamada, Y., Hodgson, P. D. & Wen, C. E.** (2008). In vitro bioactivity evaluation of titanium and niobium metals with different surface morphologies, *Acta Biomaterialia,* ***4***, 1530-1535.

[230] **Eisenbarth, E., Velten, D., Muller, M., Thull, R. & Breme, J.** (2006). Nanostructured niobium oxide coatings influence osteoblast adhesion, *Journal of Biomedical Materials Research Part A,* ***79A***, 166-175.

[231] **Chen, F., Lam, W. M., Lin, C. J., Qiu, G. X., Wu, Z. H., Luk, K. D. K. & Lu, W. W.** (2007). Biocompatibility of electrophoretical deposition of nanostructured hydroxyapatite coating on roughen titanium surface: In vitro evaluation using mesenchymal stem cells, *Journal of Biomedical Materials Research Part B-Applied Biomaterials,* ***82B***, 183-191.

[232] **Siebers, M. C., Walboomers, X. F., Leeuwenburgh, S. C. G., Wolke, J. G. C. & Jansen, J. A.** (2006). The influence of the crystallinity of electrostatic spray deposition-derived coatings on osteoblast-like cell behavior, in vitro, *Journal of Biomedical Materials Research Part A,* ***78A***, 258-267.

[233] **Hanawa, T.** (1999). In vivo metallic biomaterials and surface modification, *Materials Science and Engineering a-Structural Materials Properties Microstructure and Processing,* ***267***, 260-266.

[234] **Duan, K. & Wang, R. Z.** (2006). Surface modifications of bone implants through wet chemistry, *Journal of Materials Chemistry,* ***16***, 2309-2321.

[235] **Massaro, C., Baker, M. A., Cosentino, F., Ramires, P. A., Klose, S. & Milella, E.** (2001). Surface and biological evaluation of hydroxyapatite-based coatings on titanium deposited by different techniques, *Journal of Biomedical Materials Research,* ***58***, 651-657.

[236] **Kurella, A. & Dahotre, N. B.** (2006). Laser induced hierarchical calcium phosphate structures, *Acta Biomaterialia, **2***, 677-683.

[237] **Ward, B. C. & Webster, T. J.** (2007). Increased functions of osteoblasts on nanophase metals, *Materials Science & Engineering C-Biomimetic and Supramolecular Systems, **27***, 575-578.

[238] **Ku, Y., Chung, C. P. & Jang, J. H.** (2005). The effect of the surface modification of titanium using a recombinant fragment of fibronectin and vitronectin on cell behavior, *Biomaterials, **26***, 5153-5157.

[239] **Morra, M.** (2006). Biochemical modification of titanium surfaces: Peptides and ecm proteins, *European Cells & Materials, **12***, 1-15.

[240] **Dee, K. C., Andersen, T. T. & Bizios, R.** (1998). Design and function of novel osteoblast-adhesive peptides for chemical modification of biomaterials, *Journal of Biomedical Materials Research, **40***, 371-377.

[241] **Elmengaard, B., Bechtold, J. E. & Soballe, K.** (2005). In vivo study of the effect of rgd treatment on bone ongrowth on press-fit titanium alloy implants, *Biomaterials, **26***, 3521-3526.

[242] **Lieberman, J. R., Daluiski, A. & Einhorn, T. A.** (2002). The role of growth factors in the repair of bone - biology and clinical applications, *Journal of Bone and Joint Surgery-American Volume, **84A***, 1032-1044.

[243] **Babensee, J. E., Mcintire, L. V. & Mikos, A. G.** (2000). Growth factor delivery for tissue engineering, *Pharmaceutical Research, **17***, 497-504.

[244] **Jennissen, H. P.** (2002) Accelerated and improved osteointegration of implants biocoated with bone morphogenetic protein 2 (bmp-2), in: J. D. Sipe, C. A. Kelley & L. A. Mcnicol (Eds) *Reparative medicine: Growing tissues and organs.* (vol. 961), 139-142.

[245] **Van Den Beucken, J., Walboomers, X. F., Boerman, O. C., Vos, M. R. J., Sommerdijk, N., Hayakawa, T., Fukushima, T., Okahata, Y., Nolte, R. J. M. & Jansen, J. A.** (2006). Functionalization of multilayered DNA-coatings with bone morphogenetic protein 2, *Journal of Controlled Release, **113***, 63-72.

[246] **Van Den Beucken, J., Walboomers, X. F., Nillesen, S. T. M., Vos, M. R. J., Sommerdijk, N., Van Kuppevelt, T. H., Nolte, R. J. M. & Jansen, J. A.** (2007). In vitro and in vivo effects of deoxyribonucleic acid-based coatings funtionalized with vascular endothelial growth factor, *Tissue Engineering, **13***, 711-720.

[247] **De Jonge, L. T., Leeuwenburgh, S. C. G., Van Den Beucken, J., Wolke, J. G. C. & Jansen, J. A.** (2009). Electrosprayed enzyme coatings as bioinspired alternatives to bioceramic coatings for orthopedic and oral implants, *Advanced Functional Materials, **19***, 755-762.

[248] **Ducheyne, P. & Qiu, Q.** (1999). Bioactive ceramics: The effect of surface reactivity on bone formation and bone cell function, *Biomaterials, **20***, 2287-2303.

[249] **Moradian-Oldak, J., Wen, H. B., Schneider, G. B. & Stanford, C. M.** (2006). Tissue engineering strategies for the future generation of dental implants, *Periodontology 2000, **41***, 157-176.

[250] **Du, C., Schneider, G. B., Zaharias, R., Abbott, C., Seabold, D., Stanford, C. & Moradian-Oldak, J.** (2005). Apatite/amelogenin coating on titanium promotes osteogenic gene expression, *Journal of Dental Research, **84***, 1070-1074.

[251] **Wu, P. & Grainger, D. W.** (2006). Drug/device combinations for local drug therapies and infection prophylaxis, *Biomaterials, **27***, 2450-2467.

[252] **Zilberman, M. & Elsner, J. J.** (2008). Antibiotic-eluting medical devices for various applications, *Journal of Controlled Release, **130***, 202-215.

[253] **Trampuz, A. & Widmer, A. F.** (2006). Infections associated with orthopedic implants, *Current Opinion in Infectious Diseases, **19***, 349-356.

[254] **Jagpal, R. & Greco, R. S.** (1979). Studies of a graphite-benzalkonium-oxacillin surface, *American Surgeon, **45***, 774-779.

[255] **Piozzi, A., Francolini, I., Occhiaperti, L., Di Rosa, R., Ruggeri, V. & Donelli, G.** (2004). Polyurethanes loaded with antibiotics: Influence of polymer-antibiotic interactions on in vitro activity against staphylococcus epidermidis, *Journal of Chemotherapy, **16***, 446-452.

[256] **Piozzi, A., Francolini, I., Occhiaperti, L., Venditti, M. & Marconi, W.** (2004). Antimicrobial activity of polyurethanes coated with antibiotics: A new approach to the realization of medical devices exempt from microbial colonization, *International Journal of Pharmaceutics, **280***, 173-183.

[257] **Kwok, C. S., Wan, C. X., Hendricks, S., Bryers, J. D., Horbett, T. A. & Ratner, B. D.** (1999). Design of infection-resistant antibiotic-releasing polymers: I. Fabrication and formulation, *Journal of Controlled Release, **62***, 289-299.

[258] **Kwok, C. S., Horbett, T. A. & Ratner, B. D.** (1999). Design of infection-resistant antibiotic-releasing polymers - ii. Controlled release of antibiotics through a plasma-deposited thin film barrier, *Journal of Controlled Release, **62***, 301-311.

[259] **Liu, S. J., Chi, P. S., Lin, S. S., Ueng, S. W. N., Chan, E. C. & Chen, J. K.** (2007). Novel solvent-free fabrication of biodegradable poly-lactic-glycolic acid (plga) capsules for antibiotics and rhbmp-2 delivery, *International Journal of Pharmaceutics, **330***, 45-53.

[260] **Suzuki, A., Terai, H., Toyoda, H., Namikawa, T., Yokota, Y., Tsunoda, T. & Takaoka, K.** (2006). A biodegradable delivery system for antibiotics and recombinant human bone morphogenetic protein-2: A potential treatment for infected bone defects, *Journal of Orthopaedic Research, **24***, 327-332.

[261] **Price, J. S., Tencer, A. F., Arm, D. M. & Bohach, G. A.** (1996). Controlled release of antibiotics from coated orthopedic implants, *Journal of Biomedical Materials Research, **30***, 281-286.

[262] **Harris, L. G. & Richards, R. G.** (2006). Staphylococci and implant surfaces: A review, *Injury-International Journal of the Care of the Injured, **37***, 3-14.

[263] **Hendriks, J. G. E., Van Horn, J. R., Van Der Mei, H. C. & Busscher, H. J.** (2004). Backgrounds of antibiotic-loaded bone cement and prosthesis-related infection, *Biomaterials, **25***, 545-556.

[264] **Wininger, D. A. & Fass, R. J.** (1996). Antibiotic-impregnated cement and beads for orthopedic infections, *Antimicrobial Agents and Chemotherapy, **40***, 2675-2679.

[265] **Neut, D., Van De Belt, H., Van Horn, J. R., Van Der Mei, H. C. & Busscher, H. J.** (2003). The effect of mixing on gentamicin release from polymethylmethacrylate bone cements, *Acta Orthopaedica Scandinavica, **74***, 670-676.

[266] **Neut, D., Van De Belt, H., Van Horn, J. R., Van Der Mei, H. C. & Busscher, H. J.** (2003). Residual gentamicin-release from antibiotic-loaded polymethylmethacrylate beads after 5 years of implantation, *Biomaterials, **24***, 1829-1831.

[267] **Garvin, K. & Feschuk, C.** (2005). Polylactide-polyglycolide antibiotic implants, *Clinical Orthopaedics and Related Research,* 105-110.

[268] **Gerhart, T. N., Roux, R. D., Hanff, P. A., Horowitz, G. L., Renshaw, A. A. & Hayes, W. C.** (1993). Antibiotic-loaded biodegradable bone-cement for prophylaxis and treatment of experimental osteomyelitis in rats, *Journal of Orthopaedic Research, **11***, 250-255.

[269] **Mclaren, A. C.** (2004). Alternative materials to acrylic bone cement for delivery of depot antibiotics in orthopaedic infections, *Clinical Orthopaedics and Related Research,* 101-106.

[270] **Schnieders, J., Gbureck, U., Thull, R. & Kissel, T.** (2006). Controlled release of gentamicin from calcium phosphate - poly(lactic acid-co-glycolic acid) composite bone cement, *Biomaterials, **27***, 4239-4249.

[271] **Stigter, M., Bezemer, J., De Groot, K. & Layrolle, P.** (2004). Incorporation of different antibiotics into carbonated hydroxyapatite coatings on titanium implants, release and antibiotic efficacy, *Journal of Controlled Release, **99***, 127-137.

[272] **Witte, W.** (1999). Antibiotic resistance in gram-positive bacteria: Epidemiological aspects, *Journal of Antimicrobial Chemotherapy, **44***, 1-9.

[273] **Gold, H. S. & Moellering, R. C.** (1996). Drug therapy - antimicrobial-drug resistance, *New England Journal of Medicine, **335***, 1445-1453.

[274] **Mah, T. F. C. & O'toole, G. A.** (2001). Mechanisms of biofilm resistance to antimicrobial agents, *Trends in Microbiology, **9***, 34-39.

[275] **Stewart, P. S.** (1996). Theoretical aspects of antibiotic diffusion into microbial biofilms, *Antimicrobial Agents and Chemotherapy, **40***, 2517-2522.

[276] **Stewart, P. S.** (1998). A review of experimental measurements of effective diffusive permeabilities and effective diffusion coefficients in biofilms, *Biotechnology and Bioengineering, **59***, 261-272.

[277] **Debeer, D., Stoodley, P., Roe, F. & Lewandowski, Z.** (1994). Effects of biofilm structures on oxygen distribution and mass-transport, *Biotechnology and Bioengineering, **43***, 1131-1138.

[278] **Zhang, T. C. & Bishop, P. L.** (1996). Evaluation of substrate and ph effects in a nitrifying biofilm, *Water Environment Research, **68***, 1107-1115.

[279] **Brooun, A., Liu, S. H. & Lewis, K.** (2000). A dose-response study of antibiotic resistance in pseudomonas aeruginosa biofilms, *Antimicrobial Agents and Chemotherapy, **44***, 640-646.

[280] **Hanssen, A. M., Kjeldsen, G. & Sollid, J. U. E.** (2004). Local variants of staphylococcal cassette chromosome mec in sporadic methicillin-resistant staphylococcus aureus and methicillin-resistant coagulase-negative staphylococci: Evidence of horizontal gene transfer?, *Antimicrobial Agents and Chemotherapy, **48***, 285-296.

[281] **Dejong, E. S., Deberardino, T. M., Brooks, D. E., Nelson, B. J., Campbell, A. A., Bottoni, C. R., Pusateri, A. E., Walton, R. S., Guymon, C. H. & Mcmanus, A. T.** (2001). Antimicrobial efficacy of external fixator pins coated with a lipid stabilized hydroxyapatite/chlorhexidine complex to prevent pin tract infection in a goat model, *Journal of Trauma-Injury Infection and Critical Care, **50***, 1008-1013.

[282] **Harris, L. G., Patterson, L. M., Bacon, C., Ap Gwynn, I. & Richards, R. G.** (2005). Assessment of the cytocompatibility of different coated titanium surfaces to fibroblasts and osteoblasts, *Journal of Biomedical Materials Research Part A, **73A***, 12-20.

[283] **Sampath, L. A., Tambe, S. M. & Modak, S. M.** (2001). In vitro and in vivo efficacy of catheters impregnated with antiseptics or antibiotics: Evaluation of the risk of bacterial resistance to the antimicrobials in the catheters, *Infection Control and Hospital Epidemiology, **22***, 640-646.

[284] **Tambe, S. M., Sampath, L. & Modak, S. M.** (2001). In vitro evaluation of the risk of developing bacterial resistance to antiseptics and antibiotics used in medical devices, *Journal of Antimicrobial Chemotherapy, **47***, 589-598.

[285] **Goldschmidt, P., Cogen, R. & Taubman, S.** (1977). Cytopathologic effects of chlorhexidine on human cells, *Journal of Periodontology, **48***, 212-215.

[286] **Cheung, J. & Oleary, J. J.** (1985). Allergic reaction to chlorhexidine in an anesthetized patient, *Anaesthesia and Intensive Care, **13***, 429-439.

[287] **Ohtoshi, T., Yamauchi, N., Tadokoro, K., Miyachi, S., Suzuki, S., Miyamoto, T. & Muranaka, M.** (1986). Ige antibody-mediated shock reaction caused by topical application of chlorhexidine, *Clinical Allergy, **16***, 155-161.

[288] **Thomas, L., Russell, A. D. & Maillard, J. Y.** (2005). Antimicrobial activity of chlorhexidine diacetate and benzalkonium chloride against pseudomonas aeruginosa and its response to biocide residues, *Journal of Applied Microbiology, **98***, 533-543.

[289] **Gottenbos, B., Van Der Mei, H. C., Klatter, F., Nieuwenhuis, P. & Busscher, H. J.** (2002). In vitro and in vivo antimicrobial activity of covalently coupled quaternary ammonium silane coatings on silicone rubber, *Biomaterials, **23***, 1417-1423.

[290] **Gilbert, P. & Altaae, A.** (1985). Antimicrobial activity of some alkyltrimethylammonium bromides, *Letters in Applied Microbiology, **1***, 101-104.

[291] **Simonetti, N., Simonetti, G., Bougnol, F. & Scalzo, M.** (1992). Electrochemical ag+ for preservative use, *Applied and Environmental Microbiology, **58***, 3834-3836.

[292] **Bosetti, M., Masse, A., Tobin, E. & Cannas, M.** (2002). Silver coated materials for external fixation devices: In vitro biocompatibility and genotoxicity, *Biomaterials, **23***, 887-892.

[293] **Wassall, M. A., Santin, M., Isalberti, C., Cannas, M. & Denyer, S. P.** (1997). Adhesion of bacteria to stainless steel and silver-coated orthopedic external fixation pins, *Journal of Biomedical Materials Research, **36***, 325-330.

[294] **Alt, V., Bechert, T., Steinrucke, P., Wagener, M., Seidel, P., Dingeldein, E., Domann, E. & Schnettler, R.** (2004). An in vitro assessment of the antibacterial properties and cytotoxicity of nanoparticulate silver bone cement, *Biomaterials, **25***, 4383-4391.

[295] **Kraft, C. N., Hansis, M., Arens, S., Menger, M. D. & Vollmar, B.** (2000). Striated muscle microvascular response to silver implants: A

comparative in vivo study with titanium and stainless steel, *Journal of Biomedical Materials Research, **49***, 192-199.

[296] **Wu, J. A., Kusuma, C., Mond, J. J. & Kokai-Kun, J. F.** (2003). Lysostaphin disrupts staphylococcus aureus and staphylococcus epidermidis biofilms on artificial surfaces, *Antimicrobial Agents and Chemotherapy, **47***, 3407-3414.

[297] **Harris, L. G., Tosatti, S., Wieland, M., Textor, M. & Richards, R. G.** (2004). Staphylococcus aureus adhesion to titanium oxide surfaces coated with non-functionalized and peptide-functionalized poly(l-lysine)-grafted-poly(ethylene glycol) copolymers, *Biomaterials, **25***, 4135-4148.

[298] **Harbers, G. M., Emoto, K., Greef, C., Metzger, S. W., Woodward, H. N., Mascali, J. J., Grainger, D. W. & Lochhead, M. J.** (2007). Functionalized poly(ethylene glycol)-based bioassay surface chemistry that facilitates bio-immobilization and inhibits nonspecific protein, bacterial, and mammalian cell adhesion, *Chemistry of Materials, **19***, 4405-4414.

[299] **Chen, H., Brook, M. A., Chen, Y. & Sheardown, H.** (2005). Surface properties of peo-silicone composites: Reducing protein adsorption, *Journal of Biomaterials Science-Polymer Edition, **16***, 531-548.

[300] **Groll, J., Fiedler, J., Engelhard, E., Ameringer, T., Tugulu, S., Klok, H. A., Brenner, R. E. & Moeller, M.** (2005). A novel star peg-derived surface coating for specific cell adhesion, *Journal of Biomedical Materials Research Part A, **74A***, 607-617.

[301] **Dong, B. Y., Manolache, S., Somers, E. B., Wong, A. C. L. & Denes, F. S.** (2005). Generation of antifouling layers on stainless steel surfaces by plasma-enhanced crosslinking of polyethylene glycol, *Journal of Applied Polymer Science, **97***, 485-497.

[302] **Yoo, H. J. & Kim, H. D.** (2004). Properties of crosslinked blends of pellethene and multiblock polyurethane containing poly(ethylene oxide) for biomaterials, *Journal of Applied Polymer Science, **91***, 2348-2357.

[303] **Vandevondele, S., Voros, J. & Hubbell, J. A.** (2003). Rgd-grafted poly-l-lysine-graft-(polyethylene glycol) copolymers block non-specific protein adsorption while promoting cell adhesion, *Biotechnology and Bioengineering, **82***, 784-790.

[304] **Park, K. D., Kim, Y. S., Han, D. K., Kim, Y. H., Lee, E. H. B., Suh, H. & Choi, K. S.** (1998). Bacterial adhesion on peg modified polyurethane surfaces, *Biomaterials, **19***, 851-859.

[305] **Desai, N. P., Hossainy, S. F. A. & Hubbell, J. A.** (1992). Surface-immobilized polyethylene oxide for bacterial repellence, *Biomaterials, **13***, 417-420.

[306] **Tosatti, S., De Paul, S. M., Askendal, A., Vandevondele, S., Hubbell, J. A., Tengvall, P. & Textor, M.** (2003). Peptide functionalized poly(l-lysine)-g-poly(ethylene glycol) on titanium: Resistance to protein adsorption in full heparinized human blood plasma, *Biomaterials, **24***, 4949-4958.

[307] **Giuliani, A., Pirri, G. & Nicoletto, S. F.** (2007). Antimicrobial peptides: An overview of a promising class of therapeutics, *Central European Journal of Biology, **2***, 1-33.

[308] **Brogden, K. A.** (2005). Antimicrobial peptides: Pore formers or metabolic inhibitors in bacteria?, *Nature Reviews Microbiology, **3***, 238-250.

[309] **Zasloff, M.** (2002). Antimicrobial peptides of multicellular organisms, *Nature, **415***, 389-395.

[310] **Marshall, S. H. & Arenas, G.** (2003). Antimicrobial peptides: A natural alternative to chemical antibiotics and a potential for applied biotechnology, *Electronic Journal of Biotechnology, **6***, 271-284.

[311] **Blondelle, S. E. & Houghten, R. A.** (1992). Design of model amphipathic peptides having potent antimicrobial activities, *Biochemistry, **31***, 12688-12694.

[312] **Hancock, R. E. W. & Lehrer, R.** (1998). Cationic peptides: A new source of antibiotics, *Trends in Biotechnology, **16***, 82-88.

[313] **Powers, J. P. S. & Hancock, R. E. W.** (2003). The relationship between peptide structure and antibacterial activity, *Peptides, **24***, 1681-1691.

[314] **Yeaman, M. R. & Yount, N. Y.** (2003). Mechanisms of antimicrobial peptide action and resistance, *Pharmacological Reviews, **55***, 27-55.

[315] **Haynie, S. L., Crum, G. A. & Doele, B. A.** (1995). Antimicrobial activities of amphiphilic peptides covalently bonded to a water-insoluble resin, *Antimicrobial Agents and Chemotherapy, **39***, 301-307.

[316] **Appendini, P. & Hotchkiss, J. H.** (1999). Antimicrobial activity of a 14-residue peptide against escherichia coli o157 : H7, *Journal of Applied Microbiology, **87***, 750-756.

[317] **Appendini, P. & Hotchkiss, J. H.** (2001). Surface modification of poly(styrene) by the attachment of an antimicrobial peptide, *Journal of Applied Polymer Science, **81***, 609-616.

[318] **Etienne, O., Picart, C., Taddei, C., Haikel, Y., Dimarcq, J. L., Schaaf, P., Voegel, J. C., Ogier, J. A. & Egles, C.** (2004). Multilayer polyelectrolyte films functionalized by insertion of defensin: A new approach to protection of implants from bacterial colonization, *Antimicrobial Agents and Chemotherapy, **48***, 3662-3669.

[319] **Kwakman, P. H. S., Velde, A. A. T., Vandenbroucke-Grauls, C. M. J. E., Van Deventer, S. J. H. & Zaat, S. A. J.** (2006). Treatment and prevention of staphylococcus epidermidis experimental biomaterial-associated infection by bactericidal peptide 2, *Antimicrobial Agents and Chemotherapy,* ***50***, 3977-3983.

[320] **Rusmini, F., Zhong, Z. Y. & Feijen, J.** (2007). Protein immobilization strategies for protein biochips, *Biomacromolecules,* ***8***, 1775-1789.

[321] **Norde, W., Macritchie, F., Nowicka, G. & Lyklema, J.** (1986). Protein adsorption at solid liquid interfaces - reversibility and conformation aspects, *Journal of Colloid and Interface Science,* ***112***, 447-456.

[322] **Elwing, H., Welin, S., Askendahl, A. & Lundstrom, I.** (1988). Adsorption of fibrinogen as a measure of the distribution of methyl-groups on silicon surfaces, *Journal of Colloid and Interface Science,* ***123***, 306-308.

[323] **Morrisse.Bw & Stromber.Rr** (1974). Conformation of adsorbed blood proteins by infrared bound fraction measurements, *Journal of Colloid and Interface Science,* ***46***, 152-164.

[324] **Malmsten, M., Emoto, K. & Van Alstine, J. M.** (1998). Effect of chain density on inhibition of protein adsorption by poly(ethylene glycol) based coatings, *Journal of Colloid and Interface Science,* ***202***, 507-517.

[325] **Zhang, M. Q., Desai, T. & Ferrari, M.** (1998). Proteins and cells on peg immobilized silicon surfaces, *Biomaterials,* ***19***, 953-960.

[326] **Burns, N. L., Vanalstine, J. M. & Harris, J. M.** (1995). Poly(ethylene glycol) grafted to quartz - analysis in terms of a site-dissociation model of electroosmotic fluid-flow, *Langmuir,* ***11***, 2768-2776.

[327] **Scouten, W. H., Luong, J. H. T. & Brown, R. S.** (1995). Enzyme or protein immobilization techniques for applications in biosensor design, *Trends in Biotechnology,* ***13***, 178-185.

[328] **Fischer, U., Hempel, U., Becker, D., Bierbaum, S., Scharnweber, D., Worch, H. & Wenzel, K. W.** (2003). Transforming growth factor beta 1 immobilized adsorptively on ti6al4v and collagen type i coated ti6al4v maintains its biological activity, *Biomaterials,* ***24***, 2631-2641.

[329] **Walsh, W. R., Kim, H. D., Jong, Y. S. & Valentini, R. F.** (1995). Controlled-release of platelet-derived growth-factor using ethylene-vinyl acetate copolymer (evac) coated on stainless-steel wires, *Biomaterials,* ***16***, 1319-1325.

[330] **Love, J. C., Estroff, L. A., Kriebel, J. K., Nuzzo, R. G. & Whitesides, G. M.** (2005). Self-assembled monolayers of thiolates on metals as a form of nanotechnology, *Chemical Reviews,* ***105***, 1103-1169.

[331] **Arima, Y. & Iwata, H.** (2007). Effect of wettability and surface functional groups on protein adsorption and cell adhesion using well-defined mixed self-assembled monolayers, *Biomaterials,* ***28***, 3074-3082.

[332] **Faucheux, N., Schweiss, R., Lutzow, K., Werner, C. & Groth, T.** (2004). Self-assembled monolayers with different terminating groups as model substrates for cell adhesion studies, *Biomaterials,* ***25***, 2721-2730.

[333] **Mayer, G. & Sarikaya, M.** (2002). Rigid biological composite materials: Structural examples for biomimetic design, *Experimental Mechanics,* ***42***, 395-403.

[334] **Sakiyama-Elbert, S. E. & Hubbell, J. A.** (2001). Functional biomaterials: Design of novel biomaterials, *Annual Review of Materials Research,* ***31***, 183-201.

[335] **Sarikaya, M.** (1999). Biomimetics: Materials fabrication through biology, *Proceedings of the National Academy of Sciences of the United States of America,* ***96***, 14183-14185.

[336] **Gray, J. J.** (2004). The interaction of proteins with solid surfaces, *Current Opinion in Structural Biology,* ***14***, 110-115.

[337] **Waclawovsky, A. J., Loureiro, M. E., Freitas, R. D., Rocha, C. D., Cano, M. A. O. & Fontes, E. P. B.** (2006). Evidence for the sucrose-binding protein role in carbohydrate metabolism and transport at early developmental stage, *Physiologia Plantarum,* ***128***, 391-404.

[338] **Zhang, S. G.** (2003). Fabrication of novel biomaterials through molecular self-assembly, *Nature Biotechnology,* ***21***, 1171-1178.

[339] **Kriplani, U. & Kay, B. K.** (2005). Selecting peptides for use in nanoscale materials using phagedisplayed combinatorial peptide libraries, *Current Opinion in Biotechnology,* ***16***, 470-475.

[340] **Smith, G. P. & Petrenko, V. A.** (1997). Phage display, *Chemical Reviews,* ***97***, 391-410.

[341] **Lu, Z. J., Murray, K. S., Vancleave, V., Lavallie, E. R., Stahl, M. L. & Mccoy, J. M.** (1995). Expression of thioredoxin random peptide libraries on the escherichia-coli cell-surface as functional fusions to flagellin - a system designed for exploring protein-protein interactions, *Bio-Technology,* ***13***, 366-372.

[342] **Lee, S. Y., Choi, J. H. & Xu, Z. H.** (2003). Microbial cell-surface display, *Trends in Biotechnology,* ***21***, 45-52.

[343] **Brown, S., Sarikaya, M. & Johnson, E.** (2000). A genetic analysis of crystal growth, *Journal of Molecular Biology,* ***299***, 725-735.

[344] **Wittrup, K. D.** (2001). Protein engineering by cell-surface display, *Current Opinion in Biotechnology, **12***, 395-399.

[345] **Smith, G. P.** (1985). Filamentous fusion phage - novel expression vectors that display cloned antigens on the virion surface, *Science, **228***, 1315-1317.

[346] **Khatayevich, D., Gungormus, M., Yazici, H., So, C., Cetinel, S., Ma, H., Jen, A., Tamerler, C. & Sarikaya, M.** Biofunctionalization of materials for implants using engineered peptides, *Acta Biomaterialia, **6***, 4634-4641.

[347] **Tamerler, C. & Sarikaya, M.** (2007). Molecular biomimetics: Utilizing naturels molecular ways in practical engineering, *Acta Biomaterialia, **3***, 289-299.

[348] **Tamerler, C. & Sarikaya, M.** (2008). Molecular biomimetics: Genetic synthesis, assembly, and formation of materials using peptides, *Mrs Bulletin, **33***, 504-510.

[349] **Tamerler, C. & Sarikaya, M.** (2009). Molecular biomimetics: Nanotechnology and bionanotechnology using genetically engineered peptides, *Philosophical Transactions of the Royal Society a-Mathematical Physical and Engineering Sciences, **367***, 1705-1726.

[350] **Brown, S.** (1992). Engineered iron oxide-adhesion mutants of the escherichia-coli phage-lambda receptor, *Proceedings of the National Academy of Sciences of the United States of America, **89***, 8651-8655.

[351] **Whaley, S. R., English, D. S., Hu, E. L., Barbara, P. F. & Belcher, A. M.** (2000). Selection of peptides with semiconductor binding specificity for directed nanocrystal assembly, *Nature, **405***, 665-668.

[352] **Huang, Y., Chiang, C. Y., Lee, S. K., Gao, Y., Hu, E. L., De Yoreo, J. & Belcher, A. M.** (2005). Programmable assembly of nanoarchitectures using genetically engineered viruses, *Nano Letters, **5***, 1429-1434.

[353] **Brown, S.** (1997). Metal-recognition by repeating polypeptides, *Nature Biotechnology, **15***, 269-272.

[354] **Hnilova, M., Oren, E. E., Seker, U. O. S., Wilson, B. R., Collino, S., Evans, J. S., Tamerler, C. & Sarikaya, M.** (2008). Effect of molecular conformations on the adsorption behavior of gold-binding peptides, *Langmuir, **24***, 12440-12445.

[355] **Slocik, J. M., Stone, M. O. & Naik, R. R.** (2005). Synthesis of gold nanoparticles using multifunctional peptides, *Small, **1***, 1048-1052.

[356] **Seker, U. O. S., Wilson, B., Dincer, S., Kim, I. W., Oren, E. E., Evans, J. S., Tamerler, C. & Sarikaya, M.** (2007). Adsorption behavior of linear and cyclic genetically engineered platinum binding peptides, *Langmuir, **23***, 7895-7900.

[357] **Naik, R. R., Stringer, S. J., Agarwal, G., Jones, S. E. & Stone, M. O.** (2002). Biomimetic synthesis and patterning of silver nanoparticles, *Nature Materials, **1***, 169-172.

[358] **Naik, R. R., Brott, L. L., Clarson, S. J. & Stone, M. O.** (2002). Silica-precipitating peptides isolated from a combinatorial phage display peptide library, *Journal of Nanoscience and Nanotechnology, **2***, 95-100.

[359] **Chen, H. B., Su, X. D., Neoh, K. G. & Choe, W. S.** (2006). Qcm-d analysis of binding mechanism of phage particles displaying a constrained heptapeptide with specific affinity to sio2 and tio2, *Analytical Chemistry, **78***, 4872-4879.

[360] **Oren, E. E., Tamerler, C., Sahin, D., Hnilova, M., Seker, U. O. S., Sarikaya, M. & Samudrala, R.** (2007). A novel knowledge-based approach to design inorganic-binding peptides, *Bioinformatics, **23***, 2816-2822.

[361] **Thai, C. K., Dai, H. X., Sastry, M. S. R., Sarikaya, M., Schwartz, D. T. & Baneyx, F.** (2004). Identification and characterization of cu2o- and zno-binding polypeptides by escherichia coli cell surface display: Toward an understanding of metal oxide binding, *Biotechnology and Bioengineering, **87***, 129-137.

[362] **Sano, K. I., Sasaki, H. & Shiba, K.** (2005). Specificity and biomineralization activities of ti-binding peptide-1 (tbp-1), *Langmuir, **21***, 3090-3095.

[363] **Umetsu, M., Mizuta, M., Tsumoto, K., Ohara, S., Takami, S., Watanabe, H., Kumagai, I. & Adschiri, T.** (2005). Bioassisted room-temperature immobilization and mineralization of zinc oxide - the structural ordering of zno nanoparticles into a flower-type morphology, *Advanced Materials, **17***, 2571-+.

[364] **Liu, Y., Mao, J., Zhou, B., Wei, W. & Gong, S. Q.** Peptide aptamers against titanium-based implants identified through phage display, *Journal of Materials Science-Materials in Medicine, **21***, 1103-1107.

[365] **Lee, S. W., Mao, C. B., Flynn, C. E. & Belcher, A. M.** (2002). Ordering of quantum dots using genetically engineered viruses, *Science, **296***, 892-895.

[366] **Flynn, C. E., Mao, C. B., Hayhurst, A., Williams, J. L., Georgiou, G., Iverson, B. & Belcher, A. M.** (2003). Synthesis and organization of nanoscale ii-vi semiconductor materials using evolved peptide specificity and viral capsid assembly, *Journal of Materials Chemistry, **13***, 2414-2421.

[367] **Gungormus, M., Fong, H., Kim, I. W., Evans, J. S., Tamerler, C. & Sarikaya, M.** (2008). Regulation of in vitro calcium phosphate mineralization by combinatorially selected hydroxyapatite-binding peptides, *Biomacromolecules, **9***, 966-973.

[368] **Donatan, S., Yazici, H., Bermek, H., Sarikaya, M., Tamerler, C. & Urgen, M.** (2009). Physical elution in phage display selection of inorganic-binding peptides, *Materials Science & Engineering C-Biomimetic and Supramolecular Systems,* ***29***, 14-19.

[369] **Krauland, E. M., Peelle, B. R., Wittrup, K. D. & Belcher, A. M.** (2007). Peptide tags for enhanced cellular and protein adhesion to single-crystal line sapphire, *Biotechnology and Bioengineering,* ***97***, 1009-1020.

[370] **Gaskin, D. J. H., Starck, K. & Vulfson, E. N.** (2000). Identification of inorganic crystal-specific sequences using phage display combinatorial library of short peptides: A feasibility study, *Biotechnology Letters,* ***22***, 1211-1216.

[371] **Sanghvi, A. B., Miller, K. P. H., Belcher, A. M. & Schmidt, C. E.** (2005). Biomaterials functionalization using a novel peptide that selectively binds to a conducting polymer, *Nature Materials,* ***4***, 496-502.

[372] **Nygaard, S., Wendelbo, R. & Brown, S.** (2002). Surface-specific zeolite-binding proteins, *Advanced Materials,* ***14***, 1853-1856.

[373] **Wang, S. Q., Humphreys, E. S., Chung, S. Y., Delduco, D. F., Lustig, S. R., Wang, H., Parker, K. N., Rizzo, N. W., Subramoney, S., Chiang, Y. M. & Jagota, A.** (2003). Peptides with selective affinity for carbon nanotubes, *Nature Materials,* ***2***, 196-200.

[374] **Baneyx, F. & Schwartz, D. T.** (2007). Selection and analysis of solid-binding peptides, *Current Opinion in Biotechnology,* ***18***, 312-317.

[375] **Tamerler, C. & Sarikaya, M.** (2009). Genetically designed peptide-based molecular materials, *Acs Nano,* ***3***, 1606-1615.

[376] **Tamerler, C., Oren, E. E., Duman, M., Venkatasubramanian, E. & Sarikaya, M.** (2006). Adsorption kinetics of an engineered gold binding peptide by surface plasmon resonance spectroscopy and a quartz crystal microbalance, *Langmuir,* ***22***, 7712-7718.

[377] **Tamerler, C., Duman, M., Oren, E. E., Gungormus, M., Xiong, X. R., Kacar, T., Parviz, B. A. & Sarikaya, M.** (2006). Materials specificity and directed assembly of a gold-binding peptide, *Small,* ***2***, 1372-1378.

[378] **Oren, E. E., Tamerler, C. & Sarikaya, M.** (2005). Metal recognition of septapeptides via polypod molecular architecture, *Nano Letters,* ***5***, 415-419.

[379] **Chen, H. B., Su, X. D., Neoh, K. G. & Choe, W. S.** (2009). Context-dependent adsorption behavior of cyclic and linear peptides on metal oxide surfaces, *Langmuir,* ***25***, 1588-1593.

[380] **Sano, K. I. & Shiba, K.** (2003). A hexapeptide motif that electrostatically binds to the surface of titanium, *Journal of the American Chemical Society, **125***, 14234-14235.

[381] **Chen, H. B., Su, X. D., Neoh, K. G. & Choe, W. S.** (2008). Probing the interaction between peptides and metal oxides using point mutants of a tio2-binding peptide, *Langmuir, **24***, 6852-6857.

[382] **Seker, U. O. S., Wilson, B., Sahin, D., Tamerler, C. & Sarikaya, M.** (2009). Quantitative affinity of genetically engineered repeating polypeptides to inorganic surfaces, *Biomacromolecules, **10***, 250-257.

[383] **Evans, J. S., Samudrala, R., Walsh, T. R., Oren, E. E. & Tamerler, C.** (2008). Molecular design of inorganic-binding polypeptides, *Mrs Bulletin, **33***, 514-518.

[384] **Addadi, L. & Weiner, S.** (1985). Interactions between acidic proteins and crystals - stereochemical requirements in biomineralization, *Proceedings of the National Academy of Sciences of the United States of America, **82***, 4110-4114.

[385] **Mann, S.** (1988). Molecular recognition in biomineralization, *Nature, **332***, 119-124.

[386] **Paine, M. L. & Snead, M. L.** (1997). Protein interactions during assembly of the enamel organic extracellular matrix, *Journal of Bone and Mineral Research, **12***, 221-227.

[387] **Attwood, T. K.** (2000). Genomics - the babel of bioinformatics, *Science, **290***, 471-473.

[388] **Needlema.Sb & Wunsch, C. D.** (1970). A general method applicable to search for similarities in amino acid sequence of 2 proteins, *Journal of Molecular Biology, **48***, 443-&.

[389] **Smith, T. F. & Waterman, M. S.** (1981). Identification of common molecular subsequences, *Journal of Molecular Biology, **147***, 195-197.

[390] **Henikoff, S. & Henikoff, J. G.** (1992). Amino-acid substitution matrices from protein blocks, *Proceedings of the National Academy of Sciences of the United States of America, **89***, 10915-10919.

[391] **Suzuki, N., Gamble, L., Tamerler, C., Sarikaya, M., Castner, D. G. & Ohuchi, F. S.** (2007). Adsorption of genetically engineered proteins studied by time-of-flight secondary ion mass spectrometry (tof-sims). Part a: Data acquisition and principal component analysis (pica), *Surface and Interface Analysis, **39***, 419-426.

[392] **Suzuki, N., Sarikaya, M. & Ohuchi, F. S.** (2007). Adsorption of genetically engineered proteins studied by time-of-flight secondary ion mass spectrometry (tof-sims). Part b: Hierarchical cluster analysis (hca), *Surface and Interface Analysis, **39***, 427-433.

[393] **Kulp, J. L., Sarikaya, M. & Evans, J. S.** (2004). Molecular characterization of a prokaryotic polypeptide sequence that catalyzes au crystal formation, *Journal of Materials Chemistry,* ***14***, 2325-2332.

[394] **Braun, R., Sarikaya, M. & Schulten, K.** (2002). Genetically engineered gold-binding polypeptides: Structure prediction and molecular dynamics, *Journal of Biomaterials Science-Polymer Edition,* ***13***, 747-757.

[395] **Kantarci, N., Tamerler, C., Sarikaya, M., Haliloglu, T. & Doruker, P.** (2005). Molecular dynamics simulations on constraint metal binding peptides, *Polymer,* ***46***, 4307-4313.

[396] **Notman, R. & Walsh, T. R.** (2009). Molecular dynamics studies of the interactions of water and amino acid analogues with quartz surfaces, *Langmuir,* ***25***, 1638-1644.

[397] **So, C. R., Kulp, J. L., Oren, E. E., Zareie, H., Tamerler, C., Evans, J. S. & Sarikaya, M.** (2009). Molecular recognition and supramolecular self-assembly of a genetically engineered gold binding peptide on au{111}, *Acs Nano,* ***3***, 1525-1531.

[398] **Dickerson, M. B., Sandhage, K. H. & Naik, R. R.** (2008). Protein- and peptide-directed syntheses of inorganic materials, *Chemical Reviews,* ***108***, 4935-4978.

[399] **Crookes-Goodson, W. J., Slocik, J. M. & Naik, R. R.** (2008). Bio-directed synthesis and assembly of nanomaterials, *Chemical Society Reviews,* ***37***, 2403-2412.

[400] **Shiba, K.** Exploitation of peptide motif sequences and their use in nanobiotechnology, *Current Opinion in Biotechnology,* ***21***, 412-425.

[401] **Kacar, T., Ray, J., Gungormus, M., Oren, E. E., Tamerler, C. & Sarikaya, M.** (2009). Quartz binding peptides as molecular linkers towards fabricating multifunctional micropatterned substrates, *Advanced Materials,* ***21***, 295-299.

[402] **Ma, H., Zin, M. T., Zareie, M. H., Kang, M. S., Kang, S. H., Kim, K. S., Reed, B. W., Behar, C. T., Sarikaya, M. & Jen, A. K. Y.** (2007). Assembly of nanomaterials through highly ordered self-assembled monolayers and peptide-organic hybrid conjugates as templates, *Journal of Nanoscience and Nanotechnology,* ***7***, 2549-2566.

[403] **Zin, M. T., Munro, A. M., Gungormus, M., Wong, N. Y., Ma, H., Tamerler, C., Ginger, D. S., Sarikaya, M. & Jen, A. K. Y.** (2007). Peptide-mediated surface-immobilized quantum dot hybrid nanoassemblies with controlled photoluminescence, *Journal of Materials Chemistry,* ***17***, 866-872.

[404] **Zin, M. T., Ma, H., Sarikaya, M. & Jen, A. K. Y.** (2005). Assembly of gold nanoparticles using genetically engineered polypeptides, *Small,* ***1***, 698-702.

[405] **Wei, J. H., Kacar, T., Tamerler, C., Sarikaya, M. & Ginger, D. S.** (2009). Nanopatterning peptides as bifunctional inks for templated assembly, *Small,* ***5***, 689-693.

[406] **Nochomovitz, R., Amit, M., Matmor, M. & Ashkenasy, N.** Bioassisted multi-nanoparticle patterning using single-layer peptide templates, *Nanotechnology,* ***21***.

[407] **Kashiwagi, K., Tsuji, T. & Shiba, K.** (2009). Directional bmp-2 for functionalization of titanium surfaces, *Biomaterials,* ***30***, 1166-1175.

[408] **Meyers, S. R., Hamilton, P. T., Walsh, E. B., Kenan, D. J. & Grinstaff, M. W.** (2007). Endothelialization of titanium surfaces, *Advanced Materials,* ***19***, 2492-+.

[409] **Yoshinari, M., Kato, T., Matsuzaka, K., Hayakawa, T. & Shiba, K.** Prevention of biofilm formation on titanium surfaces modified with conjugated molecules comprised of antimicrobial and titanium-binding peptides, *Biofouling,* ***26***, 103-110.

[410] **Tsuji, T., Onuma, K., Yamamoto, A., Iijima, M. & Shiba, K.** (2008). Direct transformation from amorphous to crystalline calcium phosphate facilitated by motif-programmed artificial proteins, *Proceedings of the National Academy of Sciences of the United States of America,* ***105***, 16866-16870.

[411] **Fang, Y., Poulsen, N., Dickerson, M. B., Cai, Y., Jones, S. E., Naik, R. R., Kroger, N. & Sandhage, K. H.** (2008). Identification of peptides capable of inducing the formation of titania but not silica via a subtractive bacteriophage display approach, *Journal of Materials Chemistry,* ***18***, 3871-3875.

[412] **Sano, K. I. & Shiba, K.** (2008). In aqua manufacturing of a three-dimensional nanostructure using a peptide aptamer, *Mrs Bulletin,* ***33***, 524-529.

[413] **Naik, R. R., Jones, S. E., Murray, C. J., Mcauliffe, J. C., Vaia, R. A. & Stone, M. O.** (2004). Peptide templates for nanoparticle synthesis derived from polymerase chain reaction-driven phage display, *Advanced Functional Materials,* ***14***, 25-30.

[414] **Kacar, T., Zin, M. T., So, C., Wilson, B., Ma, H., Gul-Karaguler, N., Jen, A. K. Y., Sarikaya, M. & Tamerler, C.** (2009). Directed self-immobilization of alkaline phosphatase on micro-patterned substrates via genetically fused metal-binding peptide, *Biotechnology and Bioengineering,* ***103***, 696-705.

[415] **Hayashi, T., Sano, K. I., Shiba, K., Iwahori, K., Yamashita, I. & Hara, M.** (2009). Critical amino acid residues for the specific binding of the ti-recognizing recombinant ferritin with oxide surfaces of titanium and silicon, *Langmuir,* ***25***, 10901-10906.

[416] **Sengupta, A., Thai, C. K., Sastry, M. S. R., Matthaei, J. F., Schwartz, D. T., Davis, E. J. & Baneyx, F.** (2008). A genetic approach for controlling the binding and orientation of proteins on nanoparticles, *Langmuir, **24***, 2000-2008.

[417] **Drexler, K. E.** (1994). Molecular nanomachines - physical principles and implementation strategies, *Annual Review of Biophysics and Biomolecular Structure, **23***, 377-405.

[418] **Ryu, D. D. Y. & Nam, D. H.** (2000). Recent progress in biomolecular engineering, *Biotechnology Progress, **16***, 2-16.

[419] **Ajikumar, P. K., Vivekanandan, S., Lakshminarayanan, R., Jois, S. D. S., Kini, R. M. & Valiyaveettil, S.** (2005). Mimicking the function of eggshell matrix proteins: The role of multiplets of charged amino acid residues and self-assembly of peptides in biomineralization, *Angewandte Chemie-International Edition, **44***, 5476-5479.

[420] **Sugawara, A., Nishimura, T., Yamamoto, Y., Inoue, H., Nagasawa, H. & Kato, T.** (2006). Self-organization of oriented calcium carbonate/polymer composites: Effects of a matrix peptide isolated from the exoskeleton of a crayfish, *Angewandte Chemie-International Edition, **45***, 2876-2879.

[421] **He, G., Dahl, T., Veis, A. & George, A.** (2003). Nucleation of apatite crystals in vitro by self-assembled dentin matrix protein, 1, *Nature Materials, **2***, 552-558.

[422] **Meyers, S. R., Khoo, X. J., Huang, X., Walsh, E. B., Grinstaff, M. W. & Kenan, D. J.** (2009). The development of peptide-based interfacial biomaterials for generating biological functionality on the surface of bioinert materials, *Biomaterials, **30***, 277-286.

[423] **Reed, J. & Reed, T. A.** (1997). A set of constructed type spectra for the practical estimation of peptide secondary structure from circular dichroism, *Analytical Biochemistry, **254***, 36-40.

[424] **Cubellis, M. V., Caillez, F., Blundell, T. L. & Lovell, S. C.** (2005). Properties of polyproline ii, a secondary structure element implicated in protein-protein interactions, *Proteins-Structure Function and Bioinformatics, **58***, 880-892.

[425] **Mackerell, A. D., Bashford, D., Bellott, M., Dunbrack, R. L., Evanseck, J. D., Field, M. J., Fischer, S., Gao, J., Guo, H., Ha, S., Joseph-Mccarthy, D., Kuchnir, L., Kuczera, K., Lau, F. T. K., Mattos, C., Michnick, S., Ngo, T., Nguyen, D. T., Prodhom, B., Reiher, W. E., Roux, B., Schlenkrich, M., Smith, J. C., Stote, R., Straub, J., Watanabe, M., Wiorkiewicz-Kuczera, J., Yin, D. & Karplus, M.** (1998). All-atom empirical potential for molecular modeling and dynamics studies of proteins, *Journal of Physical Chemistry B, **102***, 3586-3616.

[426] **Ahmad, M., Gawronski, D., Blum, J., Goldberg, J. & Gronowicz, G.** (1999). Differential response of human osteoblast-like cells to commercially pure (cp) titanium grades 1 and 4, *Journal of Biomedical Materials Research,* ***46***, 121-131.

[427] **Evans, J. S.** (2008). "Tuning in" To mollusk shell nacre- and prismatic-associated protein terminal sequences. Implications for biomineralization and the construction of high performance inorganic-organic composites, *Chemical Reviews,* ***108***, 4455-4462.

[428] **Amos, F. F. & Evans, J. S.** (2009). Ap7, a partially disordered pseudo c-ring protein, is capable of forming stabilized aragonite in vitro, *Biochemistry,* ***48***, 1332-1339.

[429] **Delak, K., Giocondi, J., Orme, C. & Evans, J. S.** (2008). Modulation of crystal growth by the terminal sequences of the prismatic-associated asprich protein, *Crystal Growth & Design,* ***8***, 4481-4486.

[430] **Xu, G. Z. & Evans, J. S.** (1999). Model peptide studies of sequence repeats derived from the intracrystalline biomineralization protein, sm50. I. Gvggr and gmggq repeats, *Biopolymers,* ***49***, 303-312.

[431] **Wustman, B. A., Santos, R., Zhang, B. & Evans, J. S.** (2002). Identification of a "Glycine-loop"-like coiled structure in the 34 aa pro,gly,met repeat domain of the biomineral-associated protein, pm27, *Biopolymers,* ***65***, 362-372.

[432] **Delak, K., Harcup, C., Lakshminarayanan, R., Sun, Z., Fan, Y. W., Moradian-Oldak, J. & Evans, J. S.** (2009). The tooth enamel protein, porcine amelogenin, is an intrinsically disordered protein with an extended molecular configuration in the monomeric form, *Biochemistry,* ***48***, 2272-2281.

[433] **Kokubo, T., Kim, H. M. & Kawashita, M.** (2003). Novel bioactive materials with different mechanical properties, *Biomaterials,* ***24***, 2161-2175.

[434] **Suchanek, W. & Yoshimura, M.** (1998). Processing and properties of hydroxyapatite-based biomaterials for use as hard tissue replacement implants, *Journal of Materials Research,* ***13***, 94-117.

[435] **Hanawa, T. & Ota, M.** (1991). Calcium-phosphate naturally formed on titanium in electrolyte solution, *Biomaterials,* ***12***, 767-774.

[436] **Jonasova, L., Muller, F. A., Helebrant, A., Strnad, J. & Greil, P.** (2004). Biomimetic apatite formation on chemically treated titanium, *Biomaterials,* ***25***, 1187-1194.

[437] **Okido, M., Nishikawa, K., Kuroda, K., Ichino, R., Zhao, Z. W. & Takai, O.** (2002). Evaluation of the hydroxyapatite film coating on titanium cathode by qcm, *Materials Transactions,* ***43***, 3010-3014.

[438] **Liu, D. M., Yang, Q. Z. & Troczynski, T.** (2002). Sol-gel hydroxyapatite coatings on stainless steel substrates, *Biomaterials, **23***, 691-698.

[439] **Ding, S. J., Ju, C. P. & Lin, J. H. C.** (2000). Morphology and immersion behavior of plasma-sprayed hydroxyapatite/bioactive glass coatings, *Journal of Materials Science-Materials in Medicine, **11***, 183-190.

[440] **Nie, X., Leyland, A. & Matthews, A.** (2000). Deposition of layered bioceramic hydroxyapatite/tio2 coatings on titanium alloys using a hybrid technique of micro-arc oxidation and electrophoresis, *Surface & Coatings Technology, **125***, 407-414.

[441] **Tarasevich, B. J., Howard, C. J., Larson, J. L., Snead, M. L., Simmer, J. P., Paine, M. & Shaw, W. J.** (2007). The nucleation and growth of calcium phosphate by amelogenin, *Journal of Crystal Growth, **304***, 407-415.

[442] **Moradian-Oldak, J.** (2001). Amelogenins: Assembly, processing and control of crystal morphology, *Matrix Biology, **20***, 293-305.

[443] **Doi, Y., Eanes, E. D., Shimokawa, H. & Termine, J. D.** (1984). Inhibition of seeded growth of enamel apatite crystals by amelogenin and enamelin proteins invitro, *Journal of Dental Research, **63***, 98-105.

[444] **Fincham, A. G., Moradian-Oldak, J. & Simmer, J. P.** (1999). The structural biology of the developing dental enamel matrix, *Journal of Structural Biology, **126***, 270-299.

[445] **Hammarstrom, L.** (1997). Enamel matrix, cementum development and regeneration, *Journal of Clinical Periodontology, **24***, 658-668.

[446] **Paine, M. L., Luo, W., Zhu, D. H., Bringas, P. & Snead, M. L.** (2003). Functional domains for amelogenin revealed by compound genetic defects, *Journal of Bone and Mineral Research, **18***, 466-472.

[447] **Snead, M. L.** (2003). Amelogenin protein exhibits a modular design: Implications for form and function, *Connective Tissue Research, **44***, 47-51.

[448] **Gungormus, M., Oren, E. E., Horst, J. A., Fong, H., Hnilova, M., Somerman, M. J., Snead, M. L., Samudrala, R., Tamerler, C. & Sarikaya, M.** Cementomimetics-constructing a cementum-like biomineralized microlayer via amelogenin-derived peptides, *International Journal of Oral Science, **4***, 69-77.

[449] **Beniash, E., Simmer, J. P. & Margolis, H. C.** (2005). The effect of recombinant mouse amelogenins on the formation and organization of hydroxyapatite crystals in vitro, *Journal of Structural Biology, **149***, 182-190.

[450] **Sano, K. I. & Shiba, K.** (2008). Stepwise accumulation of layers of aptamer-ornamented ferritins using biomimetic layer-by-layer, *Journal of Materials Research, **23***, 3236-3240.

[451] **Mao, C. B., Solis, D. J., Reiss, B. D., Kottmann, S. T., Sweeney, R. Y., Hayhurst, A., Georgiou, G., Iverson, B. & Belcher, A. M.** (2004). Virus-based toolkit for the directed synthesis of magnetic and semiconducting nanowires, *Science, **303***, 213-217.

[452] **Lee, Y. J., Yi, H., Kim, W. J., Kang, K., Yun, D. S., Strano, M. S., Ceder, G. & Belcher, A. M.** (2009). Fabricating genetically engineered high-power lithium-ion batteries using multiple virus genes, *Science, **324***, 1051-1055.

[453] **Kramer, R. M., Li, C., Carter, D. C., Stone, M. O. & Naik, R. R.** (2004). Engineered protein cages for nanomaterial synthesis, *Journal of the American Chemical Society, **126***, 13282-13286.

APPENDICES

APPENDIX A1: MALDI/TOF spectrum of synthesized peptides (TiBP1, TiBP2, TiBP60, TiBP1-GGG-RGDS, TiBP2-GGG-RGDS, RGDS, TiBP1-GGG-AMP, TiBP2-GGG-AMP, AMP, TiBP2-GGG-ADP5, TiBP2-GGG- ADP7, ADP5, ADP7)

APPENDIX A1

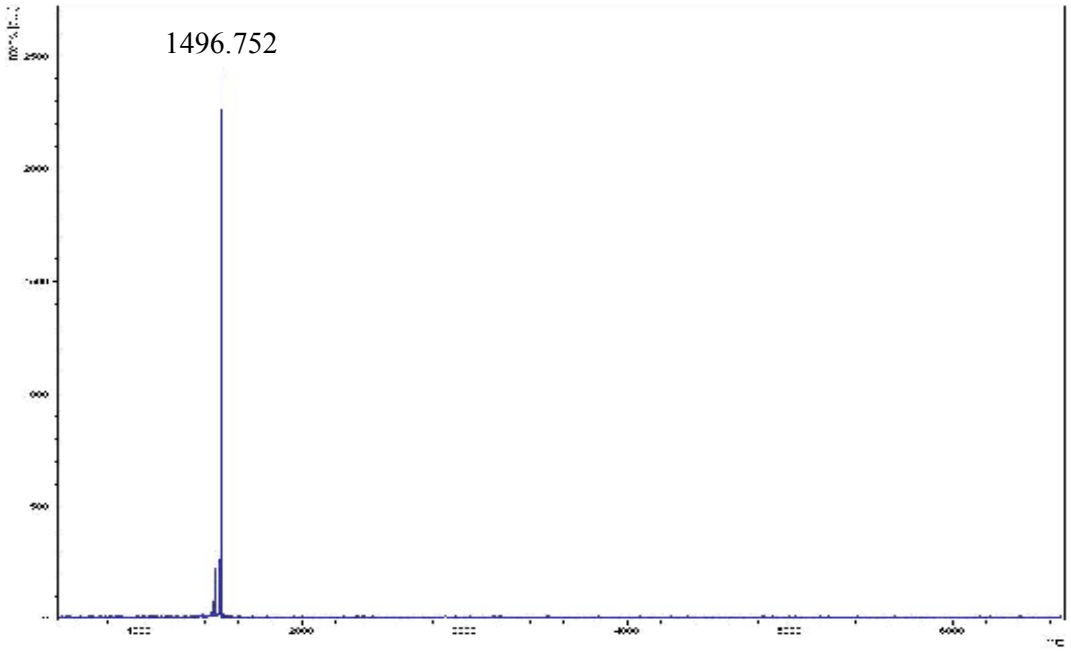

Figure A.1: The MALDI/TOF spectrum of synthesized TiBP1

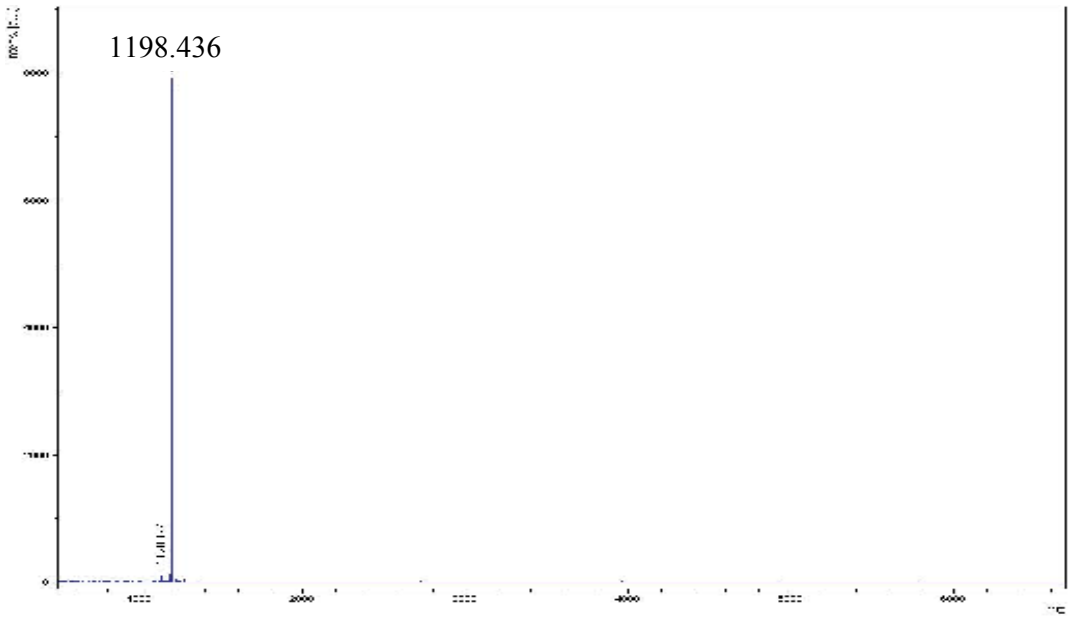

Figure A.2: The MALDI/TOF spectrum of synthesized TiBP2

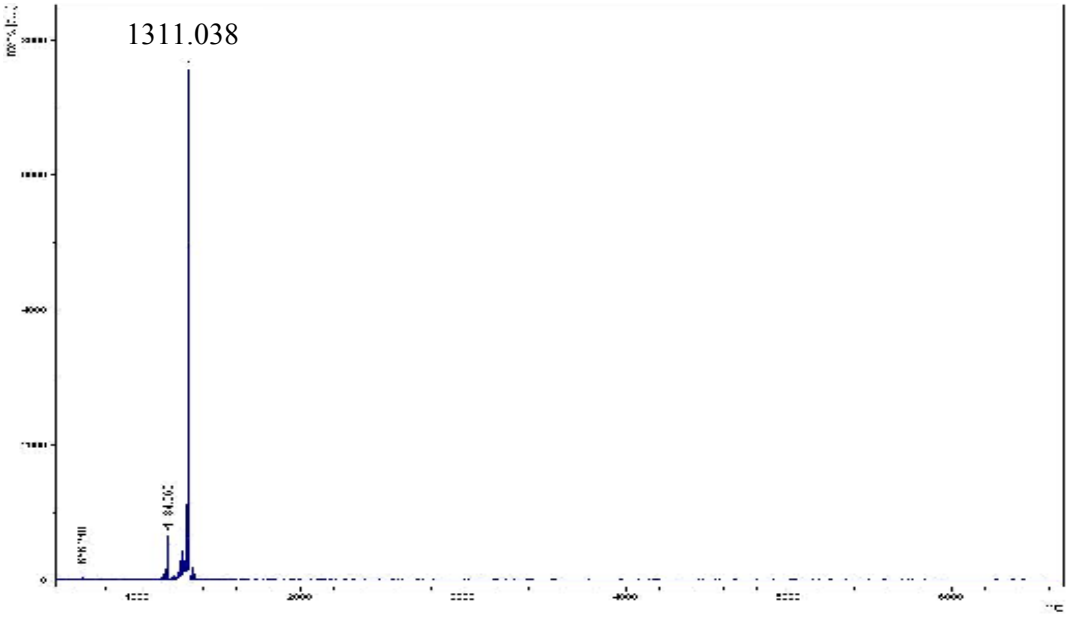

Figure A.3: The MALDI/TOF spectrum of synthesized TiBP60

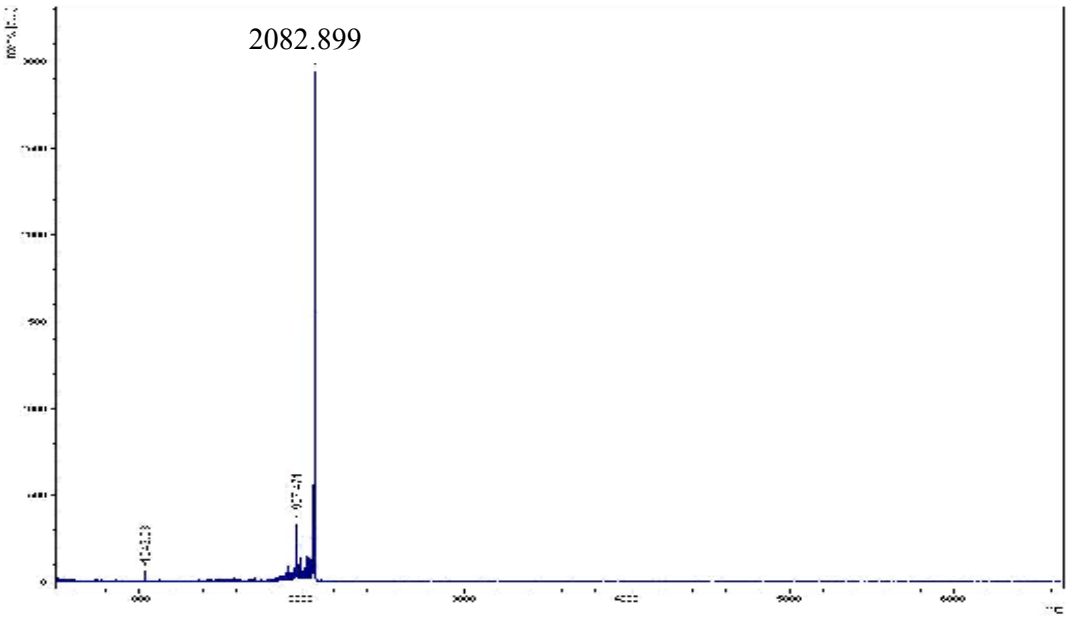

Figure A.4: The MALDI/TOF spectrum of synthesized TiBP1-GGG-RGDS

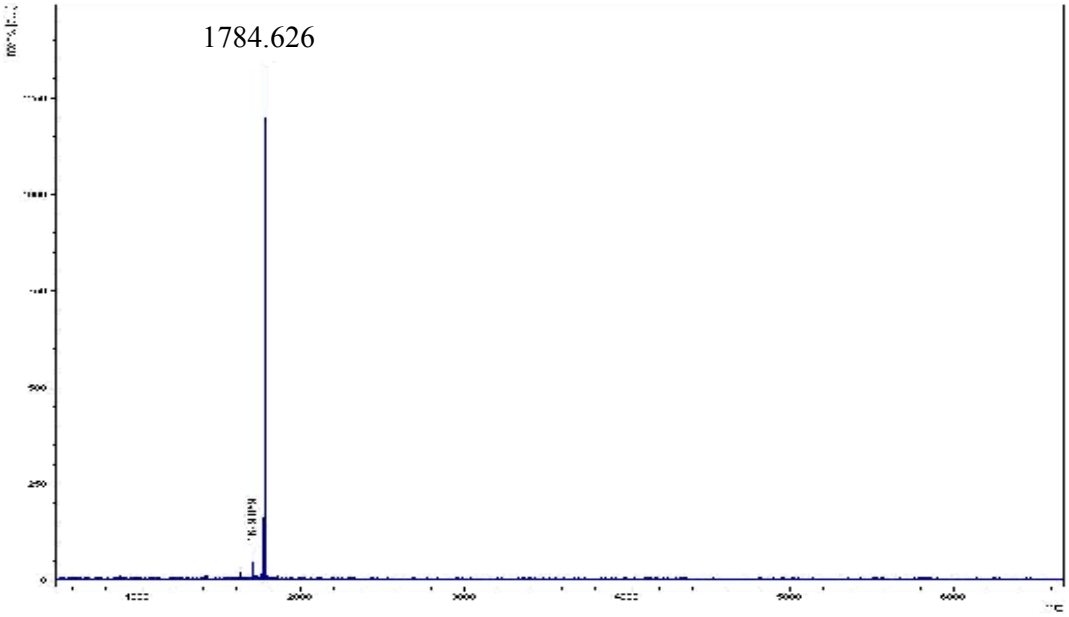

Figure A.5: The MALDI/TOF spectrum of synthesized TiBP2-GGG-RGDS

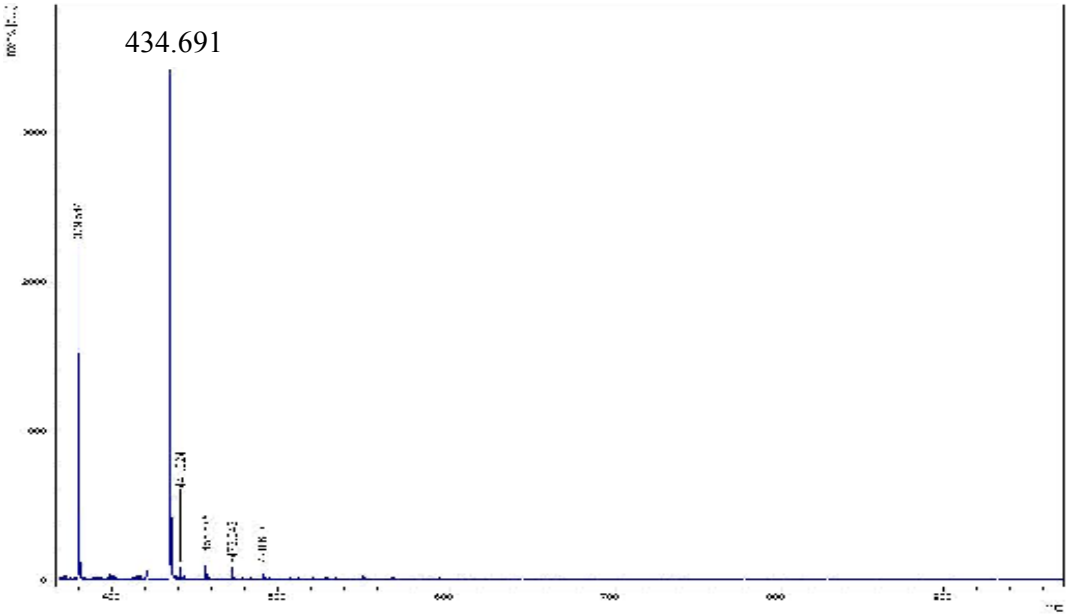

Figure A.6: The MALDI/TOF spectrum of synthesized RGDS

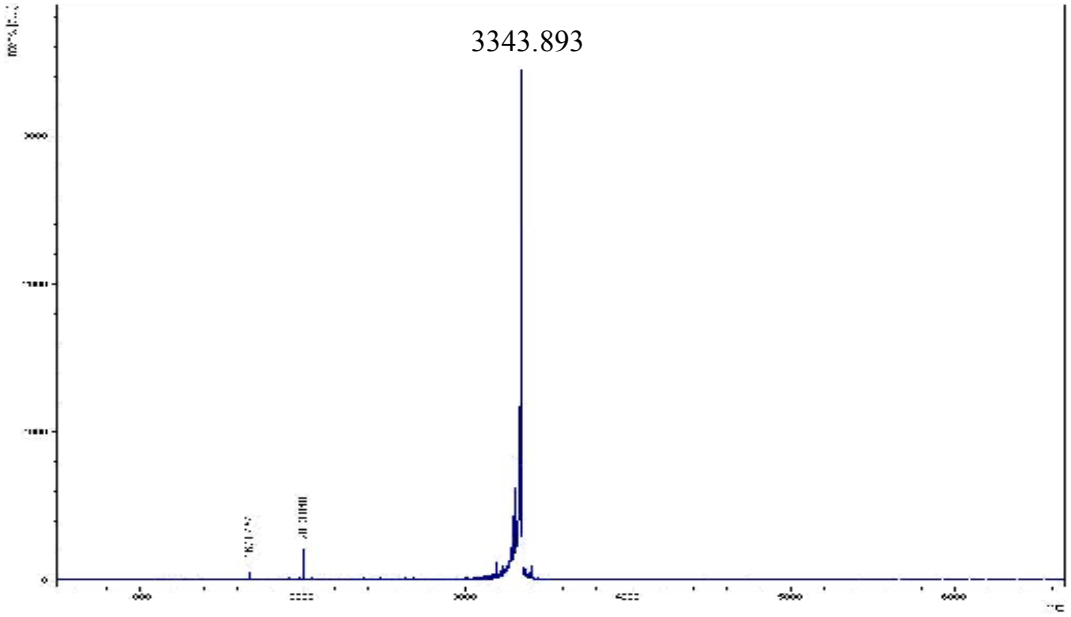

Figure A.7: The MALDI/TOF spectrum of synthesized TiBP1-GGG-AMP

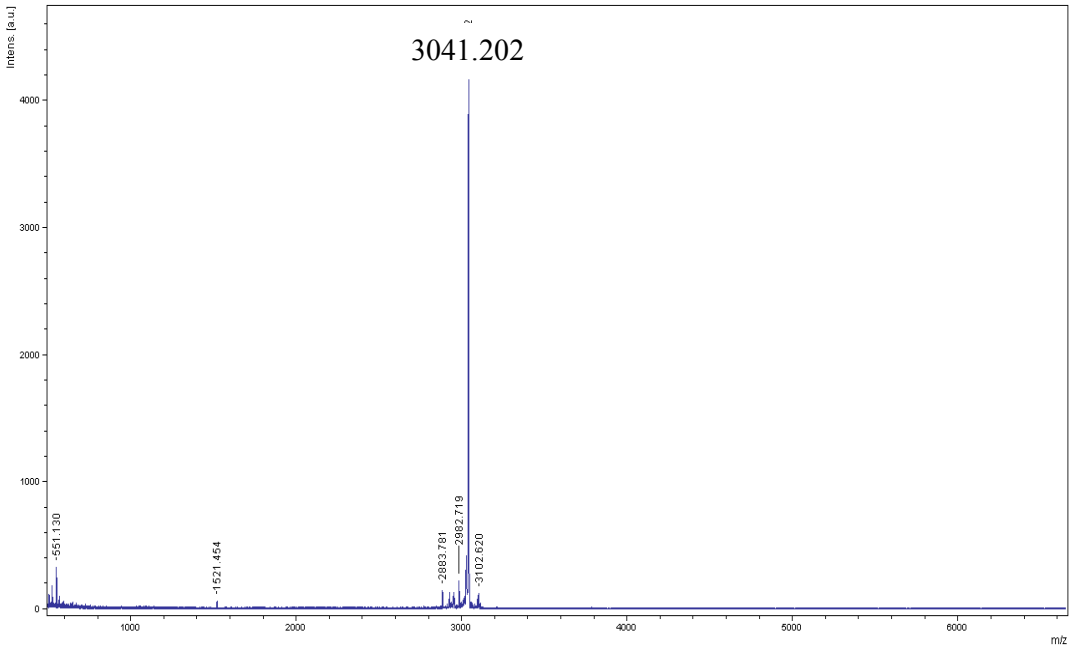

Figure A.8: The MALDI/TOF spectrum of synthesized TiBP2-GGG-AMP

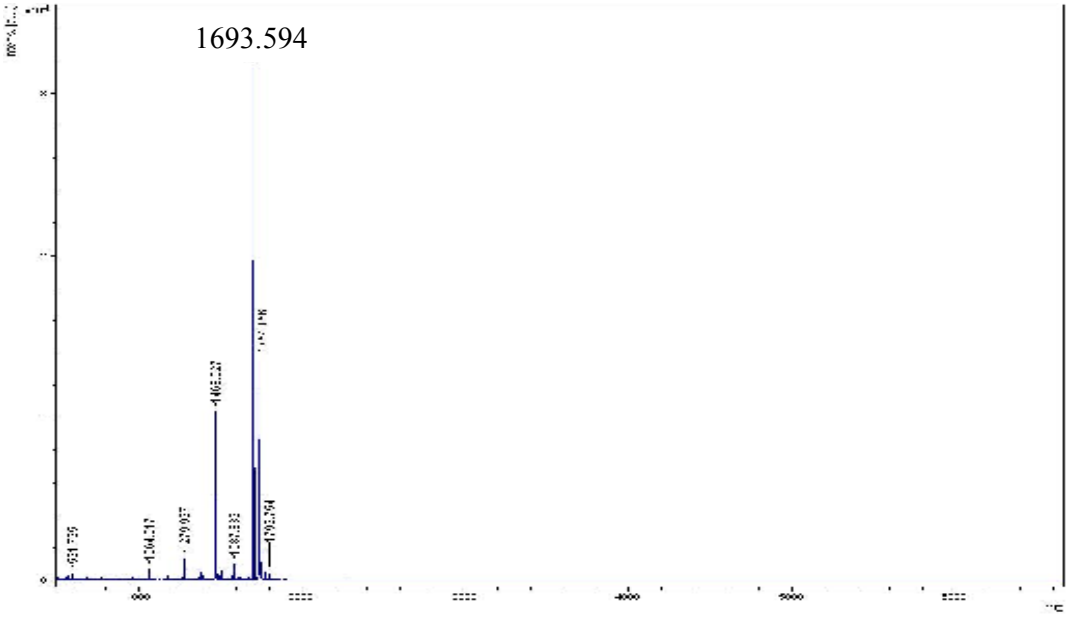

Figure A.9: The MALDI/TOF spectrum of synthesized AMP

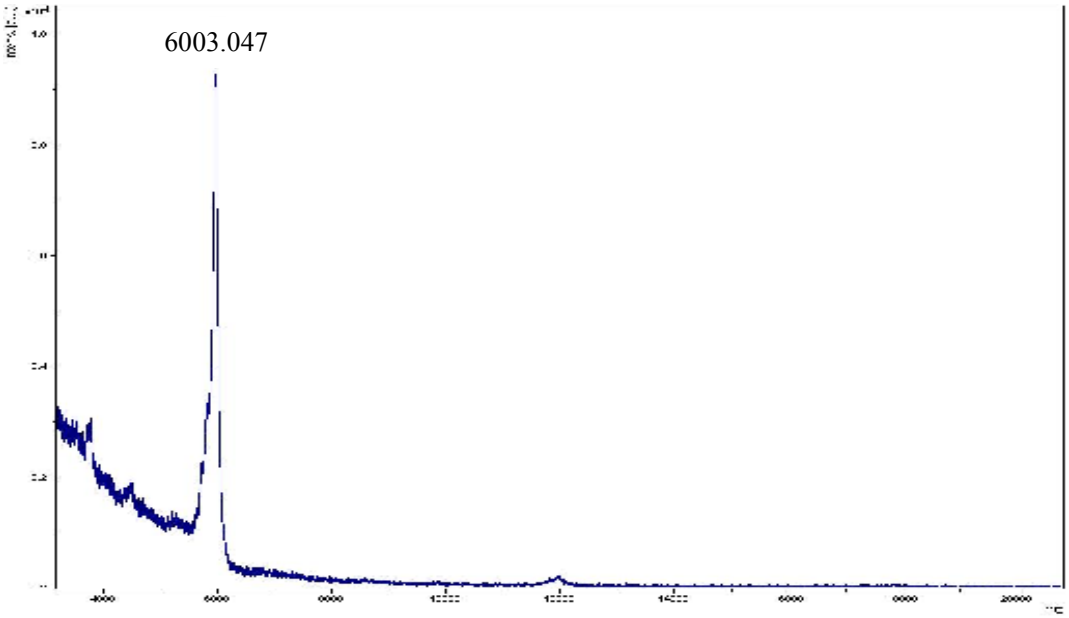

Figure A.10: The MALDI/TOF spectrum of synthesized TiBP2-GGG-ADP7

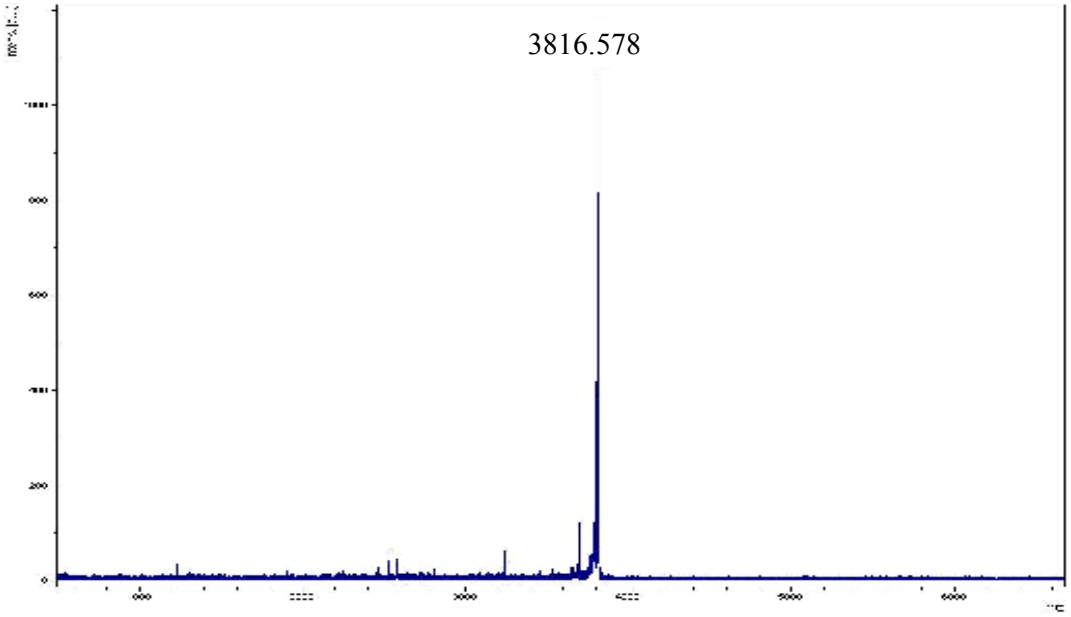

Figure A.11: The MALDI/TOF spectrum of synthesized TiBP2-GGG-ADP5

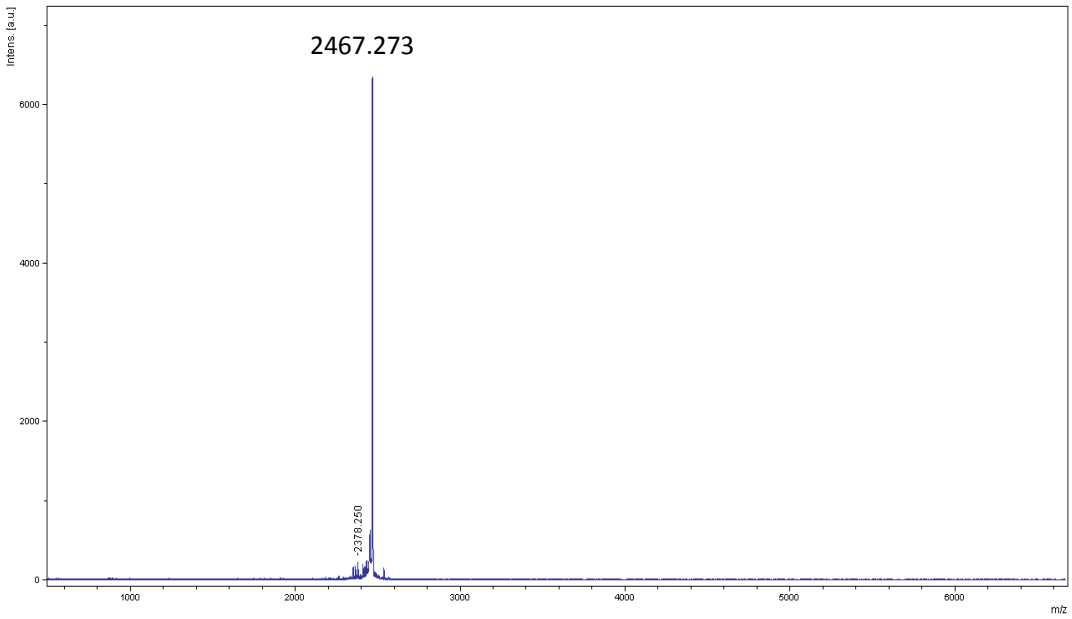

Figure A.12: The MALDI/TOF spectrum of synthesized ADP5

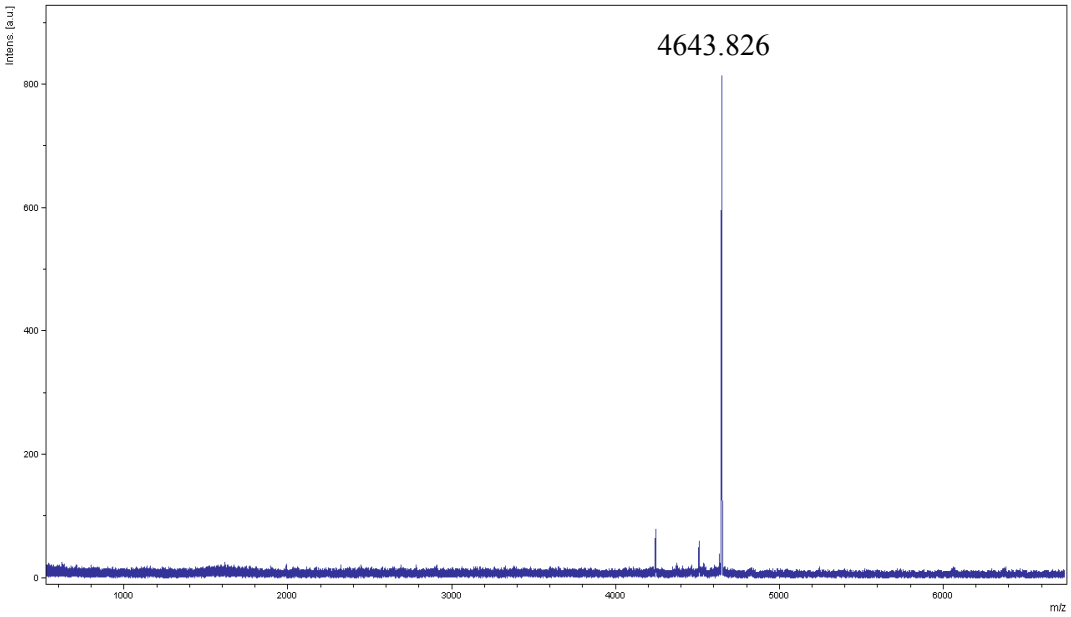

Figure A.13: The MALDI/TOF spectrum of synthesized ADP7

CURRICULUM VITAE

Hilal YAZICI

Place and date of birth: Gebze/Turkey, 1980

Permanent Address: Istanbul

E-mail : yazicihil@itu.edu.tr , hilaly@u.washington.edu

Universities and Colleges attended:

Ph.D. : 2005 – Molecular Biology-Genetics and Biotechnology, Istanbul Technical University- Turkey
M.Sc : 2005, Molecular Biology-Genetics and Biotechnology, Istanbul Technical University- Turkey
B.Sc : 2002, Biology (Genetics Group), Istanbul University- Turkey

Publications

Yazici, H., Fong, H., Wilson, B., Oren, E.E., Amos, F.A., Zhang, H., Evans, J.S., Snead, M.L., Sarikaya, M., Tamerler, C., Biological response on a titanium implant-grade surface functionalized with modular peptides, *Acta Biomaterilia*, DOI:10.1016/j.actbio.2012.11.004

C. R. So, Y. Hayamizu, **H. Yazici,** C. Gresswell, D. Khatayevich, C. Tamerler, and M. Sarikaya, "Controlling Self Assembly of Engineered Peptides on Graphite by Rational Mutation," *ACS Nano*, 6 (2) 1648-1656 (2012). (Cover Paper, February 2012

Khatayevich, D., Gungormus, M., **Yazici, H**., So, C., Cetinel, S., Ma, H., Jen, A., Tamerler, C., Sarikaya, M., Bio-functionalization of Materials for Implants Using Engineered Peptides, *Acta Biomaterialia,* 6 (12), 4634-4641, (2010)

Arin, M., **Yazici, H.,** Goller, G., Biocompability Properties of ZrO_2 Ceramics and ZrO2-TiN Composites, *Key Engineering Materials,* 396-398, 51-5, (2009)

Donatan, S., **Yazici, H**., Bermek, H., and Sarikaya, M., Tamerler, C., Urgen, M., Physical elution in phage display selection of inorganic-binding peptides, *Materials Science and Engineering C* 29, 14–19, (2009)

Liu, H., **Yazici, H.,** Ergun, C., Webster, T.J., Bermek, H., An in vitro evaluation of the Ca/P ratio for the cytocompatibility of nano-to-micron particulate calcium phosphates for bone regeneration. *Acta Biomaterialia*, 4, (5), 1472 – 1479, (2008)

Trabzon L,**Yazici H,** Đğdil M.C, Arslan E, Tamerler, C, Bermek H, Evaluation of mechanical properties and biocompatibility of plasma-nitrided laser-cut 316L cardiovascular stents, *J Mater Sci: Mater Med,* 19(5), 1851-2246, (2007)

Yazici, H, Selection of mica binding polypeptides by using Phage display technology*, Master Thesis,* Istanbul Technical University, January 2005.

Bermek. H, **Yazici, H.,** Ozturk, M.H., Tamerler, C., Jung, H., Li, K., Brown, K.M., Ding, H., Xu, F. Purification and characterization of a manganese peroxidase from wood-degrading fungus Trichophyton rubrum LSK-27. *Enzyme and Microbial Technology,* 35(1), 87-92, (2004)

Yazici, H., Glendon, G., **Yazici, H.,** Burnie, S. J., Saip, P., Buyru, F., Bengisu, E., Andrulis, I. L., Dalay, N., Ozcelik, H., BRCA1 and BRCA2 Mutations in Turkish Familial and Non-familial Ovarian Cancer Patients: High Incidence of Mutations in Non-familial Cases*, Human Mutations,* 20(1), 28-34 (2002)

Yazici, H, Rood, M., Wilson, B., Kacar, T., Oren, E.E, Sarikaya, M., Tamerler, C., GEPI-Mediated Antimicrobial Implant Surface Functionalization, *(Submitted to Biomaterials)*

Yazici, H, Wilson, B., Sarikaya, M., Tamerler, C., In Situ Mineralization of Hydroxyapatite films via bifunctional inorganic binding peptides on titanium surface *(Submitted to Biomacromolecules).*

International Conference and Symposium Presentations

Yazici, H., Rood, M., Sarikaya, M., Tamerler, C., Bi-functional peptide coatings for antimicrobial implant surface functionalization, *E-MRS 2012 Spring Meeting, Oral Presentation, Symposium G, May 14-18 2012, Strasbourg, FRANCE.*

Yazici, H., Hnilova, M., Fong, H., Zhang, H., Tamerler, C., Specific Targeting Molecular Probes: From Materials to Cells**,** *Oral Presentation, 2012 TMS Annual Meeting & Exhibition**,** Biological Materials Science Symposium**,** March 11-15, 2012, Orlando, FL*

Yazici, H., Gungormus, M., Sarikaya, M., Zhang, H., Snead, M.L., Tamerler, C., Antimicrobial Peptide Coatings on Titanium Implants, *Oral Presentation, 2012 TMS Annual Meeting & Exhibition**,** Surface Properties of Biomaterials III Symposium, March 11-15, 2012, Orlando, FL*

Yazici, H., Rood, M., Tamerler, C., Sarikaya, M., Peptide-Based Surface Modifications for antimicrobial implants*, The International Conference on Enzymes Science and Technology (ICEST) Poster Presentation, 31 October-4 November 2011, Aydin, Kusadasi, TURKEY.*

Yuca, E., **Yazici, H.,** Cetinel, S., Yücesoy, D., Sarikaya, M., Karaguler, N. G.,C. Tamerler *Inorganic Binding Peptide Mediated FDH Immobilization on Graphite Surface, The International Conference on Enzymes Science and Technology (ICEST) Poster Presentation, 31 October-4 November 2011, Aydin, Kusadasi, TURKEY*

Yazici, H., Gungormus, M., Sarikaya, M., Tamerler, C., Bi-functional Chimeric Peptide Coatings for Improved Osteointegration of Titanium Implants, *TMS, 140th Annual Meeting and Symposium*: *Biological Materials Science, Oral Presentation, February 27-March 3, 2011, San Diego, CA, USA.*

Yazici H., Wilson, B., Oren, E.E, Fong, H., Sarikaya, M., Tamerler, C., Titanium Binding Peptides as Molecular Linker for Implant Surface Funtionalization, *Eleventh International Symposium on Biomimetic Materials Processing (BMMP-11), Poster Presentation, 25-28 January 2011, Nagoya, JAPAN.*

Yazici H., Wilson, B., Oren, E.E, Evans, J.S., Sarikaya, M., Tamerler, C., Binding Characterization and cytotoxicity analysis of cell Surface display selected Titanium Binding Peptides on Titanium Implant Surfaces, *Society For Biomaterials, 2010 Annual Meeting, Poster Presentation, April 21-24, 2010, Seattle, WA,USA.*

So C., Oren, E.E., **Yazici H.,** Mulheran, P., Evans, J., Tamerler, C., Sarikaya, M., Molecular Mechanism of Genetically Engineered Peptides for Inorganics on Gold and Graphite Surfaces, *Society For Biomaterials, 2010 Annual Meeting, Oral Presentation, April 21-24, 2010, Seattle, WA,USA.*

Hayamizu, Y., So, C., **Yazici, H.,** Hnilova, M., Oren, E. E., Tamerler, C., Sarikaya, M., Electronic Transport through Materials-selective Peptides*, MRS Spring Meeting, Symposium U: Scanning Probe Microscopy - Frontiers in NanoBio Science, Oral Presentation, April 6 – 8, 2010, San Francisco, CA, USA.*

Hayamizu, Y., So, C., **Yazici, H.,** Hnilova, M., Oren, E. E., Tamerler, C., Sarikaya, M., Electric Conductivity of Peptide-Modified Graphene*, MRS Spring Meeting, Symposium S: Graphene Materials and Devices, Oral Presentation, April 6 – 8, 2010, San Francisco, CA, USA.*

Yazici, H., Rood, M., Wilson, B., Gungormus, M., Tamerler, C., Sarikaya, M., Solid-Binding peptide Based Antibacterial Implants, *TMS, 139th Annual Meeting and Symposium*: *Biological Materials Science: Surface Engineering: Biomimetics and Biological Applications, Oral Presentation, February 14–18, 2010, Seattle,WA, USA.*

So C., Noyes, M., Oren, E.E., Meskine, H., **Yazici H.,** Mulheran, P., Tamerler, C., Evans, J., Sarikaya, M., Binding and Assembly of Material-Specific Peptides on Solid Substrates by Atomic Force Microscopy, *TMS, 139th Annual Meeting and Symposium*: *Biological Materials Science: Computational Materials Science, Oral Presentation, February 14–18, 2010, Seattle, WA, USA.*

Yazici, H., Rood, M., Wilson, B., Gungormus, M., Tamerler, C., Sarikaya, M., Solid-binding Peptide-based Antibacterial Implants, *MRS Fall Meeting, Symposium, RR: Engineering Biomaterials for Regenerative Medicine, Poster Presentation,* November 30 - December 2, 2009, Boston, MA, USA.

Akin, I., **Yazici, H.,** Goller, G., Biocompatibility Evaluation of Potassium Mica-Fluorapatite Based Glass Ceramics as a Function of CeO2 Addition, *TMS 2008,137th Annual Meeting, Oral Presentation, March 9-13, 2008, New Orleans, LA,USA.*

Yazici, H., Dogan, S., Tamerler, C., Geurtsen, W., Somerman, M., and Sarikaya, M., Biomimetically Designed Peptide – Based Dental Composites*, 13th, Biomedical Science & Technology Symposium, Poster Presentation, 26-28 August 2007, Istanbul, TURKEY.*

Yazici, H., Dogan, S., Tamerler, C., Geurtsen, W., Somerman, M., and Sarikaya, M., *Molecularly designed biomimetic resin-based dental composites, Seventh International Symposium on Biomimetic Materials Processing (BMMP-7), Poster Presentation, 23-25 January 2007, Nagoya, JAPAN.*

Tamerler, C., Gungormus, M., Fong, H., Sahin, D., **Yazici, H.,** Kacar, T., Seker, U.O. S., Cetinel, S., and Sarikaya, M, Genetically Engineered Peptide-Based Functional Molecular Constructs For Materials Science and Medicine, *Seventh International Symposium on Biomimetic Materials Processing (BMMP-7), Oral presentation, 23-25, January 2007, Nagoya, JAPAN.*

Yazici, H., Donatan, S., Bermek, H., Urgen, M., Tamerler, C., and Sarikaya, M., Mica -binding polypeptides using phage display technique, *BIOMED 11. International Biomedical Science and Technology Days, Poster Presentation, 6-10 September 2004, Ankara, TURKEY.*

Donatan, S., **Yazici, H.,** Bermek, H., Urgen, M., Tamerler, C., and Sarikaya, M., Physical elution approach to selection of inorganic-binding polypeptides via phage display, *BIOMED 11. International Biomedical Science and Technology Days, Poster Presentation, 6-10 September 2004, Ankara, TURKEY.*

Donatan, S., **Yazici, H.,** Bermek, H., Urgen, M., Tamerler, C., and Sarıkaya, M., A physical elution approach to selection inorganic-binding polypeptides using ultrasonication via phage display, *MRS Fall Meeting, Poster Presentation, Nov. 29 - Dec. 3, 2005, Boston, MA, USA.*

Donatan, S. **Yazici, H.,** Bermek, H., Urgen, M., Tamerler, C., and Sarikaya, M., *A new Approach to Selection of Inorganic-Binding Polypeptides Using Ultrasonication During Phage Display, Fourth International Symposium on Biomimetic Materials Processing (BMMP-4), Poster Presentation, January 2004, Nagoya, JAPAN.*